Fall 12-22-2010

Native Functions of the Androgen Receptor are Essential to Pathogenesis in a Drosophila Model of Spinobulbar Muscular Atrophy

Natalia B. Nedelsky
University of Pennsylvania, nedelsky@mail.med.upenn.edu

Native Functions of the Androgen Receptor are Essential to Pathogenesis in a Drosophila Model of Spinobulbar Muscular Atrophy

Abstract

Spinobulbar muscular atrophy (SBMA) is a progressive, late-onset disease characterized by degeneration of motor neurons in the brainstem and spinal cord. The disease is caused by expansion of a polyglutamine tract in the androgen receptor (AR) and is dependent on exposure to AR ligand. The expanded polyglutamine tract confers toxic function to the protein through unknown mechanisms, although the ligand-dependent nature of SBMA suggests that the mechanism of pathogenesis may be tied to ligand-dependent alterations in AR function. However, whether toxicity is mediated by native AR function or a novel AR function is unknown. We systematically investigated ligand-dependent modifications of AR in a Drosophila model of SBMA. We demonstrate in vivo that nuclear translocation of mutant AR is necessary but not sufficient for toxicity and that DNA binding by AR is necessary for toxicity. Mutagenesis studies demonstrated that a functional AF-2 domain is essential for toxicity, a finding corroborated by a genetic screen that identified AF-2 interactors as dominant modifiers of degeneration. As proof of this principle, we perform epistasis experiments using the AR coregulator limpet, which we find modifies polyglutamine-expanded AR toxicity in an AF-2-dependent manner. In addition, we use expression profiling to examine the molecular phenotype of polyglutamine-expanded AR degeneration, revealing that expression of wild-type AR results in a molecular phenotype that is very similar to that caused by polyglutamine-expanded AR. These findings suggest that expanded-polyglutamine AR toxicity may be mediated by amplification of normal function, a mechanism that may be broadly applicable to other polyglutamine diseases.

Degree Type
Dissertation

Degree Name
Doctor of Philosophy (PhD)

Graduate Group
Neuroscience

First Advisor
J. Paul Taylor

Keywords
polyglutamine, neurodegeneration, Drosophila

Subject Categories
Genetics | Molecular Genetics | Nervous System Diseases | Other Neuroscience and Neurobiology

NATIVE FUNCTIONS OF THE ANDROGEN RECEPTOR ARE ESSENTIAL TO

PATHOGENESIS IN A DROSOPHILA MODEL OF SPINOBULBAR

MUSCULAR ATROPHY

Natalia B. Nedelsky

A DISSERTATION

in

Neuroscience

Presented to the Faculties of the University of Pennsylvania

In Partial Fulfillment to the Requirements for the Degree of Doctor of Philosophy

2010

_____
J. Paul Taylor, Associate Member, Developmental Neurobiology, St Jude Children's
Research Hospital
Dissertation Supervisor

_____
Rita Balice-Gordon, Professor, Neuroscience
Graduate Group Chairperson

<u>Dissertation Committee</u>
Rita Balice-Gordon, Professor, Neuroscience
Thomas Jongens, Associate Professor, Genetics
Robert Kalb, Associate Professor, Neurology
Kenneth H. Fischbeck, NIH Distinguished Investigator, NINDS, NIH

NATIVE FUNCTIONS OF THE ANDROGEN RECEPTOR ARE ESSENTIAL TO

PATHOGENESIS IN A DROSOPHILA MODEL OF SPINOBULBAR

MUSCULAR ATROPHY

ABSTRACT

NATIVE FUNCTIONS OF THE ANDROGEN RECEPTOR ARE ESSENTIAL TO PATHOGENESIS IN A DROSOPHILA MODEL OF SPINOBULBAR MUSCULAR ATROPHY

Natalia B. Nedelsky

Supervisor: J. Paul Taylor

Spinobulbar muscular atrophy (SBMA) is a progressive, late-onset disease characterized by degeneration of motor neurons in the brainstem and spinal cord. The disease is caused by expansion of a polyglutamine tract in the androgen receptor (AR) and is dependent on exposure to AR ligand. The expanded polyglutamine tract confers toxic function to the protein through unknown mechanisms, although the ligand-dependent nature of SBMA suggests that the mechanism of pathogenesis may be tied to ligand-dependent alterations in AR function. However, whether toxicity is mediated by native AR function or a novel AR function is unknown. We systematically investigated ligand-dependent modifications of AR in a *Drosophila* model of SBMA. We demonstrate *in vivo* that nuclear translocation of mutant AR is necessary but not sufficient for toxicity and that DNA binding by AR is necessary for toxicity. Mutagenesis studies demonstrated that a functional AF-2 domain is essential for toxicity, a finding corroborated by a genetic screen that identified AF-2 interactors as dominant modifiers of degeneration. As proof of this principle, we perform epistasis experiments using the AR coregulator *limpet*, which we find modifies polyglutamine-expanded AR toxicity in an AF-2-dependent manner. In addition, we use expression profiling to examine the molecular phenotype of

iii

polyglutamine-expanded AR degeneration, revealing that expression of wild-type AR results in a molecular phenotype that is very similar to that caused by polyglutamine-expanded AR. These findings suggest that expanded-polyglutamine AR toxicity may be mediated by amplification of normal function, a mechanism that may be broadly applicable to other polyglutamine diseases.

Table of Contents

List of Tables

List of Illustrations

Chapter 1: Introduction

Introduction

Polyglutamine expansion diseases together form the most common group of inherited neurodegenerative disease (Riley and Orr, 2006). The diseases are caused by expansion of trinucleotide (CAG) repeats in coding regions of DNA, yielding proteins with expanded polyglutamine tracts. These proteins cause adult-onset neurodegeneration through unknown mechanisms. Despite being caused by a common mutation, each of the polyglutamine diseases affects specific populations of neurons, resulting in diverse patterns of pathology and clinical presentations. Attempts to define and resolve this paradox have been at the heart of the most significant advances in understanding the pathogenesis of these diseases.

This chapter takes a historical approach to the field of polyglutamine disease research, aiming to demonstrate how our understanding has evolved to produce the work contained in this thesis. Starting with patient observation and guided by computational, *in vitro*, and *in vivo* models, the field has seen a range of theories that seek to unite the various members of the polyglutamine disease family with a common mechanism of pathogenesis. This work, based largely on the inherent toxicity of expanded polyglutamine peptides, suggested that toxic aggregation of polyglutamine proteins could lead to disturbances in biological activities as diverse as axonal trafficking, synaptic transmission, and the ubiquitin proteasome system (UPS). Recently, however, an alternative approach has begun to uncover a more subtle picture of toxicity. Inspired by the diversity of the diseases within the polyglutamine disease family, this approach focuses on features that are unique to each disease protein rather than their shared

2

polyglutamine expansion. These investigations have advanced the idea that toxicity arises from alterations in native protein function rather than novel function imparted by the expanded polyglutamine tract. This perspective, still largely unexplored in the polyglutamine disease field, serves as the foundation of this thesis.

Polyglutamine Disease: Discovery and Clinical Characterization

The story of the polyglutamine diseases begins, experimentally speaking, with spinal and bulbar muscular atrophy (SBMA). SBMA was first identified in 1968 as an adult-onset X-linked disease characterized by progressive muscle weakness and atrophy due to lower motor neuron degeneration (Kennedy et al., 1968). Subsequent studies expanded the clinical picture to include signs of androgen insensitivity including gynecomastia and reduced fertility (Arbizu et al., 1983), providing an important clue to mapping the mutation responsible for the disease. More than 20 years later, the causative mutation was finally defined by linkage analysis and positional cloning (La Spada et al., 1991). The mutation was found to reside in the androgen receptor (AR) gene, a result that was perhaps unsurprising given the endocrine-related clinical features of the disease. The great surprise lay in the nature of the mutation, which was defined as a novel expansion of a polymorphic trinucleotide (CAG) repeat within the coding region of the gene. While the general population had CAG repeat lengths of 9-36, patients with SBMA had repeat lengths of 38 or greater, leading to expression of AR protein with an expanded polyglutamine tract. The mutation was presumed to cause disease via a gain of function,

because loss of AR function was known to cause androgen insensitivity syndrome (AIS), a condition not characterized by degeneration or weakness (Quigley et al., 1992).

Within the same year, a number of groups identified similar mutations in other diseases, including trinucleotide repeat expansions that caused fragile X syndrome (Verkerk et al., 1991) and myotonic dystrophy (Fu et al., 1992; Mahadevan et al., 1992). However, these mutations were found in untranslated regions of genes, and the relationship between these new "trinucleotide repeat expansion diseases" remained unclear. Finally, two years later (and after 20+ years of mapping work), a collaborative research project trying to identify the genetic basis for Huntington's disease (HD) found that HD was caused by the same mutation as SBMA – expansion of a CAG repeat in a coding region of DNA, this time within a novel gene dubbed huntingtin (1993). By the time the HD mutation was confirmed to result in a protein product with an expanded polyglutamine tract (Sharp et al., 1995), an entire collection of polyglutamine diseases had been uncovered: spinocerebellar ataxia type 1 (SCA1, caused by expansion in ataxin-1) (Orr et al., 1993), dentato-rubro pallidoluysian atrophy (DRPLA, atrophin-1) (Koide et al., 1994; Nagafuchi et al., 1994), and SCA3 (ataxin-3) (Kawaguchi et al., 1994) were all found to be caused by CAG expansions in exonic regions of DNA. Over the last fifteen years, four more polyglutamine diseases have been identified: SCA2 (ataxin-2) (Pulst et al., 1996), SCA6 (CACNA1A) (Riess et al., 1997; Zhuchenko et al., 1997), SCA7 (ataxin-7) (David et al., 1997), and SCA17 (TATA-binding protein, TBP) (Nakamura et al., 2001) (Table 1.1). This family now sits within a broader class of hereditary diseases, the repeat expansion diseases (Table 1.2).

The polyglutamine disease family members have important fundamental similarities that reflect their shared mutation. Although most of the polyglutamine-expanded proteins are broadly expressed, each disease manifests as a progressive degeneration of a small subset of neurons (Table 1.1). With the exception of SBMA, all polyglutamine diseases are inherited in an autosomal dominant manner. These diseases also show robust correlations between phenotype and polyglutamine length: with longer polyglutamine lengths, disease onset occurs earlier, and disease severity increases (Orr and Zoghbi, 2007). Polyglutamine tracts are often progressively lengthened as they are transmitted from one generation to the next, a phenomenon that explains the genetic anticipation observed in these diseases, in which symptom severity increases with successive generations.

The clinical differences between the polyglutamine diseases, however, are perhaps more striking than their similarities. Despite being caused by the same mutation, the symptoms of several of the diseases have virtually no phenotypic overlap: while HD manifests as a triad of involuntary movements, dementia, and psychiatric disturbance that culminates in death, the same mutation in SBMA causes proximal muscle weakness with sparing of cognitive capacity and no significant change in longevity. These clinical differences are directly related to the subset of neurons that are affected in each disease: striatum and cortex in HD (Vonsattel et al., 1985), lower motor neurons in SBMA (Sobue et al., 1989). This selective vulnerability occurs despite overlapping patterns of huntingtin and AR expression, providing one of the first clues that polyglutamine expansion could not be solely responsible for toxicity. In addition, none of the disease proteins have any apparent

structural or functional similarities beyond their polyglutamine tracts, although a

common theme of transcription regulation may be emerging and will be discussed below

(Shao and Diamond, 2007).

Polyglutamine Disease: Lessons from the First Generation of Models

With the recognition of this new family of diseases, researchers first focused their

attention on what these disease genes had in common; namely, a polyglutamine

expansion that appeared to have a universal toxic threshold of 36-41 repeats. (As more

patients' DNA was sequenced, this threshold widened; see Table 1.1. SCA6 also stands

as a notable exception, since repeat lengths as short as 20 can cause disease.) Thus, the

biochemical and biophysical properties of expanded polyglutamine became an area of

intense interest. One of the seminal papers influencing this view came from Nobel

laureate Max Perutz, who suggested that expanded polyglutamine peptides can self-

associate to form "polar zippers" (Perutz et al., 1994; Perutz, 1996). In these structures,

polyglutamine tracts form paired antiparallel β-strands linked together by hydrogen

bonds between the main-chain and side-chain amides, excluding water molecules and

thereby rendering the protein insoluble. In modeling these structures, Perutz found that he

could replicate several fundamental properties of polyglutamine disease. First, his models

suggested that the thermodynamic threshold for polar zipper formation coincided with the

polyglutamine length threshold for disease. Second, his data suggested that longer

polyglutamine stretches would lead to tighter polar zippers that formed with faster

kinetics, an observation that provided a biophysical basis for increasing severity of disease and earlier age of onset with longer polyglutamine lengths.

At the time of Perutz's molecular models, none of the polyglutamine diseases were known to have neuropathologic changes that supported a model of aggregation. However, when the first generation of HD mouse models appeared, Perutz's hypothesis was deemed prescient. The most influential model was a transgenic strain that expressed exon 1 of the huntingtin gene, the region of the protein that contains the polyglutamine tract. The authors reported that these mice showed HD-like movement disorder phenotypes (Mangiarini et al., 1996), although decreased body weight, hind limb clasping, and poor rotarod performance have proven to be the most robust phenotypes of this model (Hockly et al., 2003). These phenotypes were accompanied by pronounced widespread neuronal intranuclear inclusions that contained huntingtin protein (Davies et al., 1997) and were also immunopositive for ubiquitin, suggesting that the inclusions were made up of misfolded and aggregated proteins that had been marked for proteasomal degradation. Within the next year, ubiquitinated neuronal intranuclear inclusions were found in patient tissue in SCA3 (Paulson et al., 1997), HD (DiFiglia et al., 1997; Becher et al., 1998), DRPLA (Becher et al., 1998), SCA1 (Skinner et al., 1997), and SBMA (Li et al., 1998).

In follow-up studies, it soon became clear that expanded polyglutamine tracts not only aggregated and formed ubiquitinated inclusions – they were also very toxic. Expression of expanded polyglutamine tracts – whether flanked by a minimal amount of disease protein context, inserted into non-disease-related genes, fused to GFP tags, or even

7

expressed with no flanking sequence whatsoever – resulted in strong toxicity in cells (Ikeda et al., 1996; Moulder et al., 1999; Yang et al., 2002), flies (Jackson et al., 1998; Warrick et al., 1998; Kazemi-Esfarjani and Benzer, 2000; Marsh et al., 2000), and mice (Ikeda et al., 1996; Ordway et al., 1997; Adachi et al., 2001), nearly always accompanied by ubiquitin-positive inclusion formation. This toxicity suggested to many researchers that aggregation and inclusion formation reflected a common pathway of cellular dysfunction and polyglutamine-mediated toxicity (Ross, 1997). Indeed, the presence of aggregates was proposed to block axonal vesicle trafficking (Gunawardena and Goldstein, 2005) and cause defects in synaptic transmission (Mattson and Sherman, 2003) in a manner that applied broadly to all diseases marked by protein aggregation. However, a significant question remained: if the diseases shared a common toxic mechanism, what could account for the differential neuronal vulnerability in the different diseases? Different levels of disease protein expression in different cell types might contribute, but were clearly not the dominant factor in determining cell-type specificity (Zoghbi and Orr, 2000; Sieradzan and Mann, 2001).

Some groups chose to call into question the causative link between inclusions and toxicity. One of the first and most direct challenges came from a transgenic model of SCA1, in which mice expressed full-length polyglutamine-expanded ataxin-1 with a point mutation to its self-association domain (Klement et al., 1998). These mice developed ataxia and pathology similar the original SCA1 model mice, although the self-association mutants did not show any signs of inclusions to accompany their phenotype. Other groups examining the temporal course of disease also found that measurable

8

phenotypic changes can occur before inclusions are detectable (Reddy et al., 1998; Hodgson et al., 1999). Elegant studies using huntingtin exon 1, ataxin-3, ataxin-7, and AR subsequently revealed inverse correlations between inclusion formation and toxicity, suggesting that inclusions may actually reflect a neuroprotective effort to relocate toxic, soluble protein into inert, insoluble protein deposits (Cummings et al., 1999; Yoshizawa et al., 2001; Taylor et al., 2003b; Arrasate et al., 2004; Bowman et al., 2005; Evert et al., 2006; Rub et al., 2006; Truant et al., 2008). Indeed, compounds that promote inclusion formation have recently shown therapeutic potential in *in vitro* models of HD (Bodner et al., 2006) and *in vitro* and *in vivo* models of SBMA (Appendix I).

While addressing the controversy regarding the nature of inclusions, however, it became clear that polyglutamine proteins did not exist in one of only two states; that is, as either soluble monomers or insoluble inclusions. Rather, researchers recognized that a continuum existed along which soluble monomers can self-associate to form oligomers, which may proceed to form larger structures, which in turn may coalesce into microscopically visible inclusions. Unfortunately, there is considerable confusion in terminology regarding these different biophysical states. In this thesis, we generally distinguish protein aggregates, which are defined primarily biochemically and include submicroscopic oligomers, from inclusions, which are defined histologically (Taylor et al., 2003b). Inclusions are likely inert and neuroprotective, as described above. In the search for the toxic polyglutamine conformer, attention has now shifted to oligomers, which have been correlated with toxicity in an animal model of SBMA (Li et al., 2007).

In the same paper that dissociated SCA1 toxicity from inclusions, Klement et al. used a second transgenic model of SCA1 with a different point mutation to full-length, polyglutamine-expanded ataxin-1 (Klement et al., 1998). This mutation disrupted the nuclear localization signal (NLS), restricting ataxin-1 to the cytoplasm. These mice did not develop disease, demonstrating that polyglutamine expansion in itself was not sufficient to cause toxicity – at least when restricted to the cytosol. Thus, the ataxin-1 NLS mutant provided critical insight into the importance of the nucleus as a site of toxicity. Some groups had already noted that several of the polyglutamine disease proteins (e.g. huntingtin, ataxin-3, and atrophin-1) are normally cytoplasmic, yet are found in inclusions in the nucleus in the context of disease (Zoghbi and Orr, 2000). These observations prompted the suggestion that although intranuclear inclusions may not be necessary for disease, nuclear translocation may be the more critical pathogenic event (Kim and Tanzi, 1998). Supporting this idea, toxicity was also mitigated by cytoplasmic retention of polyglutamine-expanded huntingtin (Saudou et al., 1998), AR (Takeyama et al., 2002), ataxin-3 (Bichelmeier et al., 2007), atrophin-1 (Nucifora et al., 2003), and even pure polyglutamine (Yang et al., 2002). Of note, the polyglutamine diseases SCA2 and SCA6 are marked by cytoplasmic inclusions, indicating that the nuclear localization is not a universal prerequisite for polyglutamine protein toxicity (Ishikawa et al., 1999; Huynh et al., 2000).

As alluded to above, the presence of certain polyglutamine disease proteins in the nucleus was a mystery in itself. HD provides the best example: given that the protein has no known NLS and that the upper size limit for passive nuclear entry of 60-70 kDa (Wei et

al., 2003), it is not clear how the large >350 kDa huntingtin protein could enter the nucleus (Truant et al., 2007). Instead, it appears that full-length huntingtin is cleaved to generate a small polyglutamine-containing N-terminal fragment that diffuses into the nucleus. This fragment has been proposed to be at the heart of toxicity, since inhibiting caspase cleavage of huntingtin can eliminate toxicity *in vivo* (Graham et al., 2006). N-terminal fragments of huntingtin have also been identified in HD patient tissue and are correlated with toxicity (DiFiglia et al., 1997). Such evidence has prompted theories that protein cleavage may be a common theme in polyglutamine disease, even providing a possible explanation for selective neuronal vulnerability. According to this theory, the subset of neurons that are affected in each disease could be defined by the presence of relevant proteases that generate toxic polyglutamine-containing fragments. However, *in vivo* evidence for cleavage of most polyglutamine-containing proteins is inconsistent across different diseases and models, and the contradictory evidence for the production and role of proteotoxic fragments suggests that protein cleavage is not a unifying mechanism of polyglutamine disease toxicity (Walsh et al., 2005).

Shortly after the first generation of mouse models appeared, *Drosophila* models of polyglutamine disease were introduced, providing their own mechanistic insights. Dominant modifier screens proved to be especially productive. The first paper to use this technique revealed two chaperone molecules as suppressors of toxicity, confirming that modification of protein folding pathways could dramatically modify polyglutamine toxicity (Warrick et al., 1999; Kazemi-Esfarjani and Benzer, 2000). Indeed, this result has been now reproduced numerous times in models of several polyglutamine diseases

11

(Opal and Zoghbi, 2002), establishing that chaperones can mitigate polyglutamine toxicity by either promoting refolding or enhancing degradation of polyglutamine-containing proteins.

The importance of protein quality control was further highlighted by the identification of modifiers of a fly SCA1 model, which included critical players in the ubiquitin-proteasome system (UPS) (Fernandez-Funez et al., 2000). The importance of this degradation pathway was confirmed by reports that proteasomes were found in the ubiquitinated inclusions in SCA1 patient tissue and HD models (Cummings et al., 1998; Waelter et al., 2001), supporting the idea that polyglutamine disease proteins accumulate in inclusions due to insufficient degradation by the UPS. Indeed, it appears that polyglutamine sequences cannot be degraded by eukaryotic proteasomes, which prefer to cleave after hydrophobic, basic, or acidic residues (Venkatraman et al., 2004). A number of groups have demonstrated that the UPS actually becomes impaired in models of polyglutamine disease (Bence et al., 2001; Bennett et al., 2005; Pandey et al., 2007b), possibly due to long polyglutamine tracts entering the proteasome and failing to exit properly (Venkatraman et al., 2004). Indeed, a recent report showed that expression of an expanded huntingtin fragment impairs UPS function (albeit transiently) *in vivo* (Ortega et al., 2010), although the relative contribution of UPS impairment to pathogenesis remains controversial. A second degradation pathway, the autophagy-lysosomal system, has recently gained attention as a compensatory pathway for protein degradation when the UPS is impaired. The relationship between the UPS and autophagy, as well as the relevance of these systems to neurodegenerative disease, is explored in Appendices II-IV.

Unexpected modifiers were also uncovered in *Drosophila* models. One particularly intriguing family of modifiers included proteins that function as coregulators in transcriptional regulation (Boutell et al., 1999; Fernandez-Funez et al., 2000). Indeed, transcriptional coregulators such as CREB-binding protein (CBP) have been found in inclusions in multiple polyglutamine diseases, and overexpression of CBP rescues polyglutamine-induced toxicity in cells (McCampbell et al., 2000; Nucifora et al., 2001) and flies (Taylor et al., 2003a). However, the nature of the interactions between polyglutamine disease proteins and transcriptional regulators is uncertain. The interactions could be due to relatively non-specific effects, as short polyglutamine tracts are found in many transcription factors (including CBP) and could potentially be incorporated into the polar zippers formed by the expanded disease proteins, resulting in functional sequestration (Schaffar et al., 2004). On the other hand, most polyglutamine disease proteins have now been shown to play some role in transcriptional regulation as part of their native function, suggesting that the modifier effects of transcriptional coregulators might reflect normal interactions that have gone awry due to polyglutamine expansion. Specifically, besides the obvious transcription regulatory role of AR and TBP, huntingtin interacts with general DNA-binding proteins such as Sp1, TFIID, and TFIIF, ataxin-7 plays a role in chromatin structure, and huntingtin, ataxin-1, and atrophin-1 interact with transcriptional coregulators (Riley and Orr, 2006). Such a common function suggests that transcriptional regulation may be a pathway that has particularly great impact on pathogenesis, and has led some to propose the polyglutamine diseases may in fact be "transcriptionopathies" (La Spada and Taylor, 2003).

13

Polyglutamine Disease: the Next Generation

With the notable exception of the SCA1 models from the Zoghbi and Orr labs, the vast majority of "first generation" polyglutamine disease models employed only truncated versions of polyglutamine disease proteins. Of particular note are the HD models that express only exon 1 of the huntingtin gene. Huntingtin is very large, with exon 1 accounting for only 3% of the total protein. And while evidence exists that polyglutamine-containing fragments of huntingtin are produced in HD, there remains a conceptual problem in modeling the disease using truncated proteins: these fragments produce toxicity in nearly every cellular context tested, yet pathology in HD occurs almost exclusively in striatal neurons. Indeed, as researchers began to compare the models expressing truncated proteins to those expressing full-length proteins, it soon became clear that truncated proteins were much more toxic than their full-length versions, and did not recapitulate the cell-type-specific neurodegeneration characteristic of each disease. Mouse models of SBMA provide an ideal example of this phenomenon: truncated, polyglutamine-expanded AR that is widely expressed in the CNS causes widespread neuronal dysfunction (Abel et al., 2001), and pure polyglutamine that is expressed specifically under the AR promoter also causes widespread neuronal dysfunction (Adachi et al., 2001). However, when full-length expanded AR is expressed under the AR promoter, the symptoms are more limited, showing specific vulnerability in lower motor neurons (Sopher et al., 2004).

Based on these and other studies, the Zoghbi and Orr labs were the first to openly speculate that the activities of polyglutamine peptides (and by implication, the pathology that arose from their expression) were distinct from those of the full-length polyglutamine-expanded proteins (Lin et al., 1999; Orr, 2001). They raised the possibility that the toxicity observed using polyglutamine peptides was a generalized toxicity that may overlap with some features of polyglutamine disease, but may not faithfully reflect pathogenesis of the human disease. Instead, taking cues from their ataxin-1 NLS mutant, these labs suggested that regions outside the polyglutamine tract could be determinants of toxicity, with the context of the polyglutamine tract defining the specificity of the disease.

Setting out to test these ideas, the Zoghbi and Orr labs developed a new experimental perspective on polyglutamine disease, one that focused on the protein context in which the polyglutamine tract was located. In a series of papers using both fly and mouse models of SCA1, these groups demonstrated that the phosphorylation status of ataxin-1 could dramatically alter toxicity: animals expressing polyglutamine-expanded ataxin-1 with a single point mutation (S776A, rendering a phosphoserine non-phosphorylatable) showed no pathogenic phenotype (Chen et al., 2003; Emamian et al., 2003). Phosphorylation of the S776 residue, located far from the polyglutamine tract, was further shown to regulate the protein complexes in which ataxin-1 could participate (Lam et al., 2006). Polyglutamine expansion enhanced interactions that were normally regulated by phosphorylation at this site, resulting in alterations in the interaction of ataxin-1 with its native partners (Lim et al., 2008). These enhanced interactions occurred

at the expense of other ataxin-1 interactions, suggesting the possibility that polyglutamine expansion contributes to disease by both gain-of-function and partial loss-of-function mechanisms. Furthermore, these imbalances in ataxin-1 complexes could contribute to the differential vulnerability of particular neuronal populations, since the levels of these interacting partners could be in particularly short (or large) supply in vulnerable neurons (Zoghbi and Orr, 2009).

Native protein function and SBMA

Although Zoghbi and Orr's studies were the first to formally test the importance of protein context in polyglutamine disease, the idea that regions outside the polyglutamine tract might play a role in toxicity was not a new one. For several years, SBMA had been used as a prime example of the importance of protein context, since polyglutamine-expanded AR is toxic only in the presence of AR ligand (testosterone, or its more potent derivative dihydrotestosterone, DHT). In experimental models, flies expressing polyglutamine-expanded AR develop pathology only if they are administered AR ligand (Takeyama et al., 2002; Pandey et al., 2007b), male SBMA mice do not develop disease if they are castrated, and female SBMA mice develop pathology only if they are injected with AR ligand (Katsuno et al., 2002). It is for this reason that SBMA affects only men; females who carry the mutation (even rare homozygotes (Schmidt et al., 2002)) are protected by their low levels of circulating androgen. However, the specific pathogenic events that occur in the presence of AR ligand remain largely unexplored.

The ligand dependence of SBMA leads to a model in which testosterone or DHT converts an innocuous protein into a toxic one, and suggests that experimental approaches that dissect ligand-dependent events may shed light on pathogenesis. In this regard, SBMA researchers have a distinct advantage over those who study other polyglutamine diseases, since the majority of polyglutamine disease proteins have unknown functions and ill-defined interactomes. In contrast, AR is a widely studied protein with a well-characterized function as a ligand-dependent transcription factor. Ligand binding to AR is known to result in a dramatic change in AR localization and function: although normally sequestered in the cytoplasm bound to heat-shock proteins (Hsps), ligand-bound AR dissociates from Hsps and translocates to the nucleus. Conformational changes occur to reveal two "activation function" domains, AF-1 and AF-2, which serve as binding sites for transcriptional coregulators. AR also undergoes ligand-dependent post-translational modifications including phosphorylation, SUMOylation, and acetylation. The protein dimerizes, binds to DNA, recruits transcriptional coregulators, and finally activates or represses its target genes. How these ligand-dependent events relate to the pathogenesis of SBMA will be addressed in Chapter 2.

Whether this experimental approach will give insight into pathogenesis, however, depends on the validity of an underlying hypothesis – specifically, that the normal behavior of wild-type AR is somehow related to the toxic behavior of polyglutamine-expanded AR. While the results of the SCA1 models argue that pathology is caused by an imbalance of native interactors of ataxin-1, this idea has remained largely untested in other polyglutamine disease models and is still far from widely accepted in the field. The

"toxic aggregate" hypothesis, for example, does not require that the toxic interactions of polyglutamine-expanded AR have any relationship to the native interactions of its wild-type counterpart; instead, this hypothesis only requires that the expanded polyglutamine adopt an aggregated conformation in a susceptible region of the cell (e.g. the nucleus). Any interactions this aggregate may initiate may be with native *or* non-native interactors that associate via the expanded polyglutamine tract.

A surprising phenomenon in SCA1 and SBMA models has yielded unexpected insight into this issue, lending support to the importance of native interactions in toxicity: in several fly and mouse models, degeneration can result from very high expression levels of wild-type, non-expanded protein. Animals expressing high levels of wild-type ataxin-1 develop the same degenerative phenotype caused by polyglutamine-expanded ataxin-1 (Fernandez-Funez et al., 2000), while expression of wild-type AR at high levels in mouse muscle leads to an SBMA-like phenotype (Monks et al., 2007). These observations suggest the possibility that amplification of native AR function may contribute to the toxicity of polyglutamine-expanded AR. Pursuing this hypothesis, Chapter 2 of this thesis illustrates how native AR function is required for toxicity in a *Drosophila* model of SBMA.

Concluding remarks

Following the discovery of the first polyglutamine mutation in 1991, it took only three years for a bona fide family of diseases to be identified. Given that these disorders were

all caused by the same mutation, it was only logical to predict that they would share a common pathogenic mechanism, and the undeniable toxicity of expanded polyglutamine peptides supported this idea. However, many years of research have led us down a much more complex path. Having started with the search for a unifying model, it is now becoming clear that the diseases' differences may be more important than their similarities. Using the precedent of SCA1 and the present findings on SBMA, we hope that these experimental perspectives will meet: perhaps our insights into aspects of pathogenesis that are *unique* to each disease will help uncover a *common* pattern of dysfunction that applies to all members of this disease family. We propose that this common pattern of dysfunction is centered on polyglutamine-induced modification of native protein function.

Table 1.1. The polyglutamine disease family

Disease	Protein	Normal Repeat	Expanded Repeat	Normal Function	Neural Expression	Tissues Affected in Disease	Clinical Features
Huntington's Disease	Huntingtin	6–34	36–121	Regulation of vesicular trafficking? Regulation of BDNF expression?	cerebellar cortex, neocortex, striatum, hippocamus	caudate and putamen, striatum	Chorea, dystonia, cognitive deficits, psychiatric problems
Kennedy's Disease (SBMA)	Androgen receptor	9–36	38–62	Transcription factor	cortex, amygdala, hippocampus, hypothalamus, midbrain, pons, medulla, cerebellum, spinal cord	anterior horn, bulbar region, dorsal root ganglion	Weakness, dysphagia, gynecomastia, decreased fertility
DRPLA	Atrophin-1	7–34	49–88	*Drosophila* ortholog is corepressor of transcription	cerebral cortex, cerebellum, pons, thalamus, basal ganglia	cerebral cortex, cerebellar cortex, globus pallidus, striatum; dentate nucleus, subthalamic nucleus, red nuclei	Ataxia, seizures, choreoathetosis, dementia
SCA1	Ataxin-1	6–44	39–82	Interacts with SMRT and Cic corepressors; RNA binding?	cerebellum, hippocampus, brainstem	brain stem, cerebellum (Purkinje cells, dentate nucleus, inferior olive)	Ataxia, slurred speech, spasticity, cognitive impairments
SCA2	Ataxin-2	15–24	32–200	Role in translational machinery?	cerebellum, brainstem nuclei	brain stem, cerebellum (Purkinje cells, granule cells)	Ataxia, polyneuropathy, decreased reflexes, infantile variant with retinopathy
SCA3	Ataxin-3	13–36	61–84	DUB, may interact with transcription deacetylase complexes	ubiquitous	basal ganglia, brain stem, spinal cord, dentate neurons of cerebellum	Ataxia, parkinsonism, spasticity
SCA6	CACNA1A	4–19	20–33	Voltage-dependent calcium channel	cerebral cortex, thalamus, hypothalamus, cerebellum	cerebellum (Purkinje), dentate nucleus, inferior olive	Ataxia, dysarthria, nystagmus, tremors
SCA7	Ataxin-7	4–35	37–306	Component of STAGA complex	widespread, most abundant in cerebellum	cerebellum, brain stem, visual cortex, macula	Ataxia, blindness, cardiac failure in infantile form
SCA17	TATA-binding protein	25–42	47–63	Component of TFIID complex	ubiquitous	caudate nucleus, putamen, thalamus, frontal cortex, temporal cortex, Purkinje cells	Ataxia, cognitive decline, seizures, and psychiatric problems

Table 1.1. The polyglutamine disease family. Nine diseases are currently known to be caused by trinucleotide (CAG) repeat expansions in exonic regions of DNA. The identity of each expanded disease protein is given, along with the normal and pathogenic polyglutamine repeat lengths and the known normal functions of these proteins (in many cases ill defined). Notably, many of the proteins are widely expressed in the nervous system, yet only particular tissues are affected in the disease. The major clinical symptoms of each disease are also listed.

Table 1.2

Type 1: Toxic gain of function mediated by protein
Huntington's disease
Kennedy's disease
Spinocerebellar ataxia types 1, 2, 3, 6, 7, and 17
Dentatorubro-pallidoluysian atrophy
Oculopharyngeal muscular dystrophy

Type 2: Toxic gain of function mediated by RNA
Spinocerebellar ataxia types 8, 10, and 12
Myotonic dystrophy types 1 and 2
Fragile X-associated tremor-ataxia syndrome

Type 3: Loss of function
Friedreich's ataxia
Fragile X syndromes
Progressive myoclonic epilepsy type 1

Table 1.2. Repeat expansion diseases. The repeat expansion diseases can be generally classified into three categories based on their pathogenic mechanism. Type 1 diseases include the polyglutamine diseases as well as oculopharyngeal muscular dystrophy, a polyalanine disease; all are caused by a toxic gain of function at the protein level. Type 2 diseases are caused by toxic gain of function mediated at the RNA level; in these diseases, repeats occur in the 5' or 3' untranslated regions (UTR) of genes and affect cellular function, including alternative splicing of various genes. Type 3 diseases caused by loss of function; these diseases are caused by mutations located in introns or 5' UTRs.

Chapter 2:

Native functions of the androgen receptor are essential to pathogenesis

in a *Drosophila* model of spinobulbar muscular atrophy

Native functions of the androgen receptor are essential to pathogenesis in a *Drosophila* model of spinobulbar muscular atrophy

Natalia B. Nedelsky[1,2], Maria Pennuto[3], Rebecca B. Smith[1], Isabella Palazzolo[4], Jennifer Moore[1], Zhiping Nie[5], Geoffrey Neale[6], J. Paul Taylor[1]

[1] Department of Developmental Neurobiology, St. Jude Children's Research Hospital, Memphis, TN 38105, USA

[2] Neuroscience Graduate Group, University of Pennsylvania School of Medicine, Philadelphia, PA 19104, USA

[3] Department of Neuroscience, Italian Institute of Technology, Genova 16163, Italy

[4] Neurogenetics Branch, National Institute of Neurological Disorders and Stroke, National Institutes of Health, Bethesda, MD 20892, USA

[5] Department of Neurology, University of Pennsylvania School of Medicine, Philadelphia, PA 19104, USA

[6] Hartwell Center for Bioinformatics and Biotechnology, St. Jude Children's Research Hospital, Memphis, TN 38105, USA

Current address of IP: Department of Neurology, Massachusetts General Hospital, Charlestown, Massachusetts 02129, USA

Correspondence should be addressed to JPT (jpaul.taylor@stjude.org)
J. Paul Taylor, MD, PhD
Developmental Neurobiology
MS 343, D-4026
St. Jude Children's Research Hospital
262 Danny Thomas Place
Memphis, TN 38105-3678
Email: jpaul.taylor@stjude.org
Phone: (901) 595-6047
FAX: (901) 595-5947

Summary

Spinobulbar muscular atrophy (SBMA) is a neurodegenerative disease caused by expansion of a polyglutamine tract in the androgen receptor (AR). This mutation confers toxic function to AR through unknown mechanisms. Mutant AR toxicity requires binding of its hormone ligand, suggesting that pathogenesis involves ligand-induced changes in AR. However, whether toxicity is mediated by native AR function or a novel AR function is unknown. We systematically investigated events downstream of ligand-dependent AR activation in a Drosophila model of SBMA. We show that nuclear translocation of AR is necessary but not sufficient for toxicity and that DNA binding by AR is necessary for toxicity. Mutagenesis studies demonstrated that a functional AF-2 domain is essential for toxicity, a finding corroborated by a genetic screen that identified AF-2 interactors as dominant modifiers of degeneration. These findings indicate that SBMA pathogenesis is mediated by misappropriation of native protein function, a mechanism that may apply broadly to polyglutamine diseases.

Running Title

Native functions of AR mediate SBMA pathogenesis

Introduction

Spinobulbar muscular atrophy (SBMA, also known as Kennedy's disease) is a progressive late-onset degenerative disorder of the motor neurons in the brainstem and spinal cord that affects only men (Kennedy et al., 1968). SBMA is a member of the polyglutamine repeat disease family, which includes at least eight other disorders, including Huntington's disease (HD), dentatorubral-pallidoluysian atrophy (DRPLA), and six forms of spinocerebellar ataxia (SCA). All of these diseases are caused by gain-of-function mutations characterized by expanded trinucleotide (CAG) repeats in exonic regions of DNA, and all result in late-onset, progressive neurodegeneration (Zoghbi and Orr, 2000). In SBMA, the CAG repeat site is located in the androgen receptor (AR) gene and causes disease when the number of repeats is 40 or greater (La Spada et al., 1991). Patients often display signs of mild feminization, likely due to partial loss of AR function. Although loss of AR function may contribute to disease (Thomas et al., 2006), it is not sufficient for degeneration, as loss-of-function mutations to AR result in androgen insensitivity syndrome without signs of neuronal degeneration (Quigley et al., 1992).

A central mystery in the field of polyglutamine disease research arises from the observation that the same mutation in nine different proteins results in nine different diseases; yet in each disease, different subsets of neurons are affected. This pattern occurs despite widespread and overlapping expression of the disease proteins, suggesting that the inherent toxicity of the expanded polyglutamine is not the sole basis of toxicity. Indeed, in SBMA mouse models, expression of polyglutamine-expanded fragments of

26

AR results in widespread neuronal degeneration, a phenotype that is not dissimilar from that observed in transgenic animal models expressing fragments of other polyglutamine-expanded proteins (Abel et al., 2001). In contrast, models employing full-length polyglutamine-expanded AR protein more accurately reflect the human disease, displaying restricted symptoms, lower motor neuron specificity in degeneration, and gender specificity (Chevalier-Larsen et al., 2004; Sopher et al., 2004).

These findings highlight the importance of protein context in polyglutamine disease, and raise the question of the role of protein domains other than the polyglutamine tract in toxicity. It is not clear whether the mutation results in the formation of novel, toxic interactions, or whether the mutation alters the normal, native interactions of the polyglutamine-containing protein in such a way as to result in neurotoxicity. While these possibilities are not mutually exclusive, recent studies in SCA1, SCA7, and SCA17 have provided evidence in favor of a model in which the normal function of the disease protein is tied to the mechanism of pathogenesis (Emamian et al., 2003; Friedman et al., 2007; Helmlinger et al., 2006; Lim et al., 2008; McMahon et al., 2005; Palhan et al., 2005; Tsuda et al., 2005). More direct evidence that native interactions may mediate toxicity comes from animal models in which overexpression of non-expanded ataxin-1 or AR result in pathology resembling SCA1 and SBMA, respectively (Fernandez-Funez et al., 2000; Monks et al., 2007).

In the majority of polyglutamine diseases, neither the primary function nor the native interactors of the disease proteins are well known. SBMA is an exception in that the

27

disease protein has a well-characterized role as a ligand-dependent transcription factor. AR is a member of the nuclear hormone receptor (NHR) superfamily and resides in the cytoplasm when inactive. A number of events occur upon ligand binding, the final result of which is AR-mediated activation or repression of target genes. These ligand-induced events include several post-translational modifications, nuclear translocation, and DNA binding. These changes occur in concert with conformational changes that result in the exposure of two coregulator interaction surfaces, termed activation function-1 (AF-1) and activation function-2 (AF-2). Ligand binding to polyglutamine-expanded AR is a requisite step in disease pathogenesis. Indeed, there is now incontrovertible evidence from animal model studies as well as human studies that gender specificity in SBMA is due to higher levels of circulating androgens in males (Katsuno et al., 2002; Takeyama et al., 2002).

Although the basis of the toxic gain of function imparted by the polyglutamine expansion remains unknown, the ligand dependence of SBMA implies that ligand-induced alterations of AR play important roles in toxicity. In this study, we used a *Drosophila* model to test the hypothesis that SBMA is mediated by ligand-induced alterations in native AR interactions. First, we present evidence that nuclear translocation of AR is necessary but not sufficient for toxicity, demonstrating that ligand-induced modifications of AR (beyond nuclear translocation) are required for pathogenesis. Second, we showed that DNA binding of polyglutamine-expanded AR is required for toxicity, indicating that the native DNA-binding function of AR is critical to pathogenesis. Third, we used a genetic screen to identify modifiers of SBMA toxicity, which revealed a pattern of AF-2-

28

based coregulators that genetically interact with polyglutamine-expanded AR. Pursuing this finding, we show rescue of polyglutamine-expanded AR toxicity through two independent point mutations designed to disrupt the AF-2 coregulator interaction surface. To more precisely define the degenerative phenotype associated with polyglutamine-expanded AR toxicity we used expression profile analysis. This analysis confirmed that interruption of either the AF-2 or DNA binding domains robustly suppressed this molecular phenotype. In addition, analysis of the molecular phenotype of flies expressing wild-type AR revealed the same (albeit weaker) molecular phenotype as polyglutamine-expanded AR, indicating that amplification of normal AR function may underlie the toxicity of polyglutamine-expanded AR. Finally, we investigated the AR coregulator ortholog *limpet*, a gene identified in our genetic screen, as proof of principle that polyglutamine-expanded AR toxicity is mediated via native function of the AF-2 binding surface following DNA binding.

Results

Expression of polyglutamine-expanded AR in Drosophila results in toxicity

In order to investigate the contributions of AR interactions to polyglutamine-expanded AR toxicity, we used a *Drosophila* model of SBMA. Although human AR has no direct ortholog in flies, the NHR system is well conserved (King-Jones and Thummel, 2005). This conservation is reflected in the domain architecture of *Drosophila* nuclear receptors, including AF-1 and AF-2 coregulator interaction domains that bind to conserved motifs in nuclear receptor coregulators. It was previously demonstrated that human AR

expressed in *Drosophila* tissues translocates to the nucleus and activates transcription of an ARE-GFP reporter transgene in response to DHT (Takeyama et al., 2002). This cross-species transactivational capacity reflects the fact that human AR interacts with endogenous *Drosophila* coactivators and corepressors; indeed, genetic modulation of *Drosophila* homologs of mammalian AR coregulators can modify the transactivational capacity of AR *in vivo* (Takeyama et al., 2004).

When human AR of varying polyglutamine lengths is expressed using the GAL4-UAS system (Brand and Perrimon, 1993), flies develop polyglutamine length- and ligand-dependent degenerative phenotypes, thus recapitulating two fundamental features of SBMA (Pandey et al., 2007b; Takeyama et al., 2002). To assess toxicity in an externally visible neuronal tissue, we expressed AR in the eye using the *glass multimer reporter* driver (GMR-GAL4), which leads to transgene expression in photoreceptor neurons and accessory pigment cells in developing eye discs (Moses and Rubin, 1991). While flies expressing AR show no eye phenotype when reared on normal food, flies reared on food containing DHT exhibit a degenerative phenotype that is limited to the posterior margin of the eye (Figure 2.1A). The severity of the phenotype is also polyglutamine-length dependent, with AR52Q-expressing flies showing severe ommatidial pitting, disorganization, and fusion, as well as abnormal and supernumerary interommatidial bristles. In contrast, AR12Q-expressing flies show only mild ommatidial and bristle phenotypes when the transgene is expressed at equivalent levels (Figure 2.1A-C). Confocal imaging of eye discs confirmed that AR undergoes DHT-dependent nuclear translocation *in vivo*. This analysis also revealed diffuse nuclear accumulation of AR and

the formation of small nuclear and cytoplasmic puncta that were particularly prominent with polyglutamine-expanded AR (Figure 2.1D).

The polyglutamine length- and DHT-dependence of SBMA is recapitulated in several larval tissues. For example, using the larval salivary gland driver (fkh-GAL4) (Andrew et al., 2000), expression of polyglutamine-expanded AR results in a dramatic reduction of salivary gland cell size (Figure 2.1 E-F). Larvae expressing AR in motor neurons under the control of the D42-GAL4 driver (Yeh et al., 1995) also show polyglutamine length- and DHT-dependent defects in locomotor ability as measured by larval crawling assay, indicating a significant functional deficit (Figure 2.1G). In addition, the number of type 1B boutons at the larval neuromuscular junction (NMJ) is significantly decreased in a DHT-dependent manner when polyglutamine-expanded AR is expressed using the motor neuron driver OK371-GAL4 (Mahr and Aberle, 2006) (Figure 2.1H-I).

Importantly, we noticed that expression of wild-type polyglutamine-length AR at high levels results in a degenerative phenotype that is indistinguishable from that caused by polyglutamine-expanded AR (Figure 2.1J-K). This is reminiscent of the SBMA-like phenotype associated with high level expression of wild-type AR in mice (Monks et al., 2007). The dose-dependent toxicity of wild-type AR suggests the possibility that amplification of native AR function may contribute to the toxicity of polyglutamine-expanded AR.

Nuclear translocation of polyglutamine-expanded AR is necessary for toxicity

The observation that ligand binding to AR is required for pathogenesis suggests a model in which non-toxic AR is converted to a proteotoxin through ligand-induced events. The first major event to occur upon ligand binding is translocation of AR to the nucleus. In most polyglutamine diseases, the primary site of cellular toxicity is thought to be the nucleus (Klement et al., 1998; Montie et al., 2009; Peters et al., 1999; Saudou et al., 1998; Takeyama et al., 2002), although cytoplasmic toxicity may also contribute (Hodgson et al., 1999; Morfini et al., 2006; Szebenyi et al., 2003). In the case of SBMA, whether nuclear translocation of polyglutamine-expanded AR is both necessary and sufficient for toxicity has not been examined *in vivo*.

AR has three major domains (Figure 2.2A): 1) an N-terminal transactivation domain (NTD) that contains activation function-1 (AF-1) and serves as a coregulator interaction surface, 2) a DNA-binding domain (DBD) that binds regulatory elements in AR-regulated promoters, and 3) a C-terminal ligand-binding domain (LBD) that binds testosterone or dihydrotestosterone (DHT) and also harbors a second coregulator interaction surface (activation function-2, or AF-2). Bridging the DBD and LBD is a flexible hinge domain that harbors a bipartite nuclear localization sequence (NLS). To address the necessity of nuclear translocation, we generated two AR constructs designed to remain in the cytoplasm even in the presence of DHT (Figure 2.2A). In the first construct, we used phosphomimetic substitutions of serines 210 and 790 (AR65Q SS/DD) that prevent DHT binding to AR (Palazzolo et al., 2007). In the second construct, we mutated residues K632 and K633 (AR73Q KK/AA) in the NLS of AR; these substitutions markedly alter DHT-induced nuclear translocation (Thomas et al., 2004).

COS-1 cells transfected with these constructs showed that the SS/DD and KK/AA mutations each caused AR to remain in the cytoplasm even in the presence of DHT (Supplemental Figure 2.1A-B).

In order to investigate whether these cytoplasmic AR mutants cause toxicity *in vivo*, we generated transgenic *Drosophila* lines that express these proteins under the control of the GAL4-UAS system. We first confirmed that these modified AR proteins resist DHT-induced nuclear translocation *in vivo* in *Drosophila* by expressing the AR transgenes with the larval salivary gland driver fkh-GAL4. Salivary glands provide an ideal model to assess subcellular localization of proteins in *Drosophila* due to their highly ordered histoarchitecture and high ratio of cytoplasm to nucleus. Using fkh-GAL4, we found that while AR52Q showed nuclear localization, AR65Q SS/DD and AR73Q KK/AA remained in the cytoplasm despite the presence of DHT in the larval medium (Figure 2.2C).

In order to test the toxicity of these constructs in a neuronal tissue, we next expressed the AR transgenes using GMR-GAL4. As previously shown, expression of AR52Q in the eye resulted in a degenerative phenotype in a DHT-dependent manner (Figure 2.2B,D). In contrast, eyes expressing AR65Q SS/DD or AR73Q KK/AA showed no degenerative phenotype even in the presence of DHT despite high expression of AR (Figure 2.2B,D and Supplemental Figure 2.2A). Consistent with prior reports (Montie et al., 2009; Takeyama et al., 2002), these results indicate that nuclear translocation of polyglutamine-expanded AR is necessary for toxicity.

Nuclear translocation of polyglutamine-expanded AR is not sufficient for toxicity

In order to address whether nuclear translocation of polyglutamine-expanded AR is

sufficient for toxicity, we designed AR constructs that translocate to the nucleus in a

DHT-independent manner, thereby dissociating nuclear translocation from ligand

binding. To this end, we fused the SV40 NLS to either the C- or N-terminus of AR

(Figure 2.2A). As an additional control, we fused an NLS to the AR65Q SS/DD protein

that is unable to bind DHT. COS-1 cells transfected with AR65Q-NLS or NLS-AR65Q

SS/DD show AR localized to the nucleus even in the absence of DHT (Supplemental

Figure 2.1C-D). In addition, AR65Q-NLS retained its transactivation ability in response

to DHT as measured by an ARE-luciferase reporter, though only at about 50% of AR65Q

(Supplemental Figure 2.1E). As expected, NLS-AR65Q SS/DD did not activate

transcription, due to its inability to bind DHT.

We next made transgenic *Drosophila* carrying UAS-AR65Q-NLS and UAS-NLS-

AR65Q SS/DD. After confirming that AR65Q-NLS and NLS-AR65Q SS/DD translocate

to the nucleus in the absence of DHT *in vivo* using fkh-GAL4 (Figure 2.2E), we

expressed these transgenes in the eye using GMR-GAL4 (Figure 2.2F and Supplemental

Figure 2.2B). Expression of AR65Q-NLS or NLS-AR65Q SS/DD did not cause toxicity

in the absence of DHT, indicating that nuclear translocation of polyglutamine-expanded

AR is not sufficient for toxicity. However, once the AR65Q-NLS animals were exposed

to DHT, they developed the characteristic SBMA eye phenotype, demonstrating that

DHT binding to AR provides the critical step in the conversion of polyglutamine-expanded AR from a non-toxic to a toxic molecule (Figure 2.2B, F).

An intact DNA-binding domain is required for polyglutamine-expanded AR toxicity

Having determined that the role of DHT in SBMA is not simply to effect translocation of AR to the nuclear compartment, but also to modify nuclear AR, we hypothesized AR's function as a DNA-binding transcription factor might play a role in pathogenesis. To investigate this hypothesis, we introduced a mutation to the AR DBD (A574D) that blocks the ability of AR to bind DNA without disrupting its ligand-binding ability (Bruggenwirth et al., 1998).

AR65Q A574D showed normal DHT-induced nuclear translocation *in vitro* (Supplemental Figure 2.3), although transactivation capacity was severely disrupted, as predicted due to the inability of the mutated AR to bind DNA (Figure 2.3A). Strikingly, transgenic flies expressing AR52Q A574D using GMR-GAL4 showed no degenerative phenotype even in the presence of DHT, indicating that the A574D mutation abolished the toxicity of polyglutamine-expanded AR despite nuclear localization of AR and high transgene expression (Figure 2.3B-D and Supplemental Figure 2.2C-D). Supporting this result, flies expressing polyglutamine-expanded AR with the A574D mutation showed no larval crawling defect when AR was expressed in motor neurons (Figure 2.3E). Additionally, introduction of the A574D mutation resulted in salivary gland cell size that was indistinguishable from AR52Q without DHT (Figure 2.3F-G). These results indicate that the native DNA-binding function of AR is critical for pathogenesis.

AF-2-interacting coregulators modify the toxicity of polyglutamine-expanded AR

In the normal life cycle of AR, DNA binding is followed by the recruitment of coregulators (either corepressors or coactivators) that associate with AR at target promoters (Heinlein and Chang, 2002). We hypothesized that coregulator binding, an event immediately downstream of DNA binding, might play a role in pathogenesis.

In order to investigate the role of AR coregulators in SBMA, we performed a candidate-based genetic screen for modifiers of polyglutamine-expanded AR toxicity. We began with 73 human coregulators that are known to interact with AR. We identified 61 putative *Drosophila* orthologs of these coregulators, including 23 coactivators, 34 corepressors, and 4 coregulators with dual function. RNAi-mediated knockdown of 19/61 (31%) of these *Drosophila* coregulators dominantly modified the SBMA fly phenotype (Table 2.1, Supplemental Figure 2.4A-B). These modifiers included some coregulators with obvious mechanisms of enhancement, including Pat1 and Pten, which normally function to inhibit AR nuclear translocation. The mechanism for other modifiers was less clear, although there was an interesting pattern among the hits because seven of them relate to the function of the AF-2 domain of AR. Specifically, CycD, gskt, jbug, Lmpt, Rad9, Smr, and wts (putative *Drosophila* orthologs of CCND1, GSK3B, FLNA, FHL2, RAD9, NCOR1/2, and LATS2, respectively) each plays a role in AF-2 interactions, either by binding AF-2 directly or by modifying the AF-2-based interaction with the NTD (Table 2.1). To confirm the specificity of these hits and to rule out off-target effects due to RNAi, we confirmed the effects of these AF-2-related hits in three additional

contexts. First, we confirmed that classical alleles and aneuploid aberrations of these same genes would similarly enhance the AR52Q eye phenotype (Supplemental Figure 2.4C). Second, after verifying that RNAi knockdown had no effect on larval crawling ability when expressed in motor neurons in the absence of AR52Q, we showed that these RNAi lines enhanced the AR52Q larval crawling defect in 6/7 cases (Table 2.1, Supplemental Figure 2.4 D-E). Third, we showed that the RNAi lines did not enhance the AR52Q eye phenotype nonspecifically, by crossing RNAi-expressing lines to an unrelated disease model of inclusion body myopathy associated with Paget's disease of bone and frontotemporal dementia (IBMPFD) that shows a modifiable degenerative eye phenotype (Ritson et al., 2010) (data not shown).

A functional AF-2 binding site is required for toxicity

AF-2 is a ligand-dependent hydrophobic surface flanked by opposing charged residues, K720 and E897 (Figure 2.4A). This surface is highly conserved across steroid hormone receptors and across species, and in most cases serves as a binding pocket for the LxxLL motifs of steroid receptor coactivator (SRC) family members (He et al., 1999). Unlike other steroid hormone receptors, however, the AF-2 of AR binds an additional motif, defined as FxxLF, with higher affinity (Dubbink et al., 2004; He et al., 2001; He et al., 2004). The FxxLF motif is found in a small number of coregulators, as well as in the N terminus of AR, which allows for an intra- or intermolecular interaction between the NTD and AF-2 domains of AR. Current models propose that AF-2 binds the NTD FxxLF motif while AR is mobile, and that the NTD/AF-2 interaction is lost upon AR binding to DNA, rendering AF-2 optimally accessible to coregulators (van Royen et al., 2007).

37

Since our targeted RNAi screen highlighted the importance of coregulator interactions with AF-2, we next investigated the role of AF-2 function in polyglutamine-expanded AR toxicity by taking advantage of three well-characterized mutations that disrupt AF-2-based interactions without influencing protein stability. The first, E897K, reverses the charge of one of the two charge clamp residues in AF-2, thereby abolishing both LxxLL- and FxxLF-mediated interactions (He et al., 1999) (Figure 2.4A). The second, K720A, which neutralizes the charge of the other charge clamp residue in AF-2, partially impairs AF-2 function by severely disrupting LxxLL-mediated interactions and decreasing FxxLF-based interactions by approximately 50% (Dubbink et al., 2004; He et al., 1999). The third, G21E, located two amino acids from the FxxLF sequence in the NTD, blocks the NTD/AF-2 interaction without affecting AF-2 structure (Callewaert et al., 2003). Neither E897K nor K720A alters the equilibrium binding affinity for ligand (He et al., 1999).

In COS-1 cells, AR E897K, K720A, and G21E showed DHT-induced nuclear translocation similar to wt AR (Supplemental Figure 2.5A-B). Luciferase-based transactivation assays indicated that while K720A and G21E mutants showed unaltered transactivation capacity, the activity of AR E897K was modestly decreased (Figure 2.4C). When expressed *in vivo* using fkh-GAL4, we found that all three mutant proteins translocated to the nucleus in response to DHT (Figure 2.4B). Importantly, the AF-2 mutations E897K and K720A strongly suppressed the phenotype caused by expression of polyglutamine-expanded AR in salivary glands cells (Figure 2.4B and Supplemental

Figure 2.5C-D). In contrast, the G21E mutation had no impact on salivary gland phenotype (Figure 2.4B).

We next tested the toxicity of these mutant proteins using GMR-GAL4. We found that introduction of the E897K mutation abolished the degenerative eye phenotype, indicating that complete disruption of AF-2 binding eliminates the toxicity of polyglutamine-expanded AR despite high levels of AR expression (Figure 2.4E, Supplemental Figure 2.2C-D, and Supplemental Figure 2.5E). The K720A mutation also suppressed degeneration, confirming that LxxLL- and FxxLF-based binding to AF-2 are critical mediators of toxicity. In contrast, the G21E mutation had no discernable impact on the eye phenotype. This latter result argues that impaired coregulator interactions with AF-2, rather than impaired NTD binding to AF-2, underlie the suppressive effect of E897K and K720A mutations.

To corroborate the suppression seen by the K720A and E897K mutations, we next used the driver elav-GAL4, which drives transgene expression in all neurons. While expressing AR52Q with elav-GAL4 resulted in early larval lethality, introducing the AF-2 mutations E897K or K720A resulted in increased viability, as evidenced by more flies surviving to the pupal stage (Figure 2.4D and Supplemental Figure 2.5F). When expressed in motor neurons with D42-GAL4, the E897K and K720A mutations also significantly suppressed the larval crawling defect seen in AR52Q flies (Figure 2.4F). In addition, AF-2 mutations suppressed the NMJ bouton phenotype, resulting in a significantly increased number of synaptic boutons, while the G21E mutation had no

effect on this phenotype (Figure 2.4G-H). These results confirm the suppression observed in the eye while extending the findings to the cell type most affected in the human disease.

Expression profile analysis of AR mutants reveals the molecular phenotype of eye degeneration

While the rescue of eye degeneration we observe with mutations to the DNA-binding domain or AF-2 domain are robust, and we have corroborated the findings in other tissues, we felt it would be valuable to generate a molecular phenotype to serve as an objective, quantifiable assay of degeneration. Using GMR-GAL4 to drive transgene expression in the eye, we used Affymetrix arrays to profile gene expression changes in flies expressing wild-type AR, polyglutamine-expanded AR, or polyglutamine-expanded AR with mutations affecting the DBD or AF-2. 149 genes were identified whose expression significantly changed in concert with ligand-induced degeneration in AR52Q-expressing flies, representing a molecular signature of degeneration (Figure 2.5A, Supplemental Figure 2.6, and Supplemental Table 2.1). Hierarchical cluster analysis revealed strong correlation between this molecular read-out and visual inspection of eye morphology (Figure 2.5A-B). Principal components analysis showed that introduction of the E897K and A574D mutations reverted the molecular phenotype back to a pattern that is indistinguishable from AR12Q or AR52Q without ligand (Figure 2.5C). The K720A mutation partially reversed the molecular phenotype observed in the AR52Q flies +DHT, reflecting the milder suppression observed in these eyes when scored according to the severity of their external degenerative phenotype.

40

For the purpose of our study, we used expression profiles as a means of quantifying eye degeneration in our model. We caution against making too much of the identity of the individual genes whose expression is changed because the molecular phenotype that accompanies eye degeneration is likely dominated by secondary gene expression changes that are a consequence rather than a cause of degeneration. Nevertheless, we recognized the possibility that embedded within these expression profiles are some gene expression changes that are primary due to AR binding. To address this possibility, we performed promoter analysis which found no evidence of enrichment of genes containing AR binding sites among the DHT-responsive gene set (data not shown). Similarly, promoter analysis showed no enrichment for genes that are responsive to endogenous nuclear hormone receptors such as the ecdysone receptor (data not shown). These results suggest that although the molecular phenotype captured by our expression profiling can be used to quantify neurodegeneration in the adult eye, secondary gene changes are likely to obscure primary gene changes that occurred in the first steps of pathogenesis.

In addition to corroborating our visual inspection with respect to E897K, A574D, and K720A mutations and toxicity, the expression profile analysis also revealed that AR12Q +DHT caused nearly the same molecular signature as AR52Q +DHT, although the degree of expression level changes was generally weaker in AR12Q compared to AR52Q (Figure 2.5A and Supplemental Figure 2.6). This observation is consistent with a model in which amplification of normal AR function may underlie the toxicity of

polyglutamine-expanded AR. Indeed, as described above, expression of AR12Q in fly

eyes can also result in degeneration when expressed at very high levels.

Modification of the SBMA phenotype by the FxxLF-containing coregulator limpet is

dependent on AF-2

The strong suppression observed in the E897K mutants (which eliminates FxxLF-based

interactions), along with the milder suppression observed in the K720A mutants (which

merely decreases FxxLF-based interactions), implicated FxxLF-based coregulator

interactions as playing a significant role in toxicity. Based on our genetic screen (Table

2.1), we further examined the identity of our genetic modifiers in the context of FxxLF-

based AF-2 interactions. Although some of these modifiers are not known to interact with

AF-2 directly and not all contain FxxLF motifs, the AR coregulator four-and-a-half LIM

domains 2 (FHL2, the human ortholog of *Drosophila limpet*) interacts with AF-2 directly

via an FxxLF motif (Hsu et al., 2003). FHL2/limpet is well-conserved between fly and

human (56.4% similarity, 74.4% identity), including the FxxLF motif (Supplemental

Figure 2.7A), and is one of a family of LIM domain-containing proteins, several of which

are known to play a role in motor neuron development (Bhati et al., 2008). The exact

mechanism whereby FHL2 modifies AR transactivation is unknown, although LIM

domain-containing proteins have been found to act as bridging molecules between

transcription factors, suggesting that they may act as scaffolds in the assembly of

transcriptional complexes (Wadman et al., 1997). Thus, *limpet* provided a good candidate

for further investigation, given that it may act to positively or negatively regulate the

assembly of AF-2 complexes.

We therefore performed epistasis experiments to examine the ability of *limpet* to modify

the toxicity of polyglutamine-expanded AR. While RNAi knockdown of limpet in the

Drosophila eye using GMR-GAL4 results in no externally visible phenotype in flies

without the mutant AR transgene, limpet knockdown in flies expressing AR52Q

enhanced the AR52Q degenerative eye phenotype (Figure 2.6A,C,M and Supplemental

Figure 2.7B-C). Similarly, a classical P-element allele (Lmpt[GE27535]) of *limpet* enhanced

the AR52Q phenotype (Figure 2.6B,C,M and Supplemental Figure 2.7B). A

chromosomal duplication that produces two copies of the *limpet* gene (Dp(3;3)st⁺g18)

(Tearle et al., 1989) suppressed the AR52Q phenotype, suggesting that depletion of

limpet by AR contributes to toxicity (Figure 2.6C,D,M and Supplemental Figure 2.7B).

This suppression was confirmed through expression profile analysis in which we

determined that 46% of the gene expression changes that accompanied ligand-dependent

degeneration in AR52Q flies were completely reversed by limpet duplication (Figure

2.6N).

Interestingly, although genetic manipulation of *limpet* did not modify the mild phenotype

of flies expressing AR12Q at moderate levels (data not shown), *limpet* alleles did modify

the more severe phenotype of flies expressing AR12Q at very high levels (Figure 2.6E-

H,M), suggesting that the molecular pathophysiology of high-expressing AR12Q flies is

related to that of AR52Q flies. Importantly, limpet knockdown did not modify the

phenotype of AR66Q E897K, indicating that the enhancement by limpet RNAi requires a

functional AF-2 binding surface (Figure 2.6I-J). In addition, limpet duplication did not

suppress the degenerative phenotype caused by pure polyglutamine protein (127Q) (Kazemi-Esfarjani and Benzer, 2000), demonstrating that increased levels of limpet are not globally protective, but instead show a specific genetic interaction with AR (Figure 2.6K-L). These results are consistent with a model in which polyglutamine-expanded AR causes toxicity through AF-2-based interactions with coregulators.

Discussion

In this study, we investigated the basis for the toxicity of polyglutamine-expanded AR by systematically interrogating ligand-dependent modifications of this nuclear hormone receptor. We showed that nuclear translocation of polyglutamine-expanded AR is necessary but not sufficient for toxicity and that DNA binding is required for toxicity. Insight from a genetic screen indicated that native interactions, those mediated by the AF-2 domain in particular, play a key role in toxicity. This suspicion was confirmed by our results indicating that toxicity is dependent upon a functional AF-2 binding surface. Specifically, we demonstrated that K720A and E897K mutations to the AF-2 coregulator interaction surface attenuated polyglutamine-expanded AR toxicity, while interruption of the NTD/AF-2 interaction had no effect. In the majority of assays, the E897K mutation resulted in a stronger suppression than K720A (Figure 2.4D-E, G-H), an observation that is consistent with the stronger AF-2 disruption due the reversal of charge (E/K) compared to the neutralization of charge (K/A). These results indicate that AF-2 function is essential for polyglutamine-expanded AR toxicity. Importantly, the morphological (Figure 2.1J) and molecular (Figure 2.5) phenotypes of AR12Q recapitulate those of AR52Q, only less strongly, suggesting that polyglutamine-expanded AR toxicity may be mediated by amplification of wild-type AR function. We conclude that SBMA pathogenesis is mediated by amplification of native AR interactions, and that functions of the AF-2 domain are essential to toxicity.

Although we have demonstrated that polyglutamine-expanded AR toxicity requires DNA binding followed by association with AF-2 coregulators, we do not yet know how this results in toxicity. We favor a model in which the AF-2 domain of AR competes with other transcription factors for a finite supply of coregulators. According to this model, amplification of AR activity could result in reduced availability of coregulators for important functions. This model is consistent with our observation that RNAi-mediated knockdown of AF-2 interactors consistently enhances toxicity. A key outstanding question not answered in this study is how AR activity in the nucleus is amplified. One possibility is that aggregation-prone polyglutamine-expanded AR adopts a toxic conformation that amplifies AF-2-based interactions. However, the fact that we did not detect polyglutamine length-dependent changes in co-immunoprecipitation of AR and FHL2 argues against this possibility (Supplemental Figure 2.8). An alternative possibility is that polyglutamine expansion amplifies AR activity (and AF-2 function in particular) independent of any change in the intrinsic ability of AR to interact with coregulators. For example, by reducing the inactivation rate of DNA-bound AR or by reducing the rate of AR nuclear efflux similar to what has been observed for ataxin-7 (Taylor et al., 2006). The mechanism by which polyglutamine expansion amplifies AR nuclear activity will be an important focus for future studies. In previous analysis we observed the presence of high molecular weight species of presumed aggregated polyglutamine-expanded AR in our *Drosophila* model of SBMA (Pandey et al., 2007b). These species are also present in the mutant forms of AR included in the current study. Quantitative analysis shows no correlation between the amount of high molecular weight species and neurodegeneration in this *Drosophila* model (Supplemental Figure 2.2 E-F). While this observation is

46

intriguing, thorough assessment of the relative contributions of aggregation and altered native function will require follow up studies in mammals.

While our results indicate that AF-2 function is essential to toxicity (Figure 2.7), it is likely that multiple native interactions influence the toxicity of polyglutamine-expanded AR, and this is substantiated by the results of our genetic screen. For example, AF-1-interacting coregulators Hey and Rbf were found to modify toxicity, indicating that coregulator interactions at AF-1 likely participate in pathogenesis. One of these proteins, Rbf, (the *Drosophila* ortholog of Rb, or Retinoblastoma protein) was also recently shown to modulate the toxicity of polyglutamine-expanded AR in another *Drosophila* model of SBMA. In this study, Rb was shown to have increased association with polyglutamine-expanded AR, leading to reduced Rb activity and subsequent loss of regulation of Rb-associated genes (Suzuki et al., 2009). Such a model may also apply to AF-2-based interactions.

These observations may easily be aligned with recent reports relating to three other polyglutamine diseases in which the data point away from the intrinsic toxicity of expanded polyglutamine and toward the toxic consequences of amplified native interactions. A series of publications from the Orr and Zoghbi labs has illuminated the role of native interactions of ataxin-1 in the pathogenesis of SCA1 (Emamian et al., 2003; Lim et al., 2008; Tsuda et al., 2005). Specifically, polyglutamine expansion favors interaction with the RNA-binding protein RBM17, contributing to SCA1 neuropathology through a gain-of-function mechanism. Concomitantly, polyglutamine expansion

47

attenuates interaction with Capicua, contributing to SCA1 through a partial loss-of-function mechanism (Lim et al., 2008). Analogous mechanisms have been implicated in the pathogenesis of SCA7 and SCA17, although less is known about the identity of the native interactions that are key to pathogenesis (Friedman et al., 2007; Helmlinger et al., 2006; McMahon et al., 2005; Palhan et al., 2005).

While the AF-2 result is interesting insofar as it highlights a model in which polyglutamine expansion drives toxicity through native function, the greatest significance is that these results reveal an opportunity for therapeutic intervention. An entire therapeutic enterprise has developed around targeting of AF-2/coregulator interactions with small molecules in efforts to combat prostate cancer, hyperandrogenic syndromes and male-pattern baldness among others (Chang and McDonnell, 2005; Schapira, 2002). Indeed, the drug ASC-J9 was found to ameliorate neurodegeneration in a mouse model of SBMA and this was attributed to increased degradation of polyglutamine-expanded AR (Yang et al., 2007). However, in light of our findings it is worth noting that ASC-J9 disrupts the interaction between AF-2 and FxxLF-containing coregulators, suggesting that the beneficial effect of ASC-J9 may represent targeted interruption of AF-2-based interactions that are essential mediators of toxicity (Ohtsu et al., 2002). Although further studies are required to replicate these results in a mammalian model, our current findings allow for the possibility that SBMA patients will not have to rely on drugs that result in global androgen deprivation, but instead hope for therapeutic agents that will act in motor neurons to specifically target toxic AR interactions.

Experimental Procedures

Antibodies

Primary antibodies used: AR (N20, Santa Cruz Biotechnology), actin (I-19-R, Santa Cruz Biotechnology), α-tubulin (T5168, Sigma), FLAG (M2 F1804, Sigma), Anti-HRP-Cy3 conjugate (Jackson Immunoresearch), Discs-Large (DSHB 4F3). Secondary antibodies used for biochemistry: IRDye 800CW Goat Anti-Mouse IgG, IRDye 680 Goat Anti-Mouse IgG, IRDye 680 Goat Anti-Rabbit IgG, IRDye 800CW Goat Anti-Rabbit IgG (Li-Cor Biosciences). For *in vivo* staining: Goat anti-mouse Alexa Fluor 488 (Invitrogen), Goat anti-rabbit Alexa Fluor 488 (Invitrogen), FITC anti-rabbit (Jackson ImmunoResearch). The mouse anti-Discs-Large hybridoma antibody developed by Corey Goodman was obtained from the Developmental Studies Hybridoma Bank developed under the auspices of the NICHD and maintained by the University of Iowa, Department of Biology, Iowa City, IA 52242.

Cloning

Mutagenesis (G21E, S210D, A574D, K720A, S790D, and E879K) was performed using Quikchange II XL Mutagenesis Kit (Stratagene). NLS sequences were added to AR using a PCR-based method.

Eye disc staining

UAS-AR flies were crossed to GMR-GAL4 flies on food with or without 1 mM DHT (Steraloids). Pupal eye discs were dissected and fixed with 4% PFA for 30 minutes at

room temperature. Discs were stained with primary antibody for 16 hours at 4°C and secondary antibody for 1 hour at room temperature. Phalloidin staining (Alexa Fluor568 Phalloidin, Invitrogen) was performed for 2 hours at room temperature. Discs were washed and embedded using Glycergel (Dako), mounted, and examined by laser scanning confocal microscopy.

Eye phenotypes

UAS-AR flies were crossed to GMR-GAL4 flies at 25°C or 29°C on food containing either 1 mM DHT (Steraloids) or 1% ethanol. Eye phenotypes of anesthetized female flies were evaluated with a Leica MZ APO or M205C stereomicroscope and photographed with a Leica DFC320 digital camera. Blinded scoring of the AR phenotype was performed as previously described (Pandey et al., 2007b).

Fly stocks

Mutant AR flies were generated by cloning human AR constructs into pUAST. DNA was injected into w^{1118} embryos by BestGene Inc (Chino Hills, CA). At least 4 independently generated transgenic lines were evaluated for all AR-expressing flies. Classical alleles and deficiency lines (Df(1)sd72b, Df(3R)tll-e, Df(2R)Exel6079, Df(3L)Cat, Df(1)N105, wts[3-17], Lmpt^{GE27535}, and Dp(3;3)st+g18) were obtained from Bloomington Stock Center (Bloomington, IN). RNAi transgenic lines were obtained from the Vienna *Drosophila* RNAi Center (Vienna, Austria).

Larval crawling

UAS-AR flies were crossed to D42-GAL4 flies at 25°C on food containing either 1 mM DHT (Steraloids) or 1% ethanol. Larval crawling was performed on a 1% agarose gel in a 245 mm^2 dish with gridlines spaced by 2.5 mm. Wandering third instar larvae were allowed to acclimate for 5 minutes, and the number of gridlines passed by the posterior end of the larvae in 30 seconds was counted. Each larva was tested 3 times.

Luciferase assays

Luciferase assays were performed in HEK293T cells as previously described (Palazzolo et al., 2007). Briefly, cells were transfected with indicated AR constructs together with both the luciferase pARE-E1b-Luc and the β-galactosidase pCMVβ reporter constructs. AR transactivation was measured in the presence and absence of DHT by luciferase assay and normalized to β-galactosidase activity.

Microarray gene expression profiling analysis

UAS-AR flies were crossed to GMR-GAL4 flies at 29°C on food containing either 1 mM DHT (Steraloids) or 1% ethanol. Heads of 15 female offspring were collected, frozen, and RNA was extracted using TRIzol (Invitrogen). Details of processing and analysis may be found in Supplemental Information.

Neuromuscular bouton counting

UAS-AR flies were crossed to OK371-GAL4 flies at 25°C on food containing either 1 mM DHT (Steraloids) or 1% ethanol. Third instar larvae were heat killed, dissected in PBS, and fixed with 4% PFA for 20 minutes. Primary antibody staining was performed at

4°C overnight and secondary antibody staining was performed at room temperature for 4 hours. After staining, pelts were mounted in Fluoromount-G (SouthernBiotech). Boutons at muscle 4 segments A2-A5 on the right and left side were quantified in the mounted muscle preparations.

RNAi screen

The list of 73 AR-interacting coregulators was generated through literature review. Orthology prediction for *Drosophila* orthologs of these coregulators was performed using the HUGO Gene Nomenclature Committee Comparison of Orthology Prediction tool along with PSI-BLAST. RNAi lines were obtained from the Vienna *Drosophila* RNAi Center. Flies expressing UAS-RNAi were crossed to flies expressing GMR-GAL4; UAS-AR52Q at 29°C on food containing either 1 mM DHT (Steraloids) or 1% ethanol. Eye phenotypes of anesthetized female flies were evaluated with a Leica MZ APO or M205C stereomicroscope and photographed with a Leica DFC320 digital camera.

Salivary gland staining

UAS-AR flies were crossed to fkh-GAL4 flies at 25°C on food containing either 1 mM DHT (Steraloids) or 1% ethanol. For antibody staining, wandering third instar larvae were collected and salivary glands were dissected into 4% PFA in PBS. Glands were stained with primary antibody for 16 hours at 4°C and secondary antibody for 2 hours at room temperature. For details of fixation and washing, see Supplemental Information. For phalloidin staining, wandering third instar larvae were collected and salivary glands were dissected and stained as previously described (Martin and Baehrecke, 2004) using

52

Texas Red-Phalloidin (Invitrogen). Slides were examined using a Leica DMIRE2 microscope and cell size was determined using phalloidin staining and Slidebook software (Intelligent Imaging Innovations).

Statistics

Statistical comparisons were performed by ANOVA and Tukey HSD Test or Student's t-test as appropriate.

Viability

UAS-AR flies were crossed to elav-GAL4 flies at 25°C on food containing either 1 mM DHT (Steraloids) or 1% ethanol. Crosses were set up using 1 female and 1 male. The number of pupae on the sides of the vial and the surface of the food were counted 16 days after parents were added.

Western blotting

UAS-AR flies were crossed to GMR-GAL4 flies at 29°C. Heads of 3 female offspring were collected, frozen, and lysed in RIPA buffer (150 mM NaCl, 6 mM Na_2HPO_4, 4 mM NaH_2PO_4, 2 mM EDTA, 1% NaDOC, 1% Triton X-100, 0.1% SDS) with protease inhibitors (Roche). The lysate was sonicated, boiled, and run on 7.5% Tris-HCl SDS-PAGE gels (Bio-Rad). Proteins were transferred to nitrocellulose membranes (GE Healthcare) and immunoblotted. Blots were developed using the Odyssey Imaging System (Li-Cor Biosciences).

Supplemental Experimental Procedures

Antibodies

Additional primary antibodies used: α-tubulin (T5168, Sigma), FLAG (M2 F1804, Sigma). Secondary antibody used for *in vitro* immunofluoresence: Alexa Fluor 488-Goat Anti-Rabbit IgG antibody (Molecular Probes).

Immunofluorescence

Immunofluorescence was performed in COS-1 cells as previously described (Palazzolo et al., 2007). Images were acquired digitally with a DeltaVision microscope and deconvolved with the softWoRx algorithm (Applied Precision). For quantification of nuclear translocation, the percentage of transfected cells with a greater concentration of AR in the nucleus than the cytoplasm was determined for each AR construct.

Real-time quantitative PCR

Total RNA was isolated from 5-10 animals of the appropriate genotype with TRIzol reagent (Invitrogen) and cDNA was generated using the iScript cDNA Syntheses kit (BioRad #170-8890) following the manufacturer's protocol. Concentrations for each primer probe set were individually optimized. Quantitative real-time PCR reactions were carried out in a total reaction volume of 25□l of iQ Supermix (BioRad #170-8860) using an BioRad iCycler iQ5 machine for 40 cycles. Quantitation of each transcript was determined using the □□CT method. The primer/probe set for *Drosophila* GAPDH2 (product number Dm01843776_S1) and for Limpet (product number Dm01836996_gH) were purchased from Applied Biosystems.

Nuclear extraction and co-immunoprecipitation

HEK293T cells were co-transfected with pcDNA3 FLAG-FHL2 and pEF AR12Q or pEF AR52Q using Fugene (Roche). 48 hours post-transfection, cells were treated with 100 nM DHT (Steraloids) for 1 hour. Cells were collected and allowed to swell for 10 minutes in Buffer A (10 mM HEPES-KOH pH 7.9, 1.5 mM $MgCl_2$, 10 mM KCl, 0.5 mM DTT) plus protease inhibitor cocktail (PIC, Roche). Cells were vortexed 10 seconds and centrifuged at max speed for 30 seconds; supernatant was discarded. The pellet was resuspended in Buffer C (20 mM HEPES-KOH pH 7.9, 25% glycerol, 420 mM NaCl, 1.5 mM $MgCl_2$, 0.2 mM EDTA, 0.5 mM DTT) plus PIC. Cells were extracted in Buffer C for 20 minutes on ice, then centrifuged at max speed for 2 minutes. The resulting supernatant (comprising nuclear extract) was diluted in bead incubation buffer to yield a final concentration of 10 mM Tris-HCl pH 8.0, 250 mM NaCl, 0.5% NP-40, 0.1ug/ul BSA plus PIC. Extracts were pre-cleared with Protein-G agarose beads for 1 hour, washed 3 times, then incubated with M2 agarose beads (F2426, Sigma) for 2.5 hours. Beads were washed 5 times with bead incubation buffer. After final wash, 25ul of 1x SDS sample buffer was added to beads and boiled for 5 minutes. Samples were loaded onto 8-16% Novex gels (Invitrogen) and transferred onto nitrocellulose membranes (GE Healthcare) using the iBlot transfer system (Invitrogen). All buffers were supplemented with 100 nM DHT or ethanol as appropriate. All steps performed at 4° except as indicated.

Microarray gene expression profiling analysis

RNA quality was confirmed by analysis on the Agilient 2100 Bioanalyzer. Total RNA (100 ng) was processed in the Hartwell Center microarray core according to the Affymetrix 3' IVT Express target labeling protocol (https://www.affymetrix.com/support/downloads/manuals/3_ivt_express_kit_manual.pdf). Biotin-labeled cRNA (10 ug) was hybridized overnight at 45°C to the *Drosophila* Genome 2.0 GeneChip array which interrogates more than 18,500 transcripts. After staining and washing, arrays were scanned and expression values summarized using the MAS5 algorithm as implemented in the GCOS v1.4 software (Affymetrix, Santa Clara, CA). Detection calls (Present, Absent and Marginal) were determined using the default parameters of the software. Signals were normalized for each array by scaling to a 2% trimmed mean of 500. Prior to statistical analysis the MAS5 signals were variance stabilized by the started logarithm transformation (Rocke & Durbin, 2003). Principal component analysis (PCA) and statistical analyses were performed using Partek Genomics Suite v6.4 (Partek Inc., St. Louis, MO). Analysis of differential expression was determined using a two-factor ANOVA model where genotype and treatment were the factors. Three or four independent replicates were analyzed for each condition. The false discovery rate was estimated as described (Benjamini and Hochberg, 1995) and was controlled at a level of 0.05 or as otherwise stated. An additional filter was applied to select transcripts with robust expression by including those with at least one Present call across the dataset. Hierarchical clustering was performed using Spotfire DecsionSite 9.1 (TIBCO, Palo Alto, CA). Probeset annotations were obtained from the Affymetrix website (http://www.affymetrix.com/analysis/index.affx).

Transcription factor binding motif analysis

The upstream sequences of the 52Q-responsive genes were analyzed for potential transcription factor binding sites using the following method. Sequences 5kb upstream from the transcription start site of all known *Drosophila* genes were downloaded using the UCSC Genome Browser (http://www.genome.ucsc.edu/; *Drosophila melanogaster* genome build BDGP R5/dms, Apr 2006). The sequences were searched for homology (minimum identity 80%) to the consensus human androgen receptor binding site (AGAACANNNTGTTCT) and the endogenous ecdysone receptor binding sequence ([A/C])GGTCANTGACCT using CLC Genomics Workbench v3.7.1 (CLC bio, Cambridge MA). The frequency of binding motifs identified in the 52Q-responsive gene set (136 total) was compared to the frequency identified in all genes (21,243 total). There was no difference in the proportion of 52Q-responsive genes predicted to have androgen receptor binding sites (125/136 vs. 19,831/21,243; Chi Square $p = 0.614$), or ecdysone receptor binding sites (22/136 vs. 4,010/21,243; Chi Square $p = 0.486$). Further, there was no signficant enrichment of the distribution of predicted binding sites within the 52Q-responsive genes as compared to all genes (Wilcoxon rank sum test: Androgen receptor $p = 0.385$, Ecdysone receptor $p = 0.491$). Statistical analyses were performed using R 2.11.0.

Cell culture and transfections

COS-1 (ATCC, CRL-1650) and HEK293T (ATCC, CRL-1573) cells were cultured as previously described (Palazzolo et al, 2007). All experiments were carried out in complete medium containing 10% charcoal dextran stripped-fetal bovine serum (CDS)

(HyClone), when not indicated otherwise. COS-1 cells were transiently transfected using the Cell Line Nucleofector kit V (Amaxa Biosystem) with 5 µg of DNA. HEK293T were transfected with 2 µg of DNA using Lipofectamine/Plus reagent (Invitrogen). Cells were treated for 48 hours with DHT (10 nM, Sigma).

Salivary gland staining details

For antibody staining, wandering third instar larvae were collected and salivary glands were dissected into 4% PFA in phosphate buffered saline (PBS). Glands were fixed in 4% PFA/heptane for 20 minutes at room temperature, rinsed 3x in methanol, rinsed 3x in PBS + 0.1% Tween-20 (PBST), rinsed 4x in PBST + 1% BSA (PBSBT), blocked in PBSBT for 2 hours at room temperature, and incubated with primary antibody for 16 hours at 4°C. Salivary glands were then washed for 2 hours in PBSBT, incubated with secondary antibody for 2 hours at room temperature, washed for 30 minutes in PBSBT at room temperature, and mounted using Prolong Gold Antifade Reagent with DAPI (Invitrogen).

Figures and Legends

Figure 2.1. Expression of polyglutamine-expanded AR in *Drosophila* results in toxicity.
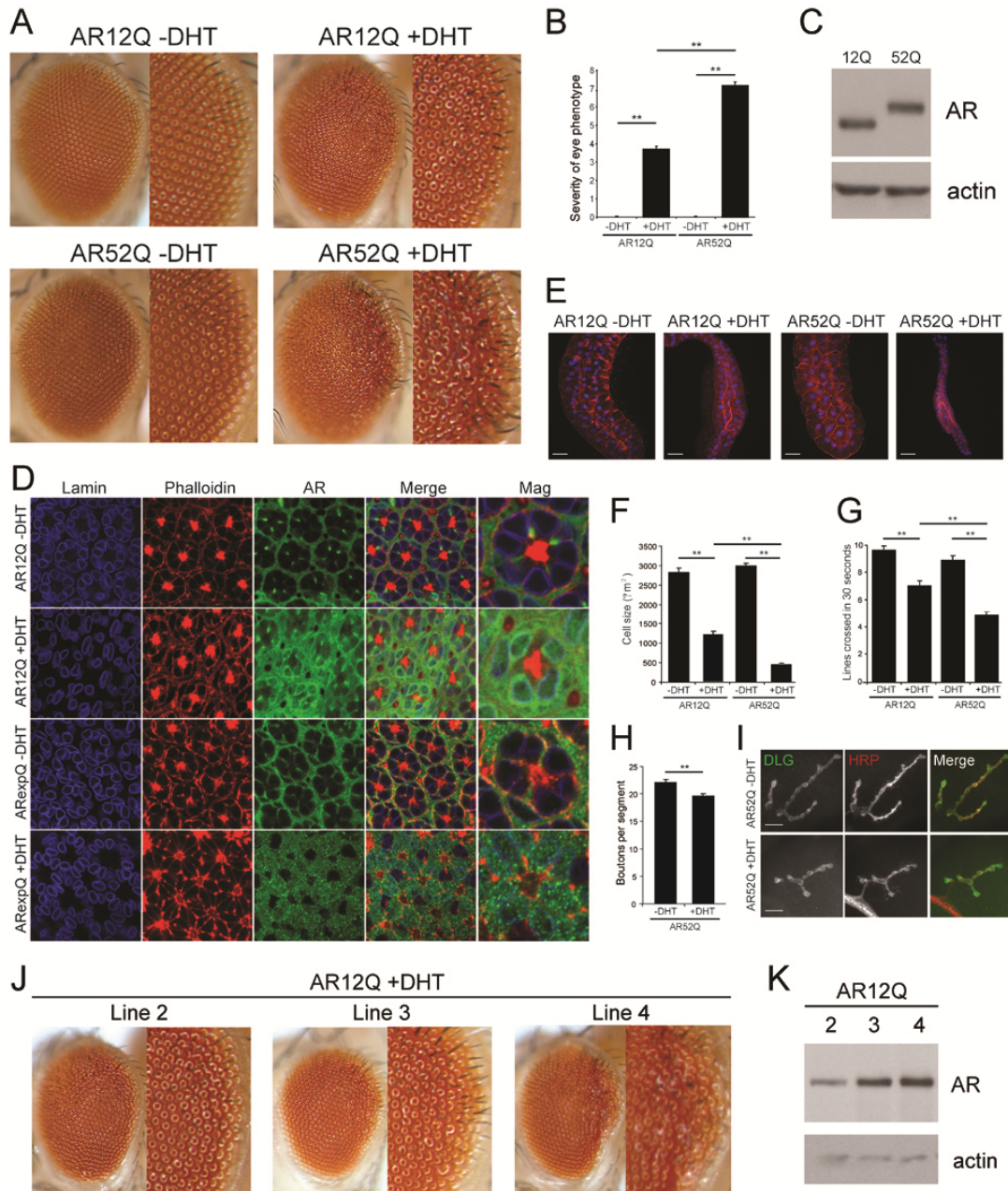
Figure 2.1 Expression of polyglutamine-expanded AR in *Drosophila* results in toxicity. (A) *Drosophila* females expressing AR in eyes using GMR-GAL4 were raised in medium containing vehicle or DHT and adult eye phenotypes were assessed by light microscopy. (B) Blinded scoring of the external eye phenotypes in (A) using a quantitative scoring system (Pandey et al., 2007b). (C) Western blot showing levels of AR expression for AR12Q- and AR52Q-expressing flies shown in (A). (D) Pupae expressing AR in eyes using GMR-GAL4 were raised in medium with or without DHT and whole mount preparations of eye discs were immunostained for lamin (blue) and AR (green). Phalloidin (red) was used to stain F-actin. Samples were examined by confocal microscopy. (E-F) Third instar larvae expressing AR using the salivary gland fkh-GAL4 were dissected and stained with DAPI (blue) and phalloidin (red). Overall gland size shown in (E), cell size shown in (F). Phalloidin staining was used to delineate cell boundaries and determine cell size. Scale bar, 50 μm. (G) Third instar larvae expressing AR12Q or AR52Q using D42-GAL4 were assessed for their ability to travel distances along the surface of an agar plate. (H-I) Larvae expressing AR52Q using OK371-GAL4 were raised in medium containing vehicle or DHT, dissected as third instar wandering larvae, and stained using the post-synaptic marker discs large (DLG, green) and the pre-synaptic marker HRP (red). Type 1B boutons were counted at muscle 4. Scale bar, 10 μm. (J) Female flies expressing AR12Q using GMR-GAL4 were raised on medium containing DHT. Each line shown represents an independent transformant line. (K) Western blot analysis of heads shown in (J). In (A) and (J), left side of each diptych shows light micrograph imaged at 63x, while right side shows increased magnification

(~140x) of the posterior region of the eye in which degeneration is concentrated. **

p<0.01 in all panels. Bars, mean + SEM in all panels.

Figure 2.2. Nuclear localization of polyglutamine-expanded AR is necessary but not sufficient for toxicity in vivo.
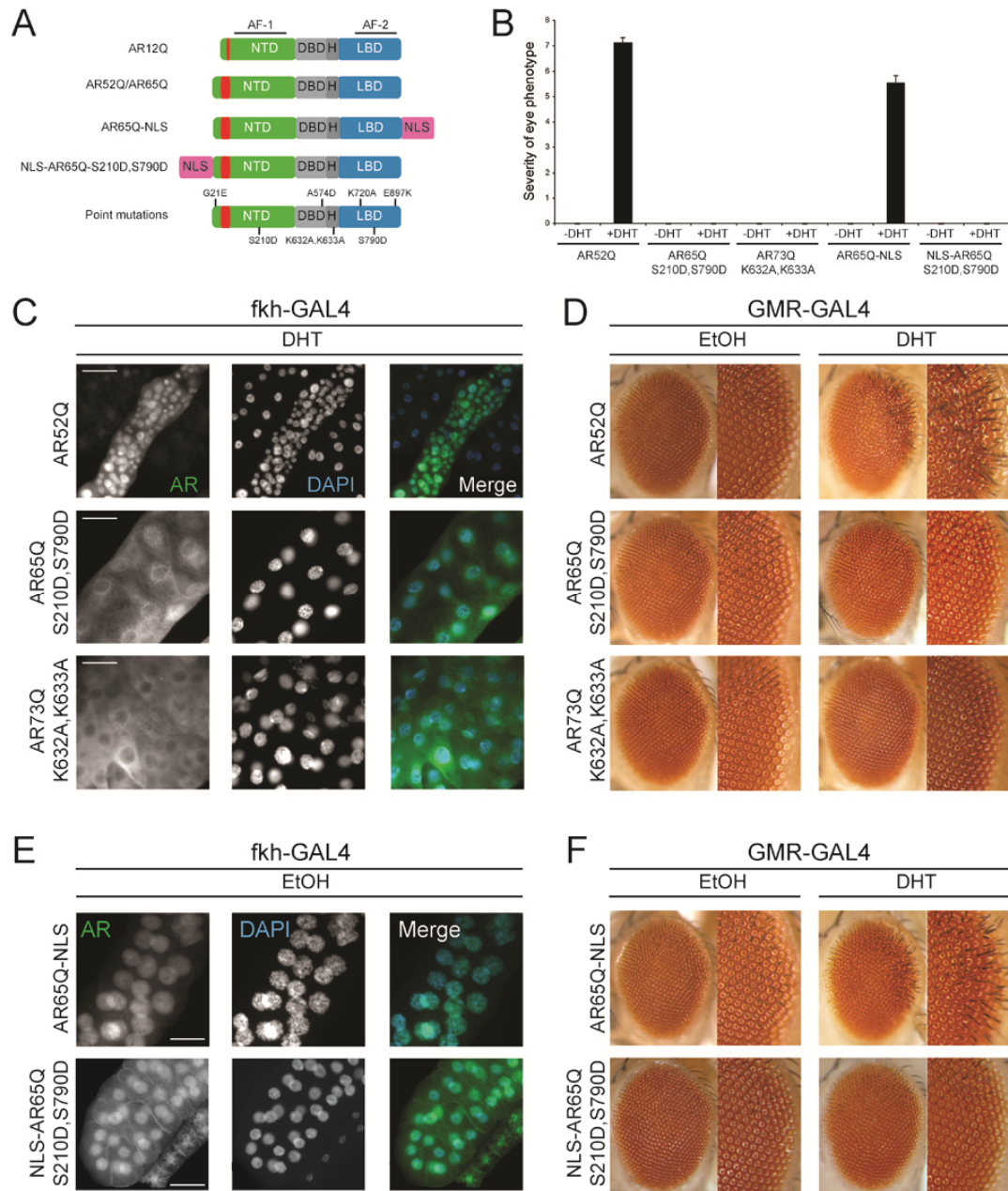
Figure 2.2. Nuclear localization of polyglutamine-expanded AR is necessary but not sufficient for toxicity in vivo. (A) Schematic of AR constructs used. NTD, N-terminal transactivation domain; DBD, DNA-binding domain; H, hinge; LBD, ligand-binding domain; NLS, nuclear localization sequence. (B) Blinded scoring of the external eye phenotypes in (D) and (F) using a quantitative scoring system. Bars, mean + SEM. (C) Salivary glands of *Drosophila* larvae expressing AR using fkh-GAL4. Larvae were raised in medium containing DHT and processed for immunocytochemistry. AR was detected with anti-AR antibody (green) and nuclei were stained with DAPI (blue). Scale bar, 50 µm. (D) *Drosophila* females expressing AR in eyes using GMR-GAL4 were raised in medium containing vehicle or DHT and adult eye phenotypes were assessed by light microscopy. (E) Salivary glands of *Drosophila* larvae expressing AR using fkh-GAL4. Larvae were raised in medium containing ethanol and processed for immunocytochemistry as in (C). Scale bar, 50 µm. (F) *Drosophila* females expressing AR in eyes using GMR-GAL4 were raised in medium containing vehicle or DHT and adult eye phenotypes were assessed by light microscopy. See also Supplemental Figure 2.1 and S2.

Figure 2.3. DNA binding by polyglutamine-expanded AR is required for toxicity.
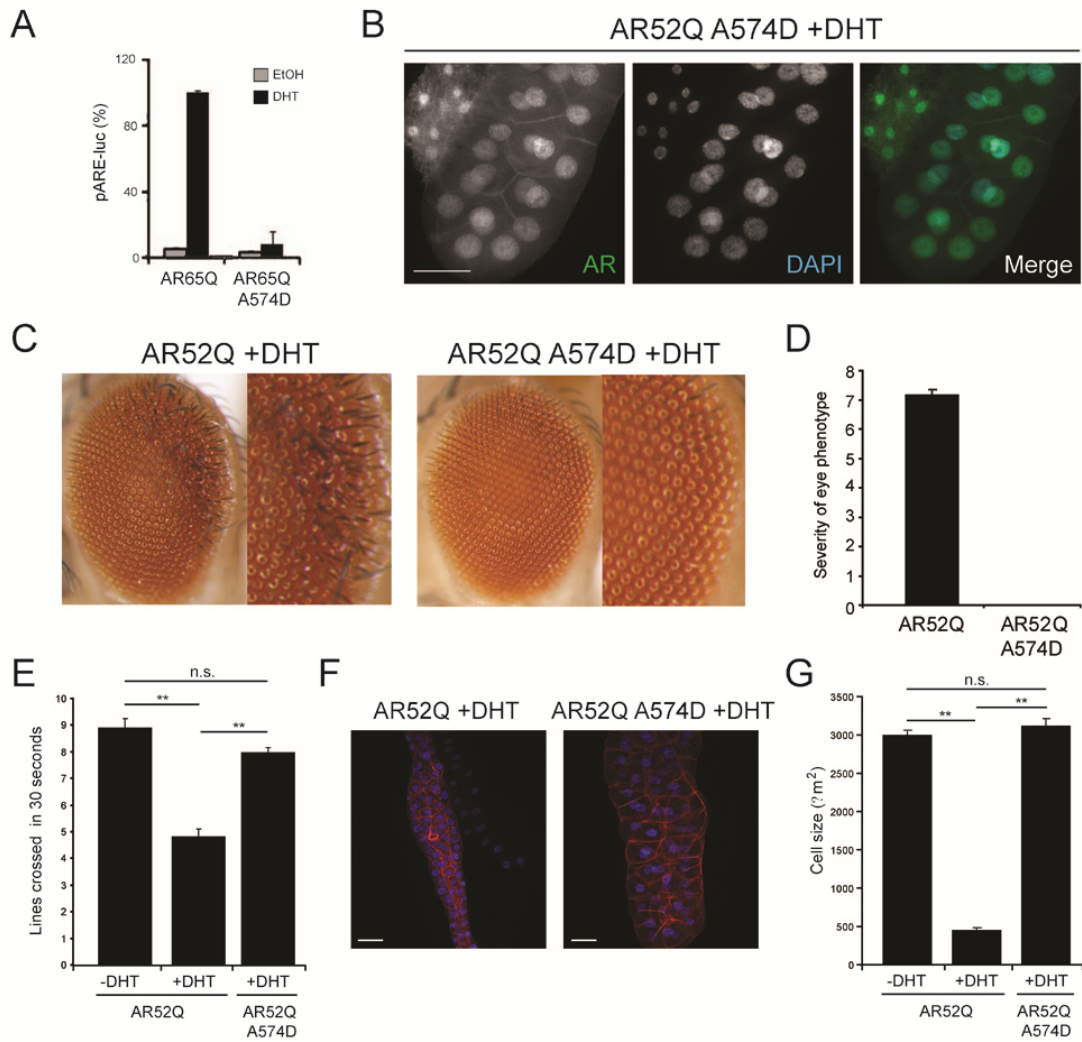
Figure 2.3. DNA binding by polyglutamine-expanded AR is required for toxicity.

(A) HEK293T cells were transfected with indicated AR constructs together with both the luciferase pARE-E1b-Luc and the ß-galactosidase pCMVß reporter constructs. AR transactivation was measured in the presence and absence of DHT by luciferase assay and normalized to ß-galactosidase activity. (B) Salivary glands of *Drosophila* larvae expressing AR using fkh-GAL4. Larvae were raised were raised in medium containing DHT and processed for immunocytochemistry. AR was detected with anti-AR antibody (green) and nuclei were stained with DAPI (blue). Scale bar, 50 μm. (C) *Drosophila* females expressing AR in eyes using GMR-GAL4 were raised in medium containing DHT and adult eye phenotypes were assessed by light microscopy. (D) Blinded scoring of the external eye phenotypes in (C) using a quantitative scoring system. (E) Third instar larvae expressing AR using the motor neuron driver D42-GAL4 were assessed for their ability to travel distances along the surface of an agar plate. (F-G) Third instar larvae expressing AR using the salivary gland fkh-GAL4 were dissected and stained with DAPI (blue) and phalloidin (red). Overall gland size shown in (F), cell size shown in (G). Phalloidin staining was used to delineate cell boundaries and determine cell size. Scale bar, 50 μm. ** $p < 0.01$ in all panels. n.s., not significant. Bars, mean + SEM in all panels. See also Supplemental Figure 2.2 and S3.

Figure 2.4. Disruption of AF-2 blocks polyglutamine-expanded AR toxicity.
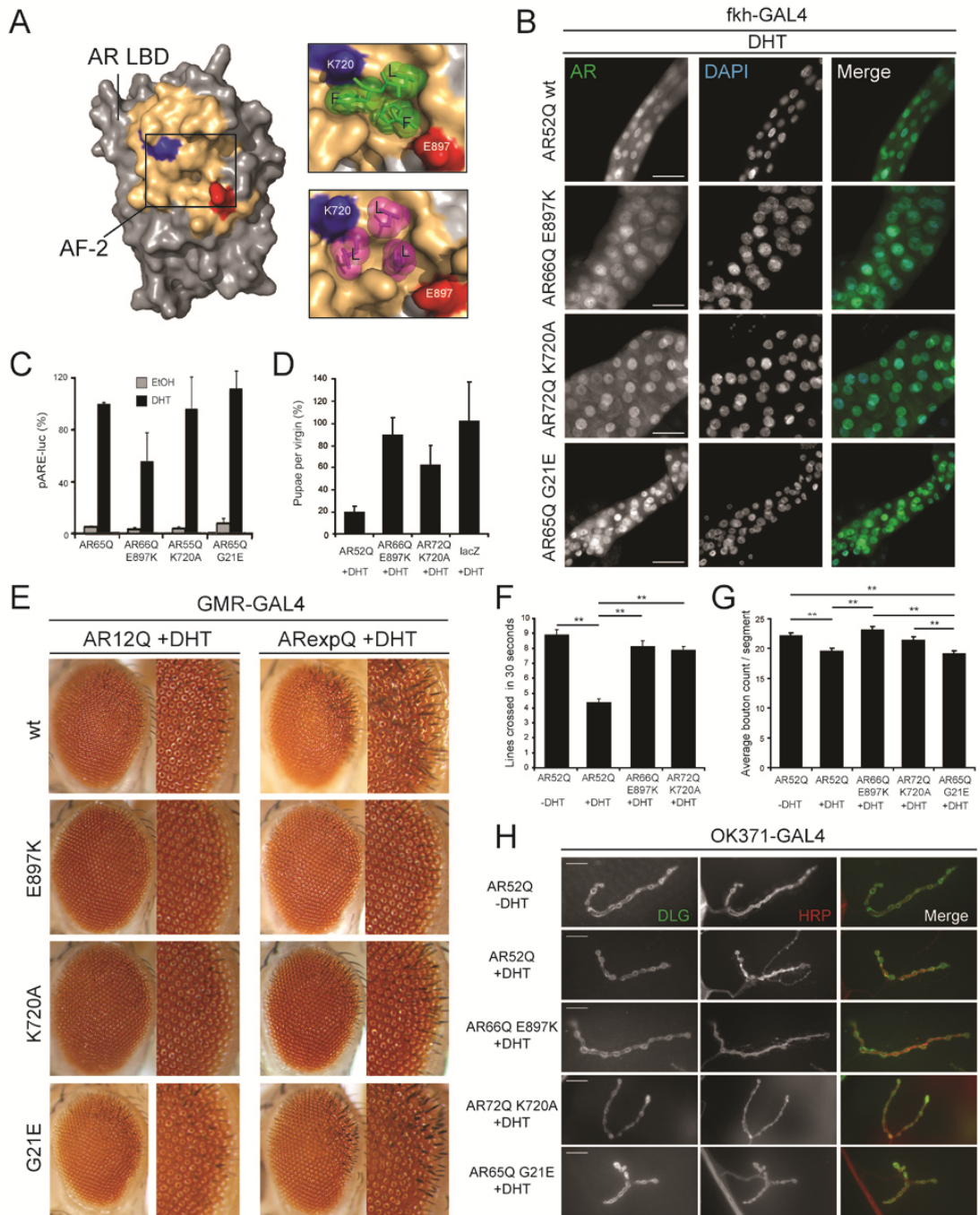
Figure 2.4. Disruption of AF-2 blocks polyglutamine-expanded AR toxicity.

(A) Crystal structure of the AR LBD (PDB ID: 2AMA) showing the AF-2 binding

surface (gold) and the two charge clamp residues in AF-2, K720 (blue) and E897 (red).

Green, FxxLF peptide co-crystallized with AF-2 (PDB ID: 1T7R). Pink, LxxLL peptide

co-crystallized with AF-2 (PDB ID: 1T7F). (B) Salivary glands of *Drosophila* larvae

expressing AR using fkh-GAL4. Larvae were raised in medium containing DHT and

processed for immunocytochemistry. AR was detected with anti-AR antibody (green) and

nuclei were stained with DAPI (blue). Scale bar, 50 μm. (C) HEK293T cells were

transfected with indicated AR constructs together with both the luciferase pARE-E1b-

Luc and the β-galactosidase pCMVβ reporter constructs. AR transactivation was

measured in the presence and absence of DHT by luciferase assay and normalized to β-

galactosidase activity. (D) Viability assay of *Drosophila* expressing indicated AR

transgenes using elav-GAL4. Crosses were performed in medium containing DHT. The

number of pupae from each 1x1 cross was counted and normalized to lacZ. Expression of

AR52Q resulted in larval lethality, while E897K or K720A mutations increased

survivability to the pupal stage. (E) *Drosophila* females expressing AR in eyes using

GMR-GAL4 were raised in medium containing DHT and adult eye phenotypes were

assessed by light microscopy. Left, AR constructs with 12Q. Right, AR constructs with

expandedQ (AR52Q wt, AR66Q E897K, AR72Q K720A, AR65Q G21E). See

Supplemental Figure 2.5E for phenotype severity scores. (F) Third instar larvae

expressing AR using the motor neuron driver D42-GAL4 were assessed for their ability

to travel distances along the surface of an agar plate. (G-H) Larvae expressing AR using

the motor neuron driver OK371-GAL4 were raised in medium containing vehicle or

DHT, dissected as third instar wandering larvae, and stained using the post-synaptic

marker discs large (DLG, green) and the pre-synaptic marker HRP (red). Type 1B

boutons were counted at muscle 4. Scale bar, 10 μm. ** p<0.01 in all panels. Bars, mean

+ SEM in all panels. See also Supplemental Figure 2.2 and S5.

Figure 2.5. Molecular phenotype of AR mutants.
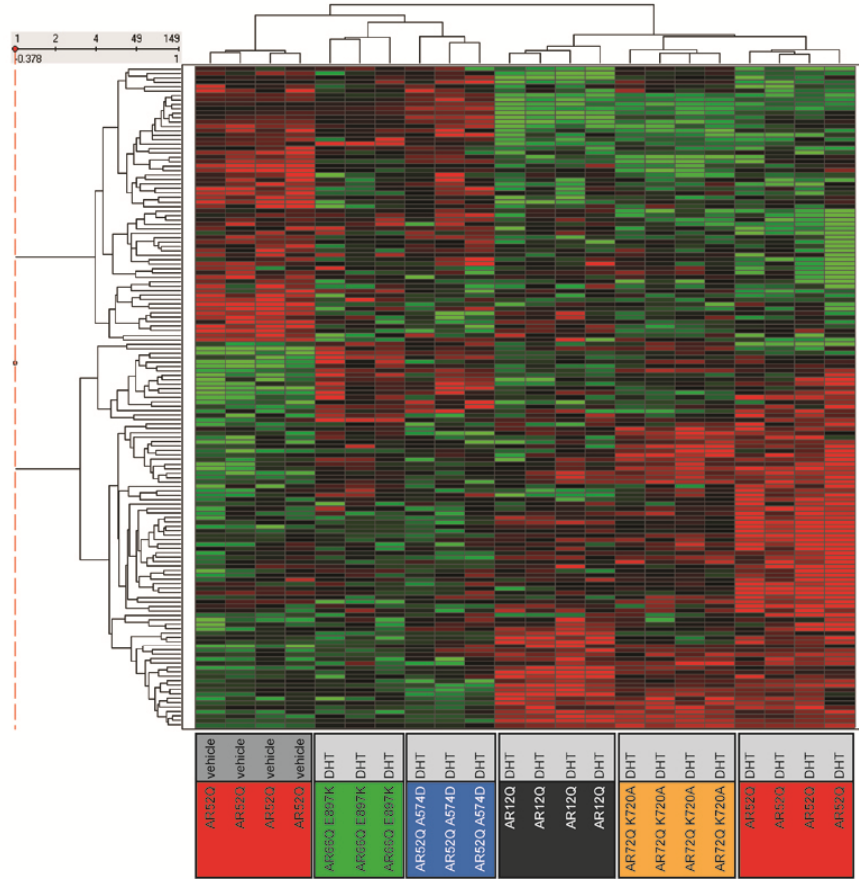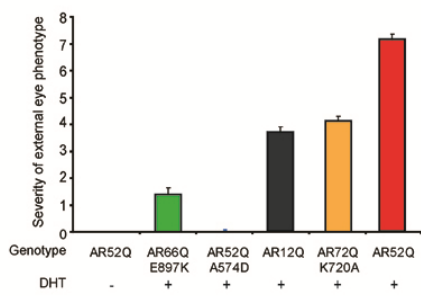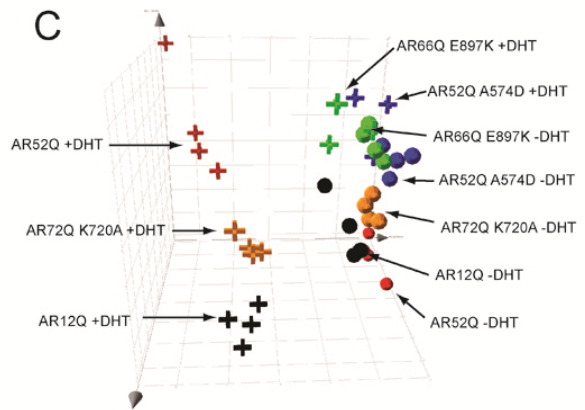
Figure 2.5. Molecular phenotype of AR mutants. (A) RNA from fly heads expressing AR using GMR-GAL4 was extracted and analyzed using Affymetrix arrays. Using a false discovery rate of 0.1, 149 genes were identified as showing significant changes in AR52Q flies due to DHT treatment and were thereby selected for further analysis. (B) Scoring of the external eye phenotype shows a correlation between the severity of the observable external phenotype and the clustering results. (C) PCA analysis using the 149 genes shown in (A). See also Supplemental Figure 2.6 and Supplemental Table 2.1.

Figure 2.6. Manipulation of limpet levels modifies polyglutamine-expanded AR toxicity in an AF-2-dependent manner.
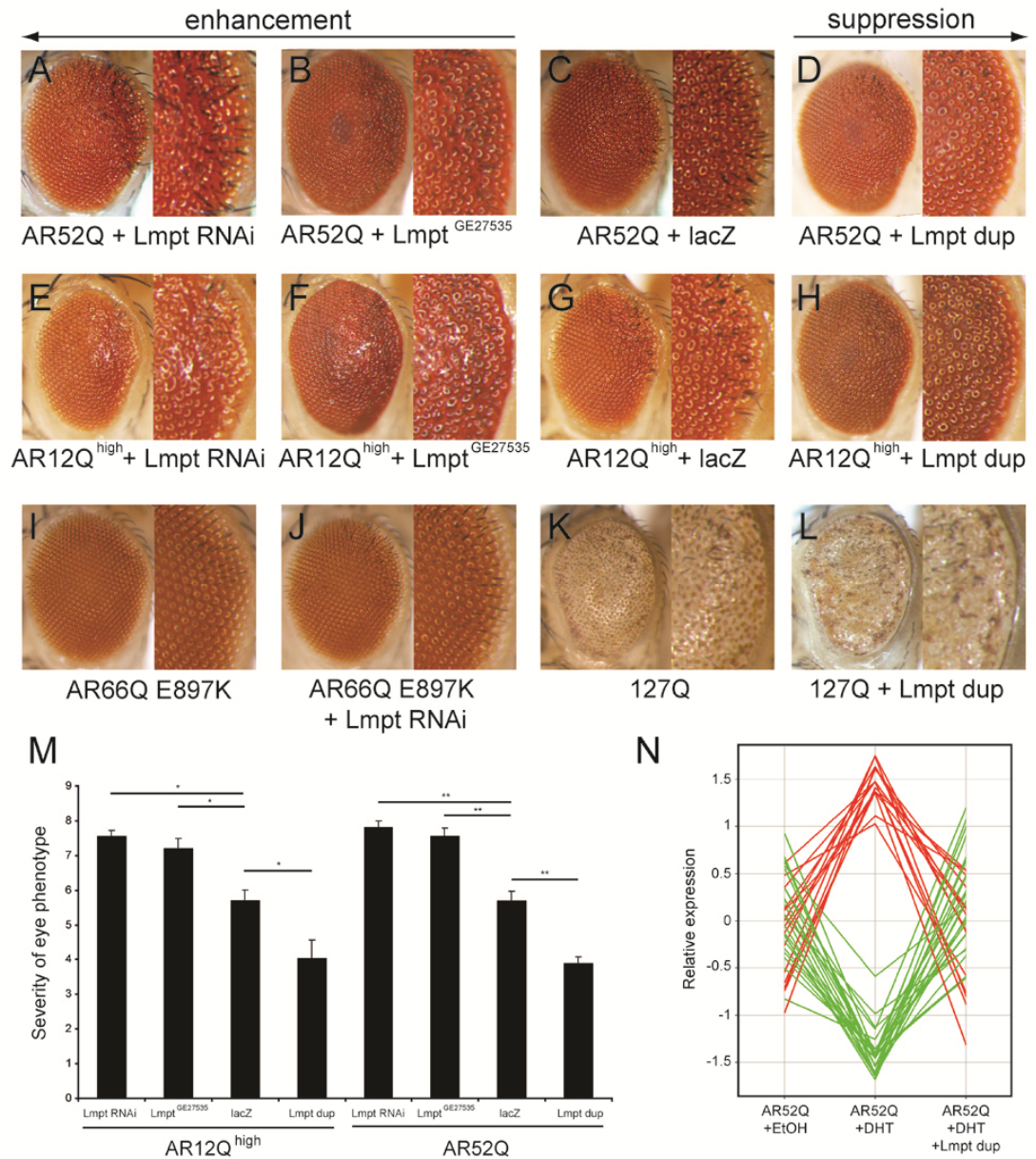
Figure 2.6. Manipulation of limpet levels modifies polyglutamine-expanded AR toxicity in an AF-2-dependent manner. (A-D) RNAi knockdown of limpet (A) and a P-element allele of limpet (limpet^{GE27535}) (B) enhance the phenotype of AR52Q alone (C). Flies with a chromosomal duplication of a region containing *limpet* (Dp(3;3)st$^+$g18) (D) show suppression of the AR52Q degenerative phenotype. (E-H) Limpet alleles similarly modify the phenotype of AR12Q flies with a strong phenotype. (I-J) Expression of limpet RNAi fails to enhance the phenotype in flies expressing AR66Q E897K. (K-L) Chromosomal duplication of *limpet* fails to suppress the phenotype in flies expressing pure polyglutamine (127Q). (M) Blinded scoring of the external eye phenotypes in (A-H) using a quantitative scoring system. All crosses performed on medium containing DHT. Bars, mean + SEM. ** $p < 0.01$, * $p < 0.05$. (N) Of 81 genes that changed in a DHT-dependent manner by expression profile analysis, 37 genes showed an opposite change in the presence of *limpet* duplication. Expression changes of these 37 genes are shown and plotted as relative expression (std dev) to the mean. See also Supplemental Figure 2.7.

Figure 2.7
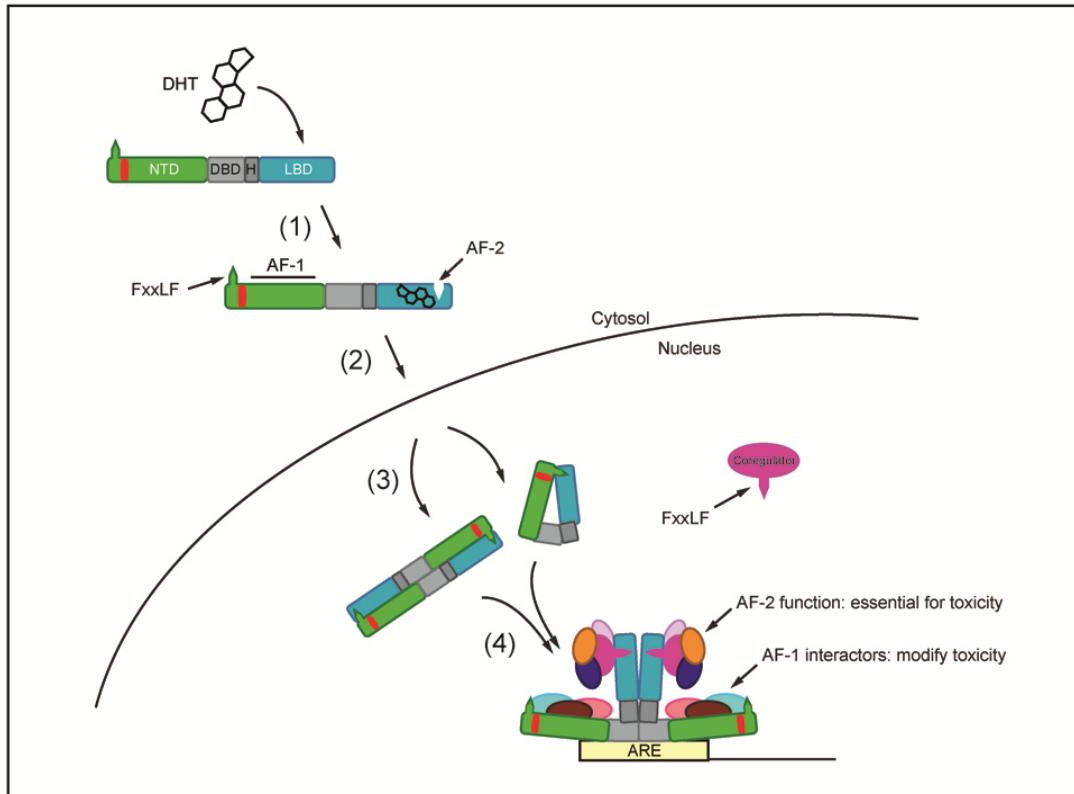
Figure 2.7. Schematic representation of the minimal ligand-dependent events that precede initiation of pathogenesis. (1) Ligand binding induces a conformational change in the LBD to create the AF-2 binding surface. Ligand also induces post-translational modifications that are not depicted. (2) Ligand-activated AR translocates to the nucleus. (3) Prior to DNA binding, the AF-2 domain is occupied by the N-terminal FxxLF in an intra- or inter-molecular interaction. (4) Following DNA binding, AF-1 and AF-2 interact with coregulators. In order to initiate pathogenesis, polyglutamine-expanded AR must bind DHT, translocate to the nucleus, bind DNA, and interact with coregulators at AF-2. While interactions at AF-1 modify toxicity, AF-2 function is essential for toxicity.

Table 2.1

Hit from screen	Putative AR ortholog	Mechanism of AR interaction	AF-2-based interaction	Validation by alternate allele	Validation by larval crawling	Ref
CycD	CCND1	CCND1 decreases AR NTD/AF-2 interaction	X	Df enhances	enhances, p<0.05	(Burd et al., 2005)
Dif	RELA	RELA competes for AR coactivators				(Palvimo et al., 1996)
Dl	RELA	RELA competes for AR coactivators				
Ets96B	ETV5	ETV5-AR interaction represses metalloproteinase expression				(Schneikert et al., 1996)
Fkh	FOXH1	FOXH1 blocks DHT-induced AR nuclear foci				(Chen et al., 2005)
Groucho	AES	AES interacts with basal transcriptional machinery				(Yu et al., 2001)
gskt	GSK3B	GSK3B decreases AR NTD/AF-2 interaction	X	Df enhances	enhances, p<0.05	(Wang et al., 2004b)
Hey	HEY1	HEY1 represses AR AF-1				(Belandia et al., 2005)
Hr78	NR2C2	NR2C2 forms heterodimer with AR				(Lee et al., 1999)
Usp	NR2C2	NR2C2 forms heterodimer with AR				
jbug	FLNA	FLNA decreases AR NTD/AF-2 interaction	X	Df enhances	enhances, p<0.05	(Loy et al., 2003)
Lmpt	FHL2	FHL2 increases AR transactivation in AF-2-dependent manner	X	P-element enhances	enhances, p<0.01	(Muller et al., 2000)
Pat1	APPBP2	APPBP2 inhibits AR nuclear translocation				(Zhang et al., 2004)
Pten	PTEN	PTEN inhibits AR nuclear translocation, promotes AR degradation				(Lin et al., 2004)
Rad9	RAD9	RAD9 decreases N/C interaction, requires AF-2	X	Df enhances	lethal with AR52Q	(Wang et al., 2004a)
Rbf	RB1	RB1 increases AR transactivation				(Yeh et al., 1998)
Smox	SMAD3	SMAD3 interrupts AR-coactivator interactions				(Hayes et al., 2001)
Smr	NCOR1/2	NCOR1/2 decreases N/C interaction, requires AF-2	X	Df enhances	n.s.	(Liao et al., 2003)
wts	LATS2	LATS2 decreases N/C interaction, requires AF-2	X	EMS mutation enhances	enhances, p<0.05	(Powzaniuk et al., 2004)

Table 2.1. Results from RNAi-based targeted genetic screen. 73 previously described AR coregulator genes were investigated for the existence of *Drosophila* orthologs. We identified 61 putative orthologs and obtained RNAi lines for these genes from the Vienna *Drosophila* RNAi Center. RNAi lines were tested for their ability to modify the SBMA fly phenotype. Shown are 19 hits from the screen which dominantly modified the AR52Q eye phenotype. Mammalian orthologs and mechanisms of AR interaction are shown. As indicated, seven of these hits were found to have AF-2-based interactions. These seven hits were validated in motor neurons by larval crawling assay, as well as with alternate alleles (classical alleles or aneuploid aberrations) in the eye. See also Supplemental Figure 2.4.

Supplemental Figure 2.1. AR mutants SS/DD and KK/AA do not show DHT-induced nuclear localization, while AR-NLS fusions show DHT-independent nuclear localization and decreased transactivation.
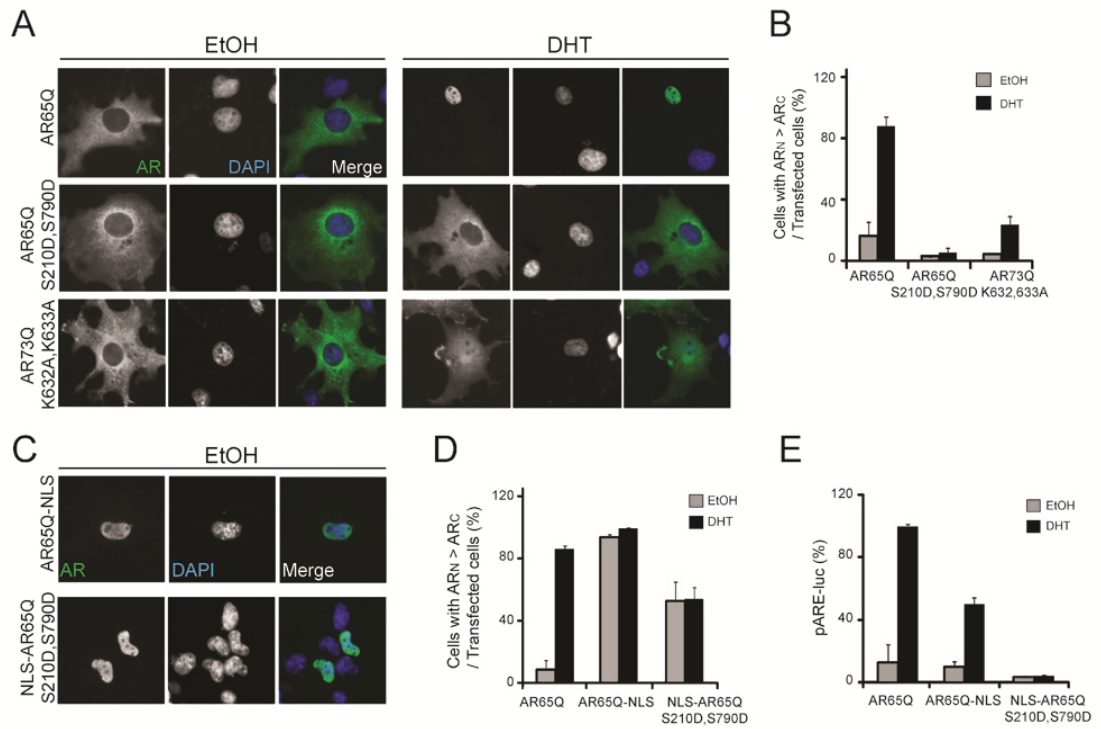
Supplemental Figure 2.1, related to Figure 2.2. AR mutants SS/DD and KK/AA do not show DHT-induced nuclear localization, while AR-NLS fusions show DHT-independent nuclear localization and decreased transactivation. (A) COS-1 cells transfected with AR were treated with vehicle or DHT and processed for immunocytochemistry. AR was detected with anti-AR antibody (green) and nuclei were stained with DAPI (blue). (B) Quantification of nuclear translocation shown in (A). The percentage of transfected cells with a greater concentration of AR in the nucleus than the cytoplasm was determined for each AR construct. (C) COS-1 cells transfected and processed as in (A). (D) Quantification of nuclear translocation shown in (C). (E) HEK293T cells were transfected with indicated AR65Q constructs together with both the luciferase pARE-E1b-Luc and the β-galactosidase pCMVβ reporter constructs. AR transactivation was measured in the presence and absence of DHT by luciferase assay and normalized to β-galactosidase activity. All bars indicate mean + SEM.

Supplemental Figure 2.2.
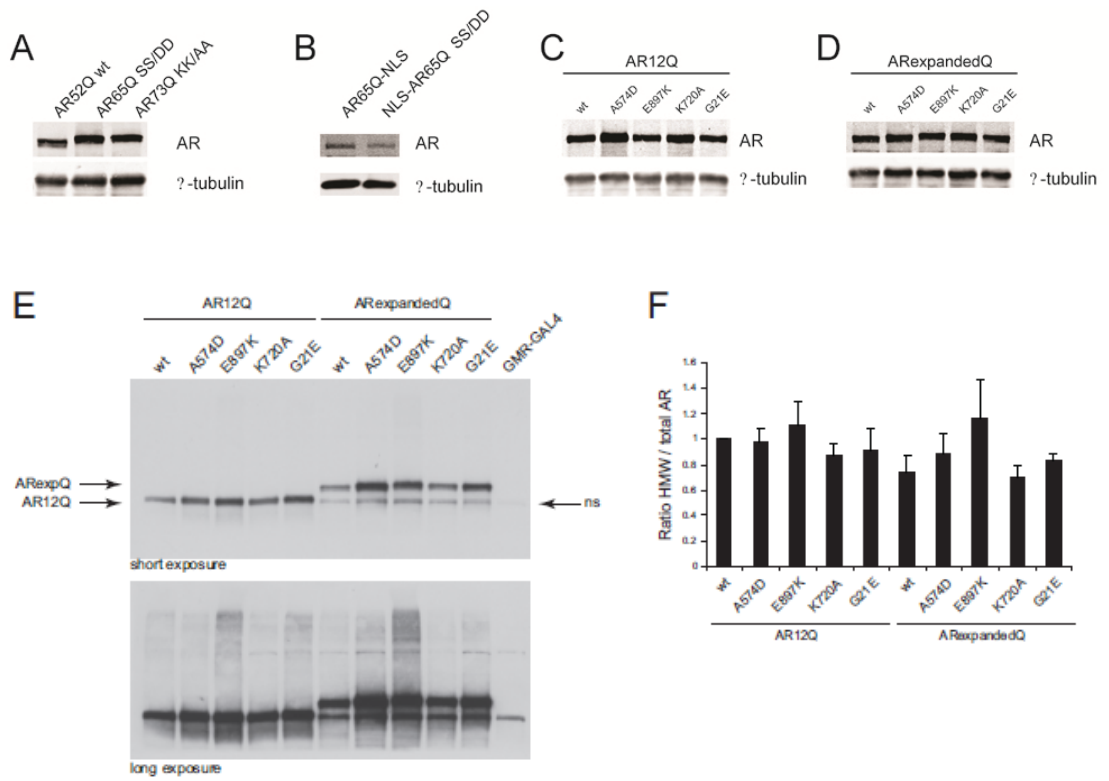
Supplemental Figure 2.2, related to Figures 2.2-2.5. Western blots of AR-expressing fly lysates. (A-D) Fly heads expressing AR driven by GMR-GAL4 were lysed and subjected to Western blotting to verify AR expression. α-tubulin is shown as loading control. (E-F) Western blots showing high molecular weight species of AR in protein extract from Drosophila eyes. Flies were crossed to GMR-GAL4 and reared on food containing DHT. Female heads were collected, lysed, and subjected to Western blotting to verify AR expression (short exposure) and look for biochemical aggregation (long exposure). No correlation was observed between the amount of high molecular weight species and degeneration. Quantitation of 5 independent experiments was performed using Image J.

Supplemental Figure 2.3.
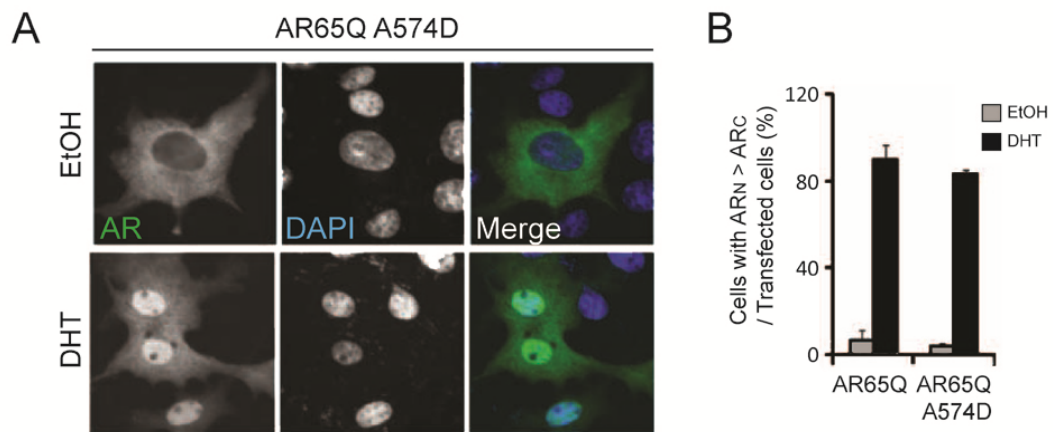
Supplemental Figure 2.3, related to Figure 2.3. A574D mutant AR undergoes DHT-induced nuclear localization. (A) COS-1 cells transfected with AR were treated with vehicle or DHT and processed for immunocytochemistry. AR was detected with anti-AR antibody (green) and nuclei were stained with DAPI (blue). (B) Quantification of nuclear translocation shown in (A). The percentage of transfected cells with a greater concentration of AR in the nucleus than the cytoplasm was determined for each AR construct. Bars, mean + SEM.

Supplemental Figure 2.4. Results from candidate-based genetic screen.
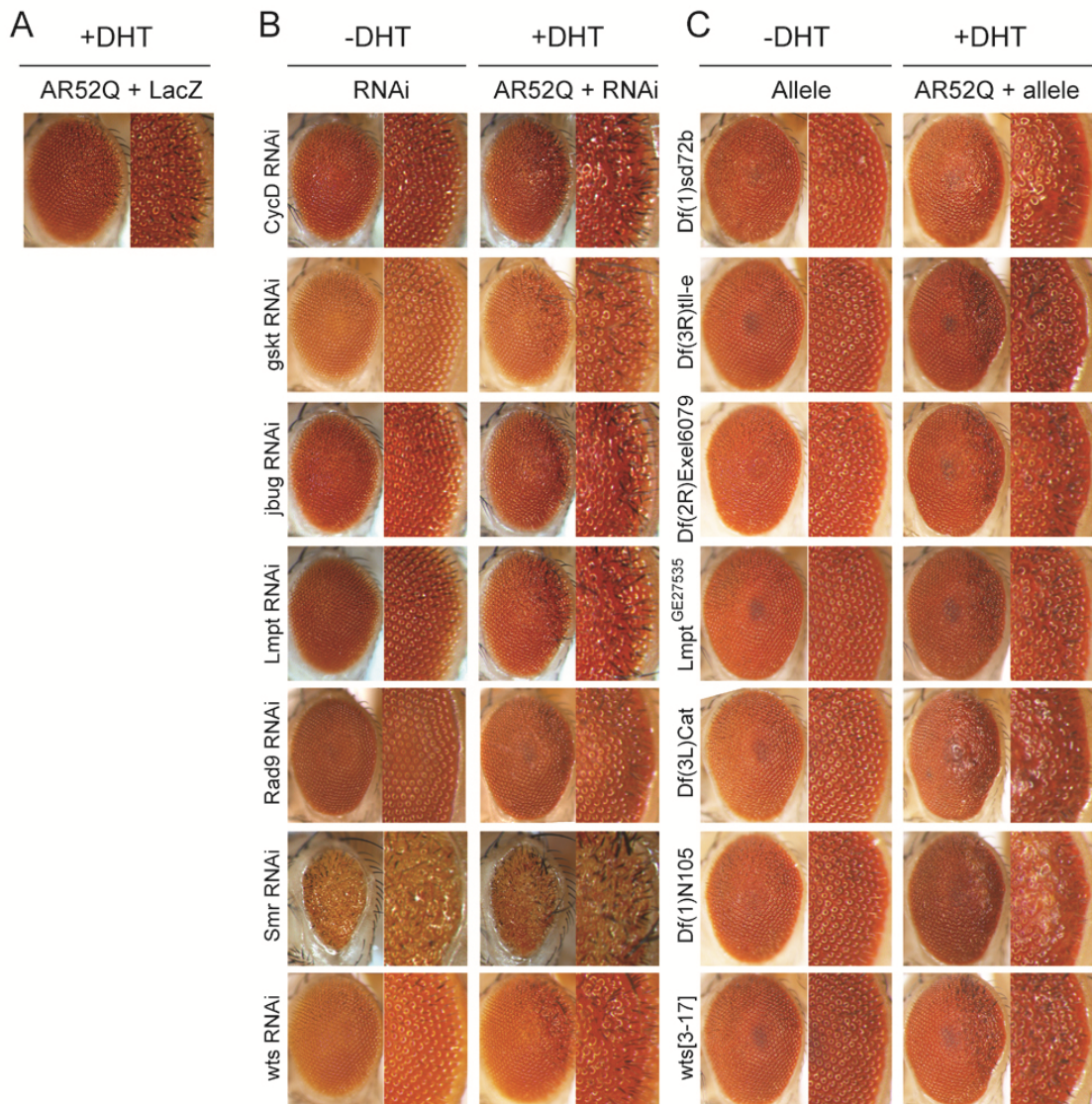
Supplemental Figure 2.4, related to Table 2.1. Results from candidate-based genetic screen. Flies expressing AR were crossed to either UAS-LacZ flies (A) or UAS-RNAi flies (B). Effects of RNAi were validated using classical alleles or aneuploid aberrations that disrupt or delete the relevant genes (C). For columns labeled "RNAi" and "Allele," flies were crossed to GMR-GAL4 to test for baseline eye phenotypes. Shown are seven genetic modifiers that play a role in AF-2 based interactions (see Table 2.1 for full list). All crosses performed at 29°C except gkst RNAi, Smr RNAi, and wts RNAi performed at 25°C.

Supplemental Figure 2.5, related to Figure 2.4. AR AF-2 mutants undergo DHT-induced nuclear localization, rescue the salivary gland and eye phentoypes caused by polyglutamine-expanded AR, and do not affect viability -DHT.

83
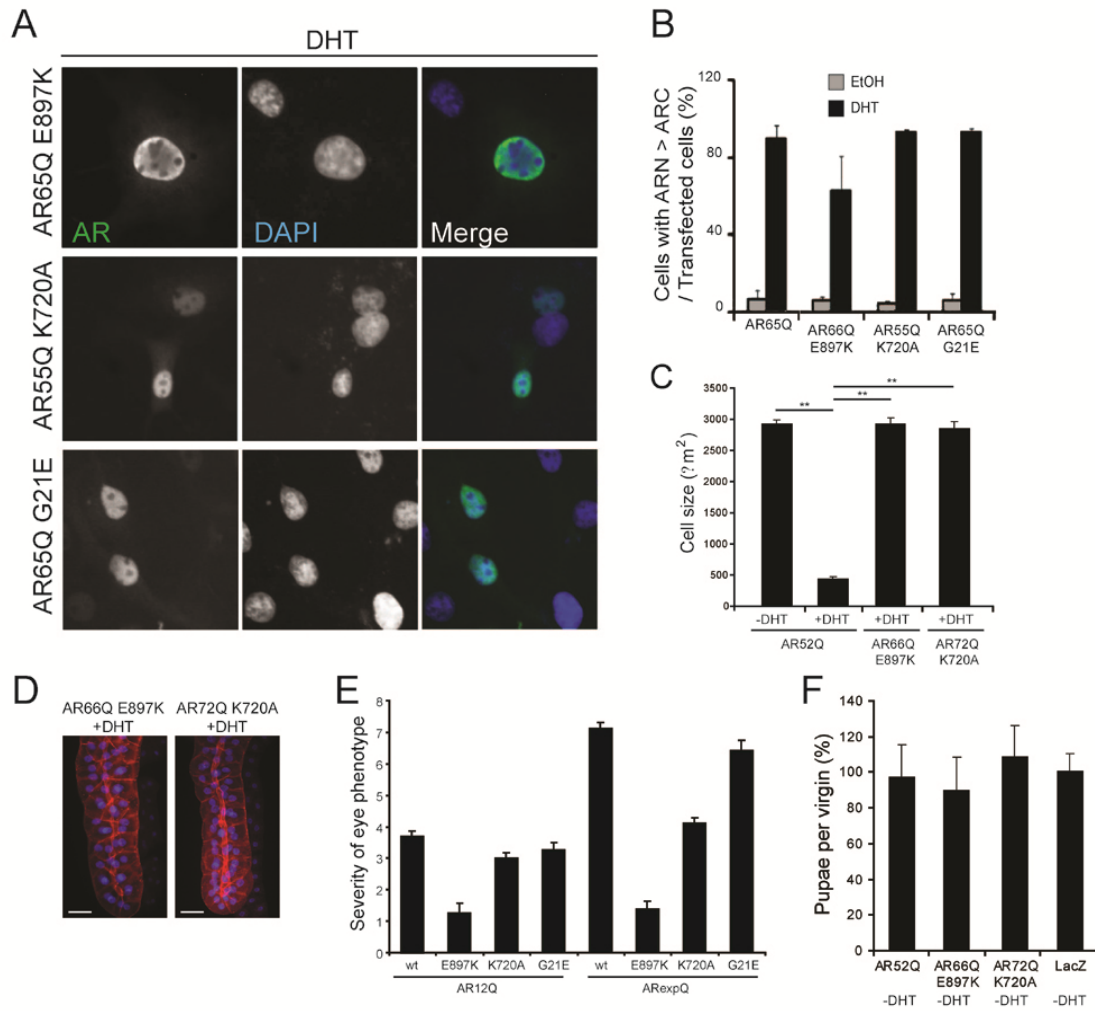
Supplemental Figure 2.5, related to Figure 2.4. AR AF-2 mutants undergo DHT-induced nuclear localization, rescue the salivary gland and eye phentoypes caused by polyglutamine-expanded AR, and do not affect viability -DHT. (A) COS-1 cells transfected with AR were treated with DHT and processed for immunocytochemistry. AR was detected with anti-AR antibody (green) and nuclei were stained with DAPI (blue). (B) Quantification of nuclear translocation shown in (A). The percentage of transfected cells with a greater concentration of AR in the nucleus than the cytoplasm was determined for each AR construct. (C-D) Salivary glands expressing AR with AF-2 mutations show rescued cell size. AR was expressed using fkh-GAL4 and dissected tissues were stained with phalloidin (red) and DAPI (blue). Salivary gland cell size was determined using phalloidin staining. Scale bar, 50 μm. ** $p<0.01$. (E) Blinded scoring of the external eye phenotypes in Figure 2.4E. (F) Viability assay performed on -DHT food. Elav-GAL4 flies were crossed to UAS-AR or UAS-LacZ flies. The number of pupae from each 1x1 cross was counted and normalized to LacZ. No significant differences were found between groups. Bars, mean + SEM in all panels.

Supplemental Figure 2.6, related to Figure 2.5. Molecular phenotype of AR-expressing flies.
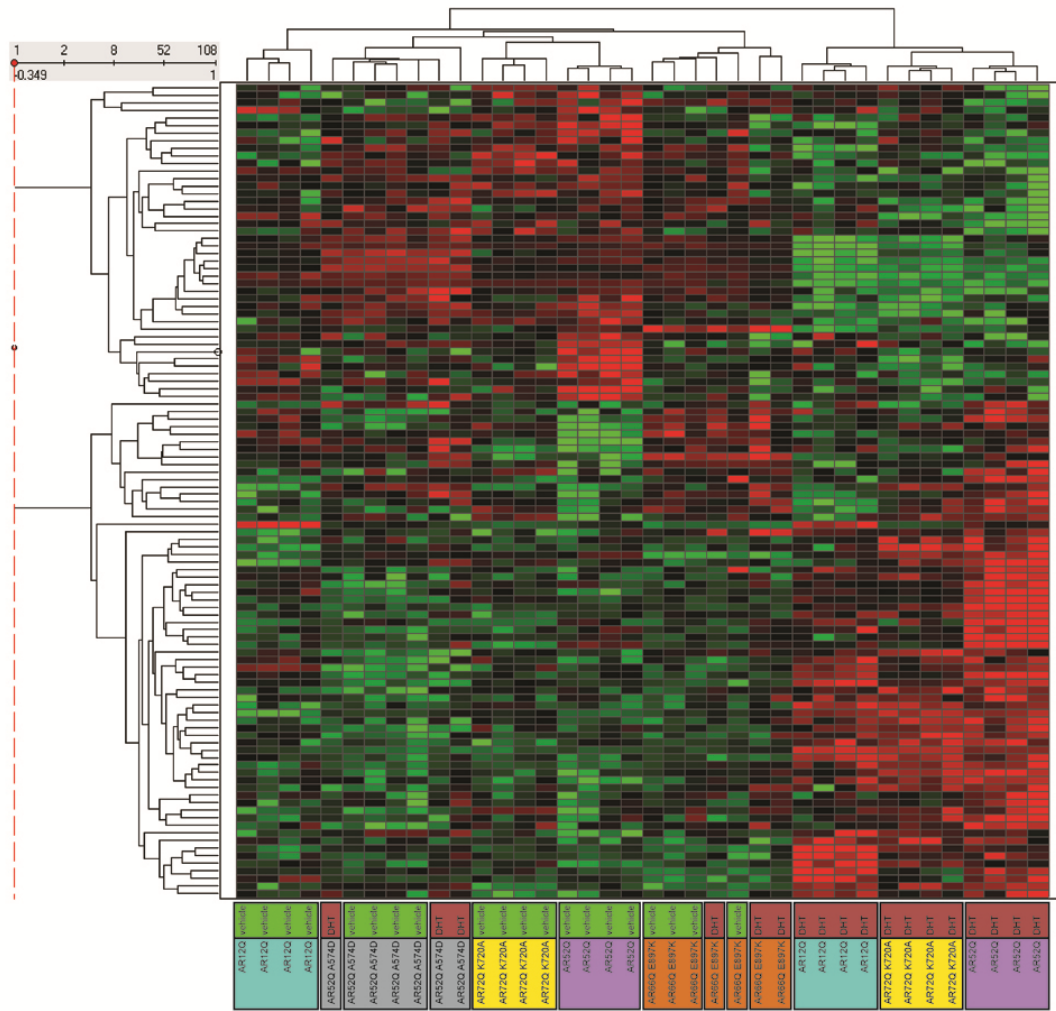
Supplemental Figure 2.6, related to Figure 2.5. Molecular phenotype of AR-expressing flies. UAS-AR flies were crossed to GMR-GAL4 flies on food containing either DHT or vehicle. Total RNA was extracted and subjected to analysis on Affymetrix chips. Using a false discovery rate of 0.05, 108 genes were identified that significantly differ in a DHT-dependent manner in AR52Q-expressing flies. Cluster analysis of these 108 genes demonstrates that A574D and E897K mutations suppress the molecular phenotype of AR52Q +DHT, while K720A mutation results in a mild suppression.

Supplemental Figure 2.7, related to Figure 2.6. Supporting information for limpet allele crosses.

A
```
lmpt   MTPSPTKELMSATPTISRRPREEFAEKGAIIREVEDGVRCEQCKSDCPGFAAHDWRKTCQ 60
FHL2   ------------------------------------------------------------
```

```
lmpt   SCKCPREAHAIYQQQTTNVHERLGFKLVSPADSGVEARDLGFTWVPPGVRASSRINRYFE 120
FHL2   ------------------------------------------------------------
```

```
lmpt   QLPDEMVPRLGSEGACSRERQISYQLPKQDLSLEHCKHLEVQHEASFEDFVTARNEIALD 180
FHL2   ------------------------------------------------------------
```

```
lmpt   IAYIKDAPYDEHCAHCDNEIAAGELVVAAPKFVESVMWHPKCFTCSTCNSLLVDLTYCVH 240
FHL2   ------------------------------------------------------------
```

```
lmpt   DDKVYCERHYAEMLKPRCAGCDELIFSGEYTKAMDKDWHSGHFCCWQCDESLTGQRYVIR 300
FHL2   -----------------------------------MTERFDCHHCNESLFGKKYILR 22
                                          :  :*  *  :*:*** *::*::*
```

```
lmpt   DDHPYCIKCYENVFANTCEECNKIIGIDSKDLSYKDKHWHEACFLCFKCHLSLVDKQFGA 360
FHL2   EESPYCVVCFETLFANTCEECGKPIGCDCKDLSYKDRHWHEACFHCSQCRNSLVDKPFAA 82
       ::  ***: *:*.:********.* ** *.*******:******* *  :*: ***** *.*
```

```
lmpt   KADKIYCGNCYDAQFASRCDGCGEVFRAGTKKMEYKTRQWHENCFCCCVCKTAIGTKSFI 420
FHL2   KEDQLLCTDCYSNEYSSKCQECKKTIMPGTRKMEYKGSSWHETCFICHRCQQPIGTKSFI 142
       * *::  *  :**. :::*:*: *  :.: .**:****   .***.** *   *: .*******
```

```
lmpt   PREQEIYCAGCYEEKFATRCIKCNKVITSGGVTYKNEPWHRECFTCTHCNITLAGQRFTS 480
FHL2   PKDNQNFCVPCYEKQHAMQCVQCKKPITTGGVTYREQPWHKECFVCTACRKQLSGQRFTA 202
       *:::: :*. ***::.* :*::*:* **:*****::***:***.** *.  *:*****:
```

```
lmpt   RDEKPYCAECFGELFAKRCTACVKPITGIGGTRFISFEDRHWHHDCFVCASCKASLVGRG 540
FHL2   RDDFAYCLNCFCDLYAKKCAGCTNPISGLGGTKYISFEERQWHNDCFNCKKCSLSLVGRG 262
       **:  .**  :** :*:**:*.*.:**:*:***::*****:*:**:*** *  .*. ******
```

```
lmpt   FITDGPDILCPDCAKQKLM 559
FHL2   FLTERDDILCPDCGKDI-- 279
       *:*:  *******.*:
```

B

GMR   Lmpt RNAi alone

Lmpt GE27535 alone   Lmpt dup alone

C

Supplemental Figure 2.7, related to Figure 2.6. Supporting information for limpet allele crosses. (A) Alignment of *Drosophila* limpet (top) and human FHL2 (bottom). Protein sequences were aligned using ClustalW. FHL2 contains two FxxLF-like sequences that interact directly with AF-2 in AR. One of these sequences is conserved as FGELF in *Drosophila* limpet (box). (B) Eye phenotype of limpet alleles expressed alone. Flies expressing GMR-GAL4 alone, UAS-limpet RNAi, or a P-element allele of limpet (limpet GE27535) exhibit no phenotype. Flies with a chromosomal duplication of a region containing limpet (Dp(3;3)st+g18) show a very mild phenotype of slight ommatidial disorganization. (C) Quantitation of RNAi knockdown. To determine the degree of knockdown of limpet, UAS-Lmpt RNAi was crossed to GMR-GAL4 and total RNA was isolated from 5-10 heads in triplicate. Real-time quantitative PCR was performed as described in Supplemental Methods. Graph shows mean transcript levels relative to GAPDH2.

Supplemental Figure 2.8
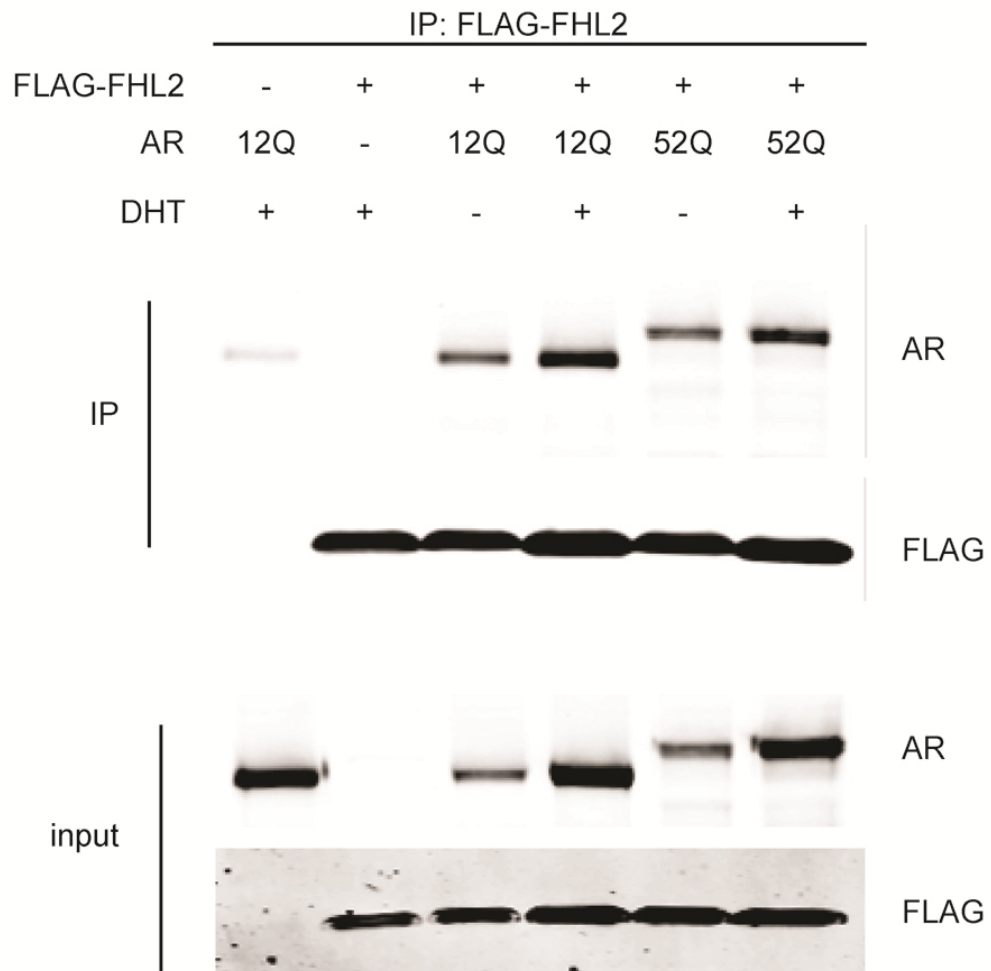
Supplemental Figure 2.8. Co-IP of AR and FLAG-FHL2. HEK293T cells were co-transfected with FLAG-FHL2 and AR followed by treatment with DHT or vehicle. Nuclear extracts were collected as described in Supplemental Methods and immunoprecipated for FLAG. No difference in FHL2-AR interaction was observed based on polyglutamine length.

Supplemental Table 2.1

Probeset	Gene Title	FlyBase	AR52Q change	AR12Q change	p-value (AR52Q)	p-value (AR12Q)
1633797_at	rhodopsin	FBgn0003248	decreased*	decreased*	1.325E-18	1.573E-18
1625382_at	Osiris	FBgn0027527	decreased*	decreased*	6.770E-10	6.928E-15
1634148_at	CG4842	FBgn0036620	decreased*	decreased*	8.824E-06	4.339E-14
1626740_at	CG4784	FBgn0036619	decreased*	decreased*	3.741E-11	2.273E-12
1637801_at	sepia	FBgn0086348	decreased*	decreased*	4.416E-06	3.110E-10
1628635_at	Osiris	FBgn0037416	decreased*	decreased*	2.262E-06	7.963E-07
1627499_at	CG2016 /// --- /// ---	FBgn0250839 /// FBgn0260206 /// FBgn0260207	decreased*	decreased*	3.210E-04	4.217E-09
1625764_at	CG17572	FBgn0032753	decreased*	decreased*	1.053E-04	4.363E-09
1636078_at	CG13670	FBgn0035873	decreased*	decreased*	7.007E-06	3.957E-05
1627829_at	rhodopsin	FBgn0003249	decreased*	decreased*	3.173E-10	4.440E-10
1623757_at	drosocrystallin	FBgn0005664	decreased*	decreased*	2.781E-05	1.504E-04
1640912_s_at	scarface	FBgn0033033	increased*	increased*	3.409E-10	5.052E-04
1640184_at	CG17002	FBgn0033122	increased*	increased*	6.921E-05	1.097E-04
1636005_at	CG14495	FBgn0034293	increased*	increased*	2.049E-04	8.802E-05
1641490_s_at	Thrombospondin	FBgn0031850	increased*	increased*	6.445E-08	2.063E-04
1627872_at	CG3770	FBgn0035085	increased*	increased*	1.812E-06	2.852E-04
1636505_at	CG15083	FBgn0034399	increased*	increased*	2.093E-05	6.353E-08
1632185_s_at	SCP-containing protein A /// SCP-containing protein B /// SCP-containing protein C	FBgn0037879 /// FBgn0037888 /// FBgn0037889	increased*	increased*	9.896E-06	3.294E-04
1635191_at	tetraspanin 42E	FBgn0029507	increased*	increased*	7.055E-08	2.247E-07
1634688_at	RabX5	FBgn0035255	increased*	increased*	7.188E-04	1.051E-04
1625266_at	antigen 5-related	FBgn0015010	increased*	increased*	5.459E-14	1.237E-04
1630579_at	Cyclin-dependent kinase 8	FBgn0015618	increased*	increased*	2.830E-04	4.400E-07
1639718_at	CG18764	FBgn0042205	increased*	increased*	4.729E-04	3.956E-06
1629553_at	CG14153	FBgn0036094	increased*	increased*	3.937E-04	1.065E-07
1629029_at	CG5160	FBgn0031906	increased*	increased*	1.146E-05	2.424E-05
1627105_at	thioredoxin	FBgn0029752	increased*	increased*	5.013E-06	3.720E-05
1629963_at	sugar transporter 1	FBgn0028563	increased*	increased*	4.535E-04	1.177E-09
1635507_at	CG30031 /// CG4269	FBgn0034741 /// FBgn0050031	increased*	increased*	3.241E-11	4.477E-05
1624724_at	b6	FBgn0024897	increased*	increased*	1.358E-07	6.687E-10
1624579_at	CG13934	FBgn0035279	increased*	increased*	8.706E-07	8.941E-08
1631480_at	CG2652	FBgn0025838	increased*	increased*	2.802E-04	9.152E-06
1633607_at	CG2444	FBgn0030326	increased*	increased*	1.125E-09	4.899E-10
1625307_at	sugar transporter 2	FBgn0028562	increased*	increased*	1.510E-05	3.008E-09
1629455_at	CG8925	FBgn0038404	increased*	increased*	2.173E-06	2.053E-16
1638279_at	CG13840	FBgn0039028	increased*	increased*	9.195E-16	1.380E-18
1629565_s_at	CG30160 /// tetraspanin 42E	FBgn0042086 /// FBgn0050160	increased*	increased*	7.143E-15	2.607E-17
1637012_at	E(spl) region transcript m2	FBgn0002592	decreased*	decreased	3.864E-04	0.0183
1624373_at	Circadianly Regulated Gene	FBgn0021738	decreased*	decreased	4.934E-04	0.0013
1623140_at	ionotropic receptor 94e	FBgn0259194	decreased*	decreased	4.722E-04	0.1598
1639269_a_at	pigment cell dehydrogenase reductase	FBgn0011693	decreased*	decreased	4.055E-04	0.0031

Probeset	Gene Title	FlyBase	AR52Q change	AR12Q change	p-value (AR52Q)	p-value (AR12Q)
1633499_at	retinin	FBgn0040074	decreased*	decreased	2.619E-05	0.0236
1633207_at	Na^{+}-driven anion exchanger 1	FBgn0259111	decreased*	decreased	6.723E-05	0.0025
1634438_at	Munster	FBgn0023489	decreased*	decreased	8.951E-05	0.0009
1628689_at	CG17211	FBgn0032414	decreased*	decreased	4.226E-05	0.0657
1626742_at	CG8964	FBgn0033674	decreased*	decreased	3.478E-04	0.0381
1633651_at	tachykinin-3	FBgn0037976	decreased*	decreased	7.955E-05	0.0479
1636488_at	CG4468 /// CG4468	FBgn0038749 /// FBgn0064532	decreased*	decreased	8.286E-05	0.0159
1634988_a_at	CG17352	FBgn0035880	decreased*	decreased	2.530E-04	0.0166
1626918_at	CG13879	FBgn0035120	decreased*	decreased	3.095E-05	0.0097
1632392_s_at	giant slob	FBgn0024290	decreased*	decreased	6.042E-04	0.0654
1641333_s_at	prominin-like protein	FBgn0026189	decreased*	decreased	2.909E-05	0.0449
1639408_a_at	shaking B	FBgn0085387	decreased*	decreased	1.133E-04	0.0310
1627288_a_at	calcium-binding protein	FBgn0010218	decreased*	decreased	6.846E-04	0.1123
1633801_s_at	CG9171	FBgn0031738	decreased*	decreased	2.873E-04	0.1876
1632319_at	CG18598	FBgn0038589	decreased*	decreased	9.082E-06	0.0609
1627498_at	Syndapin	FBgn0053094	decreased*	decreased	3.511E-04	0.0217
1638314_at	CG12418 /// CG12802	FBgn0040536 /// FBgn0250818	decreased*	decreased	4.607E-04	0.3249
1631094_s_at	CG9339	FBgn0032901	decreased*	decreased	4.705E-04	0.2245
1627971_s_at	serrano	FBgn0034408	decreased*	decreased	5.119E-05	0.1346
1638588_at	CG15522	FBgn0039723	decreased*	decreased	2.617E-05	0.2937
1641083_at	CG3257	FBgn0034978	decreased*	decreased	4.622E-04	0.1942
1631368_s_at	CG8108	FBgn0027567	decreased*	decreased	3.683E-04	0.1492
1636539_at	Dak1 /// Sld5	FBgn0028833 /// FBgn0039403	decreased*	decreased	4.176E-04	0.2200
1628143_a_at	Drosophila A kinase anchor protein	FBgn0086911	decreased*	decreased	1.635E-04	0.2806
1633939_at	CG13563	FBgn0034966	decreased*	decreased	1.002E-05	0.5606
1637637_at	dynamin	FBgn0003392	decreased*	decreased	6.877E-05	0.3056
1628859_at	dynamin	FBgn0003392	decreased*	decreased	4.834E-04	0.5495
1629996_at	CG11910	FBgn0039332	decreased*	decreased	3.955E-05	0.7194
1638828_a_at	CG17378	FBgn0031858	decreased*	decreased	3.130E-04	0.8916
1635585_at	CG9264	FBgn0032911	decreased*	decreased	9.552E-05	0.9657
1628493_at	Kallmann	FBgn0039155	decreased*	decreased	1.373E-04	0.9841
1629446_at	CG1136	FBgn0035490	increased*	increased	3.405E-04	0.9910
1630145_s_at	tetraspanin 42E	FBgn0029508	increased*	increased	1.875E-05	0.9367
1626452_at	CG2121	FBgn0033289	increased*	increased	4.362E-07	0.9539
1628884_at	semmelweis	FBgn0030310	increased*	increased	4.880E-14	0.9114
1624312_at	fidgetin_DROME	FBgn0031519	increased*	increased	2.394E-04	0.8939
1632808_at	CG6012	FBgn0032615	increased*	increased	7.353E-04	0.8952
1631660_at	CG15065	FBgn0040734	increased*	increased	8.688E-07	0.7397
1624057_at	CG16713	FBgn0031560	increased*	increased	1.736E-05	0.5342
1632381_at	verstopft	FBgn0043903	increased*	increased	1.345E-04	0.2752
1638542_at	CG15685	FBgn0038789	increased*	increased	6.001E-04	0.6985
1624655_at	CG6472	FBgn0034166	increased*	increased	7.885E-05	0.6944

Probeset	Gene Title	FlyBase	AR52Q change	AR12Q change	p-value (AR52Q)	p-value (AR12Q)
1634012_at	CG5002	FBgn0034275	increased*	increased	4.093E-04	0.3499
1631697_at	Drosocin	FBgn0010388	increased*	increased	8.433E-06	0.5011
1633998_s_at	---	---	increased*	increased	1.342E-04	0.0564
1627327_at	Drosomycin B	FBgn0035434	increased*	increased	1.154E-04	0.0604
1629138_at	---	---	increased*	increased	4.442E-04	0.3387
1625012_s_at	virus-induced RNA 1	FBgn0043841	increased*	increased	5.401E-05	0.0902
1631701_a_at	CG8502	FBgn0033725	increased*	increased	7.527E-04	0.3803
1629507_a_at	no action potential	FBgn0002774	increased*	increased	7.557E-05	0.1134
1632591_at	Pherokine 3	FBgn0035089	increased*	increased	1.390E-04	0.0567
1625743_at	beta-carotene dioxygenase	FBgn0002937	increased*	increased	5.582E-04	0.0115
1626839_s_at	bloated tubules	FBgn0027660	increased*	increased	2.858E-04	0.0340
1625185_at	Carbonic anhydrase 2	FBgn0027843	increased*	increased	1.685E-04	0.0421
1632212_at	CG14401	FBgn0032900	increased*	increased	1.236E-06	0.0075
1634546_at	tiggrin	FBgn0011722	increased*	increased	2.145E-04	0.0064
1637577_at	Zinc/iron regulated transporter-related protein 3	FBgn0038412	increased*	increased	4.814E-05	0.0840
1641496_a_at	CG5896	FBgn0039494	increased*	increased	5.394E-05	0.0139
1634201_at	CG13841 /// CG4000	FBgn0038820 /// FBgn0040588	increased*	increased	3.524E-05	0.0050
1625313_at	CG12826	FBgn0033207	increased*	increased	1.777E-06	0.0807
1637936_at	CG32512	FBgn0052512	increased*	increased	4.529E-04	0.0118
1631121_at	CG7267	FBgn0030079	increased*	increased	6.698E-06	0.0015
1640983_at	CG5909	FBgn0039495	increased*	increased	2.501E-10	0.0055
1629919_at	CG12045	FBgn0039805	increased*	increased	1.876E-06	0.0027
1639418_at	Acp65Aa	FBgn0020765	increased*	increased	1.980E-11	0.0199
1625124_at	attacin	FBgn0012042	increased*	increased	2.523E-05	0.3793
1623388_at	CG15861	FBgn0035084	increased*	increased	5.183E-06	0.0007
1633211_a_at	CG7795	FBgn0032019	increased*	increased	2.187E-04	0.0045
1635844_at	CG15887	FBgn0038132	increased*	increased	7.377E-05	0.0026
1628617_at	drosomycin-F	FBgn0052282	increased*	increased	1.121E-05	0.0156
1627551_s_at	attacin /// attacin	FBgn0012042 /// FBgn0041581	increased*	increased	1.159E-05	0.0663
1640978_at	CG14567	FBgn0037126	increased*	decreased*	4.483E-07	0.0003
1638021_at	CG4757	FBgn0027584	increased*	decreased	4.570E-09	0.0220
1629530_at	Immune induced molecule 23	FBgn0034328	increased*	decreased	4.624E-04	0.1615
1640144_at	CG18067	FBgn0034512	increased*	decreased	3.797E-04	0.0019
1628387_s_at	CG30080	FBgn0050080	increased*	decreased	3.940E-06	0.0356
1628404_at	CG2767	FBgn0037537	increased*	decreased	8.041E-04	0.0017
1639019_s_at	CG33470 /// Immune induced molecule 10	FBgn0033835 /// FBgn0053470	increased*	decreased	9.495E-08	0.0247
1639571_s_at	heat shock 70 /// heat shock 70	FBgn0013275 /// FBgn0013276	increased*	decreased	3.826E-05	0.0312
1640768_at	CG13965	FBgn0032834	increased*	decreased	1.328E-04	0.1201
1626319_a_at	Immune induced molecule 10	FBgn0033835	increased*	decreased	1.049E-05	0.2830
1628229_at	serpin27A	FBgn0028990	increased*	decreased	8.563E-05	0.0378
1627759_at	CG30080	FBgn0050080	increased*	decreased	2.086E-04	0.5929

Probeset	Gene Title	FlyBase	AR52Q change	AR12Q change	p-value (AR52Q)	p-value (AR12Q)
1640884_at	CG15784	FBgn0029766	increased*	decreased	3.023E-04	0.3535
1640405_at	lethal (2) 01810	FBgn0010497	increased*	decreased	1.420E-04	0.6607
1634278_at	CG6409	FBgn0036106	increased*	decreased	3.199E-05	0.4527
1639907_at	CG11951	FBgn0039656	increased*	decreased	6.956E-04	0.6006
1640327_at	CG6023	FBgn0030912	increased*	decreased	6.128E-04	0.7254
1635416_at	CG31100	FBgn0051100	increased*	decreased	2.480E-05	0.7979
1635175_at	CG17121	FBgn0039043	increased*	decreased	5.026E-04	0.9506
1635968_at	CG3604	FBgn0031562	increased*	decreased	5.214E-07	0.9801
1628536_s_at	CG11880	FBgn0039637	increased*	decreased	4.089E-04	0.9752
1622920_at	Cosens-Manning mutant	FBgn0003861	decreased*	increased	1.643E-04	0.9682
1634570_at	CG5375	FBgn0032221	decreased*	increased	9.355E-05	0.9564
1632478_a_at	protein kinase C	FBgn0003091	decreased*	increased	2.920E-04	0.9018
1639095_at	pharbin-like	FBgn0036273	decreased*	increased	5.043E-04	0.8129
1628913_at	CG32365	FBgn0052365	decreased*	increased	7.690E-04	0.8476
1625922_a_at	CG10508	FBgn0037060	decreased*	increased	2.508E-04	0.6613
1628382_at	Srp54	FBgn0024285	decreased*	increased	3.327E-04	0.7212
1629962_at	CG8916	FBgn0030707	decreased*	increased	2.453E-04	0.6585
1625917_s_at	---	---	decreased*	increased	6.338E-05	0.8259
1640950_at	CG15739	FBgn0030347	decreased*	increased	6.142E-06	0.5448
1636615_at	---	---	decreased*	increased	5.767E-04	0.6677
1623261_at	RabX4	FBgn0051118	decreased*	increased	1.974E-04	0.3445
1638708_s_at	grappa	FBgn0014963	decreased*	increased	1.592E-04	0.3098
1627082_at	CG15465	FBgn0029746	decreased*	increased	2.135E-04	0.2177
1640790_at	CG11293	FBgn0034889	decreased*	increased	8.548E-06	0.1629
1630961_at	CG17193	FBgn0040571	decreased*	increased	1.478E-04	0.2033
1632424_at	CG13995	FBgn0031770	decreased*	increased	5.512E-04	0.2336

Supplemental Table 2.1, related to Figure 2.5 and Supplemental Figure 2.6.

Identities of 149 genes that change in response to DHT in AR52Q-expressing flies.

Identifiers given are Probeset IDs from Affymetrix, Gene Title, and FlyBase ID. For each gene, the relative change (DHT vs. vehicle) is shown as an increase or decrease. Of the 149 genes DHT-responsive genes identified for AR52Q flies, 111 genes (indicated in bold) show a similar DHT-responsive trend in AR12Q flies. * indicates that the gene achieved significance at false discovery rate of 0.1.

Chapter 3: Conclusions

General Conclusions

The work described in the previous chapter extends our understanding of SBMA pathogenesis in several important ways. First, it strengthens the concept that native protein functions are key to polyglutamine pathogenesis, an idea that was still largely untested outside SCA1. More specifically, it defines the precise molecular events that are required for pathogenesis of SBMA, elucidating the molecular basis for the ligand dependence of the disease and identifying targets for therapeutic intervention.

It is important to note the scientific climate in which these results are being published. The dominant hypothesis within the polyglutamine disease field holds that degeneration results from the generation of polyglutamine-containing cleavage fragments that are prone to oligomerization and acquisition of neurotoxic properties due to the intrinsic toxicity of expanded polyglutamine. In contrast, the idea that native protein function might play a role in pathogenesis has remained largely unexplored. To a certain extent, the lack of investigation in this research vein is due to practical limitations; in many cases, the native function of polyglutamine disease proteins is ill defined, and in those proteins with known functions, the domains required for such functions have not been mapped. Certainly, the richness of the basic scientific knowledge of AR allowed us to pursue our hypothesis farther than would be possible with another protein in the same disease family.

Although prior studies have suggested that polyglutamine toxicity may be influenced by protein context (reviewed in (La Spada and Taylor, 2003, 2010)), these investigations

have had limited impact on the debate about the relative pathogenic contribution of intrinsic polyglutamine toxicity vs. altered native function. Indeed, two prior publications that are relevant to our study demonstrate the prism through which most polyglutamine disease research in viewed. The first showed that nuclear localization of AR is necessary for toxicity *in vivo* (Takeyama et al., 2002), and the second showed that nuclear localization of AR is not sufficient for toxicity *in vitro* (Montie et al., 2009). These manuscripts concluded that the nucleus presented an environment in which AR undergoes ligand-dependent cleavage (Montie et al., 2009) and subsequent polyglutamine-mediated aggregation (Takeyama et al., 2002; Montie et al., 2009). Indeed, Takeyama et al. state that "[the neurotoxic] events are thought to be mediated through factors associated with the expanded polyQ stretches in the aggregates and not through any innate function of the disease proteins" (Takeyama et al., 2002). On the basis of our current study, we advance the alternative hypothesis that the pathogenesis of SBMA is mediated by native coregulator interactions of AR in its full-length, DNA-bound form. These findings are consistent with a mechanism wherein polyglutamine expansion results in toxicity that is mediated by the normally-folded protein that is trying to carry out its native function, but is altered in a minor way such that its ratio of native interactions is subtly altered. It is important to note that AR might not have a single "normal" conformation, but instead has multiple subtly different native conformations, the ratio of which may be altered by polyglutamine expansion.

More specific to SBMA, our work provides a promising list of therapeutic targets to combat pathogenesis. Previous work that determined that androgen binding to AR was

necessary for toxicity led to clinical trials of anti-androgen drugs that target the hypothalamic-pituitary-gonadal axis (Banno et al., 2009); however promising, these drugs decrease levels of androgen globally and cause a wide range of undesired side effects. In the present work, we have identified a number of detailed molecular events that underlie this requirement for ligand binding: in order to cause toxicity, ligand-bound mutant AR must translocate to the nucleus, bind DNA, and interact with coregulators at AF-2. Although myriad AR antagonists could be used to restrict the mutant protein to the cytoplasm, to outcompete endogenous ligand at the AR LBD, or to prevent AR binding to DNA, each of these approaches suffers from the same global drawbacks as anti-androgen therapy. Instead, it is the last identified requirement – AF-2-based interactions – that presents an unprecedented opportunity for therapeutic intervention.

Inspired by the clinical success of SERMs (selective estrogen receptor modulators) in treating breast cancer, an entire pharmaceutical enterprise has developed to produce SARMs (selective androgen receptor modulators), defined as compounds that act as AR agonists or antagonists in a tissue-specific manner (Chang and McDonnell, 2005). Although initially designed to combat AR-related conditions such as hirsutism, benign prostatic hypertrophy, prostate cancer, and others, SARMs provide a tantalizing therapeutic approach to promote tissue-selective (in)activation of AR in SBMA. The tissue specificity of these drugs is thought to be tied to the distinct AF-2 conformations that are induced by DHT vs various SARMs, with the result being preferential binding of particular AF-2-based coregulators over others (Baek et al., 2006; Estebanez-Perpina et al., 2007). Given our findings, it is not unreasonable to predict that SBMA patients might

be able to take particular SARM(s) that alter the complement of transcriptional

coregulators in such a way as to restore the balance of AR complexes in motor neurons

while leaving AR activity in other tissues unaltered.

Future directions

Obviously, the results presented in the previous chapter must be replicated in a

mammalian system before thoughts of SARM-based therapeutics can be reasonably

entertained. We have already begun to pursue this avenue of research, generating

transgenic mouse models of SBMA that express each of the key mutations described in

this work. These mice were designed using a Cre-Lox system that will allow mutant AR

to be expressed either ubiquitously or in a tissue-specific manner, with motor neurons

being of primary interest. If we can replicate the rescue of mutant AR toxicity using the

mutants A574D and E897K, these mice can be further used to answer important

mechanistic questions.

For example: in the present work, we show that native protein function is essential to

initiate degeneration. However, we do not rule out a role for polyglutamine length-

dependent aggregation in toxicity, largely because our *Drosophila* model of SBMA does

not show appreciable ligand- or polyglutamine length-dependent biochemical

aggregation. Instead, using a mouse model of SBMA (where biochemical aggregation has

traditionally been more prominent), we can address the respective roles of aggregation

and altered native function in pathogenesis. Although our model predicts that the

suppressive mutations A574D, K720A, and E897K will have no effect on polyglutamine length-dependent aggregation, it is important to examine this question in order to reconcile our results with the aggregation-centric history of the field.

Mammalian systems will also provide a key source of material with which to investigate the proteomic consequences of the AF-2 mutations. As described in the previous chapter, we favor a model in which the AF-2 domain of AR competes with other transcription factors for a limited supply of coregulators, and that polyglutamine expansion alters the balance of AR-coregulator interactions in such as way as to deplete coregulators away from their normal functions. Proteomic work in mammalian systems, likely beginning in immortalized cell culture and leading to work in mouse, may provide insight into these altered complexes – not only those complexes that change with polyglutamine expansion, but also those that occur in the context of K720A and E897K mutations. In an ideal experiment, these proteomic data could be aligned with proteomic profiles of AR bound to a collection of candidate SARMs.

According to our proposed mechanism of pathogenesis, amplification of AR activity by polyglutamine expansion would be expected to result in reduced availability of coregulators for important coactivating or corepressing functions. As mentioned in the preceding chapter, however, a crucial outstanding question is how AR activity in the nucleus is amplified. One possibility involves aggregation-prone polyglutamine-expanded AR adopting a conformation that amplifies AF-2-based interactions. However, arguing against this possibility is our failure of detect any polyglutamine length-

dependent changes in co-immunoprecipitation of AR and the AF-2-interacting coregulator FHL2. Testing for polyglutamine length-dependent alterations in binding of additional AF-2-based interactors would be necessary to rule out this possibility, ideally using endogenous proteins rather than overexpressed epitope-tagged proteins as in our FHL2 co-IP. An alternative possibility is that polyglutamine expansion amplifies AR activity (and AF-2 function in particular) independent of any change in the intrinsic ability of AR to interact with coregulators. For example, this could occur by reducing the inactivation rate of DNA-bound AR or by reducing the rate of AR nuclear efflux similar to what has been observed for ataxin-7 (Taylor et al., 2006). In fact, reduced nuclear efflux might be a parsimonious explanation for the diffuse nuclear accumulation of AR that is found in SBMA patient tissue, a phenomenon that correlates with increasing polyglutamine length (Adachi et al., 2005). The mechanism by which polyglutamine expansion amplifies AR nuclear activity will be an important focus for future studies, and may in fact lead to additional therapeutic targets.

Appendix I:

B2 attenuates polyglutamine-expanded androgen receptor toxicity in cell and fly models of spinal and bulbar muscular atrophy

B2 attenuates polyglutamine-expanded androgen receptor toxicity in cell and fly models of spinal and bulbar muscular atrophy

Isabella Palazzolo[1,2], Natalia B. Nedelsky[3,4], Caitlin E. Askew[1], George G. Harmison[1], Aleksey G. Kasantsev[5], J. Paul Taylor[3], Kenneth H. Fischbeck[1], Maria Pennuto[6] *

[1]Neurogenetics Branch, NINDS, NIH, Bethesda, Maryland

[2]Instituto di Endocrinologia, Universitá degli Studi di Milano, Milan, Italy

[3]Department of Developmental Neurobiology, St. Jude Children's Research Hospital, Memphis, Tennessee

[4]Neuroscience Graduate Group, University of Pennsylvania, Philadelphia, Pennsylvania

[5]Department of Neurology, Harvard Medical School, Massachusetts General Hospital, Boston, Massachusetts

[6]Department of Neuroscience, Italian Institute of Technology, Genoa, Italy

*Correspondence to Maria Pennuto, Department of Neuroscience and Brain Technologies, Italian Institute of Technology, Via Morego 30, Genoa, 16163 Italy

Abstract

Expanded polyglutamine tracts cause neurodegeneration through a toxic gain-of-function mechanism. Generation of inclusions is a common feature of polyglutamine diseases and other protein misfolding disorders. Inclusion formation is likely to be a defensive response of the cell to the presence of unfolded protein. Recently, the compound B2 has been shown to increase inclusion formation and decrease toxicity of polyglutamine-expanded huntingtin in cultured cells. We explored the effect of B2 on spinal and bulbar muscular atrophy (SBMA). SBMA is caused by expansion of polyglutamine in the androgen receptor (AR) and is characterized by the loss of motor neurons in the brainstem and spinal cord. We found that B2 increases the deposition of mutant AR into nuclear inclusions, without altering the ligand-induced aggregation, expression, or subcellular distribution of the mutant protein. The effect of B2 on inclusions was associated with a decrease in AR transactivation function. We show that B2 reduces mutant AR toxicity in cell and fly models of SBMA, further supporting the idea that accumulation of polyglutamine-expanded protein into inclusions is protective. Our findings suggest B2 as a novel approach to therapy for SBMA.

Introduction

Polyglutamine diseases are late-onset, inherited neurodegenerative diseases caused by expansion of CAG repeats encoding polyglutamine tracts in nine different genes (Orr and Zoghbi, 2007). Expansion of polyglutamine in the androgen receptor (AR), huntingtin,

103

atrophin 1, and ataxin-1, -2, -3, -6, -7, and -17 causes spinal and bulbar muscular atrophy (SBMA), Huntington's disease, dentatorubral-pallidoluysian atrophy, and six types of spinocerebellar ataxia, respectively. All the polyglutamine diseases are inherited in an autosomal dominant fashion, except for SBMA, which is X-linked (La Spada et al., 1991) and gender-specific (Katsuno et al., 2002; Schmidt et al., 2002; Yu et al., 2006). There is no available effective therapy for SBMA and the other polyglutamine diseases, although several therapeutic approaches have been proposed to date (for review see (Pennuto and Fischbeck, 2010). Polyglutamine diseases share several features, such as a positive correlation between repeat length and disease severity and the phenomenon of genetic anticipation, which causes the next generation to inherit a longer repeat than the previous one, and so to have an earlier age of onset or a more severe phenotype. Expansion of polyglutamine confers a toxic gain of function on the mutant protein. Evidence also indicates a contribution of loss of protein function to the disease pathogenesis (Zuccato et al., 2001; Thomas et al., 2006; Lim et al., 2008). Although disease-specific features imply the contribution of protein-specific features in polyglutamine disease pathogenesis, the observation that the same mutation in nine unrelated genes causes neurodegeneration suggests a common disease mechanism.

Expansion of polyglutamine leads the protein to acquire a stable, non-native -sheet conformation (Perutz et al., 1994), which results in protein unfolding and deposition into microaggregates and inclusions (Ross and Poirier, 2004). Microaggregates are small oligomeric species detectable by biochemistry (Taylor et al., 2003b; Li et al., 2007; Palazzolo et al., 2009). Inclusions are large macromolecular species detectable primarily

by immunohistochemistry (Taylor et al., 2003b). Inclusions contain several cellular constituents, including molecular chaperones and components of the ubiquitin-proteasome system and autophagic degradation (Garcia-Mata et al., 1999; Wigley et al., 1999; Taylor et al., 2003b). The observation that polyglutamine-positive inclusions are present in the nuclei of the degenerating neurons from patients and animal models of polyglutamine diseases led to the idea that inclusions are toxic species (for review see (Taylor et al., 2002). Toxicity was attributed to sequestration of essential cellular constituents and aberrant protein-protein interactions, with consequent disruption of cellular homeostasis (Gidalevitz et al., 2006). However, a series of findings has not only dissociated inclusions from neurodegeneration (Saudou et al., 1998; Cummings et al., 1999; Slow et al., 2005; Rub et al., 2006) but also highlighted a protective role for inclusions in neurodegenerative diseases (Taylor et al., 2003b; Arrasate et al., 2004). These findings suggest that enhancing inclusion formation may be a therapeutic target for polyglutamine diseases. The compound B2 (5-[4-(4-chlorobenzoyl)-1-piperazinyl]-8-nitroquinoline) has been shown to increase inclusion formation and reduce the toxicity of mutant huntingtin *in vitro* (Bodner et al., 2006).

Here we investigated the effect of B2 on SBMA. We show that B2 increases formation of mutant AR-positive nuclear inclusions, without altering mutant AR ligand-dependent aggregation, expression, or subcellular localization. The effect of B2 on inclusions correlates with a reduction of AR transactivation, which is not due to altered ligand binding. Finally, we show that B2 reduces the toxicity of mutant AR in both cell and fly models of SBMA. Our results provide evidence that B2 reduces the toxicity of mutant

AR by increasing the deposition of the protein into inclusions and highlight B2 as a potential therapy for SBMA.

Materials and Methods

Plasmids

The pCMV-AR65Q-K632A,K633A and pARE-E1b-luc expression vectors were kindly provided by Drs. A. Lieberman (University of Michigan, Ann Arbor, MI) and C. Smith (Baylor College of Medicine, Huston, TX), respectively; pFHRE-luc reporter vector was purchased from Addgene.

Cell Cultures and Transfections

HEK293T (ATCC, CRL-1573) and PC12-TET ON cells stably expressing AR112Q (Walcott and Merry, 2002) were cultured as previously described (Walcott and Merry, 2002; Palazzolo et al., 2007). HEK293T cells (6 x 10^5) were transiently transfected with 1 g DNA using Lipofectamine Plus (Invitrogen, Carlsbad, CA). PC12-AR112Q cells (8 x 10^5) were cultured on collagen-coated dishes for 24 hr in differentiation medium (1% heat-inactivated horse serum, 5% heat-inactivated charcoal-stripped fetal bovine serum, 4 mM glutamine, 100 U/ml penicillin, 100 g/ml streptomycin, 132 g/ml G-418, 70 g/ml hygromycin B, and 100 ng/l nerve growth factor) in the presence of doxycycline (10 g/l; Calbiochem, La Jolla, CA) and treated with B2 (3448-6548; ChemDiv, San Diego, CA) and R1881 (Sigma, St. Louis, MO) at the indicated concentrations. Motor neuron-derived MN-1 cells stably expressing AR65Q were previously described (Brooks et al., 1997).

106

The cells were maintained in culture in the presence of G418 (350 g/ml), plated (1 x 10^6 cells) in charcoal-dextran-stripped fetal bovine serum (HyClone, Logan, UT)-containing medium for 48 hr and processed for caspase 3 assay. Where indicated, the cells were treated with staurosporin (1 M) for 6 hr and z-VAD-FMK (30 M) for 48 hr.

Immunocytochemistry and Microscopy

PC12 cells were grown for 24 hr on collagen-coated dishes in differentiation medium, induced for 4 hr with doxycycline, pretreated for 20 hr with B2 (10 M), and then treated for 48 hr with R1881 (10 nM) and B2. Immunofluorescence was performed as previously described (Palazzolo et al., 2007). The person who analyzed the images was blind for the treatments. For the graph in Figure A1.1A, the cells treated with R1881 together with either vehicle or B2 were classified into cells with diffuse nuclear AR or cells with nuclear inclusions. The percentage of cells with nuclear inclusions was calculated for each treatment. Data in the graph represent the fold increase in the number of cells with nuclear inclusions in the B2/R1881-treated sample compared with the R1881-treated sample, which was set as 1. The graph represents the average of four independent experiments; in each experiment, three different fields (n = 150 cells) for each treatment were analyzed.

Western Blotting and Nuclear/Cytoplasmic Fractionation

For Western blotting, cells were washed in ice-cold 1x PBS and scraped in lysis buffer [150 mM NaCl, 6 mM Na2HPO4, 4 mM NaH2PO4, 5 mM ethylenediaminetetraacetic acid, 1% Na-deoxycholate, 1% Triton X-100, 0.1% sodium dodecyl sulfate (SDS)] plus

protease inhibitor cocktail (Roche Diagnostics, Indianapolis, IN). The lysate was

sonicated and then centrifuged at 18,000g for 10 min at 4°C. Cell lysates were denatured

at 95°C in 5x sample buffer (60 mM Tris, pH 6.8, 2% SDS, 25% glycerol, 0.1%

bromophenol blue, 20% -mercaptoethanol) and processed for 7.5-10% SDS-

polyacrylamide gel electrophoresis (SDS-PAGE) and electrotransferred to a PVDF

membrane (Millipore, Bedford, MA). Immunoblottting was done in 5% nonfat dry milk

in Tris-buffered saline. Antibodies used were anti-AR (N20; sc-816; Santa Cruz

Biotechnology, Santa Cruz, CA), anti-tubulin (T6199; Sigma), anti-Hsp90 (SPA-830;

Assay Design), anti-Hsp40 (SPA-400; Assay Design), anti-Hsp70 (Spa810; Assay

Design), and anti-actin (sc-1616; Santa Cruz Biotechnology). Immunoreactivity was

detected using peroxidase-conjugated AffiniPure goat anti-rabbit or anti-mouse IgG

(Jackson Immunoresearch, West Grove, PA), and visualized using Lightning

chemiluminescence reagent (Perkin Elmer, Norwalk, CT), following the manufacturer's

instructions. Nuclear/cytosolic fractionation was performed per manufacturer's

instructions (NE-PER; Pierce, Rockford, IL).

XTT, Caspase 3, Ligand Binding, and Transcriptional Assays

Caspase 3 activity, cell survival (XTT assay), and transcriptional activity were measured

according to manufacturers' instructions using the ApoTarget fluorometric assay

(Biosource International, Camarillo, CA), Cell Proliferation Kit II (Roche Diagnostics),

and LucLite Luminescence Reporter Gene Assay System (Perkin Elmer), respectively.

For the XTT assay, the cells were incubated in aphidicolin (0.4 g/ml; Calbiochem) to

inhibit cell proliferation. For transcriptional assay to measure AR transactivation, cells

were transfected with pARE-E1b-luc reporter vector, pre-treated for 24 hr with B2 at the

indicated concentrations, and incubated with the ligand together with either B2 or vehicle

for other 24 hr. For FOXO-mediated transcriptional activity, cells were transfected with

pFHRE-luc reporter vector, pre-treated with B2 for 24 hr, and incubated with IGF-1 or

under serum-deprivation conditions for 24 hr prior to the assay. To normalize for

transfection efficiency, luciferase activity was compared with β-galactosidase activity.

For the ligand binding assay, 24 hr after transfection, HEK293T cells were incubated for

2 hr in 0.5% bovine serum albumin and 10 M triamcinolone acetonide in Dulbecco's

modified Eagle's medium (binding medium) with 10 nM [^{3}H]R1881 (72.0 Ci/mmol;

Perkin Elmer). Specific binding of [^{3}H]R1881 was calculated as previously described

(Palazzolo et al., 2007).

SBMA Flies

Generation of transgenic flies expressing AR52Q was previously described (Pandey et

al., 2007b). *Drosophila* stocks were crossed on standard cornmeal agar media at 29°C.

GMR-GAL4 virgin females were mated to UAS-AR52Q male flies on media containing

either 1 mM dihydrotestosterone (DHT) + 0.5% DMSO or 1 mM DHT + 50 M B2

diluted in DMSO. The phenotype of female flies was assessed blindly on day 1 post-

eclosion. The scoring method was modified from (Pandey et al., 2007b), as follows: 1

point for presence of bristle phenotype (supernumerary interommatidial bristles or

abnormal bristle orientation), 1 point for presence of ommatidial phenotype (fusion or

disorganization), 1 point for ommatidial pitting, 3 points for retinal collapse, 3 points if

the phenotype covered more than 20% of the eye, 6 points if the phenotype covered more

than 50% of the eye. The number of flies analyzed was n = 45 for DHT + vehicle and n =

57 for DHT + B2.

Statistical Analysis

Each experiment was repeated a minimum of three times. One-way ANOVAs were used

to evaluate the effect of B2 and ligand among treatment groups. Two-sample t-tests were

used for post hoc comparisons.

Results

B2 Increases the Formation of AR-Positive Nuclear Inclusions in Cultured Cells

B2 increases the deposition of mutant huntingtin into inclusions (Bodner et al., 2006). We

asked whether B2 has similar effect on mutant AR. Mutant AR accumulates into nuclear

inclusions in motor neurons in patients (Katsuno et al., 2006). Generation of mutant AR-

positive nuclear inclusions with features similar to those observed in patient tissues can

be reproduced in an inducible PC12 cell line, which expresses human full-length AR with

112 glutamine residues (PC12-AR112Q; (Walcott and Merry, 2002)). In these cells,

transgene AR expression is induced by treatment of the cells with doxycycline, and

inclusion formation is promoted by exposure of the cells to androgens (Walcott and

Merry, 2002). To test whether B2 affects inclusion formation in SBMA, the PC12-

AR112Q cells were treated with doxycycline and the synthetic androgen analog R1881

together with either vehicle or B2, and the AR-positive inclusions were detected by

immunocytochemistry using the AR-specific antibody N20 (Figure A1.1A). In the

110

absence of ligand, mutant AR localizes in the cytosol. Treatment of the cells with ligand resulted in nuclear translocation and formation of AR-positive nuclear inclusions. Treatment of the cells with B2 did not induce AR inclusion formation in the absence of ligand. Instead, treatment of the cells with B2 in the presence of ligand significantly increased the number of cells with nuclear inclusions by 13% compared with the cells exposed to ligand alone. Expansion of polyglutamine leads the mutant protein to form not only inclusions but also microaggregates (Taylor et al., 2002; Ross and Poirier, 2004). Mutant AR-positive microaggregates can be detected by Western blotting as high-molecular-weight species accumulating in the stacking portion of polyacrylamide gels (Palazzolo et al., 2009). Therefore, we asked whether B2 affects mutant AR aggregation in the PC12-AR112Q cells (Figure A1.1B). Treatment of the cells with ligand significantly increased AR aggregation. Treatment of the cells with B2 increased mutant AR aggregation in the absence of ligand but did not affect the biochemical aggregation of mutant AR induced by ligand.

To investigate whether the effect of B2 on AR inclusions is due to an increase in the AR expression levels, we analyzed the levels of human AR mRNA (Supplemental Figure A1.1A) and protein (Figure A1.1B). By real-time PCR and Western blotting analyses, we found that neither the levels of transgene AR transcript nor the levels of monomeric mutant AR protein change upon B2 treatment. Then, we asked whether B2 increases nuclear inclusion formation because it increases the translocation of mutant AR into the nucleus. To test this, we performed nuclear/cytosolic fractionation in HEK293T cells transiently transfected with vector expressing mutant AR with 65 glutamine residues

111

(AR65Q) and treated with R1881 together with either vehicle or B2 (Figure A1.1C). B2 did not change the amount of AR accumulating in the nucleus in the presence of ligand. Because AR interacts with the heat shock proteins (Hsps; (Poletti, 2004)), we asked whether the effect of B2 occurs through induction of Hsp90, Hsp70, and Hsp40 (Figure A1.1D). Expression of these proteins was analyzed by Western blotting in the PC12-AR112Q cells. Treatment of the cells with B2 did not alter the levels of expression of Hsp90, Hsp70, and Hsp40 in either the absence or the presence of ligand, indicating that the B2 effect on AR inclusion is independent of the Hsps. Collectively, these results indicate that B2 increases the deposition of mutant AR into nuclear inclusions without affecting AR ligand-dependent aggregation, expression, or subcellular distribution in cultured cells.

B2 Alters AR Function

AR is a transcription factor activated by androgens (Poletti, 2004). We reasoned that B2 by entrapping mutant AR into macromolecular complexes may alter the ability of AR to activate transcription. We tested this hypothesis in HEK293T cells transiently transfected with an expression vector encoding AR65Q together with a reporter vector in which luciferase expression is driven by a regulatory region containing three androgen-responsive elements (ARE), as previously described (Palazzolo et al., 2007). The cells were treated with vehicle or B2 (10 M) and increasing amounts of R1881 (from 0.1 to 10 nM), and AR transactivation was measured by luciferase assay (Figure A1.2A). Treatment of the cells with R1881 induced mutant AR transactivation in a dose-dependent fashion. Treatment of the cells with B2 significantly reduced the AR

112

transactivation induced by ligand. As with the effect of B2 on AR inclusions observed in the PC12-AR112Q cells, the effect of B2 on mutant AR transcription observed in HEK293T cells was not due to a decrease in transgene mRNA transcript or protein levels (Supplemental Figure A1.1B). To investigate whether the effect of B2 also occurs on non-expanded AR and is dose-dependent, we treated cells transfected with either normal or mutant AR with a constant dose of R1881 (10 nM) and a range of concentrations of B2 from 1 M to 10 M (Figure A1.2B). The effect of B2 on polyglutamine AR transactivation was dose-dependent. At 1 M, B2 slightly increased normal, but not mutant, AR transactivation, whereas, at 5 M, B2 had no significant effect on either normal or mutant AR transcription. At 10 M, B2 reduced both normal and mutant AR transactivation. Similar results were obtained with B21 (Supplemental Figure A1.2), which is a compound structurally similar to B2 and that has been shown to have the same effect as B2 on mutant huntingtin inclusion formation (Bodner et al., 2006). It is relevant to note that B21 had no effect on normal AR transactivation.

One explanation for the effect of B2 on AR transactivation is the recruitment of AR into inclusions. However, we explored other possibilities. To rule out the possibility that treatment of the cells with B2 disrupts the cellular transcription machinery, we tested whether B2 alters the transcription mediated by FKHRL1, a member of the Forkhead family of transcription factors (Brunet et al., 1999). The Forkhead transcription factors are active in the absence of survival factors, a condition that we reproduced here by serum deprivation, and are inactivated by the insulin-like growth factor 1 (IGF-1) through Akt phosphorylation. HEK293T cells were transfected with a reporter vector in which the

113

luciferase gene is under the control of the forkhead-responsive element (pFHRE-luc; (Holtz-Heppelmann et al., 1998)). As expected, transcription of the reporter gene was observed upon serum starvation and was decreased by IGF-1 treatment (Figure A1.2C). Treatment of the cells with B2 did not have any effect on this reporter. These results indicate that B2 does not alter the cellular transcription machinery. Moreover, these data suggest that the effect of B2 on transcription is likely to be specific to mutant AR.

B2 has recently been shown to have inhibitory activity against sirtuin 2 (SIRT2) microtubule deacetylase (Outeiro et al., 2007). Normal AR is acetylated at specific lysine residues lying in the acetylation consensus site KXKK at position 630-633 (NM_000044), where K is lysine and X any amino acid (Fu et al., 2000). To test whether B2 reduces AR transactivation through acetylation at this site, we used an acetylation-defective mutant AR in which the lysine residues were replaced by alanine (AR65Q-K632A,K633A; (Thomas et al., 2004)). In HEK293T cells, the acetylation-defective mutant had enhanced transactivation compared with the non-substituted AR (Figure A1.2D). Similar results were obtained with the non-polyglutamine-expanded AR (Supplemental Figure A1.3). This is consistent with previous results obtained with non-polyglutamine-expanded AR but different promoter regions (Haelens et al., 2007; Faus and Haendler, 2008). B2 treatment decreased the transactivation of the acetylation-defective mutant, indicating that B2 effect on AR transactivation does not occur through regulation of acetylation at lysines 632 and 633.

Because AR transactivation is strikingly ligand dependent (Poletti, 2004), we wondered

whether B2 works as a competitive antagonist. To test this, we incubated HEK293T cells

transiently expressing AR65Q cells with nonmetabolizable radioactive ligand [^{3}H]R1881

and measured the displacement of radioactive bound R1881 by increasing amounts of B2

(Figure A1.2E). If B2 competes with R1881 for binding to the same site, incubation of

the cells with increasing concentrations of B2 is expected to result in a dose-dependent

displacement of radioactive ligand from the AR. As positive control, we treated the cells

with increasing amounts of cold R1881. B2 did not displace the bound [^{3}H]R1881,

whereas cold R1881 completely displaced [^{3}H]R1881 at 100 nM and 1 M, as expected.

These data indicate that B2 does not compete for binding to the same site on the mutant

AR where androgens bind, thereby excluding the possibility that B2 acts as a competitive

antagonist of AR. At high doses, B2 inhibits normal AR transactivation (Figure A1.2B).

To rule out the possibility that B2 alters binding of normal AR to ligand, we measured

ligand binding in HEK293T cells transfected with normal AR as previously described

(Palazzolo et al., 2007). We found that B2 does not alter the binding of ligand to normal

AR (Figure A1.2F). Altogether, these results show that B2 specifically decreases mutant

AR transactivation in a manner that is independent of acetylation at the KXKK site and

does not affect ligand binding. Rather, these results are consistent with the idea that the

B2-induced formation of AR-positive inclusions results in a reduction of AR function.

B2 Reduces the Toxicity of Mutant AR in Cultured Cells

Because increased accumulation of polyglutamine-expanded proteins into inclusions has

been correlated with reduced toxicity in both cell and animal models of polyglutamine

disease (Taylor et al., 2003b; Arrasate et al., 2004), we asked whether B2 attenuates the toxicity of mutant AR. We tested this in the PC12-AR112Q cells. The cells were treated with R1881 and either vehicle or B2, and cell viability was measured by XTT assay (Figure A1.3A). Treatment of the cells with increasing concentrations of R1881 resulted in a dose-dependent decrease in cell viability (Figure A1.3A, open bars). Treatment of the cells with B2 significantly increased cell viability by 29% compared with the cells treated with ligand alone (Figure A1.3A, solid bars). Similar results were obtained measuring cell death by propidium iodide incorporation (Supplemental Figure A1.4A).

SBMA is characterized by the loss of lower motor neurons from spinal cord and brainstem (Adachi et al., 2007). Therefore, we asked whether B2 has any effect on mutant AR toxicity in motor neuron-derived MN-1 cells stably expressing polyglutamine-expanded AR with 65 glutamine residues (AR65Q; (Brooks et al., 1997)). Although these cells do not show ligand-dependent toxicity, they do show polyglutamine length-dependent toxicity. Indeed, we have previously shown that expression of polyglutamine-expanded AR in these cells results in increased caspase 3 activity and reduced cell viability compared with cells expressing non-polyglutamine-expanded AR (Palazzolo et al., 2007). Treatment of the mutant MN-1 cells with B2 reduced caspase 3 activation by 31% (Figure A1.3B). The effect of B2 on toxicity was specific to polyglutamine-dependent caspase 3 activation, as B2 did not have any effect on caspase 3 activation induced by staurosporin (Figure A1.3, inset). We also asked whether the B2 analog compound B21 impacts the toxicity of mutant AR in the MN-1 cells. Similarly to B2, B21 reduced the caspase 3 activation induced by mutant AR (Supplemental. Figure

116

A1.4B). These results indicate that B2 attenuates the toxicity of mutant AR in cell cultures.

B2 Protects Flies from the Toxicity Induced by Mutant AR

Next, we sought to determine whether B2 counteracts mutant AR-induced neurodegeneration *in vivo*. With this aim, we used transgenic flies that express mutant AR with 52 glutamine residues (AR52Q; (Takeyama et al., 2002; Pandey et al., 2007b)). Flies expressing polyglutamine-expanded AR recapitulate the unique feature of SBMA, which is the ligand dependence of the disease (Pandey et al., 2007b). Transgenic flies expressing AR52Q in the eye do not show any sign of neurodegeneration in the absence of hormone (Pandey et al., 2007b). In contrast, the flies show alteration of the eye phenotype when fed with the AR natural ligand dihydrotestosterone (DHT; Figure A1.4). Exposure of the flies to B2 together with ligand attenuated the extent of damage. To quantify the effect of B2 on disease severity, we analyzed the phenotype of about 50 flies per group and scored the disease severity as described in Materials and Methods (Figure A1.4, middle panel). We found that B2 treatment significantly decreased the extent of alteration of the eye phenotype in this fly model of SBMA. The effect of B2 was not due to a decrease in the level of expression of the mutant AR (Figure A1.4, bottom panel). This is the first evidence that B2 protects against polyglutamine-expanded toxicity *in vivo*. These results are important, because they highlight B2 as a novel potential therapy for SBMA.

Discussion

The current study tested the effect of B2 on SBMA. We found that B2 increases deposition of mutant AR into inclusions. This was associated with reduced transactivation of mutant AR. Furthermore, we show that B2 reduces the toxicity of mutant AR in cell models of the disease. We show for the first time that B2 attenuates polyglutamine-expanded toxicity *in vivo*. Our results provide further evidence that inclusions represent a protective response of the cell to cope with misfolded protein. Moreover, because we found that the increased accumulation of mutant AR into inclusions correlates with decreased AR function, we speculate that B2 attenuates polyglutamine-expanded toxicity through a mechanism that involves compartmentalization of the mutant protein and reduction of native protein function. Finally, we propose B2 as a potential therapy for SBMA.

B2 Increases the Compartmentalization of Mutant AR Into Inclusions and Reduces Toxicity

B2 was isolated from a drug screen to increase the formation of inclusions while reducing proteasome dysfunction in cell models of Huntington's disease (Bodner et al., 2006). B2 has a similar effect on α-synuclein toxicity, suggesting a general protective role in protein misfolding diseases, such as Parkinson's disease. We report that B2 increases inclusion formation in cell models of SBMA. It is relevant to note that, unlike the case in Huntington's disease, B2 does not induce AR inclusion formation per se. In the absence of ligand, a condition in which there is no effect on inclusion formation, B2 increases the accumulation of mutant AR into microaggregates, further suggesting that inclusions and

microaggregates behave differently. In contrast, B2 increases the deposition of mutant AR into inclusions in the presence of ligand. This suggests that the effect of B2 occurs at a stage that follows ligand binding. A unique feature of SBMA among the polyglutamine diseases is gender specificity. In SBMA, only males show full disease symptoms, and this is a result of high levels of circulating androgens in the serum. In the absence of ligand, AR is in the cytosol in an inactive state bound to Hsps, such as Hsp90, Hsp70, and Hsp40. Ligand binding induces a conformational change, which results in dissociation from the Hsps, translocation to the nucleus, and generation of inclusions. AR-positive inclusions have been found in motor neurons from SBMA patients (Li et al., 1998) as well as in cultured cells (Walcott and Merry, 2002). We explored the mechanism through which B2 increases formation of mutant AR-positive inclusions. We tested whether the induction of inclusion formation in the nucleus is a consequence of increased expression of the mutant protein or increased nuclear translocation. However, we did not find any difference in mutant AR expression or in the ligand-induced nuclear translocation in the presence or absence of B2. We also tested whether the mechanism through which B2 works involves the induction of the Hsps, such as Hsp90, Hsp70, and Hsp40. However, we could not detect any change in expression of these Hsps. From these results, we excluded the possibility that the effect of B2 on mutant AR toxicity and inclusion formation is due to an alteration of chaperone levels. These results are consistent with a previous report that B2 attenuates polyglutamine-expanded huntingtin toxicity through a mechanism that does not involve chaperone activity (Bodner et al., 2006).

Although inclusions had initially been considered toxic, the observations that accumulation of mutant huntingtin into inclusions in cultured striatal neurons inversely correlates with cell death (Arrasate et al., 2004) and that drugs that interfere with the ability of the cell to form inclusions cause cell death (Taylor et al., 2003b) suggest a protective role for inclusions. Consistent with this model, mutant AR has been shown to accumulate more frequently and extensively in a diffuse nuclear pattern rather than in nuclear inclusions, with the extent of diffuse nuclear accumulation correlating with polyglutamine repeat length (Adachi et al., 2005). We show here that B2 decreases the toxicity of mutant AR not only in cultured cells but also in a fly model of SBMA. B2 had no effect on the toxicity induced by agents, such as staurosporin, that cause apoptosis independently of inclusion formation (Tamaoki et al., 1986; Matsumoto and Sasaki, 1989). However, we cannot exclude additional effects of B2 on cellular toxicity independent of polyglutamine inclusion formation. Our results provide the first evidence that B2 counteracts the toxicity of polyglutamine-expanded protein *in vivo* and suggest that agents that promote the deposition of unfolded proteins into inclusions may have therapeutic potential.

B2 Alters Mutant AR Function in Cultured Cells

Recent evidence suggests that altered protein function is an important component of polyglutamine disease pathogenesis (Lim et al., 2008). AR is a transcription factor activated by the male hormones testosterone and its derivative DHT (Poletti, 2004). Upon ligand binding, AR translocates to the nucleus to activate transcription of those genes whose regulatory regions contain specific androgen-responsive element sequences.

Polyglutamine-expanded AR has been shown to have altered transcriptional activity in motor neuron-derived cells, which may contribute to disease pathogenesis (Lieberman et al., 2002). We found that B2 reduces AR transactivation in cultured cells without disrupting the general cellular transcription machinery. Although this is unlikely, B2 might have a repressive effect on the transactivation of other steroid receptors whose structure is similar to that of AR. Were this to occur, B21 might represent a valid alternative to B2. In fact, we found that B21 has no effect on normal AR transactivation, suggesting that it specifically targets the disease protein.

B2 inhibits activity of SIRT2 deacetylase, catalyzing the NAD+-dependent reaction of acetyl group removal from lysine residues of protein substrates such as α-tubulin and histones (Outeiro et al., 2007). Acetylation of non-polyglutamine-expanded AR at the KXKK acetylation consensus site is important for AR transactivation (Fu et al., 2003) and is regulated by sirtuin activity (Fu et al., 2006). However, when we tested whether B2 affects transactivation of an acetylation-defective AR, we found that B2 is still active on this AR variant, indicating that B2 does not require this site to alter AR function. Rather, B2 may affect AR transcription by regulating acetylation of AR at different lysine residues or through a mechanism that is independent of AR acetylation. The observation that B2 increases the deposition of mutant AR into inclusions, while decreasing AR function and toxicity, leads us to speculate that, by increasing the compartmentalization of mutant AR into inclusions, B2 affects AR function and reduces mutant AR toxicity.

Is B2 a Potential Therapy for SBMA?

There is no effective therapy available for SBMA. A unique feature of SBMA among the polyglutamine diseases is gender specificity. This feature of SBMA has been reproduced in animal models of the disease, including mice (Katsuno et al., 2002; Yu et al., 2006) and flies (Takeyama et al., 2002; Pandey et al., 2007b), and may be attributed to androgen-dependent toxicity of the mutant AR protein. The androgen dependence of the disease offers the opportunity to develop therapy based on the reduction of testosterone levels in the serum. Indeed, reduction of testosterone levels by leuprorelin has had promising results in mouse models of SBMA (Katsuno et al., 2003) and, more recently, in a phase 2 clinical trial (Banno et al., 2009). However, the use of anti-androgens can be accompanied by several undesired side effects. We show here that B2 reduces the toxicity of mutant AR in cell cultures and fly models of SBMA. Based on these results, we propose B2 as a novel therapeutic approach for SBMA.

Figures and Legends

Figure A1.1. B2 increases the accumulation of mutant AR into nuclear inclusions.
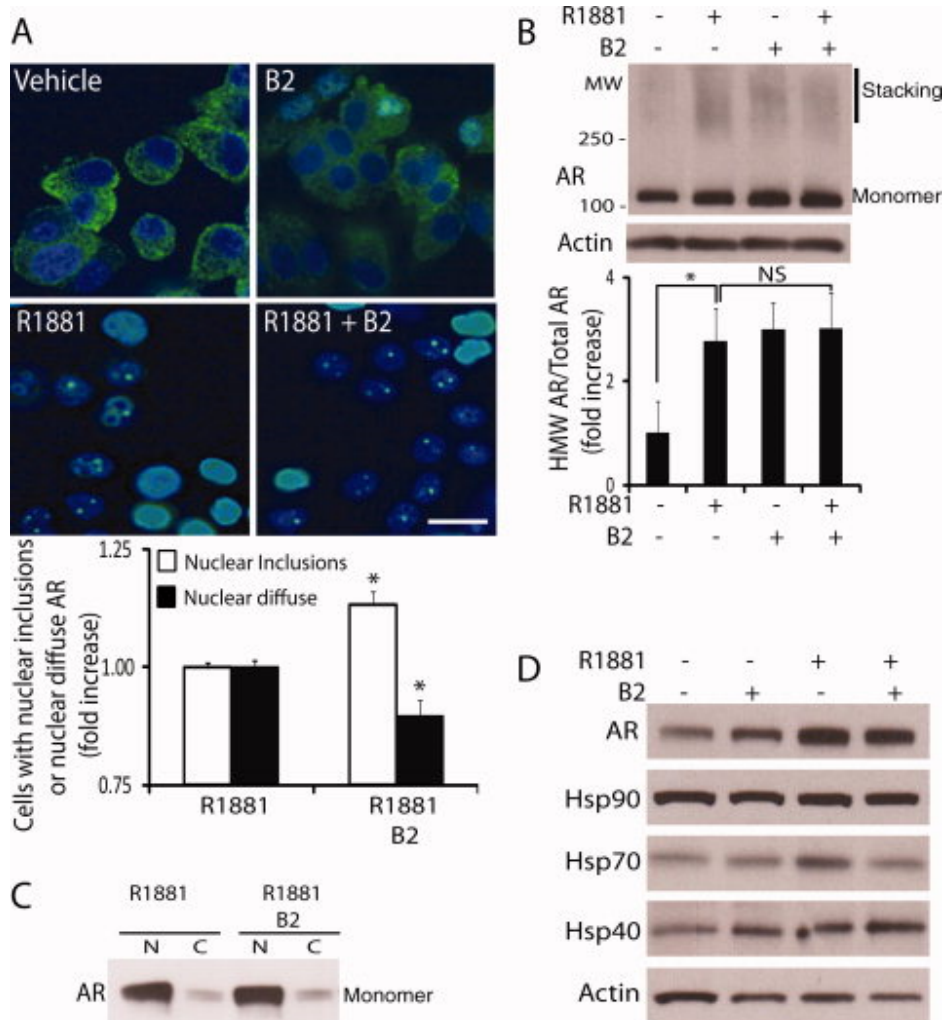
Figure A1.1. B2 increases the accumulation of mutant AR into nuclear inclusions.

A: PC12 cells stably expressing mutant AR (AR112Q) were induced with doxycycline: treated with vehicle, B2 (72 hr), and R1881 (48 hr) as indicated: and processed for immunocytochemistry. AR was detected with N20 antibody (green) and nuclei with DAPI (blue). Quantification of the number of cells with AR-positive nuclear inclusions and of cells with nuclear diffused AR is shown at the bottom. Graph, mean ± sem, n = 4, *P = 0.002 (post hoc t-test). B: Upper panel: Western blotting of PC12-AR112Q cells showing AR protein in cells treated with R1881 and B2 as indicated in A. Actin is shown as loading control. Shown is one experiment representative of three. MW, molecular weight. Bottom panel: Quantification of mutant AR aggregation reveals that B2 increases AR aggregation in the absence of ligand but has no effect on aggregation in the presence of ligand. HMW, high molecular weight. Graph, mean ± sem, n = 3, *P = 0.02; NS, non-significant (post hoc t-test). C: Nuclear-cytoplasmic fractionation of HEK293T cells transiently transfected with vector expressing AR65Q and treated as indicated shows that B2 does not affect nuclear translocation induced by ligand. Shown is one experiment representative of three. N, nuclear fraction; C, cytosolic fraction. D: Western blotting analysis of PC12-AR112Q cells treated as described for A shows that B2 treatment does not change the expression levels of Hsp90, Hsp70, or Hsp40. Actin is shown as loading control. This is one experiment representative of three. Scale bar = 10 μm.

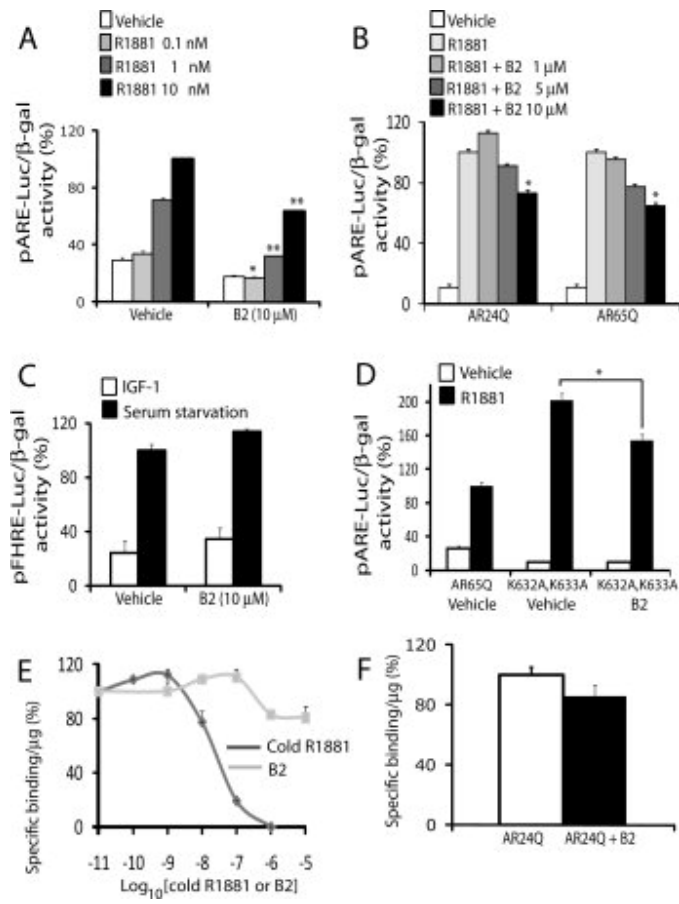**Figure A1.2. B2 alters AR transactivation.**

Figure A1.2. B2 alters AR transactivation. A,B: Transcriptional assay of HEK293T

cells transfected with vectors expressing AR65Q (A) or as indicated (B) and the reporter

vectors pARE-E1b-luc and pCMV for luciferase and β-galactosidase expression,

respectively, and treated with B2 (48 hr) and R1881 (24 hr) shows that B2 reduces

mutant AR transactivation. Data are represented relative to AR65Q-expressing cells

treated with 10 nM R1881, which are set as 100%. Graphs, mean ± sem, n = 3

independent experiments; A: *P = 0.05 and **P = 0.001; B: R1881 10 nM, *P = 0.004

(post hoc t-test). C: Transcriptional assay of HEK293T cells transfected with the pFHRE-

luc and pCMV reporter vectors, treated with B2 (48 hr), and either serum starved or

treated with IGF-1 for 24 hr revealed that B2 does not affect pFHRE reporter activity.

Data were analyzed as described for A. Graph, mean ± sem, n = 3. D: Transcriptional

assay of HEK293T cells transfected with the AR expression vectors indicated and the

reporter vectors as for A shows that B2 is active on the acetylation-defective AR mutant.

Data were analyzed as in A. Graph, mean ± sem, n = 3, *P = 0.02 (post hoc t-test). E:

Ligand binding assay of HEK293T cells transfected with vector expressing AR65Q,

treated with radioactive ligand for 2 hr, then treated with either B2 or cold ligand for 1 hr,

shows that B2 does not compete with ligand for binding to mutant AR. Schatchard

analysis shows that B2 does not compete for binding with radioactive ligand. Graph,

mean ± sem, n = 3 independent experiments. F: Ligand binding assay of HEK293T cells

transiently expressing normal AR and treated with either vehicle (AR24Q) or 10 M B2

(AR24Q + B2) shows that B2 does not alter binding of normal AR to ligand. Graph,

mean ± sem, n = 3 independent experiments.

Figure A1.3
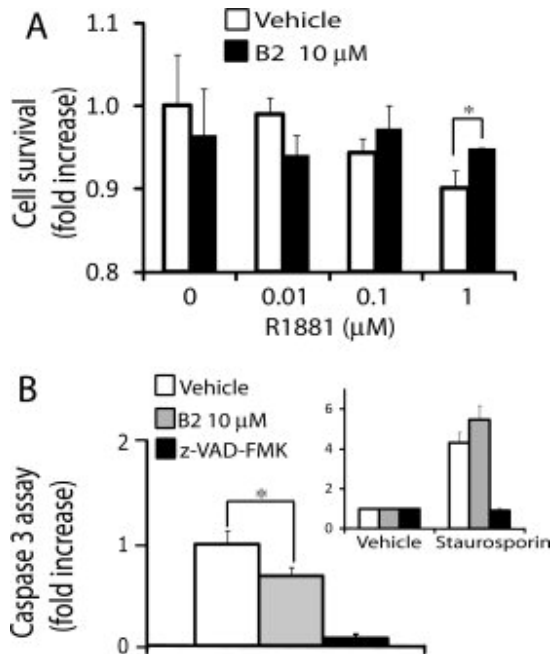
Figure A1.3. B2 reduces the toxicity of mutant AR in cultured cells. A: XTT assay of PC12-AR112Q cells treated with R1881 (48 hr) together with either B2 or vehicle (72 hr) shows that cell survival is decreased by ligand and that this effect is attenuated by B2. Graph, mean ± sem, n = 3, *P = 0.05 (post hoc t-test). B: Caspase 3 assay of MN-1 cells stably expressing AR65Q and treated as indicated for 48 hr shows that B2 decreases caspase 3 activity but has no effect on the caspase 3 activation induced by staurosporin (inset). The caspase inhibitor z-VAD-FMK (10 M, 48 hr treatment) and the caspase activator staurosporin (1 M, 6 hr treatment) were used as controls. Graph, mean ± sem, n = 3, *P = 0.004 (post hoc t-test).

Figure A1.4. B2 attenuates the toxicity of mutant AR in vivo.
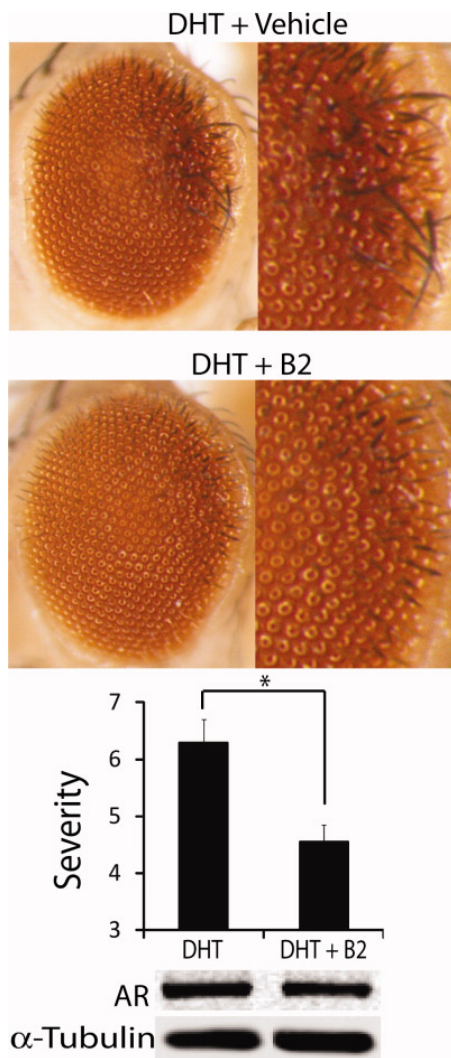
Figure A1.4. B2 attenuates the toxicity of mutant AR in vivo. Upper panel: Transgenic flies expressing AR52Q in the eye were fed with dihydrotestosterone (DHT) and either vehicle or B2. Exposure of the flies to DHT resulted in the alteration of the eye phenotype, which was attenuated by B2. A magnification of the posterior side of the eye is shown on the right of each panel. Middle panel: Quantification of disease severity is shown in the graph (see Materials and Methods). Graph, mean ± sem, n = 45 for the DHT-fed flies and 57 for the DHT/B2-fed flies, *P = 0.001 (two-sample t-test). Bottom panel: Western blotting analysis of AR transgene expression levels reveals that B2 does not change mutant AR expression in flies. Tubulin (Tub) is shown as loading control.

Supplemental Figure A1.1
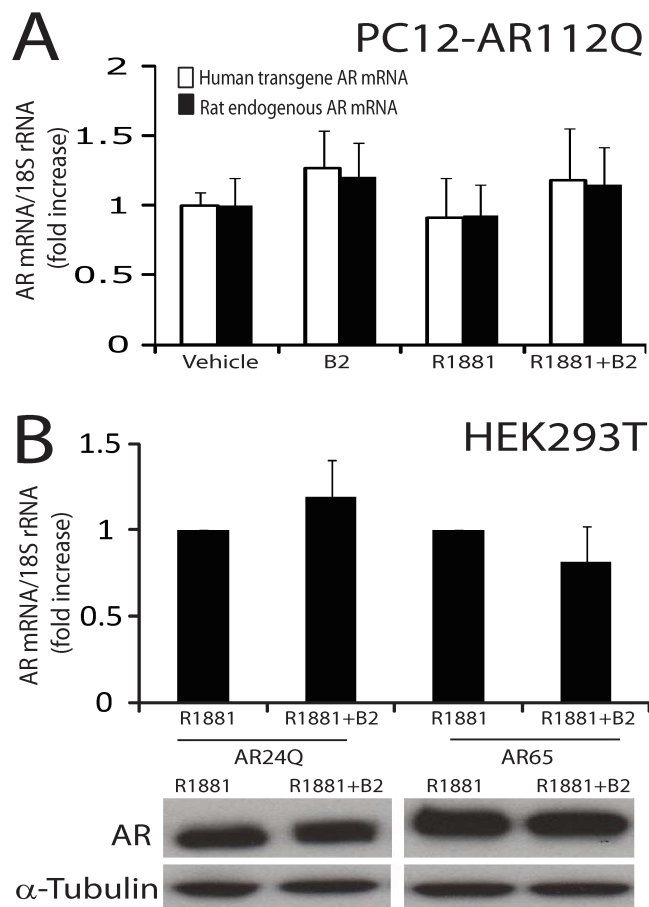
Supplemental Figure A1.1. B2 does not alter AR transcript levels in cultured cells.

Real-time PCR analysis of (A) PC12-AR112Q cells and (B) HEK293T cells transiently

expressing either normal (AR24Q) or mutant (AR65Q) AR and treated with the androgen

analog R1881 together with either B2 or vehicle. The AR mRNA was normalized to 18S

rRNA. Graph, mean ± s.e.m., n = 3. (B, bottom panel) AR protein was detected by

western blotting. Tubulin is shown as loading control.

Supplemental Figure A1.2
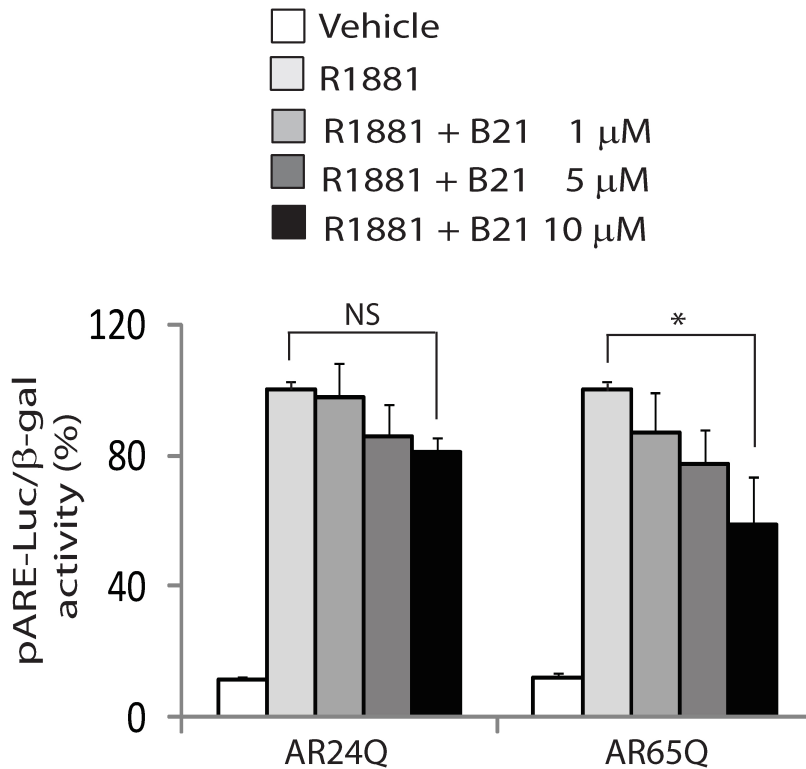
Supplemental Figure A1.2. B21 alters AR function in cultured cells. Transcriptional assay was performed in HEK293T cells transiently transfected with vector expressing either AR24Q or AR65Q and the reporter vectors pARE-E1b-Luc and pCMVβ. The cells were treated with B21 for 48 hours and R1881 (10 nM) for 24 hours as indicated, and processed for luciferase and beta-galactosidase assays. Luciferase activity was normalized to beta-galactosidase activity. Graph, mean ± s.e.m., n = 3, p = 0.001, (post-hoc t-test).

Supplemental Figure A1.3
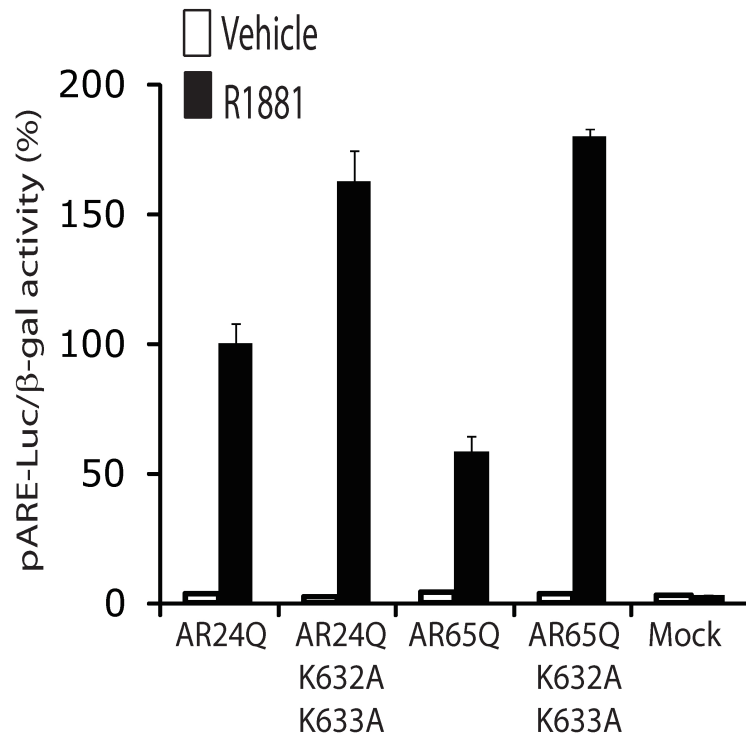
Supplemental Figure A1.3. Acetylation-defective AR has increased transactivation function. Transcriptional assay of HEK293T cells transfected with the indicated AR constructs and the reporter vectors pARE-E1b-Luc and pCMVβ and treated with either vehicle or R1881 for 48 hours shows that lack of acetylation at the KXKK consensus site results in increased AR transactivation. Graph, mean ± s.e.m., n = 3.

Supplemental Figure A1.4
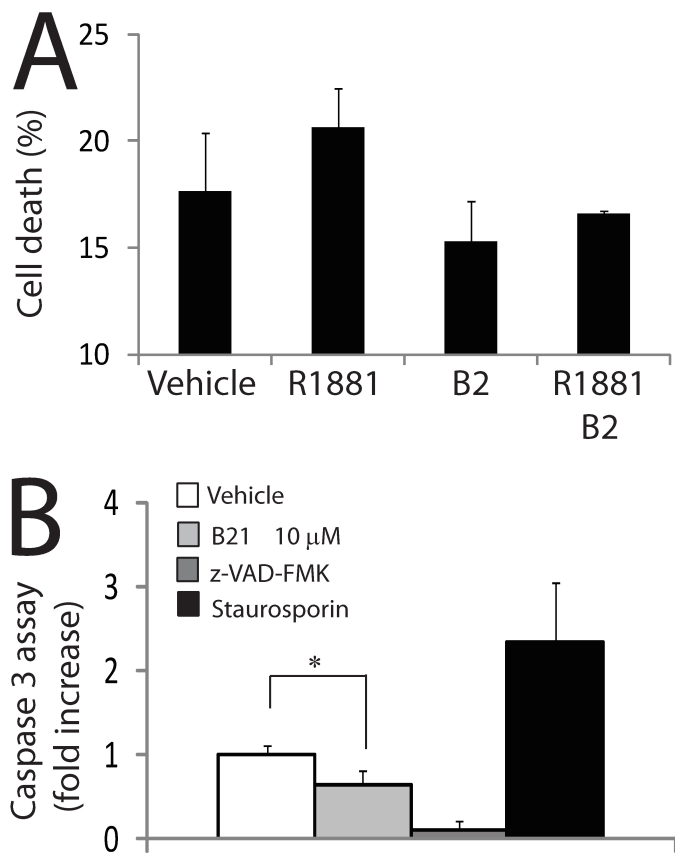
Supplemental Figure A1.4. B2 decreases mutant AR toxicity in cultured cells. A) Propidium iodide incorporation followed by fluorescence-activated cell sorter analysis of PC12-AR112Q cells exposed to ligand and B2 for 48 and 72 hours, respectively, shows that B2 decreases ligand-induced cell death. Graph, mean $\pm$ SD, n = 2. B) Caspase 3 assay of motor neuron-derived MN-1 cells treated with vehicle or B21 for 48 hours shows that B21 decreases caspase 3 activity. Z-VAD-FMK and staurosporin were used as negative and positive controls, respectively. Graph, mean $\pm$ s.e.m., n = 3, p = 0.01 (two-sample t-test).

Appendix II:

Autophagy and the Ubiquitin-Proteasome System –

Protein Catabolism Comes Full Circle

Autophagy and the Ubiquitin-Proteasome System – Protein Catabolism Comes Full Circle

Natalia B. Nedelsky and J. Paul Taylor

Department of Developmental Neurobiology, St. Jude Children's Research Hospital, 262 Danny Thomas Place, Memphis, TN 38120 USA

Abstract

All cells are endowed with two catabolic pathways for degrading protein: the ubiquitin-proteasome system (UPS) and autophagy. While these routes of protein degradation were long considered to be parallel and complementary systems, new evidence has revealed interaction between the UPS and autophagy, suggesting a coordinated relationship that becomes critical in times of cellular stress. Here we introduce the basics and parallels of the UPS and autophagy, review the evidence for cross-regulation of the two systems, and highlight their emerging coordinated relationship. Throughout, we review the evidence suggesting that impairment of autophagy could contribute to the initiation or progression of age-related neurodegeneration.

Introduction

In awarding the Nobel Prize in Chemistry to Aaron Ciechanover, Avram Hershko and Irwin Rose in 2004, the Royal Swedish Academy of Sciences praised these scientists as innovators. After decades of work focusing on how the cell produces proteins, these pioneers had broken with tradition and highlighted the equally important process of how the cell *degrades* proteins. Indeed, the idea that the proteome (a term yet to be invented) was dynamic, with proteins continually synthesized and degraded, was challenged well into the 1950s. What Ciechanover, Hershko, and Rose discovered in the mid-1980s was an exquisitely controlled and efficient system of selectively labeling and targeting proteins for degradation, now well known as the ubiquitin-proteasome system (UPS).

According to Ciechanover, the identification of the UPS marked the end of a long search for a non-lysosomal proteolytic system (Ciechanover, 2005). Although the lysosome had been characterized as a catabolic organelle some 30 years before, several lines of evidence indicated that some portion of intracellular protein degradation could not be explained based on the known mechanisms of lysosomal activity. If the lysosome non-selectively degraded all proteins, one might predict that all proteins would be degraded at approximately the same rate. Yet, empirically, protein half-lives varied widely from a few minutes to as long as several days. Secondly, the discovery that the stability of only a subset of proteins was sensitive to physiological conditions (most notably nutrient availability) was difficult to reconcile with a single, bulk lysosome-based degradation system. A third line of evidence for a non-lysosomal proteolytic system was the differential sensitivity of particular proteins to lysosomal inhibitors, suggesting that distinct groups of proteins are degraded by distinct degradation pathways, only one of which is dependent on lysosomal proteases. Finally, the fact that degradation of some proteins was ATP-dependent suggested that lysosomal proteases (which degrade proteins in an exergonic manner) could not be the sole means of degradation. This delineation between lysosomal- and non-lysosomal-based degradation permitted these astute investigators to intuit an alternative degradation system, culminating in elucidation of the UPS as we understand it today.

The manner in which the UPS was discovered and initially characterized underscored the differences between the UPS and lysosome-mediated degradation. Indeed, for many years these two catabolic pathways were viewed as distinct catabolic pathways with no point of

intersection. Recent years have seen renewed interest in that which the UPS specifically

is *not* – that is, relatively non-selective bulk degradation of intracellular proteins that

requires lysosomal proteases – a process broadly defined as *autophagy*. The recent

heightened interest in autophagy, combined with the wealth of knowledge of the UPS,

has highlighted the similar goals of the two catabolic pathways: first, their

complementary role in recycling macromolecules, and second, their turnover of

misfolded and/or damaged proteins. Further studies have begun to identify functional and

physical interactions between the two systems, uncovering what may be a hierarchical

relationship between the pathways. Thus the two systems that were identified based on

their differences are presently being revealed to be surprisingly similar and intimately

interrelated.

The UPS and Autophagy: A Division of Labor

The distinctions used by researchers in the 1980s to differentiate the UPS from autophagy

remain the key characteristics of these systems as they are defined today. The UPS is a

highly selective catabolic process which serves as the primary route of degradation for

thousands of short-lived proteins, many of which serve regulatory functions in such key

processes as cell cycle control, transcriptional regulation, and signal transduction. An

important class of substrates for degradation by the UPS is misfolded and damaged

proteins, since elimination of these proteins is important to prevent their accumulation in

protein aggregates that are inherently toxic. UPS substrates are first marked for

degradation by the covalent addition of a ubiquitin molecule to particular lysine(s) within

138

the target protein; these ubiquitin molecules are added in an ATP-dependent manner

through the sequential action of ubiquitin-activating (E1), -conjugating (E2), and -ligating

(E3) enzymes. An additional ubiquitin moiety is added to a specific lysine residue in the

preceding ubiquitin molecule, and this process is repeated to form a polyubiquitin chain

on the substrate, sometimes involving the activity of a polyubiquitin (E4) ligase.

Ubiquitin molecules have a total of seven lysine residues (at positions 6, 11, 27, 29, 33,

48, and 63), and the particular lysine residue used for conjugation of one ubiquitin

monomer to another – defining distinct ubiquitin topologies – appears to have important

functional consequences for the substrate. For example, K48-linked polyubiquitin chains

are targeted to the proteasome, while K63-linked polyubiquitin chains are involved in

other functions, as will be explored below (Chau et al., 1989; Arnason and Ellison, 1994).

Those substrates targeted for UPS degradation are directed to the proteasome, where

ubiquitin molecules are recycled and substrates are enzymatically degraded to

oligopeptides. These oligopeptides are subsequently broken down into amino acids by

non-specific peptidases, thereby regenerating molecules essential to metabolic

homeostasis.

In contrast, autophagy (literally "self-eating") describes a process in which cellular

components such as organelles and longer-lived proteins are delivered to the lysosome

for degradation. While autophagy serves a diverse array of functions (reviewed in

(Mizushima, 2005)), this chapter will focus on its evolutionarily conserved function as

the critical mediator of metabolic homeostasis in the face of changing nutrient availability

(Abeliovich and Klionsky, 2001) as well as its role in neuroprotection. Autophagy is

generally considered to be a less selective degradative system than the UPS, and is typically described as a process in which large portions of cytoplasm are engulfed within membranes and delivered to the lysosome in bulk. This characterization describes the best-studied subtype of autophagy, known as macroautophagy. However, more several specialized forms of autophagy exist, including microautophagy and chaperone-mediated autophagy (CMA). These subsystems are distinguished by the identity of the substrates and the route by which these substrates reach the lysosomal compartment. Microautophagy consists of direct engulfment of small volumes of cytosol by lysosomes, while CMA involves selective, receptor-mediated translocation of proteins into the lysosomal lumen. In contrast, macroautophagy involves the *de novo* formation of an isolation membrane which expands to engulf a portion of the cytosol, eventually fusing to form a new vacuole termed an autophagosome. Autophagosomes undergo a series of maturation steps before fusing with lysosomes to deliver their cargo for degradation by lysosomal proteases. Breakdown products from the lysosome are translocated across the lysosomal membrane to the cytosol, where they are reused in metabolic processes. There appears to be capacity for selectivity within the process of macroautophagy, as some processes have been observed that appear to be specific for mitochondria (mitophagy), portions of the nucleus (*nucleophagy*), peroxisomes (*pexophagy*), endoplasmic reticulum (*reticulophagy*), microorganisms (*xenophagy*), ribosomes *(ribophagy)* or protein aggregates (*aggrephagy*) (reviewed in (Kundu and Thompson, 2008)). Macroautophagy forms the basis of this chapter and will be referred to hereafter simply as "autophagy".

The UPS and Autophagy: Functional Parallels

Despite such gross differences between the UPS and autophagy at a mechanistic level, two key functional parallels have been well-established. First, both systems play important roles in maintaining cellular pool of free amino acids, particularly in the setting of limited nutrient availability. Protein catabolism mediated by the UPS and autophagy are crucial for recycling amino acids during acute and chronic starvation, respectively. Second, both systems play essential roles in protecting the integrity of the proteome which is continually threatened by non-native protein-protein interactions and can lead to the formation of insoluble aggregates. Even under normal conditions cells constitutively produce aberrant proteins, and the challenge to protein quality control can become even greater with proteotoxic insults such as protein oxidation, aberrant translation, or mutant gene products. To counteract protein aggregation and its consequences, cells are equipped with protective mechanisms that scrutinize the cell for non-native proteins and assist in their refolding or degradation. The UPS and autophagy are both important to this quality control system and deficiency of either system is associated with accumulation of defective proteins in insoluble aggregates with attendant cytotoxicity.

The importance of eliminating misfolded or defective proteins is perhaps most evident in the context of the nervous system. As post-mitotic, highly metabolically active cells, neurons are particularly vulnerable to the long-term accumulation of proteins that engage in aberrant interactions or acquire other toxic properties. Indeed, a broad array of neurodegenerative diseases are characterized by the accumulation of misfolded proteins in affected brain regions. These deposits are frequently immuno-positive for ubiquitin

141

and other UPS components, suggesting a failure in the cell's capacity to clear proteins

marked for degradation. In addition, accumulations of autophagic vacuoles in affected

brain regions of patients with Alzheimer's disease, Parkinson's disease, Creutzfeldt-

Jakob disease, and many of the polyglutamine diseases suggest that autophagy could play

a role in the initiation or progression of disease (Anglade et al., 1997; Sapp et al., 1997;

Sikorska et al., 2004; Nixon et al., 2005).

The observation that these protein deposits in the setting of disease occur alongside (and

despite) signs of both UPS and autophagic activity raises the question of which system

has failed in its task of degrading these misfolded proteins. The answer may be both: the

in vitro turnover of neurodegenerative disease-causing proteins such as polyglutamine-

expanded proteins, polyalanine-expanded proteins, and α-synuclein can be altered by

manipulation of either the UPS or the autophagy-lysosomal system (Bennett et al., 1999;

Cummings et al., 1999; Kegel et al., 2000; Martin-Aparicio et al., 2001; Ravikumar et al.,

2002; Taylor et al., 2003b; Webb et al., 2003; Davies et al., 2006). Such wide-ranging

sensitivities indicate that more than one degradative route may be available to some

proteins, and have led to the suggestion that the choice of route for a particular substrate

may be influenced by which system is most capable of degrading it. For example, in the

case of α-synuclein, it has been suggested that soluble forms of the protein can be

efficiently degraded by the proteasome, while aggregated or oligomeric forms require the

bulk degradation of the autophagic pathway (Webb et al., 2003). Such a model further

suggests that autophagy could provide an alternate, compensatory route of degradation

142

when a particular substrate cannot be cleared efficiently by the proteasome, or when the UPS is more globally compromised.

While the clearance of disease proteins is likely to be cytoprotective in and of itself, degradation of intracellular proteins in general – whether misfolded, damaged, or simply no longer useful – has the advantage of recycling amino acids for further use by the cell. As mentioned above, the best-characterized and evolutionarily conserved role for autophagy lies in its response to chronic starvation. As such, autophagy is negatively regulated by the nutrition-dependent insulin/PI3K and TOR signaling pathways; when nutrients are removed, active PI3K inhibits TOR, allowing autophagy to reallocate nutrients from nonessential cytoplasmic components to vital cellular processes. The UPS has also been implicated in response to starvation, though its major role appears to be mobilization of nutrients in the context of acute starvation.

The UPS and Autophagy: Molecular Parallels

Apart from functional parallels between the UPS and autophagy with respect to recycling amino acids and implications of impaired function in the setting of neurodegenerative disease, a number of molecular parallels between autophagy and the UPS have emerged as the details of each system have been delineated. Of particular note is the striking similarity between the processes of autophagy induction and ubiquitin conjugation. Both processes utilize molecules that have come to be defined as UBLs (ubiquitin-like proteins): while the UPS uses the eponymous ubiquitin molecule, autophagy induction is

143

regulated by post-translational modification by two UBL proteins, known as Atg8 and Atg12. Atg8 and Atg12 are also members of a family of evolutionarily conserved proteins known as the Atg (autophagy-related) proteins; these Atg proteins are the effectors and regulatory proteins that initiate and elongate the autophagosomal membrane (reviewed in (Xie and Klionsky, 2007)). UBLs share similar structural domains and are likely ancestrally related (Figure A2.1) (Love et al., 2007). Moreover, the UBL conjugation system is also highly conserved between the UPS and autophagy (Figure A2.2): in both cases, the carboxyl group of the C-terminal glycine of the UBL is activated and attacked by a thiol-group-containing E1-activating enzyme to generate an E1-UBL thiolester. The activated UBL is then transferred to an E2-conjugating enzyme, and finally ligated to the target. In the case of the UBL Atg8, this target is not a protein, but the membrane-bound phospholipid phosphotidylethanolamine (PE). As PE is a component of the autophagosomal membrane, this PE-Atg8 reaction results in the studding of the inner and outer membrane of the autophagosome with Atg8. A mammalian homolog of Atg8 known as MAP-LC3 (microtubule-associated protein light chain 3, typically abbreviated as LC3) associates with phagophores in an analogous manner, and is therefore used as a primary histological marker of autophagosomes. Pro-LC3 is cleaved cotranslationally to yield a protein known as "LC3-I." When LC3-I becomes conjugated to PE and covalently associates with the phagophore, it forms "LC3-II." Consequently, the generation and turnover of LC3-II is used as an index of autophagy induction and/or flux (Klionsky et al., 2008). Because LC3-II remains on the inner membrane of autophagosomes until lysosomal enzymes degrade it, increased steady-state levels of LC3-II may be due to induction of autophagosome formation, a blockade in

their maturation, or both. The striking similarities between the ubiquitination system that precedes proteasomal digestion and the autophagy induction system that culminates in lysosomal digestion have led to the suggestion that these two catabolic pathways may have evolved from a common, ancestral biological pathway.

Points of Intersection Between the UPS and Autophagy: Cross-Regulation

As the list of similarities between the UPS and autophagy continued to grow, several groups began to realize that these shared characteristics did not simply reflect two parallel systems, but that these pathways could intersect in meaningful ways. This intersection was not predicted by the early researchers working to characterize the UPS, because of the apparently strict rule that agents that disrupt lysosomal function have no effect on the ATP-dependent turnover of short-lived and abnormal proteins (Pickart, 2004).

The first solid evidence that the UPS intersected with autophagy emerged in the mid-1990s, when ubiquitin modification was identified as an essential signal in the endosomal-lysosomal system that permits lysosomal degradation of certain integral membrane proteins. Specifically, several groups showed that a subset of endocytosed proteins requires ubiquitin conjugation in order to achieve internalization from the plasma membrane (Kolling and Hollenberg, 1994; Hicke and Riezman, 1996) and that monoubiquitination is sufficient as an endocytic internalization signal (Terrell et al., 1998). In addition, K63-linked ubiquitin topologies were found to stimulate endocytosis

(Galan and Haguenauer-Tsapis, 1997). Ubiquitination was also found to serve as a sorting signal for endosomes, targeting endosomal cargo to multivesicular bodies (MVBs) in the lysosomal degradation pathway (Komada and Kitamura, 2005). This pathway is also used in lysosome biogenesis, indicating that ubiquitination can influence the autophagy-lysosomal pathway at its most fundamental level. This latter observation was also the first of several observations suggesting a hierarchical relationship between these catabolic pathways, with autophagy under the control of the ubiquitin-proteasome system, as discussed below.

More recent evidence linking the UPS and autophagy comes from research into p53, a short-lived transcription factor whose steady-state levels are tightly controlled by the UPS. p53 plays multiple well-described roles in the regulation of the cell cycle and cell death, and several groups have now confirmed an additional function for p53 in the regulation of autophagy. Activation of p53 is believed to activate autophagy through both transcription-dependent and -independent mechanisms (Feng et al., 2005; Crighton et al., 2006; Amaravadi et al., 2007; Zeng et al., 2007; Abida and Gu, 2008; Maclean et al., 2008), while inhibition of p53 also appears to activate autophagy, though strictly in a transcription-independent manner (Tasdemir et al., 2008). The paradox in which autophagy may be induced by both activation and inhibition of p53 remains to be resolved, though it has been suggested that the different types of p53-dependent autophagy activation could potentially be dictated by the nature of the stress signal (Levine and Abrams, 2008). The notion that the UPS can dictate the steady-state levels of a key autophagy signaling molecule such as p53 suggests a model in which the UPS

146

holds the reins of autophagy induction, acting upstream of autophagy to control the signals that induce or inhibit this degradative pathway.

Further intersection of the UPS and autophagy can be found in the specialized form of macroautophagy known as mitophagy (mitochondria-specific autophagy), a process vital to protecting cells from oxidative stress (Kim et al., 2007). Parkin, a protein best known as a gene deleted in juvenile Parkinson's disease, is also an E3 ubiquitin ligase that was recently shown to be recruited to impaired mitochondria, where it mediates the engulfment of mitochondria by autophagosomes (Narendra et al., 2008). Though the ubiquitination activity of Parkin was not directly tested in this paper, it will be interesting to determine whether its ubiquitination signal involves mono- or poly-ubiquitination. Of particular interest is Parkin's ability to assemble K63-linked polyubiquitin chains, which form a ubiquitin chain topology that has been linked to autophagy and will be discussed more below (Lim et al., 2005).

Autophagy and the UPS: Coordinated Function

While these points of intersection highlighted regulatory crosstalk between the UPS and autophagy, there was until recently little evidence to show functional overlap between the two systems beyond their shared abilities to degrade disease-associated proteins. However, two papers published back-to-back in *Nature* in 2006 revealed a level of interaction that few would have predicted (Hara et al., 2006; Komatsu et al., 2006). Both of these papers described conditional knockouts of individual Atg genes within the

147

nervous system, and both reported that these mice showed neurodegeneration with extensive ubiquitin-positive pathology despite evidence of an intact UPS (Figure A2.3). These papers were significant in two respects. First, they revealed an essential role for basal autophagy (as opposed to nutritionally-induced autophagy) in the development and maintenance of the central nervous system, even in the absence of any disease-related mutant proteins. Second, the accumulation of ubiquitin conjugates despite an intact, functioning UPS was the first evidence that autophagy might play a role the degradation of ubiquitin-tagged substrates. Subsequent to the determination that a deficiency of autophagy leads to neurodegeneration with accumulation of ubiquitin conjugates, it was determined that induction of autophagy was able to suppress degeneration associated with UPS impairment and accelerate the clearance of misfolded protein in *Drosophila melanogaster*. These results demonstrated for the first time that not only does autophagy functionally complement the UPS, but is able to compensate for an impaired UPS (Pandey et al., 2007b). In fact, impairment of the UPS is such a potent and consistent stimulus of autophagy that it has become a frequent method of experimentally inducing autophagy both *in vitro* and *in vivo* (Rideout et al., 2004; Iwata et al., 2005a).

Molecular links between the UPS and autophagy

The UPS and autophagy clearly share roles in maintaining metabolic homeostasis and degrading abnormal proteins, while ubiquitin modification evidently can lead substrates into the autophagic system. What signals might mediate this coordination between the UPS and autophagy? Several clues have come to light from *in vitro* studies in which cells

are challenged by either high-level expression of misfolded protein or direct impairment of the UPS. In such contexts, many cells actively transport ubiquitinated, misfolded proteins to juxtanuclear bodies termed aggresomes (Johnston et al., 1998). Aggresomes are thought to be cytoprotective, acting as a mechanism to sequestrate potentially toxic proteins and facilitate their clearance by autophagy (Taylor et al., 2003b). While controversy surrounds the question of whether aggresomes are formed *in vivo*, they have provided significant insight into the molecular machinery that protects cells from misfolded stress. In particular, several proteins involved in aggresome formation have subsequently been shown to play roles in managing toxic proteins *in vivo,* including Parkin, histone deacetylase 6 (HDAC6) and p62. The common threads linking HDAC6 and p62 to aggresomes are K63-linked polyubiquitin chains, which are thought to target proteins to aggresomes, among other functions. The E3 ubiquitin ligase Parkin is capable of generating such K63 linkages (Lim et al., 2005), and overexpression of Parkin leads to aggresome formation (Junn et al., 2002). HDAC6 is a cytoplasmic deacetylase whose targets include α-tubulin, Hsp90, and cortactin. HDAC6 interacts with polyubiquitinated proteins through a Zn-finger ubiquitin-binding domain, and also interacts with dynein motors, suggesting that it may provide a link between ubiquitinated proteins and transport machinery (Kawaguchi et al., 2003; Kopito, 2003; Iwata et al., 2005a). Indeed, HDAC6 was recently demonstrated to operate as an adaptor between Parkin-mediated K63-linked polyubiquitinated substrates and the dynein motor complex, effectively coordinating delivery of substrates to autophagic machinery (Olzmann et al., 2007; Olzmann and Chin, 2008). In *Drosophila,* HDAC6 overexpression was found to suppress degeneration associated with UPS impairment as well as degeneration caused by toxic polyglutamine

expression; this suppression was autophagy-dependent, supporting a role for HDAC6 in linking the UPS with compensatory autophagy (Pandey et al., 2007b). p62 is a second aggresome-related cytosolic protein that is thought to operate as an adaptor between ubiquitinated proteins and autophagic machinery, as it harbors both a ubiquitin-associated domain and an LC3-interacting region (Geetha and Wooten, 2002; Seibenhener et al., 2004; Pankiv et al., 2007). p62 has been observed in ubiquitin-positive inclusions in a variety of neurodegenerative disease brains (Kuusisto et al., 2001a, 2002; Zatloukal et al., 2002), and converging evidence from experimental studies suggest that p62 protects against misfolded stress by facilitating a connection between ubiquitinated substrates and autophagic machinery (Bjorkoy et al., 2005; Komatsu et al., 2007; Pankiv et al., 2007; Ichimura et al., 2008; Nezis et al., 2008; Ramesh Babu et al., 2008). In a model similar to that described for HDAC6, p62 has been proposed to partner specifically with K63-linked polyubiquitin to promote the clearance of protein inclusions by autophagy (Tan et al., 2007).

Autophagy is Cytoprotective (Except When it Isn't)

Whereas the neurodegeneration with ubiquitin-pathology observed in autophagy-deficient mice was unexpected, it was consistent with prior observations that genetic alteration of lysosomal activity has dramatic impact on the central nervous system. For example, knockout of cathepsin D, a lysosomal protease enriched in neuronal tissues, resulted in neurodegeneration and accumulation of autophagosomes and lysosomes in both mice and *Drosophila* (Koike et al., 2000; Myllykangas et al., 2005; Shacka et al.,

2007). On the basis of these observations one might predict that impairment of autophagy could contribute to neurodegenerative disease in humans. Indeed, primary lysosomal dysfunction in inherited congenital "lysosomal storage disorders" has long been recognized to cause severe neurodegenerative phenotypes characterized pathologically by accumulations of lysosomes and autophagic vacuoles (Nixon et al., 2008). For example, the neuronal ceroid lipofuscinoses (NCLs) are a heterogeneous group of inherited, neurodegenerative disorders with onset ranging from infancy to late adulthood that are caused by a variety of defects in lysosomal function. Furthermore, a growing list of adult-onset, familial neurological diseases have been linked to mutations expected to have an impact on autophagy-lysosomal function (reviewed in (Nixon et al., 2008)), including Parkinson's disease (mutations in the lysosomal protein ATP13A2 are linked to early-onset PD) (Ning et al., 2008), Charcot- Marie-Tooth type 2B (a dominantly inherited form of peripheral neuropathy caused by mutations in the endosomal-lysosomal trafficking protein Rab7) (Verhoeven et al., 2003), and distal-spinobulbar muscular atrophy (a form of motor neuron disease caused by mutations in the lysosomal trafficking protein dynactin) (Puls et al., 2005). These latter two diseases are caused by mutations in components of the vesicular transport machinery, implicating impaired trafficking of autophagic components as important to pathogenesis. Indeed, microtubule-based vesicular trafficking is essential to the delivery of autophagosomes to lysosomes (Kimura et al., 2008), and the relatively long axons of the sensory and motor neurons affected in these diseases may impart particular vulnerability.

How might autophagy be cytoprotective? One possibility, given the evidence that autophagy can degrade disease-causing proteins, is that autophagy's protective action is mediated through accelerated turnover of misfolded proteins. This idea is supported by experimental evidence in models of neurodegenerative disease. In these studies, genetic inhibition of autophagy enhanced degeneration in spinobulbar muscular atrophy (SBMA) and Alzheimer's disease models (Pandey et al., 2007b; Pickford et al., 2008) and was associated with higher levels of disease-related proteins, suggesting that augmenting autophagic clearance of these cytotoxic proteins could provide benefit. Indeed, pharmacological activation of TOR using rapamycin suppressed toxicity in *in vitro* and *in vivo* models of SBMA and Huntington's disease (Ravikumar et al., 2002; Ravikumar et al., 2004; Berger et al., 2006; Pandey et al., 2007b).

Such a model, however, may be too simplistic. Accelerated turnover of mutant disease-causing proteins would be predicted to be cytoprotective, but such a mechanism does not explain how autophagy can suppress degeneration in models of proteasome impairment. It seems unlikely that autophagy upregulation can normalize the turnover of short-lived proteins that are normally degraded by the UPS, effectively replacing the UPS function with respect to regulatory networks. Instead, it seems reasonable to invoke another shared function of the UPS and autophagy – that of maintaining metabolic balance. Perhaps, through induction of autophagy, the metabolic balance that is disrupted with UPS impairment can be restored, replenishing the cellular pool of nutrients and allowing the cell to regain essential functions.

However, the role for autophagy in neurodegeneration may not always be so straightforward. In the case of Alzheimer's disease, a complex picture is emerging in which impaired autophagosome-lysosome fusion, combined with decreasing efficiency of the lysosomal system, causes accumulation of autophagic vacuoles (Nixon, 2007). These vacuoles may contribute to pathology by interfering with normal cellular functions such as intracellular trafficking and metabolic turnover of nutrients. In addition, recent studies have suggested that the toxic amyloid-β species may be generated by autophagic degradation of the amyloid beta precursor protein (Yu et al., 2005). These findings support a model of Alzheimer's disease pathogenesis in which autophagy induction produces toxic species, while defective clearance of autophagic vacuoles lead to exacerbation of disease (Nixon, 2007).

Final thoughts

The complex relationship between autophagy and neurodegeneration, as illustrated by the example of Alzheimer's disease, highlights several unresolved questions. As mentioned above, many neurodegenerative diseases show accumulations of autophagic vacuoles; in addition, autophagosomes are frequently found in dying neurons. However, these morphological studies cannot determine whether the increased frequency of autophagic vacuoles in disease brain is due to induced autophagy or impaired autophagic flux. Furthermore, these studies cannot distinguish between the role of autophagy in cytoprotection or in cell death. Finally, if the increased autophagic vacuoles reflect

153

endogenous upregulation of autophagy, it is unclear why this induction is insufficient to protect against proteotoxicity.

Further questions concern the details of the interrelatedness of the UPS and autophagy. Several questions in particular concern the compensatory function of autophagy in the context of UPS impairment. For example, it is not known whether this compensatory relationship is reciprocal – that is, whether induction of the UPS is able to compensate for impaired autophagy. Few reagents exist to upregulate the UPS, though one study found that upregulation of the UPS may afford neuroprotection from toxicity caused by disease proteins (Seo et al., 2007). However, the authors did not examine the effects of UPS upregulation in autophagy-deficient cells. In addition, the molecular players that might transduce signals to induce compensatory autophagy remain unknown. Also, how is the decision made between degradative pathways for any particular protein substrate when more than one route is available? HDAC6 and p62 have both been implicated in directing ubiquitinated proteins for autophagic degradation, but the mechanisms whereby these proteins identify their targets and influence their degradation are still unknown. Some evidence suggests that different ubiquitin topologies might identify different classes of substrates, with K48-linked chains being degraded by the UPS, while K63-linked chains are recognized by HDAC6 and p62 and possibly degraded by autophagy (Figure A2.4). However, experimental limitations in distinguishing the effects of K48- and K63-ubiquitin chains must be overcome in order these questions, and *in vivo* evidence for a link between K63-linked chains and autophagy is still lacking.It is further evidence of the irony of nature that the molecule that Ciechanover, Hershko, and Rose discovered at the

heart of their search for a non-lysosomal proteolytic pathway appears to be intimately linked to lysosomal proteolysis. At the very least, their decision to name the molecule "ubiquitin" turns out to have been made with remarkable foresight.

Figures and Legends

Figure A2.1. Ubiquitin-like (UBL) molecules share three-dimensional structures and common ancestry.
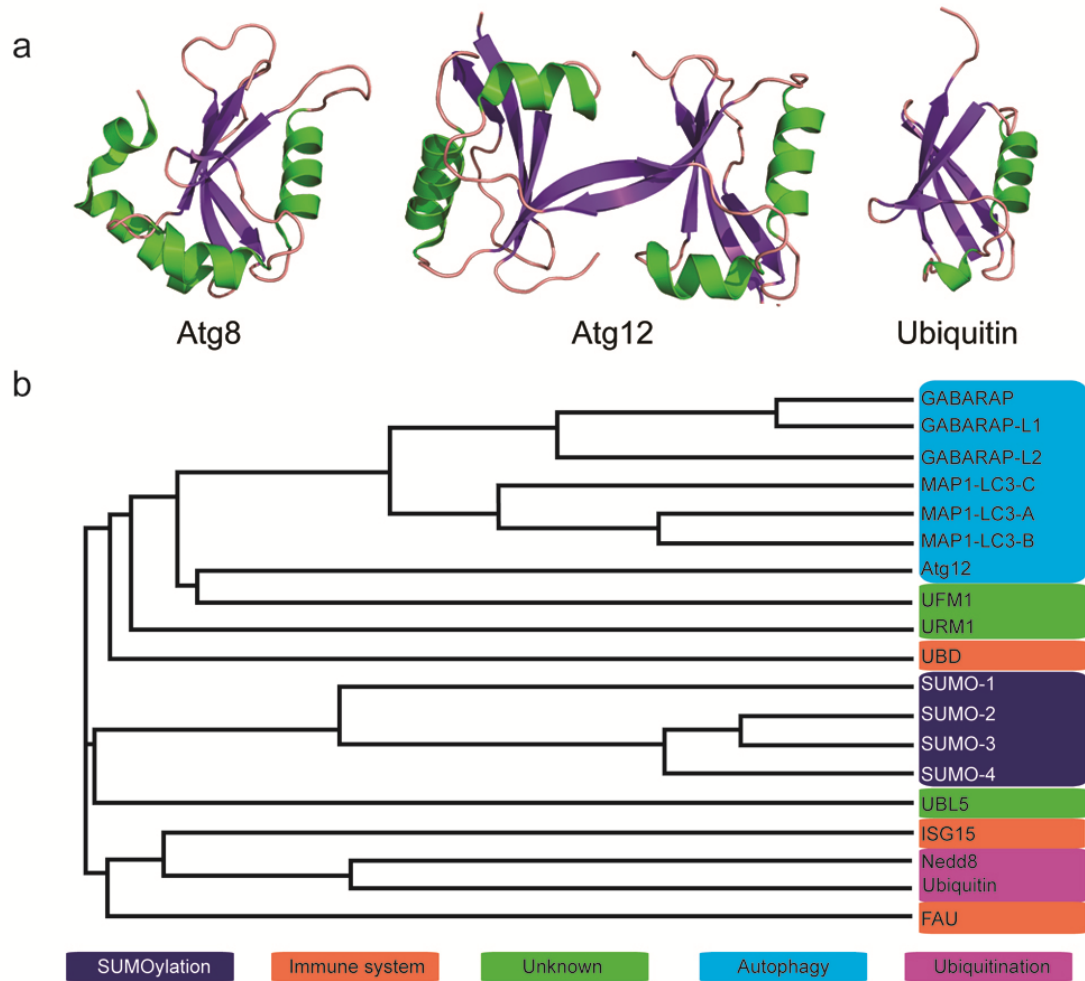
Figure A2.1. Ubiquitin-like (UBL) molecules share three-dimensional structures and common ancestry. (a) Ribbon diagrams of the UBL proteins Atg8, Atg12, and ubiquitin reveal a common ubiquitin fold. ⬚-helices are shown in green, ⬚-strands in purple, and unstructured loops in orange. Images were generated using PDB codes 1UBQ (ubiquitin), 1UGM (Atg8), and 1WZ3 (Atg12) and PYMOL. (b) Cladogram of human UBL proteins demonstrate the evolutionary relationships between UBL molecules and illustrate the ancestral relationship between ubiquitin and autophagy-related genes. Cladogram generated by multiple sequence alignment of human UBL proteins using Clustal W2.0.10.

Figure A2.2. Autophagy, the UPS, and SUMOylation use parallel conjugation systems of UBL modification.
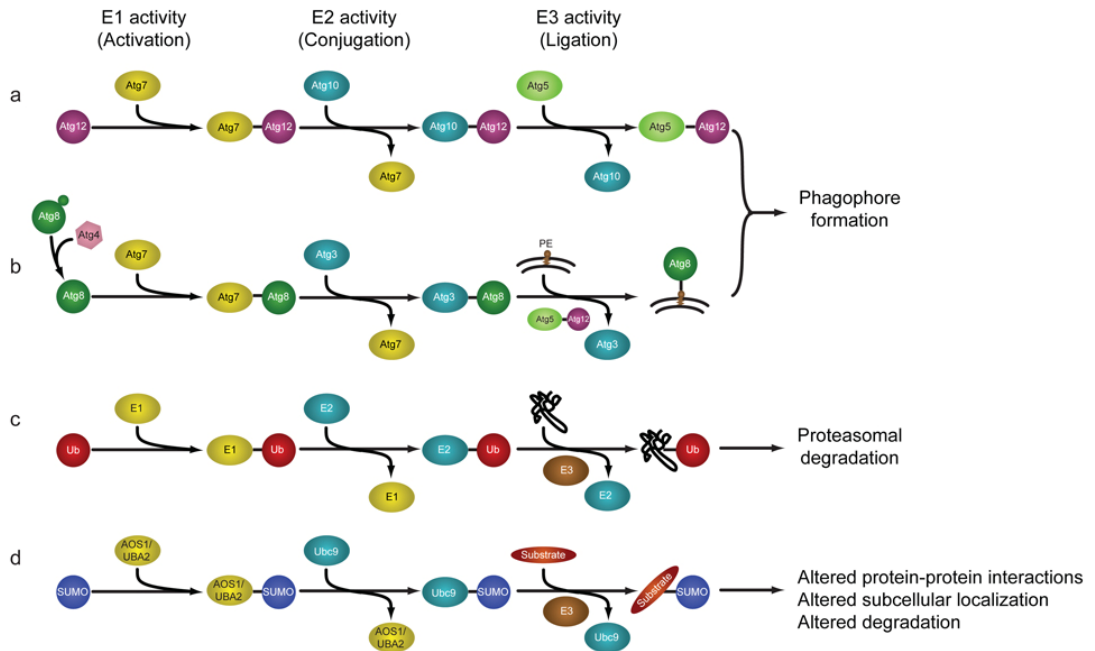
Figure A2.2. Autophagy, the UPS, and SUMOylation use parallel conjugation systems of UBL modification. (a) In the autophagy pathway, the UBL Atg12 is activated by the E1-like molecule Atg7, transferred to the E2-like Atg10, and is subsequently conjugated to Atg5. No E3-like protein has been identified in this pathway. (b) Also in the autophagy pathway, the UBL Atg8 is activated by the E1-like molecule Atg7, transferred to the E2-like Atg3, and is conjugated to phosphotidylethanolamine (PE) via the E3-like activity of the Atg5-Atg12 complex. (c) In the UPS, the UBL protein ubiquitin is activated by an E1-activating enzyme, transferred to an E2-conjugating enzyme, and linked to its target substrate through the action of an E3-ligating enzyme. (d) In the SUMOylation pathway, SUMO is first activated via the E1-like complex formed by AOS1 and UBA2, transferred to the E2-conjugating enzyme Ubc9, and finally ligated to its substrate through an E3-ligating enzyme. Though each conjugation pathway is similar, each has significantly different downstream effects.

Figure A2.3
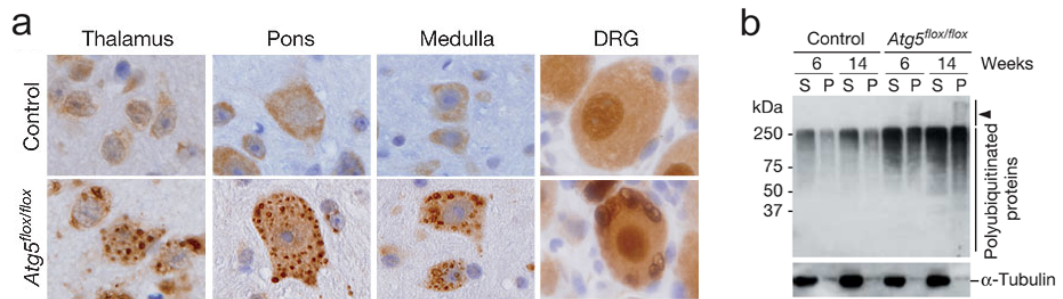
Figure A2.3. Conditional knockout of Atg5 in the mouse nervous system results in ubiquitin-positive inclusions and accumulation of polyubiquitinated proteins.

(a) Immunohistochemistry of brain sections from control and Atg5 conditional knockout mice at six weeks of age. Ubiquitin staining (1B3) reveals ubiquitin-positive inclusion bodies in the cytoplasm of large neurons in the thalamus, pons, medulla, and dorsal root ganglion (DRG). Genotypes shown: control (Atg5flox/+; nestin-Cre) and Atg5 knockout (Atg5flox/flox; nestin-Cre). Scale bar 10μm. (b) Triton-X-100-soluble polyubiquitinated proteins accumulate in Atg5flox/flox; nestin-Cre brains. Brain homogenate was prepared at indicated times and separated into Triton-X-100-soluble (S) and –insoluble (P) fractions and immunoblotted with anti-ubiquitin antibodies. Arrowhead indicates the stacking gel. Reprinted from (Hara et al., 2006) with permission.

160
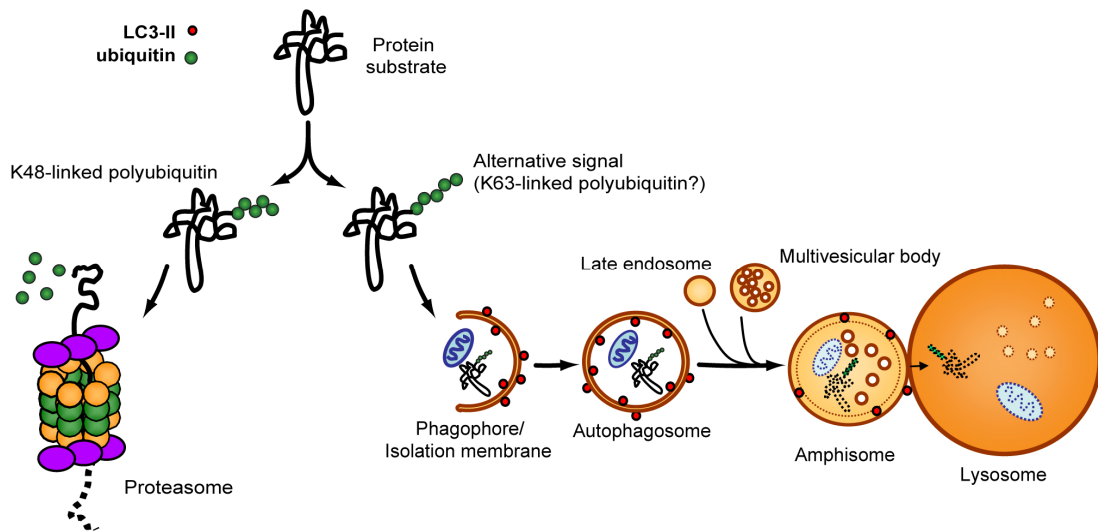
Figure A2.4

Figure A2.4. Protein degradation can be accomplished by two major intracellular pathways: the UPS and autophagy. In the UPS pathway, misfolded protein substrates are tagged with K48-linked polyubiquitin chains and targeted to the proteasome for degradation. The signal for degradation by macroautophagy is not known, but *in vitro* evidence suggests that K63-linked polyubiquitination leads to aggresome formation and subsequent degradation of misfolded proteins by autophagy. The process of macroautophagy involves the expansion of a phagophore or isolation membrane that surrounds a portion of the cytoplasm. The phagophore seals and matures to form an autophagosome, which in mammals joins with late endosomes and multivesicular bodies (MVBs) to form a new structure termed an amphisome. Amphisomes then fuse with lysosomes to deliver their cargo for lysosomal degradation.

161

Appendix III:

Autophagy and the Ubiquitin-Proteasome System:

Collaborators in Neuroprotection

Autophagy and the ubiquitin-proteasome system: collaborators in neuroprotection

Natalia B. Nedelsky[1,3], Peter K. Todd[1,2], and J. Paul Taylor[1,3]

1. Department of Neurology, University of Pennsylvania School of Medicine, Philadelphia, PA 19104 USA

2. Department of Neurology, University of Michigan, Ann Arbor, MI 48109 USA

3. Department of Developmental Neurobiology, St. Jude Children's Research Hospital, Memphis, TN 38105 USA

Abstract

Protein degradation is an essential cellular function that, when dysregulated or impaired, can lead to a wide variety of disease states. The two major intracellular protein degradation systems are the ubiquitin-proteasome system (UPS) and autophagy, a catabolic process that involves delivery of cellular components to the lysosome for degradation. While the UPS has garnered much attention as it relates to neurodegenerative disease, important links between autophagy and neurodegeneration have also become evident. Furthermore, recent studies have revealed interaction between the UPS and autophagy, suggesting a coordinated and complementary relationship between these degradation systems that becomes critical in times of cellular stress. Here we describe autophagy and review evidence implicating this system as an important player in the pathogenesis of neurodegenerative disease. We discuss the role of autophagy in neurodegeneration and review its neuroprotective functions as revealed by experimental manipulation in disease models. Finally, we explore potential parallels and connections between autophagy and the UPS, highlighting their collaborative roles in protecting against neurodegenerative disease.

A precarious balance

The energy expenditure needed to produce protein is substantial; thus, the degradation of these macromolecules comes at a high cost. Nevertheless, protein turnover is essential for removing defective proteins and for contributing to the pool of amino acids required for

164

continued protein synthesis, particularly in times of limited nutrient availability. Furthermore, many essential cellular functions – including cell division, transcription, and signal transduction – are regulated by fluctuation in protein levels accomplished by altering the balance of protein synthesis and degradation. The role of protein catabolism in protecting cells from defective, misfolded proteins has been the subject of increased attention as its relevance to human disease has become apparent. A substantial fraction of newly synthesized proteins are translated incorrectly or fold incorrectly due to errors in synthesis or genetic mutations (Wheatley and Inglis, 1980; Schubert et al., 2000; Vabulas and Hartl, 2005; Yewdell, 2005). Oxidative or nitrosylative damage adds to the burden of defective proteins. Efficient degradation of these proteins is essential, as cells cannot risk the long-term accumulation of proteins that engage in aberrant protein-protein interactions, form insoluble aggregates, or acquire other toxic properties. Considering the importance of protein catabolism in maintaining cell homeostasis, it is not surprising that dysregulation of protein turnover is associated with myriad disease states such as cancer and neurodegeneration (Kundu and Thompson, 2008).

Two major pathways accomplish regulated protein catabolism: the ubiquitin-proteasome system (UPS) and the autophagy-lysosomal system. The UPS serves as the primary route for degradation for thousands of short-lived proteins and provides the exquisite specificity and temporal control needed for fine-tuning the steady-state levels of many regulatory proteins (Ciechanover et al., 2000). UPS-mediated catabolism is also essential to maintain amino acid pools in acute starvation and contributes significantly to the degradation of defective proteins (Wheatley and Inglis, 1980; Ciechanover and Brundin,

2003; Vabulas and Hartl, 2005). Autophagy, by contrast, is primarily responsible for degrading long-lived proteins and maintaining amino acid pools in the setting of chronic starvation, although its contribution to the degradation of defective proteins may equal that of the UPS. Though it has received less attention than the UPS historically, breakthroughs in the molecular genetics of autophagy have led to a renaissance of interest in this catabolic pathway and has revealed many surprising insights about its regulation, function, and contribution to protein degradation, in both normal and disease states. This review will (1) highlight the parallels between the UPS and autophagy in their roles and regulation, (2) explore the role of autophagy in neurodegeneration, noting parallels with the UPS, and (3) discuss emerging evidence of a functional relationship between the UPS and autophagy and its relevance to neurodegeneration.

The basics: roles and regulation

"Autophagy", literally "self-eating", describes a catabolic process in which cell constituents such as organelles and proteins are delivered to the lysosomal compartment for degradation. Autophagy is an evolutionarily conserved process whose primary task in lower organisms is the maintenance of metabolic homeostasis in the face of changing nutrient availability (Abeliovich and Klionsky, 2001). This role in recycling is complementary to that of the UPS, which degrades proteins to generate oligopeptides that are subsequently degraded into amino acids while replenishing the cell's supply of free ubiquitin. Recent advances have demonstrated that autophagy also serves a surprisingly diverse array of additional functions, including organelle clearance, antigen presentation,

166

elimination of microbes, as well as regulation of development and cell death (Mizushima, 2005). Traditionally, autophagy has been considered a less selective degradative pathway than the UPS and is frequently illustrated as the engulfment of large portions of cytoplasm (including nearby cytosolic bystanders) and delivery of the contents to the lysosome in bulk. This view of autophagy as a crude, nonselective form of catabolism has been challenged by the appreciation of specialized forms of autophagy that are distinguished by the identity of the substrates and the route by which these substrates reach the lysosomal compartment (Figure A3.1). *Microautophagy* consists of direct engulfment of small volumes of cytosol by lysosomes (Ahlberg et al., 1982), whereas *chaperone-mediated autophagy* (CMA) involves selective, receptor-mediated translocation of proteins into the lysosomal lumen (Dice, 1990). These processes are distinguished from *macroautophagy*, in which an isolation membrane expands to engulf a portion of the cell, eventually fusing to form a new autophagic vacuole that subsequently fuses with a lysosome (Arstila and Trump, 1968). Even within the category of macroautophagy, there appears to be capability for selectivity, as autophagic processes have been observed that appear to be specific for mitochondria (*mitophagy*), portions of the nucleus (*nucleophagy*), peroxisomes (*pexophagy*), endoplasmic reticulum (*reticulophagy*), microorganisms (*xenophagy*), ribosomes *(ribophagy)* or protein aggregates (*aggrephagy*) (reviewed in (Kundu and Thompson, 2008)).

While the molecular regulation of microautophagy remains obscure, there has been substantial insight into the regulation of CMA and macroautophagy. CMA is a process in which proteins harboring a pentapeptide motif related to the sequence KFERQ are specifically recognized by a cytosolic chaperone, the heat shock cognate protein of 70

167

kDa (hsc70). The substrate-chaperone complex is then targeted to the lysosome by binding to lysosome-associated membrane protein 2A (LAMP-2A) which carries out receptor-mediated translocation of the substrate into the lysosome for degradation (Dice, 1990; Cuervo and Dice, 1996). Up to 30% of all cytosolic proteins harbor the CMA recognition motif and are potentially subject to degradation by this catabolic pathway during long-term nutrient deprivation (Dice, 1990, 2007).

While it remains unclear how substrates are specifically marked for degradation by macroautophagy (hereafter referred to as autophagy), the identification of a family of autophagy-related (Atg) genes in yeast and their homologues in higher organisms has permitted minute dissection of the general process by which autophagy engulfs and degrades its targets. The initial step in autophagy involves expansion of a membranous structure called the "isolation membrane" or "phagophore" that engulfs a portion of the cell; the membrane eventually fuses to form a new double-membraned structure known as an autophagosome (Figure A3.1). The process of autophagy is controlled by parallel activation cascades that involve ubiquitin-like (UBL) protein modification, strikingly similar to the activation cascade that regulates the UPS (Figure A3.2a). In the first arm of the Atg conjugation system, phagophore membrane elongation is triggered through the sequential action of an E1-like protein (Atg7) and an E2-like protein (Atg10) leading to an isopeptide linkage between the C-terminal glycine in the UBL protein Atg12 and a lysine residue of Atg5 (Figure A3.2b). These Atg12-Atg5 conjugates are further cross-linked to Atg16 to form a large (~350 kDa) multimeric complex, which has been thought to act as a structural support for membrane expansion (Reggiori and Klionsky, 2005).

168

More recent work has demonstrated that the Atg12-Atg5 conjugate can function as an E3-like enzyme in the second arm of the Atg conjugation cascade to promote lipidation of Atg8 (Hanada et al., 2007). In a second arm of the Atg conjugation system, Atg4 cleaves the UBL protein Atg8 to promote interaction with Atg7. Atg8 is then conjugated with the phospholipid phosphotidylethanolamine (PE) by the concerted action of the E2-like Atg3 and the E3-like Atg12-Atg5 conjugate. Of note, this E3-like activity results in a protein-lipid conjugation, in contrast to the classical E3 protein-protein conjugation of the UPS. As PE is a component of the autophagosomal membrane, the lipidation reaction results in studding of the inner and outer membranes of autophagosomes with Atg8 (Figure A3.2c).

Once formed, new autophagosomes move through a stepwise maturation process that culminates with fusion to a lysosome permitting degradation of the lumenal contents. In mammals, autophagosomes first fuse with endosomes and multivesicular bodies to form amphisomes, which subsequently fuse with lysosomes to create degradative vacuoles termed autolysosomes (Berg et al., 1998). Autophagosomes and autolysosomes can be distinguished morphologically, as autophagosomes contain contents with densities similar to cytosol, while autolysosomes appear as electron-dense material with a hollow rim beneath the limiting membrane. However, because of occasional ambiguity in distinguishing autophagosomes, amphisomes, and autolysosomes morphologically, the term "autophagic vacuole" frequently appears in the literature to refer to all three structures.

Four metazoan homologs of Atg8 have been identified: MAP-LC3 (microtubule-associated protein light chain 3), GABARAP (γ-aminobutyric-acid-type-A-receptor-associated protein), GATE-16 (Golgi-associated ATPase enhancer of 16 kDa), and Atg8L, although GABARAP, GATE-16, and Atg8L have not been extensively characterized. While GABARAP and GATE-16 may also be conjugated to PE in experimental systems, at present MAP-LC3 (typically abbreviated LC3) is the only protein that is known to remain associated with the autophagosome in higher eukaryotes. Pro-LC3 is cleaved co-translationally to create a form of LC3 denoted "LC3-I". LC3-I becomes conjugated to PE to form "LC3-II" and thereby covalently associates with the phagophore. Consequently, the generation and turnover of LC3-II is used as an index of autophagy induction and/or flux (Klionsky et al., 2008). LC3-II staining is also used as a primary histological marker of autophagosomes. Because LC3-II remains on the inner membrane of autophagosomes until lysosomal enzymes degrade it, increased steady-state levels of LC3-II may be due to induction of autophagosome formation, a blockade in their maturation, or both. Distinguishing between these possibilities for experimental purposes is readily accomplished with the use of chemical inhibitors of maturation (Klionsky et al., 2008).

A role for autophagy in neurodegeneration

Many neurodegenerative diseases are characterized by accumulation of misfolded protein deposits in affected brain regions, suggesting a failure in the cell's degradative capacity (Taylor et al., 2002). Neurons, as highly metabolically active, post-mitotic cells, are

170

especially vulnerable to the accumulation of defective proteins, and this may account for the frequency with which conformational diseases affect the nervous system. In most cases, these proteinaceous deposits are composed of ubiquitin conjugates, suggesting a failure in the clearance of proteins targeted for proteasomal degradation. Indeed, experimental evidence indicates that neurodegeneration is frequently associated with impaired UPS function, although whether this is a cause or consequence of neurodegeneration is a contested issue, as is reviewed elsewhere in this special issue. It has also been suggested that autophagy plays a role in the initiation or progression of some neurodegenerative diseases (McCray and Taylor, 2008). This suggestion originates from the observed accumulation of autophagic vacuoles in neurons from affected brain regions in a number of neurodegenerative diseases, including Alzheimer's disease, Parkinson's disease, Creutzfeldt-Jakob disease, and many of the polyglutamine diseases (Anglade et al., 1997; Sapp et al., 1997; Sikorska et al., 2004; Nixon et al., 2005). This notion has since been validated by experimental evidence and insights provided by human genetics, as described below.

Neurodegeneration is frequently characterized by increased frequency of autophagic vacuoles

Huntington's and Alzheimer's diseases are among the best-studied examples where histopathology implicates autophagy as playing a role in disease pathogenesis. Alzheimer's disease pathology features massive accumulation of autophagic vacuoles within large swellings along dystrophic and degenerating neurites in neocortical and

hippocampal pyramidal neurons (Nixon et al., 2005). In Huntington's disease, affected

neurons show accumulation of huntingtin in cathepsin D-positive vacuoles (Sapp et al.,

1997). Cathepsin D is a lysosomal protease enriched in neuronal tissues, suggesting that

these are autolysosomes. However, the observed increased frequency of autophagic

vacuoles in disease brain is ambiguous with respect to whether autophagy is induced or

whether autophagy flux is impaired. Furthermore, autophagosomes are frequently

observed in dying neurons, where it is unclear whether autophagy is operating as a futile

cytoprotective response, whether autophagy mediates cell death, or whether it is induced

secondarily in a cell already otherwise committed to dying. Insight into the role of

autophagy in neurodegeneration has been provided by studies indicating that: 1) some

neurodegenerative disease-related proteins are degraded by autophagy, 2) impairment of

autophagy promotes neurodegeneration in animal models and several human

neurodegenerative diseases, and 3) manipulation of autophagy modifies phenotypes in

animal models of neurodegeneration.

Neurodegenerative disease-related proteins are degraded by autophagy

That neurodegenerative disease-causing proteins are frequently degraded by autophagy

was demonstrated by a series of *in vitro* studies which showed that pharmacological

induction or inhibition of macroautophagy alters the rate of turnover of a number of

disease-related proteins including polyglutamine-expanded proteins, polyalanine-

expanded proteins, as well as wild type and mutant forms of α-synuclein (Ravikumar et

al., 2002; Webb et al., 2003). Moreover, ultrastructural analysis by immuno-electron

microscopy showed that in cell culture models, disease-related proteins are delivered to autophagic vacuoles (Kegel et al., 2000; Taylor et al., 2003b). CMA has also been found to contribute to the degradation of α-synuclein (Cuervo et al., 2004). Collectively, these studies suggested that autophagy contributes to the degradation of multiple disease proteins and the efficiency of this pathway could relate to the onset or progression of disease. Of note, there is evidence that many of these same disease-causing proteins are also degraded by the UPS (Bennett et al., 1999; Cummings et al., 1999; Martin-Aparicio et al., 2001), suggesting that more than one degradative route may be available to them. In the case of α-synuclein, for example, Webb et al. concluded that soluble forms of the disease protein are efficiently degraded by the UPS, while aggregated or oligomeric α-synuclein require autophagy for clearance (Webb et al., 2003). These observations have led to the suggestion that autophagy provides an alternate, compensatory route of degradation when clearance by the UPS and CMA are compromised. The relative contribution of autophagy and the UPS to degrading disease-related substrates, and the relationship of this to the onset and progression of various diseases, remains to be elucidated – and this may differ amongst different diseases.

Impairment of autophagy promotes neurodegeneration

It is becoming increasingly evident that the autophagy-lysosomal system is essential to neuronal homeostasis, and may in some settings be neuroprotective. The consequences of impaired lysosome function, for example, may be observed in cathepsin D knockout mice and *Drosophila melanogaster* cathepsin D mutants which show neurodegeneration and

173

associated accumulation of autophagosomes and lysosomes (Koike et al., 2000; Myllykangas et al., 2005; Shacka et al., 2007). The importance of autophagy to neuronal homeostasis is further illustrated by characterization of mice with conditional knockout of Atg genes. These mice die prematurely with extensive neurodegeneration and ubiquitin-positive pathology (Hara et al., 2006; Komatsu et al., 2006). On the basis of these observations one might predict that impairment of autophagy could contribute to neurodegenerative disease in humans. Indeed, primary lysosomal dysfunction in inherited congenital "lysosomal storage disorders" has long been recognized to cause severe neurodegenerative phenotypes characterized pathologically by accumulations of lysosomes and autophagic vacuoles (Nixon et al., 2008). For example, the neuronal ceroid lipofuscinoses (NCLs) are a heterogeneous group of inherited, neurodegenerative disorders with onset ranging from infancy to late adulthood that are caused by a variety of defects in lysosomal function. Furthermore, a growing list of adult-onset, familial neurological diseases have been linked to mutations expected to have an impact on autophagy-lysosomal function (reviewed in (Nixon et al., 2008)), including Kufor-Rakeb syndrome (a form of early-onset parkinsonism with dementia) (Ning et al., 2008), Charcot-Marie-Tooth type 2B (CMT2B) (Verhoeven et al., 2003), and distal-spinobulbar muscular atrophy (distal-SBMA) (Puls et al., 2005). Mutations in CLN3, a transmembrane protein that localizes to the late endosomal/lysosomal membrane, cause a form of NCL. CLN3-related neurodegeneration appears to be a consequence of reduced autophagosome-lysosome fusion (Cao et al., 2006). Mutations in ATP13A2, which encodes a primarily neuronal lysosomal ATPase, were recently found to cause Kufor-Rakeb syndrome (previously designated PARK9). Disease-causing mutations in

174

ATP13A2 result in protein retention in the endoplasmic reticulum and enhanced

proteasomal degradation, suggesting that neurodegeneration could be caused by

overwhelming the UPS and/or loss of function in lysosomal protein degradation (Ning et

al., 2008). Mutations in Rab7 cause the dominantly inherited axonal neuropathy CMT2B.

Rab7 participates in trafficking autophagosomes and fusion with lysosomes and disease-

causing mutations are predicted to impair this process (Gutierrez et al., 2004; Jager et al.,

2004; Kimura et al., 2007). Mutations in p150/dynactin are responsible for the motor

neuron disease distal-SBMA. Microtubule-based vesicular trafficking is essential for

delivery of autophagosomes to lysosomes and subsequent fusion (Kimura et al., 2008),

and impaired dynein-mediated trafficking is associated with impaired

autophagosome/lysosome fusion and reduced protein turnover (Ravikumar et al., 2004;

Fader et al., 2008). Thus, motor neuron loss in distal-SBMA may result from impaired

autophagosome trafficking and/or fusion with lysosomes. Indeed, a mouse model of

distal-SBMA that expresses mutant p150/dynactin is characterized by accumulation of

ubiquitin-positive aggregates and autophagic vacuoles in affected neurons (Laird et al.,

2008).

**Manipulation of autophagy modifies neurodegenerative phenotypes in animal
models**

While deficiency in autophagy results in neurodegeneration, a separate question concerns

the role of autophagy in the context of diseases initiated by mutations in genes unrelated

to autophagic function. To investigate this perspective, researchers have turned to animal

models of common neurodegenerative diseases that are amenable to genetic and pharmacological manipulation of autophagy. These studies have largely shown that reduced autophagy worsens disease phenotypes whereas augmented autophagy provides benefit, leading to the conclusion that autophagy is cytoprotective. For example, in a *Drosophila* model of X-linked spinobulbar muscular atrophy (SBMA), a polyglutamine disease, degeneration was strongly enhanced by genetic inhibition of autophagy (Pandey et al., 2007b). Similarly, in transgenic mice expressing amyloid precursor protein, a model of Alzheimer's disease, genetic inhibition of autophagy by heterozygous depletion of beclin-1 results in enhancement of neurodegeneration (Pickford et al., 2008). In both of these studies it was determined that autophagy deficiency resulted in greater accumulation of the offending, disease-related protein (Pandey et al., 2007b; Pickford et al., 2008), suggesting that autophagy was needed to degrade cytotoxic proteins. This provided the rationale for investigating whether increasing autophagic activity might provide benefit. Pharmacological upregulation of autophagy can be accomplished using the drug rapamycin, which works by inhibiting TOR (target of rapamycin), a pleiotropic molecule that negatively regulates autophagy, among other functions. Indeed, treatment with rapamycin ameliorates the degenerative phenotype in a *Drosophila* model of SBMA, as well as in *Drosophila* and mouse models of Huntington's disease (Ravikumar et al., 2004; Berger et al., 2006; Pandey et al., 2007b). In addition, inducing autophagy in an TOR-independent manner using lithium (Sarkar et al., 2008b) or trehalose (Tanaka et al., 2004; Davies et al., 2006; Sarkar et al., 2007) has been shown to accelerate clearance of disease proteins *in vitro* (Sarkar et al., 2007) and protect against neurodegeneration in mouse and *Drosophila* models of Huntington's disease (Tanaka et al., 2004; Sarkar et al.,

2008b). These exciting results have opened the door to the possibility that pharmacological upregulation of autophagy by rapamycin, lithium, trehalose, or a newer generation of small molecules might be of therapeutic benefit for patients with neurodegenerative disease. Recently, high throughput screening efforts have identified small molecule activators of autophagy. Some of these compounds inhibit TOR and activate autophagy in a manner analogous to rapamycin, but other compounds are TOR-independent and reflect multiple points of potential therapeutic intervention (Sarkar et al., 2008a). There have been fewer efforts to manipulate UPS function for therapeutic benefit in neurodegenerative disease, but it was recently shown that use of a proteasome activator enhanced survival in an *in vitro* model of Huntington's disease (Seo et al., 2007), suggesting that augmenting other routes of protein degradation may also provide neuroprotection.

However, it should be pointed out that the relationship of autophagy to the accumulation of disease protein may not always be straightforward. There is evidence that in some cases cellular attempts to degrade cytotoxic protein aggregates interfere with normal autophagy function leading to lysosomal "indigestion" that ultimately compromises cell function or viability. For example, α-synuclein is degraded at least in part by CMA (Cuervo et al., 2004). Mutations in α-synuclein that are causative of familial Parkinson's disease are poorly transferred to the lysosomal lumen and accumulate on the lysosomal surface, resulting in blockade of receptor-mediated translocation. This results in disrupting degradation of other CMA substrates (Cuervo et al., 2004; Massey et al., 2006). With respect to Alzheimer's disease, an even more complex story is emerging.

Several lines of evidence suggest that there is an impairment of autophagy resulting from impaired autophagosome-lysosome fusion combined with decreasing efficiency of the lysosomal system (Nixon, 2007). These vacuoles may further contribute to pathogenesis by interfering with normal intracellular trafficking and/or by leaking undigested toxic contents into the cytosol, or more generally by disrupting normal metabolic turnover required for neuronal homeostasis. Recent evidence suggests that the autophagic turnover of amyloid beta precursor protein (APP) may underlie the generation of toxic amyloid-□ species (Yu et al., 2005).Thus, the relationship of autophagy to Alzheimer's disease progression is complex, with autophagy-related production of toxic amyloid-□that culminates in impaired autophagy and exacerbation of disease.

Links between UPS and autophagy

The UPS and autophagy were long viewed as independent, parallel degradation systems with no point of intersection. This view was initially challenged by the observation that monoubiquitination operates as a key signal in endocytosis, a process important for numerous cell functions including lysosomal biogenesis (Ross and Pickart, 2004). Subsequently, several lines of evidence have developed suggesting that the UPS and autophagy are functionally interrelated catabolic processes (Rideout et al., 2004; Iwata et al., 2005a; Pandey et al., 2007b). Specifically, these degradation systems share certain substrates and regulatory molecules, and show coordinated and, in some contexts, compensatory function. Thus, in contrast to the traditional notion of the UPS and autophagy providing discrete routes of degradation for short-lived and long-lived

proteins, respectively, it is increasingly clear that a substantial subset of proteins may be

degraded by either pathway. Short-lived proteins normally degraded by the UPS can be

selectively degraded by autophagy under certain conditions (Fuertes et al., 2003a; Li,

2006), while longer-lived proteins can also be degraded by the UPS (Fuertes et al.,

2003b). The neuronal protein α-synuclein, for example, can be degraded by the UPS,

macroautophagy and chaperone-mediated autophagy (Webb et al., 2003; Cuervo et al.,

2004). Under conditions in which one degradation system is compromised, enhanced

degradation by an alternate pathway may become critical to maintaining pools of amino

acids for protein synthesis and may protect against the accumulation of a toxic species.

As mentioned above, dramatic illustration of the interrelatedness of the UPS and

autophagy was provided by characterizations of mice with conditional knockout of the

essential autophagy genes Atg5 or Atg7 in the central nervous system, which resulted in

neurodegeneration with accumulation of ubiquitin-positive pathology (Hara et al., 2006;

Komatsu et al., 2006). Given that these mice showed no observable defect in UPS

function, these results suggest that some ubiquitin-tagged proteins may in fact normally

be degraded by autophagy. This model is consistent with an older study showing that

inactivation of the ubiquitin-activating enzyme E1 leads to a defect in autolysosomal

degradation and to an absence of ubiquitin-positive proteins within lysosomes (Lenk et

al., 1992).

Further illustration of the relationship between the UPS and autophagy can be found in a

series of *in vitro* studies that examined the behavior of cells following challenge to the

UPS. When cultured cells are challenged with excess misfolded protein that overwhelms

the UPS, or treated with proteasome inhibitors, ubiquitinated misfolded proteins are

actively transported to a cytoplasmic, juxtanuclear structure that has been termed an "aggresome" (Johnston et al., 1998). It has been inferred that aggresome formation *in vitro* is a cytoprotective response in cultured cells since their formation correlates inversely with cell death, whereas interventions that block aggresome formation enhance cytotoxicity and slow the rate of turnover of misfolded proteins (Kawaguchi et al., 2003; Taylor et al., 2003b; Arrasate et al., 2004; Iwata et al., 2005a; Yamamoto et al., 2006). While aggresomes superficially resemble the cytoplasmic inclusions present in some neurodegenerative diseases, evidence of aggresome formation *in vivo* is lacking, and most pathological inclusions found in neurodegenerative disease are clearly not aggresomes. Nevertheless, studying the phenomenon of aggresome formation *in vitro* has provided insight into the cellular management of misfolded proteins; for example, helping to identify molecular machinery that protects cells from misfolded protein stress. It has now been established that clearance of misfolded proteins from aggresomes is mediated at least in part by autophagy, implicating this pathway as a compensatory mechanism for degrading misfolded proteins when the proteasome is impaired (Taylor et al., 2003b; Iwata et al., 2005b; Iwata et al., 2005a; Yamamoto et al., 2006).

In addition to aggresome formation, impairment of the UPS *in vitro* has been found to induce autophagy (Rideout et al., 2004; Iwata et al., 2005a). This is observed, for example, in HeLa cells after prolonged proteasomal inhibition as evidenced by redistribution of LC3 into numerous puncta (Figure A3.3a-c) and the accumulation of autophagic vacuoles based upon ultrastructural evaluation (Figure A3.3d-g). Similar induction of autophagy is observed in response to genetic impairment of the proteasome

180

in *Drosophila* (Pandey et al., 2007b). The role of autophagy induction in the setting of UPS impairment appears to be cytoprotective since degenerative phenotypes associated with proteasome impairment are enhanced in an autophagy-deficient background (Figure A3.4a-c), whereas this degeneration is suppressed when autophagy is induced with the TOR-inhibitor rapamycin (Figure A3.3d). Similar results have recently been observed *in vitro* using the proteasome inhibitor lactacystin, as pre-treatment with rapamycin attenuates lactacystin-induced apoptosis and reduces lactacystin- induced ubiquitinated protein aggregation (Pan et al., 2008).

Although the mechanism whereby autophagy and UPS function are coordinated is little understood, several regulators have emerged as important players in mediating this crosstalk, including histone deacetylase 6 (HDAC6) (Iwata et al., 2005a; Pandey et al., 2007a; Pandey et al., 2007b), p62/sequestosome 1 (p62) (Bjorkoy et al., 2005), and the FYVE-domain containing protein Alfy (Simonsen et al., 2004); notably, these proteins have all been found to regulate or be essential for aggresome formation. HDAC6 is a cytoplasmic microtubule-associated deacetylase whose targets include α-tubulin, Hsp90, and cortactin. HDAC6 interacts with polyubiquitinated proteins through a highly conserved Zn-finger ubiquitin-binding domain, and also interacts with dynein motors, suggesting that the molecule may provide a physical link between ubiquitinated cargo and transport machinery (Kawaguchi et al., 2003). HDAC6 activity appears to be important for trafficking ubiquitinated proteins and lysosomes *in vitro* and this has led to the suggestion that HDAC6 coordinates delivery of substrates to autophagic machinery (Kawaguchi et al., 2003; Kopito, 2003; Iwata et al., 2005a). In *Drosophila*, HDAC6

181

overexpression was found to suppress degeneration associated with impaired UPS

activity and also suppressed degeneration caused by toxic polyglutamine expression. In

both cases, this rescue by HDAC6 was found to be autophagy dependent, consistent with

a role for HDAC6 in linking the UPS and compensatory autophagy (Pandey et al.,

2007b). HDAC6 activity was also reported to regulate chaperone expression in response

to heat shock by deacetylating Hsp90 leading to release and activation of the transcription

factor HSF-1 (Boyault et al., 2007).

p62 is another cytosolic protein whose structure suggests a function as an adaptor

molecule linking ubiquitinated proteins to autophagic machinery. The C-terminal portion

of p62 harbors both a ubiquitin-associated (UBA) domain which interacts non-covalently

with ubiquitinated proteins (Geetha and Wooten, 2002; Seibenhener et al., 2004) as well

as an LC3- interacting region (LIR) (Pankiv et al., 2007). Cellular stresses such as

polyglutamine expression, proteasome impairment, oxidative stress, and increased

misfolded protein burden activate transcription and translation of p62, suggesting that it

functions broadly in stress situations (Kuusisto et al., 2001b; Nagaoka et al., 2004). p62

localizes to a variety of ubiquitin-positive neuropathological inclusions including Lewy

bodies in Parkinson's disease, neurofibrillary tangles in tauopathies, polyglutamine-

expanded huntingtin aggregates in Huntington's disease, and aggregates of mutant SOD1

in familial amyotrophic lateral sclerosis (Kuusisto et al., 2001a, 2002; Zatloukal et al.,

2002). A role for p62 in protecting against misfolded protein stress is supported by the

observation that RNAi-mediated knockdown of p62 exacerbates polyglutamine toxicity

in vitro and diminishes the formation of ubiquitin-positive inclusions in response to

misfolded protein stress (Bjorkoy et al., 2005) while reducing the ability of LC3 to co-precipitate ubiquitinated proteins (Pankiv et al., 2007). Very recently, p62 was found to contain an LC3 recognition sequence that, when mutated, resulted in ubiquitin- and p62-positive inclusion formation (Ichimura et al., 2008). Thus, it has been suggested that p62 provides a key link between autophagy and the UPS by facilitating autophagic degradation of ubiquitinated proteins. As predicted by this model, p62 null mice fail to form ubiquitin-positive protein aggregates in response to misfolded protein stress (Komatsu et al., 2007) and show age-related neurodegeneration (Ramesh Babu et al., 2008). Consistent results were obtained in studies of *Drosophila* deficient in Ref(2)p, the *Drosophila* homologue of p62 (Nezis et al., 2008). Recent models propose that p62 and HDAC6 function analogously to facilitate autophagic degradation of proteins that display specific polyubiquitin topology. Specifically, it is suggested that K63-linked polyubiquitin chains recruit p62 and HDAC6 providing a signal for autophagic degradation (Olzmann et al., 2007; Tan et al., 2007).

Alfy (autophagy-linked FYVE protein) is a third possible molecular link between autophagy and the UPS. Alfy is a member of the FYVE-domain family of proteins. In cells that are exposed to stressors such as starvation or UPS inhibition, Alfy relocalizes from the nuclear envelope to filamentous cytoplasmic structures that are near autophagic membranes and ubiquitinated protein inclusions, as well as within autophagosomes (Simonsen et al., 2004). Mutations in *blue cheese*, the *Drosophila* homology of human Alfy, lead to reduced longevity and the accumulation of ubiquitinated neural aggregates,

suggesting that its role in autophagic degradation may be involved in the clearance of ubiquitin aggregates (Finley et al., 2003; Simonsen et al., 2004).

Summary and unresolved questions

The last few years have led to substantial insight into the relationship between autophagy and the UPS. It has become apparent that there is significant similarity, and in some cases overlap, in the regulation of these catabolic pathways by UBL modification, leading to the suggestion that they evolved from a common biological origin (Hughes and Rusten, 2007). Further, it has become evident that the function of autophagy and the UPS are coordinated. For example, impairment of the UPS results in upregulation of autophagy ((Iwata et al., 2005a; Pandey et al., 2007b) and Figure A3.3), and in some contexts this upregulation of autophagy can compensate for impaired UPS function (Pandey et al., 2007b). However, it is not known whether this compensatory relationship is reciprocal, as few reagents exist to upregulate the UPS. One study found that upregulation of UPS may afford neuroprotection from toxicity caused by disease proteins, though the authors did not examine the effects of UPS upregulation in autophagy-deficient cells (Seo et al., 2007). The mechanism and the molecular players that regulate the relationship between autophagy and the UPS are beginning to be elucidated and, perhaps not surprisingly, recognition of UBL modification is emerging as a consistent theme.

CMA is also clearly involved in the coordinated functioning of proteolytic pathways. CMA can selectively degrade some subunits of the proteasome, highlighting a

184

relationship between CMA and the UPS (Cuervo et al., 1995). In addition, acute blockage

of CMA results in short-term impairment of both the UPS and macroautophagy, followed

by a recovery of these catabolic systems as CMA blockade persists (Massey et al., 2008).

Chronic blockage of CMA results in constitutive activation of macroautophagy, which

appears to be compensatory (Massey et al., 2006). These interrelationships suggest a

model in which the preferred route of degradation for a particular substrate may be linked

to which system is most capable of efficiently degrading it.

While much has been revealed in recent years, substantial questions remain. Most

notable, it is largely unknown how the decision is made between degradative routes for

any particular protein substrate when more than one pathway is available. HDAC6, p62,

and Alfy have been implicated in directing ubiquitinated proteins for autophagic

degradation, but the mechanisms whereby these proteins identify their targets and

influence their degradation are still unknown. Tantalizing recent evidence suggests that

different classes of substrates may be identified by polyubiquitin chains of differing

topology, providing the signal for degradation by one proteolytic system or the other

(Lim et al., 2005; Olzmann et al., 2007). More specifically, it has been suggested that

polyubiquitin chains with K48-linked chains are primarily degraded by the UPS, whereas

those with K63-linked chains are directed to autophagy. Indeed, one might envision a

"ubiquitin code" that translates into interaction with specific ubiquitin binding proteins,

including HDAC6, Alfy, p62 or other members of the UBA family (Elsasser and Finley,

2005), which may in turn determine the fate of the substrate. However, experimental

limitations in distinguishing between K48-, K63- and mixed-linkage ubiquitin chains

185

must be overcome in order to answer this question effectively, and many of these relationships remain largely unexplored.   This concept of different classes of substrates that are destined for degradation by differing pathways is consistent with one recent report in which disease-associated proteins were found to partition into two distinct intracellular compartments, with soluble ubiquitinated proteins accumulating in a proteasome-rich juxtanuclear region, and insoluble aggregated proteins accumulating in perivacuolar inclusions that colocalize with Atg8 (Kaganovich et al., 2008). It would be interesting to determine whether these proteins could be distinguished by differing UBL modifications.

The mechanism by which upregulation of autophagy mitigates neurotoxicity associated with UPS impairment is also unresolved. It is unlikely that autophagy is able to compensate for the role of the UPS in fine-tuning the steady-state levels of short-lived regulatory proteins. More likely, augmentation of autophagy is neuroprotective by 1) maintaining the overall rate of catabolism, "freeing" amino acids that would otherwise lie useless in aggregated, nonfunctioning proteins, 2) eliminating specific protein substrates that would otherwise accumulate, aggregate and acquire toxic properties, or 3) a combination of these.

Further illumination of the relationship between the UPS, autophagy and the relationship to human disease is vitally important and could lead to harnessing intrinsic catabolic pathways for therapeutic benefit.

Acknowledgments

Figures and Legends

Figure A3.1. The UPS and the autophagy-lysosomal systems are the two main protein degradation systems in the cell.
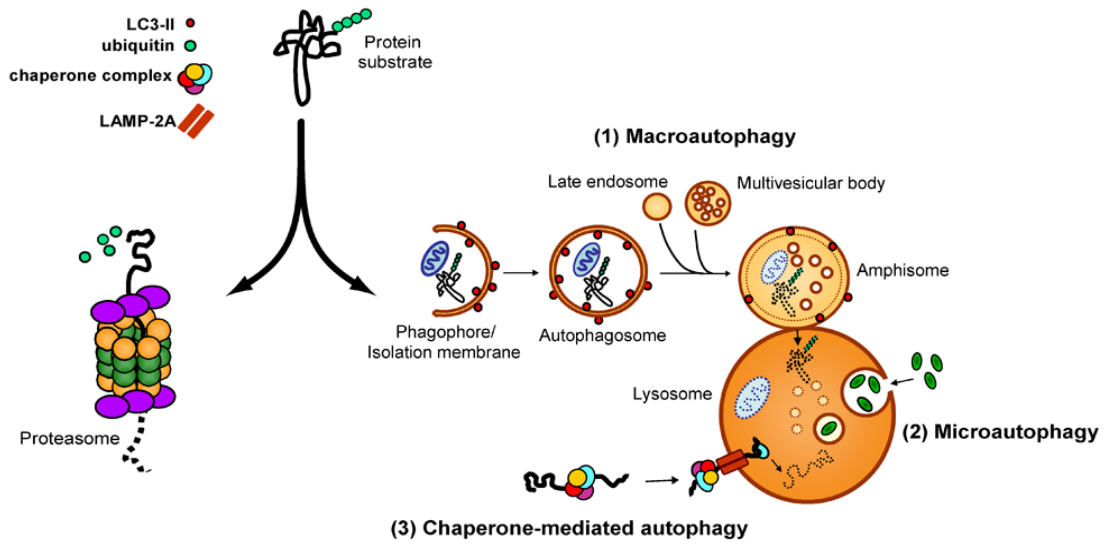
Figure A3.1. The UPS and the autophagy-lysosomal systems are the two main protein degradation systems in the cell. Proteins that are tagged with polyubiquitin chains are generally considered to be substrates for the UPS, which feeds unfolded proteins through the barrel of the 26S proteasome and generates small digested peptides. Recent evidence suggests that some ubiquitinated substrates can also be degraded via the autophagy-lysosomal system. This system is comprised of (1) macroautophagy, in which cytosolic components are engulfed and delivered to the lysosome in bulk, (2) microautophagy, in which small volumes of cytosol are directly engulfed by lysosomes, and (3) chaperone-mediated autophagy (CMA), in which soluble substrates associated with a specific chaperone complex are translocated into the lysosome through the LAMP-2A lysosomal receptor. Macroautophagy involves a series of maturation steps: first, a portion of cytoplasm is surrounded by an expanding isolation membrane or phagophore. The phagophore seals to form an autophagosome, which in mammals fuses with late endosomes and multivesicular bodies to form an amphisome. The amphisome then fuses with a lysosome to form an autolysosome, in which cytosolic cargo is degraded by lysosomal hydrolases. LC3-II is a protein that associates with the inner and outer surfaces of autophagic membranes and provides a histological marker of autophagic vacuoles.

Figure A3.2. Assembly and elongation of autophagic membranes are accomplished via sequential action of UPS-like E1-E2-E3 cascades.
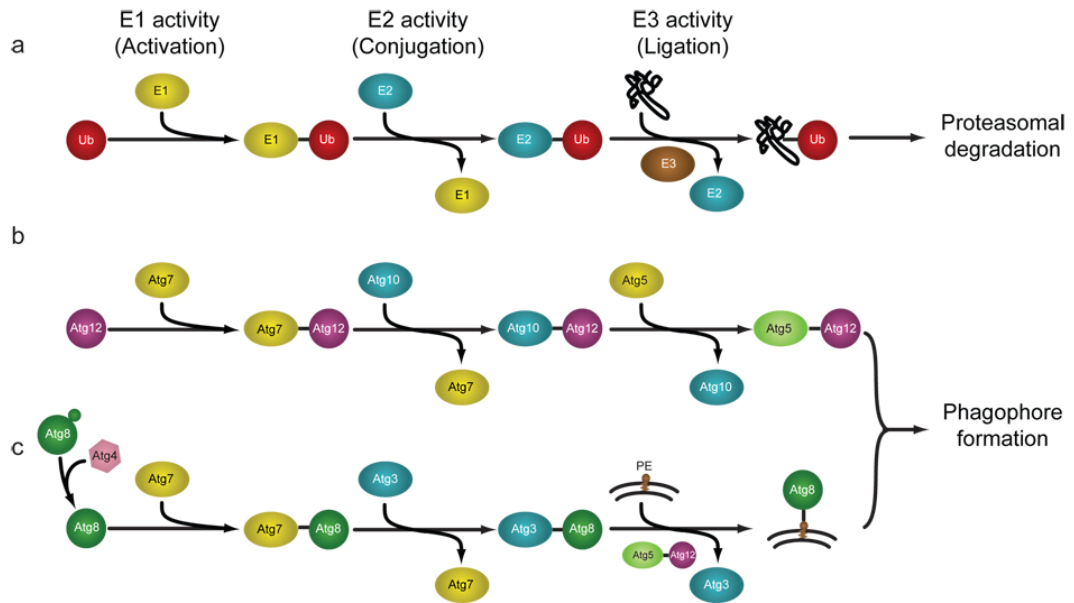
Figure A3.2. Assembly and elongation of autophagic membranes are accomplished via sequential action of UPS-like E1-E2-E3 cascades. In each case, an E1 enzyme activates a ubiquitin-like protein (UBL) such as ubiquitin, Atg12, or Atg8. The UBL is then transferred to an E2 conjugating enzyme, followed by an association with an E3 ligase that promotes association of the UBL and its target. (a) In the UPS, ubiquitination of substrates is accomplished by an E1-activating enzyme, E2-conjugating enzyme, and an E3-ligase. (b) In the first arm of the Atg conjugation pathway, Atg12 associates with the E1-like Atg7, is transferred to the E2-like Atg10, and is subsequently conjugated to Atg5. No E3-like protein has been identified in this pathway. (c) In the second arm of the Atg conjugation pathway, Atg8 associates with the E1-like Atg7, is transferred to the E2-like Atg3, and is conjugated to PE via the E3-like action of the Atg12-Atg5 complex. Adapted from (Geng and Klionsky, 2008) with permission.

Figure A3.3. Proteasome impairment leads to upregulation of autophagic activity.
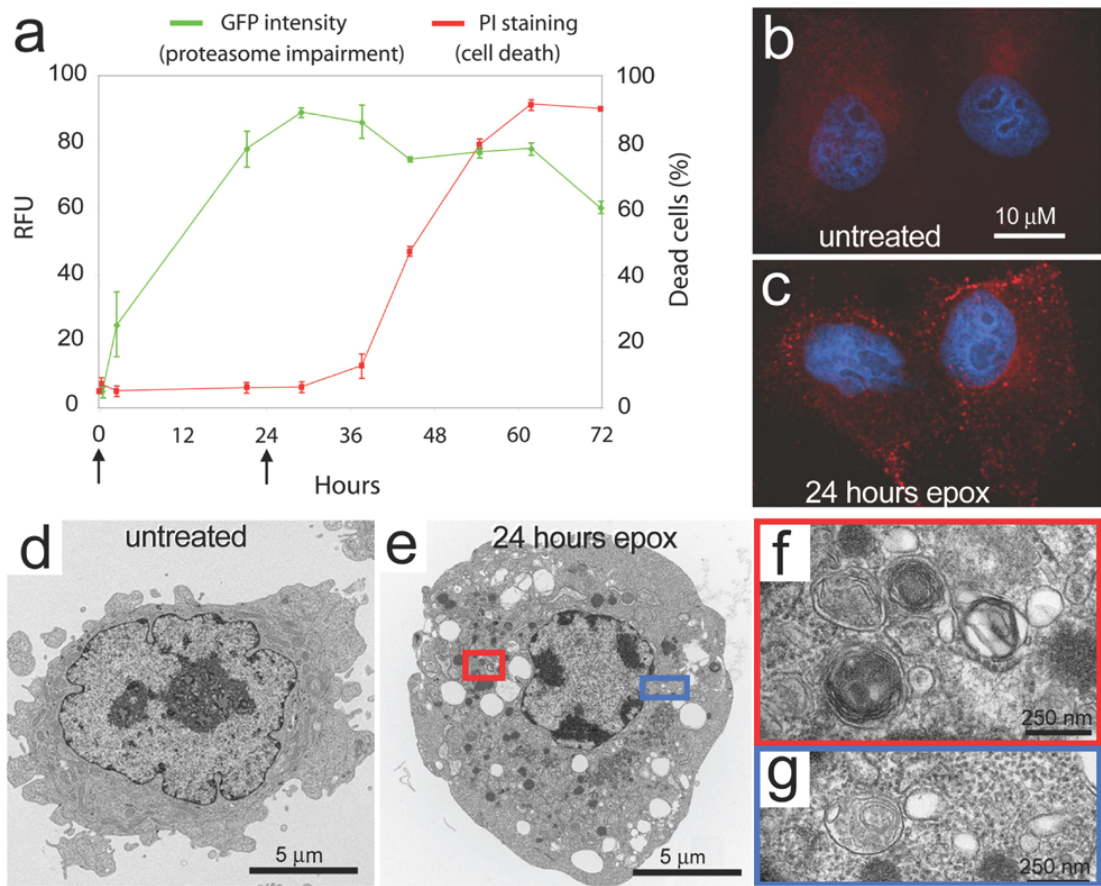
Figure A3.3. Proteasome impairment leads to upregulation of autophagic activity.

(a) HeLa cells that stably express the UPS reporter UbG76V-GFP were treated with the irreversible proteasome inhibitor epoximicin for 72 hours and monitored for cell death. Increasing levels of the GFP substrate indicate impaired UPS function. Note the 24 hours time point used in (b)-(g) is within the window during which proteasome function is impaired, but the cells remain viable. (b-c) Images of LC3 staining (red) and DAPI (blue) show accumulation of LC3 puncta in epoximicin-treated cells. (d-e) Transmission electron microscopy images of cells reveal autophagic structures and prominent vacuolization in epoximicin-treated cells. (f-g) Increased magnification of structures in (e) reveal multi-membraned structures consistent with autophagic activity.
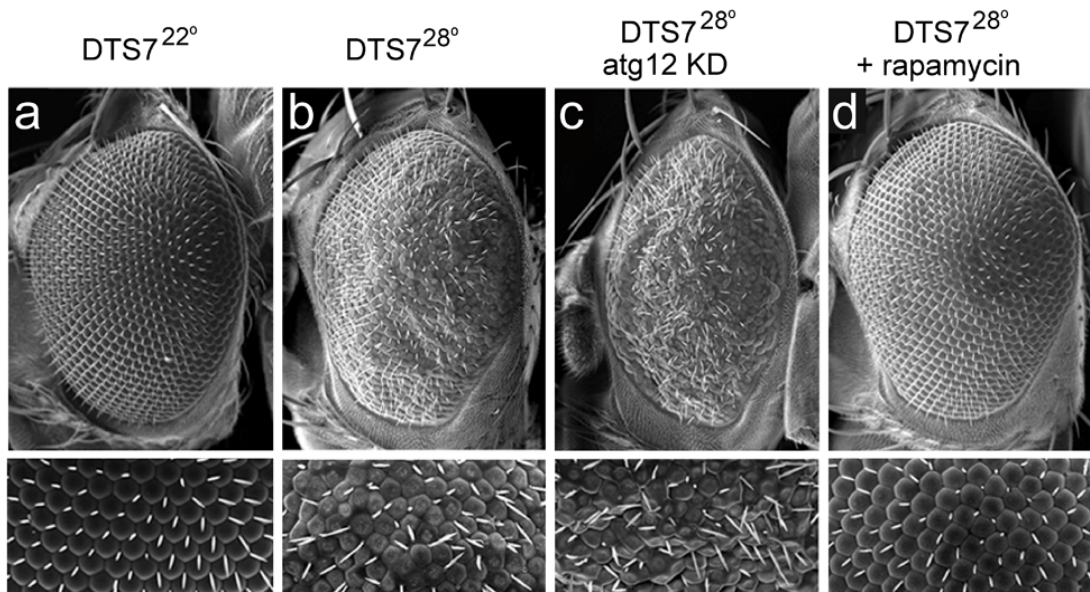
Figure A3.4

Figure A3.4. A *Drosophila* model of proteasome impairment is modified by manipulation of autophagic activity. (a-b) The temperature-sensitive DTS7 mutant shows a normal eye phenotype at the permissive temperature of 22°C and a significant degenerative phenotype at the restrictive temperature of 28°C. (c) RNAi knockdown of the autophagy gene *atg12* results in an enhancement of the DTS7 degenerative phenotype, suggesting that the autophagic activity that is induced in response to proteasome impairment is compensatory. (d) Treatment of DTS7 flies with rapamycin suppresses the degenerative phenotype, demonstrating that induction of autophagy can compensate for impaired proteasome function. Adapted from (Pandey et al., 2007b).

Appendix IV:

HDAC6 Rescues Neurodegeneration and

Provides an Essential Link Between Autophagy and the UPS

HDAC6 rescues neurodegeneration and provides an essential link between autophagy and the UPS

Udai Bhan Pandey[1], Zhiping Nie[1], Yakup Batlevi[2], Brett A. McCray[1], Gillian P. Ritson[1],

Natalia B. Nedelsky[1], Stephanie L. Schwartz[1], Nicholas DiProspero[3], Melanie Knight[3],

Oren Schuldiner[4], Ranjani Padmanabhan[5], Marc Hild[5], Deborah L. Berry[2], Dan Garza[5],

Charlotte C. Hubbert[6], Tso-Pang Yao[6], Eric H. Baehrecke[2], and J. Paul Taylor[1][§]

1. Dept. of Neurology, University of Pennsylvania School of Medicine, Philadelphia, PA 19104 USA
2. Center for Biosystems Research, University of Maryland Biotechnology Institute, College Park, MD 20742 USA
3. Neurogenetics Branch, NINDS, NIH, Bethesda, MD 20817 USA
4. Dept. of Biological Sciences, Stanford University, Stanford, CA 94305 USA
5. Novartis Institutes for Biomedical Research, Cambridge, MA 02139 USA
6. Dept. of Pharmacology and Cancer Biology, Duke University, Durham, NC 27710 USA

Abstract

A prominent feature of late-onset neurodegenerative diseases is accumulation of misfolded protein in vulnerable neurons (Taylor et al., 2002). When levels of misfolded protein overwhelm degradative pathways, the result is cellular toxicity and neurodegeneration (Trojanowski and Lee, 2000). Cellular mechanisms for degrading misfolded protein include the ubiquitin-proteasome system (UPS), the major non-lysosomal degradative pathway for ubiquitinated proteins, and autophagy, a lysosome-mediated degradative pathway (Rubinsztein, 2006). The UPS and autophagy have long been viewed as complementary degradation systems with no point of intersection (Ciechanover et al., 1984; Pickart, 2004). This view was challenged by two observations suggesting an apparent interaction: impairment of the UPS induces autophagy *in vitro*, and conditional knockout of autophagy in the mouse brain leads to neurodegeneration with ubiquitin-positive pathology (Rideout et al., 2004; Iwata et al., 2005a; Hara et al., 2006; Komatsu et al., 2006). It is not known whether autophagy is strictly a parallel degradation system, or whether it is a compensatory degradation system when the UPS is impaired; furthermore, if there is a compensatory interaction between these systems, the molecular link is not known. Here we show that autophagy acts as a compensatory degradation system when the UPS is impaired, and that histone deacetylase 6 (HDAC6), a microtubule-associated deacetylase that interacts with polyubiquitinated proteins (Kawaguchi et al., 2003), is an essential mechanistic link in this compensatory interaction. We found that compensatory autophagy was induced in response to mutations affecting the proteasome and in response to UPS impairment in a fly model of the neurodegenerative disease spinobulbar muscular atrophy (SBMA). Autophagy compensated for impaired UPS function in an HDAC6-dependent manner. Furthermore, expression of HDAC6 was sufficient to rescue degeneration associated with UPS dysfunction *in vivo* in an autophagy-

dependent manner. These findings have implications regarding the pathogenesis of neurodegenerative proteopathies as well as potential interventions for these devastating diseases.

Results and Discussion

DTS7 is a temperature sensitive, dominant negative mutant of the $\beta2$ subunit of the proteasome (Smyth and Belote, 1999). Using the UAS/GAL4 system (Brand and Perrimon, 1993), we targeted DTS7 expression to the eye to cause tissue-restricted proteasome impairment. At 22°C, proteasome function is intact and eye morphology was normal (Figure A4.1a). However, at 28°C substantial degeneration of the retina occurred due to proteasome impairment (Figure A4.1b). To investigate the role of HDAC6 in the setting of misfolded protein stress, we generated transgenic flies expressing wild type *Drosophila* HDAC6 (dHDAC6) as well as wild type and mutant versions of human HDAC6 (hHDAC6). Expression of either dHDAC6 or hHDAC6 strongly suppressed the degenerative phenotype associated with proteasome impairment (Figure A4.1c-d). However, expression of a catalytically dead mutant of hHDAC6 (H216A;H611A) failed to modify the degenerative phenotype, indicating that the deacetylase function of HDAC6 is required for suppression. To assess the role of endogenous HDAC6, we used RNAi knockdown (Supplemental Figure A4.3). Targeted knockdown of dHDAC6 did not noticeably alter eye morphology on its own (Supplemental Figure A4.4), but strongly enhanced degeneration when the proteasome was impaired (Supplemental Figure A4.5). HDAC6 did not modify the rough eye phenotype caused by ectopic expression of the positive regulator of cell death *reaper*, indicating that HDAC6 is not a general suppressor

198

of cell death pathways (Supplemental Figure A4.6). Ectopic expression of dHDAC3 and dHDAC11 did not suppress degeneration caused by proteasome impairment indicating that this is not a general response of HDACs (not shown).

Impaired UPS function has been implicated in a broad array of neurodegenerative disorders, but *in vivo* evidence is lacking (Ciechanover and Brundin, 2003). SBMA is an inherited neurodegenerative disease that is caused by polyglutamine (polyQ) repeat expansion in the androgen receptor (AR) gene (La Spada et al., 1991). Like most adult-onset neurodegenerative diseases, SBMA pathology features accumulation of ubiquitin-positive protein aggregates in vulnerable neurons (Li et al., 1998). To develop a *Drosophila* model of SBMA, we generated transgenic flies expressing full-length human AR with 12-121 glutamine repeats using the UAS/GAL4 system. Flies expressing polyQ-expanded AR recapitulate key features of human SBMA, including ligand-dependent, polyQ length-dependent degeneration (Figure A4.1f, g and Supplemental Figure A4.7), as previously reported (Takeyama et al., 2002).

To evaluate UPS function in this fly model of SBMA, we generated transgenic flies expressing a fluorescent reporter of UPS function. CL1-GFP is a fusion protein created by introducing a degradation signal to otherwise stable green fluorescent protein (GFP) (Bence et al., 2001). This protein is rapidly degraded by the UPS and its steady state levels reflect the functional status of this pathway (Neefjes and Dantuma, 2004). When stable GFP was expressed in eye imaginal discs from third instar larvae, a robust fluorescent signal was detected by confocal microscopy (Figure A4.1k). In contrast, eye

199

imaginal discs from control flies expressing the CL1-GFP reporter emitted a low

fluorescent signal reflecting an active UPS (Figure A4.1l). To test the ability of the UPS

reporter flies to detect proteasome impairment *in vivo*, we co-expressed CL1-GFP in the

eye with DTS7. At 22°C, CL1-GFP reporter levels remained low in eye imaginal discs

co-expressing DTS7, consistent with normal proteasome function (Figure A4.1m). In

contrast, at 28°C, there was a significant increase in the CL1-GFP signal, demonstrating

the ability of the reporter to detect proteasome impairment associated with a degenerative

phenotype *in vivo* (Figure A4.1n and Supplemental Figure A4.8). UPS reporter RNA

levels were not altered by the conditions used in our experiments (Supplemental Figure

A4.9).

We next expressed the CL1-GFP reporter in SBMA flies. In AR121 flies not exposed to

ligand, fluorescent signal from the UPS reporter remained low indicating that proteasome

function was normal despite high expression of polyQ-expanded AR (Figure A4.1o).

However, flies reared on DHT exhibited a significant increase in reporter signal,

indicating proteasome impairment in association with induction of toxicity (Figure A4.1p

and Supplemental Figure A4.8). The ligand-dependent nature of this finding indicates

that UPS impairment is not merely a consequence of over-expressed AR121. Proteasome

impairment by AR expression is a polyQ length-dependent phenomenon because no

impairment was observed in flies expressing AR12 (Supplemental Figure A4.8). The

finding of proteasome impairment in SBMA flies is consistent with a prior report that

polyQ toxicity *in vivo* is enhanced by proteasome mutations (Chan et al., 2002).

The determination that there is impairment of the UPS in SBMA flies led us to examine the ability of HDAC6 to modify the degenerative phenotype in this model of human neurodegenerative disease. Consistent with the results using proteasome mutant flies, ectopic expression of either dHDAC6 or hHDAC6 suppressed the ligand-dependent degenerative phenotype in flies expressing polyQ-expanded AR (Figure A4.1h, i). Expression of the catalytically dead mutant of hHDAC6 (H216A; H611A) failed to modify the degenerative phenotype, indicating that the deacetylase function of HDAC6 is also required for suppression of polyQ toxicity (Figure A4.1j). Knockdown of endogenous HDAC6 with RNAi enhanced ligand-dependent degeneration in AR52 flies (Supplemental Figure A4.5). Thus, endogenous HDAC6 also plays a role in protecting cells from polyQ toxicity.

We previously reported induction of autophagy and sequestration of polyQ-expanded AR in autophagic vacuoles *in vitro* (Taylor et al., 2003b). Induction of autophagy *in vitro* in response to proteasome impairment has also been described (Rideout et al., 2004; Iwata et al., 2005a). To determine whether autophagy is induced *in vivo* when the UPS is impaired, we performed ultrastructural evaluation by transmission electron microscopy (TEM) in the DTS7 and SBMA flies. In both cases, we found a significant increase in morphological features of autophagy (Figure A4.2f). These included autophagic vacuoles (AVs) such as early autophagosomes in which membranes surrounded cytoplasmic components (Figure A4.2a, b), more mature AVs (Figure A4.2c), multilamellar bodies (MLBs, Figure A4.2d) and multivesicular bodies (MVBs, Figure A4.2e).

To assess the role of autophagy when the UPS is impaired, we inhibited autophagy by RNAi knockdown of the autophagy genes *atg6* and *atg12*. Knockdown of either *atg6* or *atg12* did not affect eye morphology (Supplemental Figure A4.10), indicating that the *Drosophila* eye can tolerate reduced autophagy when UPS function is intact, at least in 1-day-old flies. In contrast, knocking down either *atg6* or *atg12* strongly enhanced the rough eye phenotype associated with UPS impairment in DTS7 flies reared at 28°C (Figure A4.2g-i) and in AR52 flies reared on DHT (Figure A4.2j-l). From these data, we can infer that the autophagy induced by UPS impairment is compensatory.

We hypothesized that ectopic expression of HDAC6 suppressed degeneration by promoting autophagic degradation of aberrant protein. Thus, we examined AR levels *in vivo* and determined that expression of HDAC6 led to lower steady state levels of polyQ-expanded AR *in vivo*, whereas inhibition of autophagy by knockdown of *atg6* or *atg12* resulted in higher steady state levels (Figure A4.3a). These altered steady state levels occurred despite no significant change in RNA levels (Supplemental Figure A4.11), suggesting that HDAC6 accelerates the rate of AR degradation. To investigate this further, we adapted the inducible Geneswitch expression system (McGuire et al., 2004) to monitor protein turnover. In *elav*-GS;UAS-AR52 flies, no expression was detected prior to exposure to the inducing agent RU486 (data not shown). To induce expression, starved flies were fed sucrose media containing RU486 for one hour, which resulted in a pulse of expression that became detectable within 2 hours, peaked after approximately 10 hours, and then gradually decayed with a half-life of ~100 minutes (Figure A4.3b-c and Supplemental Figure A4.12). In *elav*-GS;UAS-AR52;UAS-dHDAC6 flies, there was a

parallel induction of AR52 expression, but an accelerated rate of decay, with a half-life of ~50 minutes (Figure A4.3c-d and Supplemental Figure A4.12). Importantly, co-expression of dHDAC6 not only accelerated the turnover of AR52 monomers ~2-fold, but also high molecular weight aggregates that were trapped in the stacking gel (Figure A4.3d).

We determined that treatment with rapamycin suppressed degeneration caused by either proteasome impairment or polyQ toxicity (Figure A4.4a-d). This finding is consistent with a prior report in which rapamycin suppressed degeneration in fly and mouse models of Huntington's disease (Ravikumar et al., 2004). Rescue by rapamycin has been attributed to inhibition of TOR and induction of autophagy, although a role for other TOR-regulated pathways could not be excluded (Harris and Lawrence, 2003; Ravikumar et al., 2004). We found that knockdown of *atg12* blocked the ability of rapamycin to suppress degeneration when the proteasome was impaired, verifying that rapamycin rescue is autophagy-dependent (Figure A4.4e, f). Importantly, we also determined that knockdown of dHDAC6 blocked the ability of rapamycin to suppress degeneration, indicating that dHDAC6 is essential in order for induction of autophagy to compensate for proteasome impairment (Figure A4.4g, h). Furthermore, we determined that the ability of dHDAC6 to suppress degeneration was autophagy-dependent since rescue was blocked by knockdown of *atg12* (Figure A4.4i-l). Thus, HDAC6 is integral to rescue of degeneration by autophagy and essential for autophagy to compensate for impaired UPS function.

Our findings extend previous studies in three important ways. First, we determined that induction of autophagy is sufficient to rescue degeneration associated with UPS impairment, dramatically illustrating the compensatory relationship between autophagy and the UPS. Second, we determined that HDAC6 activity is essential for autophagy to compensate for impaired UPS function. Finally, we determined that ectopic expression of HDAC6 alone is sufficient to rescue degeneration caused by proteasome mutations and polyQ toxicity, and does so in an autophagy-dependent manner. These observations are consistent with a mechanism in which HDAC6 facilitates turnover of aberrant protein by autophagy, lowering their steady state levels and mitigating toxicity. We recently determined that over-expression of HDAC6 also suppressed degenerative phenotypes in additional models of neurodegenerative disease including flies expressing pathologic Aβ fragments and other polyQ-expanded proteins (Pandey and Taylor, unpublished results). Thus, the HDAC6-mediated pathway of protein clearance may have broad relevance to degenerative proteopathies.

While the current study indicates that the mechanism of HDAC6 rescue involves accelerated turnover of misfolded protein by autophagy, further study is required to determine the precise details of how this occurs. The mechanism could involve modulation of HSP90 activity, since this chaperone is a substrate of HDAC6 deacetylase activity (Kovacs et al., 2005). Alternatively, HDAC6 may be involved in shuttling polyubiquitinated substrates to a location conducive to engulfment by autophagosomes, consistent with a known role for HDAC6 in the formation of aggresomes *in vitro* (Kawaguchi et al., 2003). A third possibility is that HDAC6 may contribute to the

transport of lysosomes to the site of autophagy, as suggested by the observation that HDAC6 knockdown results in dispersal of lysosomes away from the microtubule organizing center (Iwata et al., 2005a). Elucidating the precise role of HDAC6 in linking autophagy and the UPS promises to reveal tremendous insight to cellular management of misfolded protein.

Author Contributions

Experimental work was performed by U.B.P., Z.N., Y.B., B.A.M., G.P.R., S.L.S., B.L.B. and J.P.T. Vital Reagents were provided by N.D., M.K., O.S., R.P., M.H., D.G., and T.P.Y. The manuscript was written by N.B.N., E.H.B. and J.P.T. All authors discussed of results and commented on the manuscript.

Author Information Reprints and permissions information is available at npg.nature.com/reprintsandpermissions. The authors declare no competing financial interests. Correspondence and requests for materials should be addressed to J.P.T.

205

Methods

Fly stocks

All *Drosophila* stocks were maintained on standard media in 25°C incubators unless otherwise noted. DHT (Steraloids) was mixed with freshly made food once it had cooled to $<50^{o}$C to a final concentration of 1 mM. Rapamycin (Sigma) was mixed with freshly made food once it had cooled to $<50^{o}$C to a final concentration of 1 μM. To generate AR transgenic flies, cDNA encoding full length human AR with 12, 77, or 121 CAG repeats was subcloned into pUAST[12]. The cDNA for dHDAC6 was generated from EST LD43531 which encodes 1128 amino acids corresponding to HDAC6-RA on Flybase. KpnI and XbaI restriction sites were included in the 5' and 3' primers, respectively, for subcloning into the vector pAc5.1/V5 (Invitrogen). The cDNA for human HDAC6 and mutant human HDAC6 were previously described (Grozinger et al., 1999). The dHDAC6 cDNA plus in-frame V5 tag was subsequently subcloned into pUAST. Transgenic *Drosophila* were generated using standard techniques (Rubin and Spradling, 1982). The GMR-GAL4 line was obtained from the Bloomington Stock Center (Bloomington, IN). UAS-DTS7 flies were provided by John Belote. AR20 and AR52 flies were provided by Ken-ichi Takeyama. Plasmid containing the cDNA for UPS reporter CL1-GFP was provided by Ron Kopito. To generate UPS reporter flies, cDNA encoding CL1-GFP was subcloned into pUAST and transgenics were generated as above. UAS-atg6^{KD} flies were generated as described previously (Scott et al., 2004). Inverted repeats for UAS-atg12^{KD} flies were generated with primers 5'-GGCGCGCCTATCC TTCTGAACGCCACTG-3' and 5'-GCGGAATTCCTTAGCAAAGTCATGTGCG TATCG-3' as described previously (Scott et al., 2004). For dHDAC6 knockdown, amplicon sequences were

206

obtained from the Heidelberg Fly Array Database (Hild et al., 2003) and a 500bp

fragment was amplified by PCR and inserted into the AvrII and NheI sites of the pWIZ

vector as described previously (Lee and Carthew, 2003). Quantitation of the degree of

knockdown in the RNAi knockdown lines is shown in Supplemental Figure A4.3. Eye

phenotypes of 1-day-old anesthetized flies were evaluated with a Leica MZ APO

stereomicroscope and photographed with a Leica DFC320 digital camera. For each

genotype and condition, at least 200 to >1000 flies were evaluated. Quantitation of eye

phenotypes is shown in Supplemental Figure A4.2.

TEM and confocal microscopy

For TEM evaluation, fly heads were fixed with 2.5% glutaraldehyde/2% formaldehyde

with 0.1 M sodium cacodylate and stored at 4°C until embedding. Heads were post-fixed

with 2% osmium tetroxide followed by an increasing gradient dehydration step using

ethanol and propylene oxide. Heads were then embedded in LX-112 medium (Ladd) and

sections were cut ultrathin (90 nm), placed on uncoated copper grids, and stained with

0.2% lead citrate and 1% uranyl acetate. Images were examined with a JEOL1010

electron microscope at 80 kV. To quantitate morphologic features by TEM, we used

longitudinal sections through the retina and identified photoreceptor neurons by the

presence of rhabdomeres. 59-82 neurons from 5 flies per condition were scored for the

presence of AVs, MVBs, and MLBs, and comparisons between conditions were made

with a paired t-test. To evaluate GFP fluorescence in UPS reporter flies, imaginal eye

discs were dissected from wandering third-instar larvae in a buffer containing 128 mM

NaCl, 4 mM MgCl2, 2 mM KCl, 0.4 mM CaCl2, 70 mM sucrose and 5 mM HEPES.

After dissection, the discs were fixed in 4% paraformaldehyde for 30 minutes on ice, washed with standard saline three times, and mounted in Glycergel Mounting Medium (DAKO). Imaging was performed on a Bio-Rad MRC1024ES confocal laser scanning module on a Nikon Eclipse E600 and analyzed by using LaserSharp software.

SEM

SEM samples were collected and fixed in 2.5% gluteraldehyde (EMS) in PBS and post-fixed for 15-30 minutes in 1.5% osmium tetroxide (Stevens Metallurgical) in PBS. Samples were then dehydrated in ethanol, immersed in hexamethyldisilazane (Polysciences Inc.) and dried in a desiccator for three days. Specimens were then coated with gold:palladium using a Denton DV-503 vacuum evaporator, and analyzed using an AMRAY 1820D scanning electron microscope.

Biochemistry

Immunoblots were performed as described previously (Taylor et al., 2003b) using antibodies against GFP (ab6556, Novus Biologicals), AR (N20, Santa Cruz Biotech), 119 β-actin (119, Santa Cruz Biotech), tubulin (Sigma), V5 epitope (Invitrogen), and affinity-purified antibody against dHDAC6. Protein signals were detected by chemiluminescence (Millipore Immobilon). To monitor protein turnover *in vivo*, 1-day-old adult flies of the appropriate genotype were collected and starved for 12 hours in a vial that contained only a Kimwipe soaked with 3 ml of water. After starvation, flies were placed in a vial that contained a Kimwipe soaked with 3 ml of 500 μM RU486 (Steraloids) dissolved in a 2% sucrose solution (minus DHT condition) or 500 μM RU486 and 1 mM DHT in a 2%

sucrose solution (plus DHT condition) for 1 hour, and then transferred to a vial

containing normal food (minus DHT condition) or food containing 1 mM DHT (plus

DHT condition) until collected for extract preparation. Five flies were collected every 2.5

hours up to 20 hours, heads were removed, crushed in RIPA buffer, sonicated, and

analyzed by Western blot. AR and β-actin protein levels were assessed by immunoblot.

Quantitation of luminescence was performed with a Kodak IS2000RT instrument and

Kodak Molecular Imaging software. The mean AR/actin ratios and standard error of the

mean from ☐3 replicates were plotted on a logarithmic scale and used to determine the

line of best fit by regression analysis ($y = Ae^{-Kx}$). The slope of the best fit line was used to

estimate half-life with the equation $t_{1/2} = 0.693/K$.

Objective criteria for scoring retinal phenotypes

All of the genotypes presented here exhibit highly uniform retinal phenotypes. We

examined the eye phenotypes of at least 200 flies per genotype (>1000 in most cases) and

the phenotypes represented in the SEM images are present in 100% of the animals.

Among genetically identical flies, there was no appreciable variability in the phenotypes.

In cases where enhancement or suppression is reported, it was present in 100% of the

animals. In most cases, changes in the relative severity of the retinal phenotypes were

qualitatively obvious. Nevertheless, to apply quantitative analysis, we randomly selected

50-100 1-day-old flies per genotype and scored phenotypic severity using objective

features. Eyes were examined for the presence or absence of the following features and

given 1 point for each if present:

Feature	Absent	Present
Supernumerary IOB	0	1
Abnormal bristle orientation	0	1
Ommatidial fusion	0	1
Ommatidial pitting	0	1
Disorganization of ommatidial array	0	1
Retinal collapse	0	1

IOB, interommatidial bristles

Two points were added if the affected area involved more than 5% of the eye and 4 points were added if the affected area involved more than 50% of the eye. Comparisons between genotypes were made using Student's t-test assuming equal variances.

Real Time Quantitative PCR

Total RNA was isolated from 5-10 animals of the appropriate genotype with TRIzol reagent (Invitrogen) and cDNA was generated using the SuperScript III First Strand Synthesis System (Invitrogen) following the manufacturer's protocol. Concentrations for each primer probe set were individually optimized. Quantitative real-time PCR reactions were carried out in a total reaction volume of 50 µl of TaqMan Universal Master Mix (ABI) using an Applied Biosystems Fast 7500 machine for 40 cycles. Quantitation of each transcript was determined using the $\Delta\Delta C_T$ method. Transcript levels relative to dGAPDH2 are shown in Supplemental Figure A4.3 for (**a**) two UAS-dHDAC6[KD] lines, (**b**) two UAS-atg6[KD] lines, and (**c**) one UAS-atg12[KD] line.

The primer/probe set for *Drosophila* GAPDH2 (product number CT25538) were

purchased from Applied Biosystems. Primer probe sets for other genes were as follows:

dHDAC6:
Forward primer: 5'-CGCTGTCGCGAACTAAATCTG-3'
Reverse primer: 5'-TCCTTGGTCGCCGATCTC-3'
Probe: 5'-6FAM-CCTGGAGTTGCCC-TAMRA -3'

Atg6:
Forward primer: 5'-GCCTCTCCTCCAACTCTGAGATT-3'
Reverse primer: 5'-GCATGGAGTCGGCACACTCT-3'
Probe: 5'-6FAM-ACCATCCGCTGTGCG-TAMRA -3'

Atg12:
Forward primer: 5'-TGTGCCCATCATCAAAAAGC-3'
Reverse primer: 5'-TCCAGCCGACTGTCTTGTTG-3'
Probe: 5'-6FAM-AACCTGGACCGTAGATC-TAMRA -3'

GFP:
Forward primer   5'-CTGCTGCCCGACAACCA-3'
Reverse   5'-GAACTCCAGCAGGACCATGTG-3'
Probe   5'-6FAM-AAAGACCCCAACGAGAAGCGCGA-TAMRA-3'

AR:
Forward primer: 5'-GCAGGCAAGAGCACTGAAGATA-3'
Reverse primer: 5'-CCTTTGGTGTAACCTCCCTTGA-3'
Probe: 5'-6FAM-TGCTGAGTATTCCCC-TAMRA-3'

Figures and Legends

Figure A4.1. HDAC6 rescues degeneration in flies with proteasome impairment and in a fly model of SBMA that exhibits impaired UPS function.
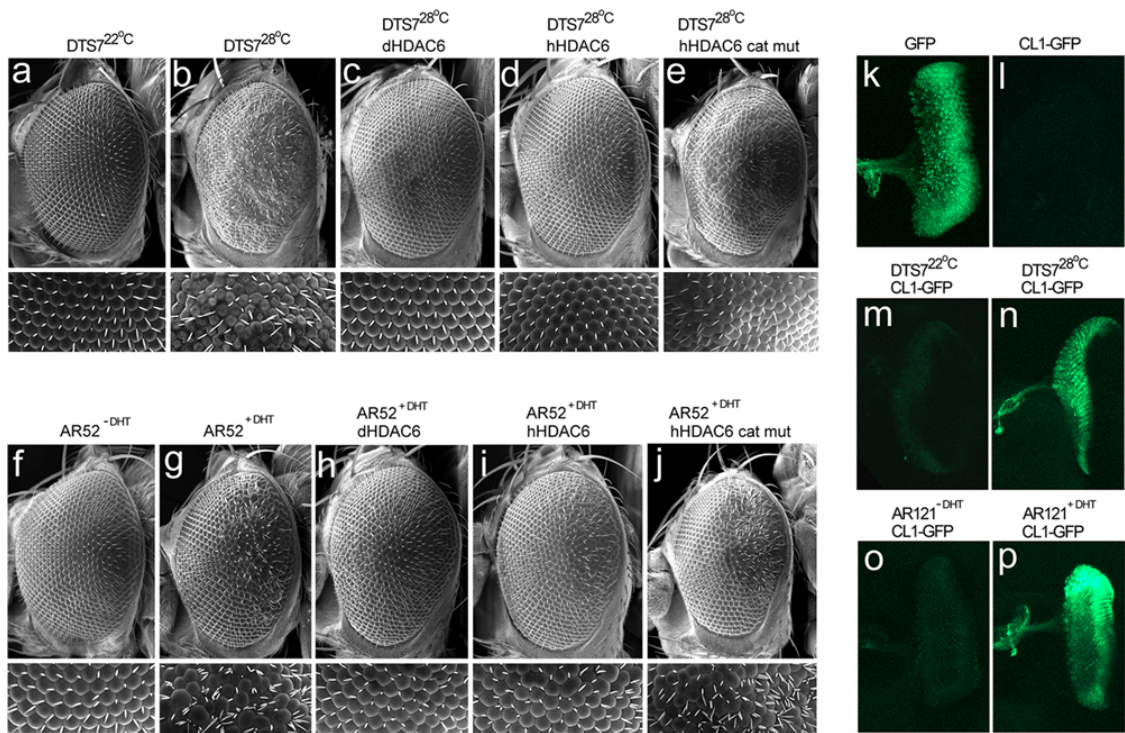
Figure A4.1. HDAC6 rescues degeneration in flies with proteasome impairment and in a fly model of SBMA that exhibits impaired UPS function. (a-e) Scanning electron microscopy (SEM) images of fly eyes expressing DTS7 with or without the indicated HDAC6 transgenes. (a) Normal eyes in DTS7 flies reared at 22°C. (b) Rough eyes in DTS7 flies reared at 28°C. Degeneration was suppressed by expression of dHDAC6 (c) or hHDAC6 (d), but not a catalytically dead mutant of hHDAC6 (e). (f-j) SEM images of fly eyes expressing AR52 with or without the indicated HDAC6 transgenes. (f) Normal eyes in AR52 flies reared without DHT. (g) Rough eyes in AR52 flies reared with DHT. Degeneration was suppressed by expression of dHDAC6 (h) or hHDAC6 (i), but not a catalytically dead mutant of hHDAC6 (j). (k-p) Detection of UPS reporter in imaginal eye discs from third instar larvae by confocal microscopy. High level fluorescence was found in flies expressing GFP (k, positive control), but fluorescence was barely detectable in control flies expressing CL1-GFP (l, negative control). CL1-GFP accumulates in DTS7 flies with temperature-dependent proteasome impairment (compare m to n) and in AR52 flies with ligand-dependent degeneration (compare o to p). The retinal phenotypes of 200 to >1000 flies of each genotype were examined. Quantitative analyses of eye phenotypes and proteasome impairment are presented in Supplemental Figure A4.2 and Supplemental Figure A4.3, respectively. (DHT, dihydrotestosterone).

Figure A4.2. Induction of compensatory autophagy in flies with proteasome mutations and in SBMA flies.
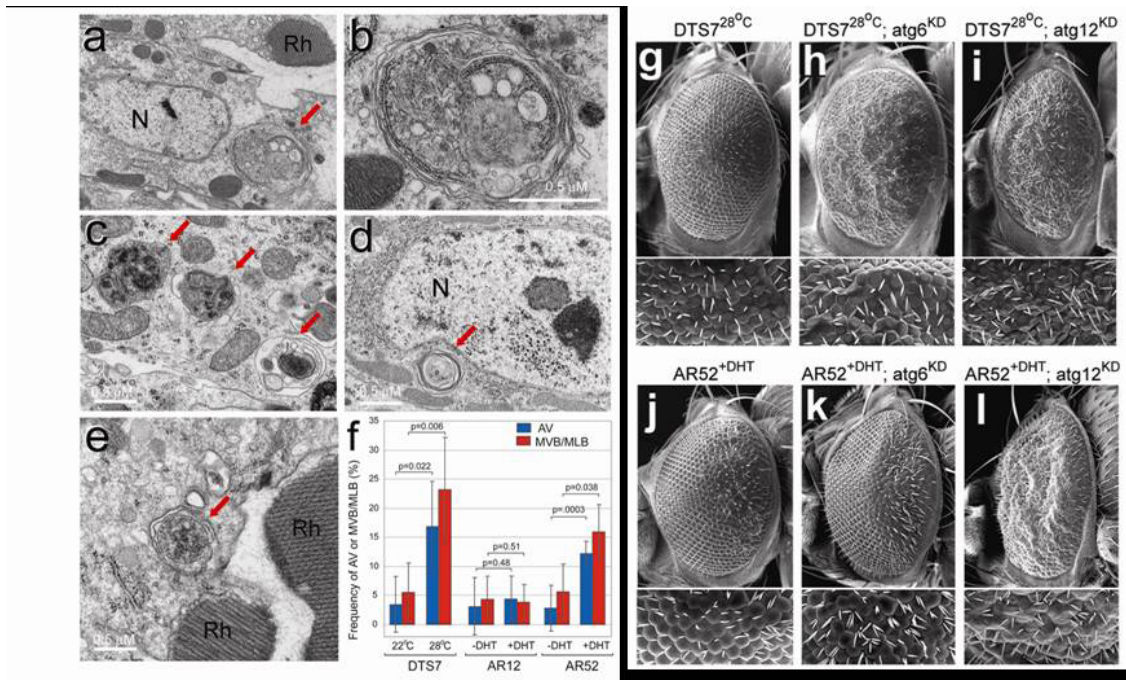
Figure A4.2. Induction of compensatory autophagy in flies with proteasome mutations and in SBMA flies. (a-e) Representative examples of autophagic vacuoles detected by TEM in retinal sections used to generate the quantitative data shown in (f). (a) An autophagosome (red arrow) containing cytoplasmic contents in a photoreceptor neuron from an AR52 fly reared on DHT. (b) Higher magnification of the autophagosome in a. (c) Multiple autophagolysosomes (red arrows) containing dense, amorphous material from an AR52 fly reared on DHT. (d) A juxtanuclear multilamellar body (red arrow) from a DTS7 fly reared at 28°C. (e) A multivesicular body (red arrow) from a DTS7 fly reared at 28°C. (f) A significant increase in the frequency of neurons with autophagic figures in DTS7 flies reared at 28°C compared to those reared at 22°C and in AR52 flies reared on DHT compared to those reared off DHT. Data show mean $\pm$s.d., $n = 59\text{-}82$ neurons in 5 sections/condition. No accumulation of autophagic figures was found in AR12 flies. (g-l) SEM images of fly eyes expressing the indicated transgenes. RNAi knockdown of *atg6* and *atg12* enhances degeneration in DTS7 flies reared at 28°C (compare h, i to g) and AR52 flies reared on DHT (compare k, l to j). 200 to >1000 fly eyes of each genotype were examined. Quantitative analyses of eye phenotypes are presented in Supplemental Figure A4.2. (N, nucleus; Rh, rhabdomere).

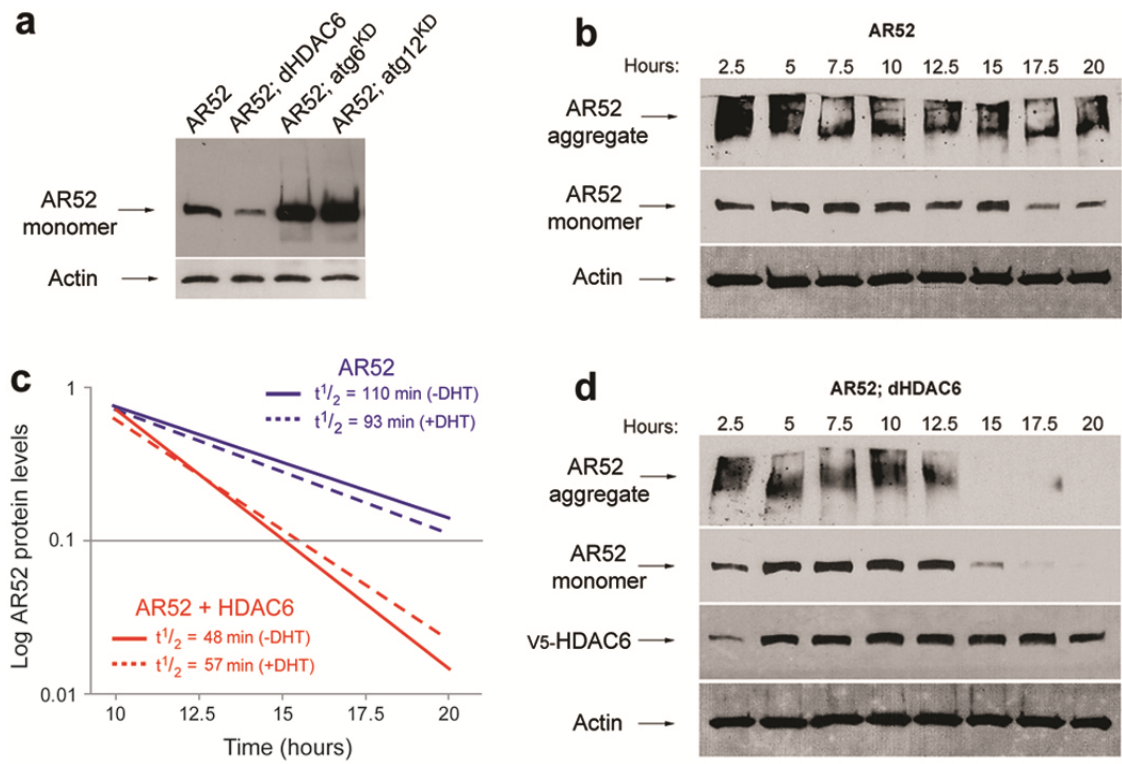**Figure A4.3. HDAC6 accelerates the turnover of polyQ-expanded AR.**

Figure A4.3. HDAC6 accelerates the turnover of polyQ-expanded AR. (a, b, d)

Western blots from flies expressing the indicated transgenes. (a) Steady state levels of

AR52 protein are reduced in flies over-expressing dHDAC6, but are elevated in flies in

which *atg6* or *atg12* has been knocked down. (b) Western blots showing the temporal

profile of AR52 protein monomer and high molecular weight aggregate levels after a

brief pulse of expression. AR52 protein became detectable by 2.5 hours after treatment

with RU486, reached a peak at 10 hours, and then slowly decayed. (c) A logarithmic plot

of AR52/actin ratios was used to determine the line of best fit by regression analysis ($y =$

Ae^{-Kx}). $R^2 = 0.9117$ (AR52^{-DHT}), $R^2 = 0.7808$ (AR52^{+DHT}), $R^2 = 0.9719$ (HDAC6 +

AR52^{-DHT}), $R^2 = 0.9644$ (HDAC6 + AR52^{+DHT}). Half-life was determined by the slope of

the best fit line with the equation $t_{1/2} = 0.693/K$. Half-life of AR52 *in vivo* was reduced

~2-fold in flies co-expressing dHDAC6 and did not differ significantly depending on the

presence (broken lines) or absence (solid lines) of DHT. Plots of the mean AR52/actin

ratios are shown in Supplemental Figure A4.12. (d) Flies co-expressing dHDAC6 showed

a nearly identical profile of induced expression as in b, but AR protein decayed at an

accelerated rate. Exogenous dHDAC6 was detected by immunoblot against the V5
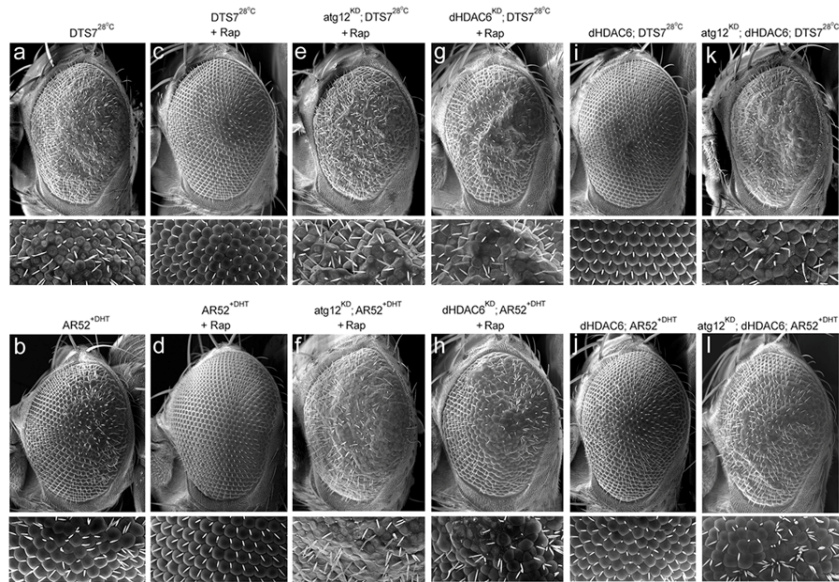
epitope.

Figure A4.4

**Figure A4.4. Rescue of degeneration by HDAC6 is autophagy-dependent.**

(a-l) SEM images of fly eyes expressing the indicated transgenes. The rough eye phenotypes caused by (a) proteasome mutation or by (b) expression of polyQ-expanded AR were both suppressed by rearing flies on the TOR inhibitor rapamycin (c, d). (e,f) Rapamycin failed to suppress degeneration in an autophagy-deficient background created by knockdown of *atg12,* confirming that rescue by rapamycin is autophagy-dependent. (g, h) Rapamycin also failed to suppress degeneration when HDAC6 levels were knocked down, demonstrating that autophagy induction via the TOR pathway is HDAC6-dependent. (k-j) HDAC6 failed to suppress degeneration in an autophagy-deficient background, confirming that rescue by HDAC6 is dependent on autophagy (compare k, l to i, j). 200 to >1000 fly eyes of each genotype were examined. Quantitative analyses of eye phenotypes are presented in Supplemental Figure A4.2.

Supplemental Figure A4.1

(a) Complementary Relationship   (b) Compensatory Relationship
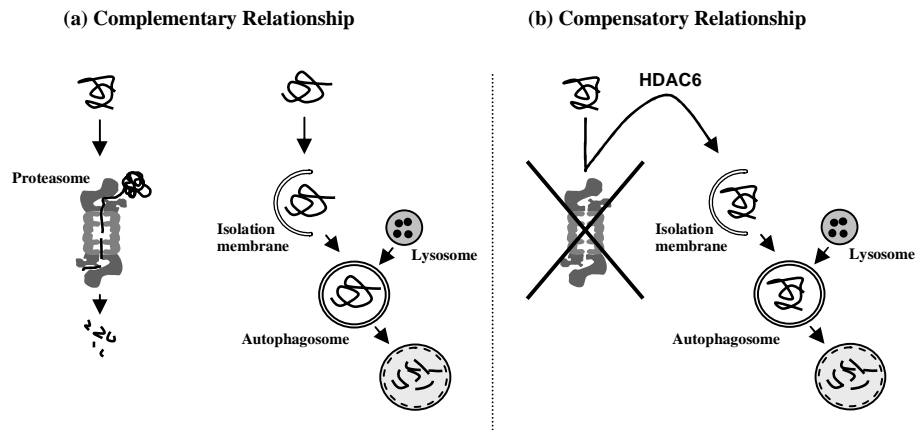
Supplemental Figure A4.1. It was long held that the UPS and autophagy were distinct degradation systems with no point of intersection. This view was challenged by the finding of prominent ubiquitin-positive pathology that accumulates in autophagy-deficient mice despite normal UPS function. Those studies strongly suggest that autophagy participates in the degradation of ubiquitinated substrates under basal conditions and, by so doing, plays a vital neuroprotective role complementary to that of the UPS (**a**). The data here indicates that when the UPS is overwhelmed, for example by proteasome mutations or excess misfolded protein, autophagy also provides compensatory degradation of misfolded proteins (**b**). Furthermore, we find that the microtubule-associated deacetylase HDAC6 is essential for autophagy to compensate for impaired UPS function. Most important with respect to therapeutic implications, we find that over-expression of HDAC6 is sufficient to rescue degeneration in *Drosophila* models of neurodegenerative disease and does so in an autophagy-dependent manner, a finding that has important therapeutic implications.

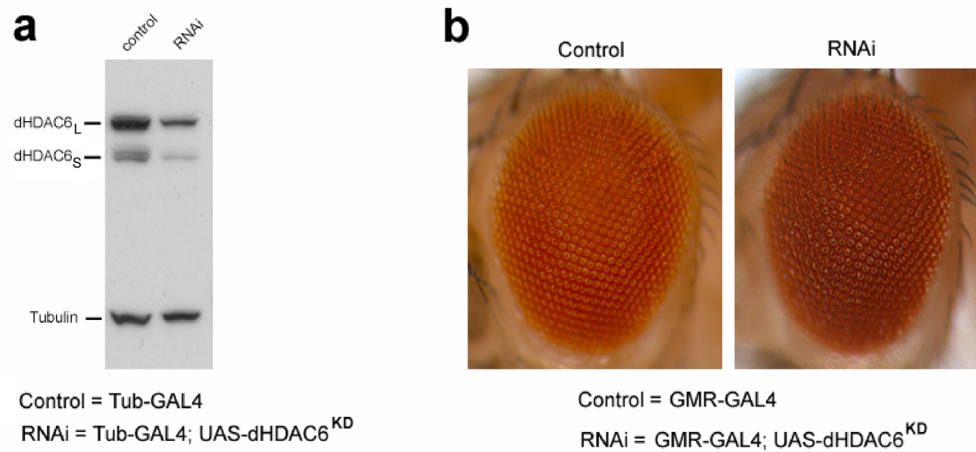**Supplemental Figure A4.2. Quantitative analyses of eye phenotypes.**
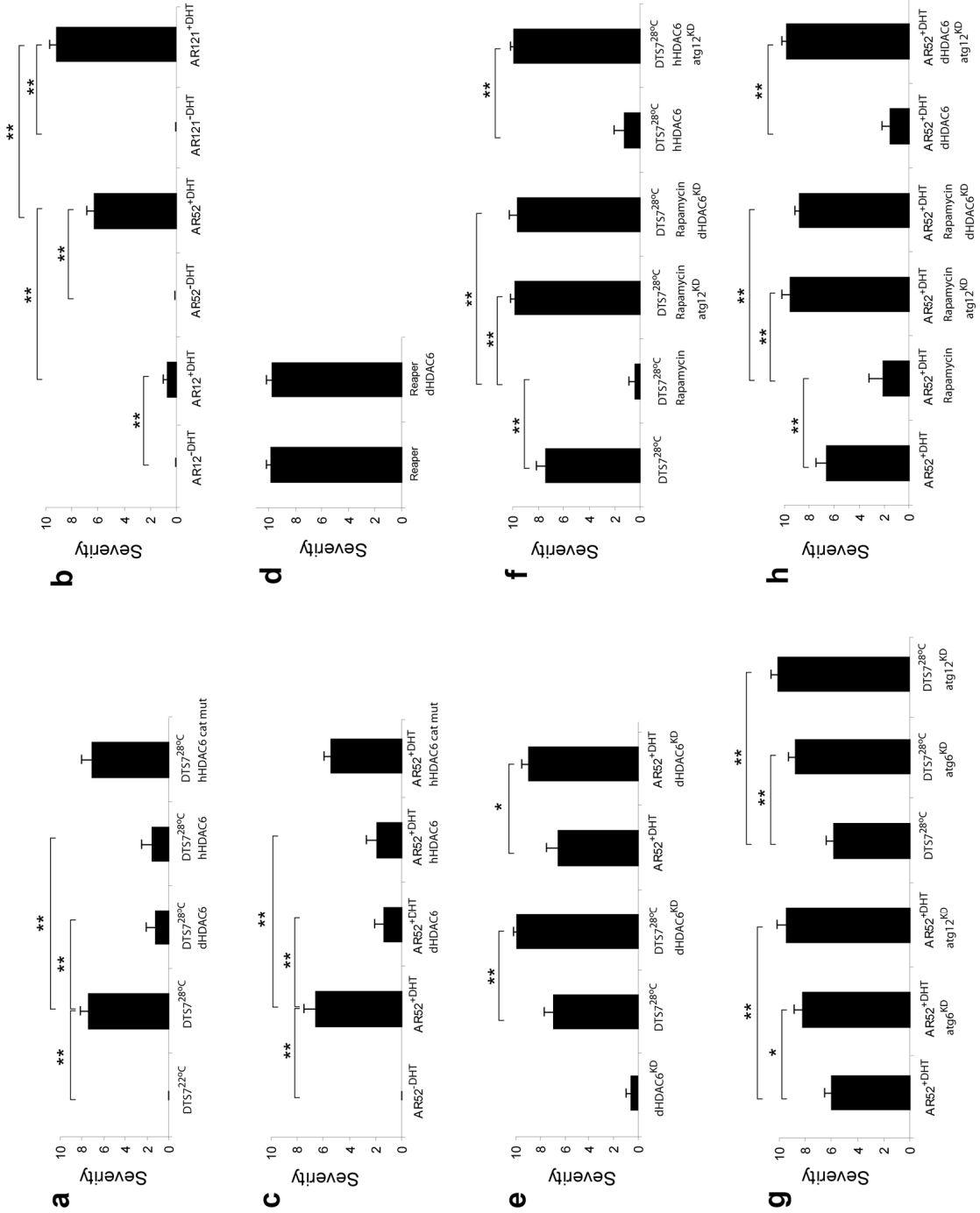
Supplemental Figure A4.2. Quantitative analyses of eye phenotypes. We examined the eye phenotypes of at least 200 flies per genotype (>1000 in most cases) and the phenotypes represented in the SEM images are present in 100% of the animals. Among genetically identical flies, we did not observe significant variability in the phenotypes. In cases where enhancement or suppression is reported, it was present in 100% of the animals. In most cases, changes in the relative severity of the retinal phenotypes were qualitatively obvious. Nevertheless, to apply quantitative analysis, 50-100 flies per genotype were randomly selected for objective scoring according to the criteria described in Supplemental Methods. Comparisons were made using Student's t-test. Data show mean phenotype score ± s.d. * =p<0.01. ** =p<0.001.
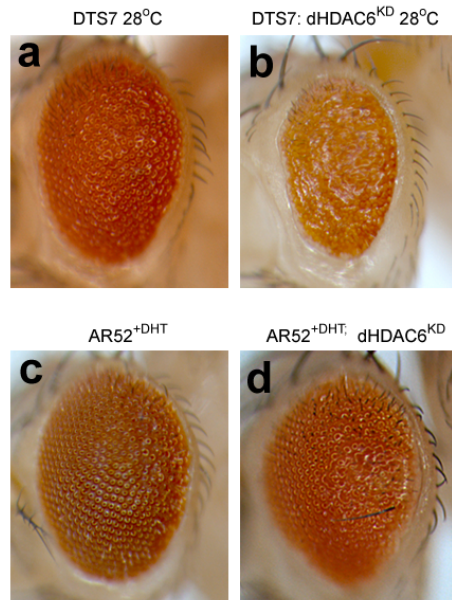
Supplemental Figure A4.3
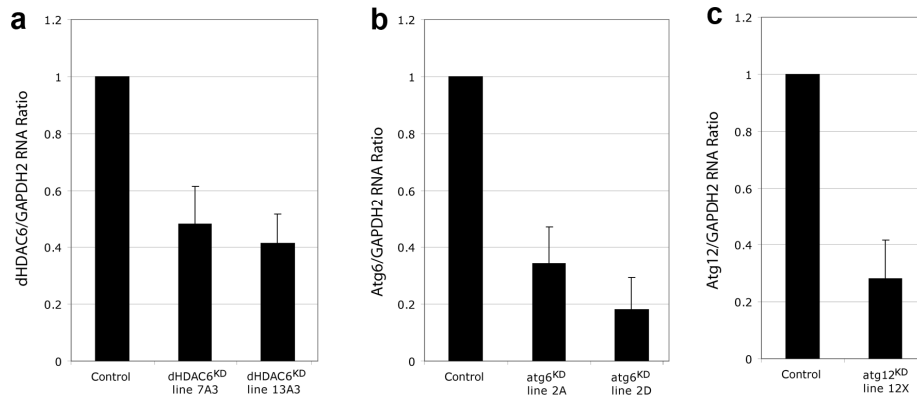
Supplemental Figure A4.3. Quantitation of RNAi knockdown. UAS-dHDAC6[KD],

UAS-atg6[KD], and UAS-atg12[KD] lines were generated as described in Supplemental

Methods. To determine the degree of knockdown of each relevant transcript, these lines

were crossed with the driver line Actin5c-GAL4 and total RNA was isolated from 5-10

larvae. Quantitation was performed as described in Supplemental Methods. Data show

mean transcript levels relative to GAPDH2 and standard error. Transcript levels relative

to dGAPDH2 are shown for (**a**) two UAS-dHDAC6 [KD] lines, (**b**) two UAS-atg6[KD] lines,

and (**c**) one UAS-atg12[KD] line. Knockdown of dHDAC6 was also examined at the protein

level by immunoblot as shown in Supplemental Figure A4.4. Consistent with the results

shown here, the UAS-atg12[KD] knockdown line used here was previously shown to reduce

autophagy induction by approximately 75% in the *Drosophila* fat body based on a

Lysotracker assay (Scott et al., 2004).
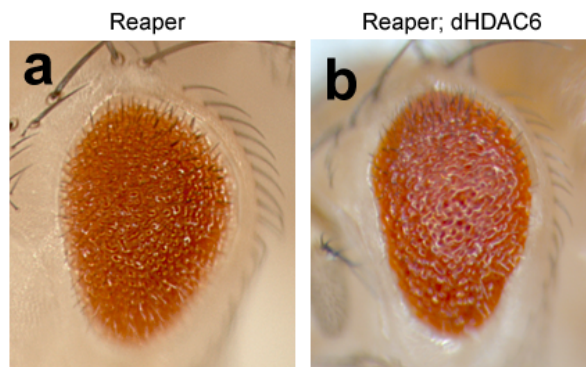
Supplemental Figure A4.4

Supplemental Figure A4.4. Knockdown of endogenous dHDAC6 in the eye causes no overt phenotype in 1-day-old adult flies. (**a**) Western blot with affinity-purified anti-dHDAC6 validating knockdown of dHDAC6 when the dsRNA is ubiquitously expressed in larvae using the driver Tub-GAL4. Western blot for tubulin serves as a loading control. (**b**) Targeted RNAi knockdown of dHDAC6 in the eye using the driver GMR-GAL4 has no overt effect on the external morphology of the eye of a 1-day-old fly. UAS-HDAC6^{KD} line 13A3 is shown. ~200 fly eyes of each genotype have been examined. Quantitative analyses of eye phenotypes are presented in Supplemental Figure A4.2.
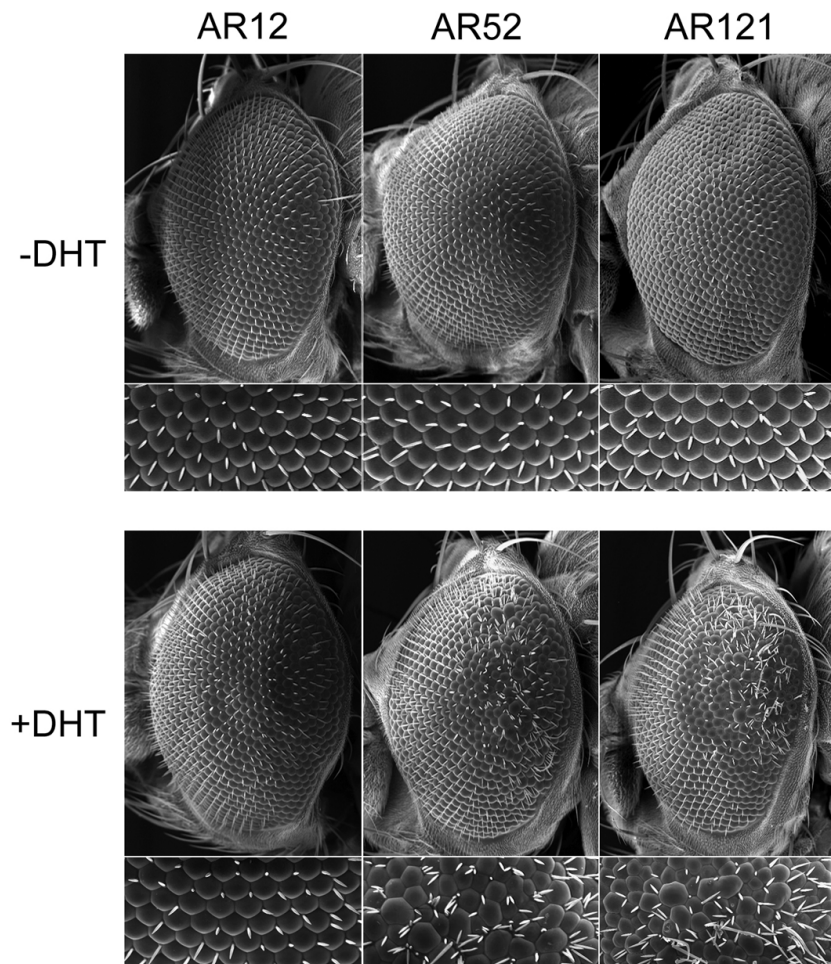
Supplemental Figure A4.5

Supplemental Figure A4.5. Targeted knockdown of dHDAC6 enhances the degenerative phenotype in flies with mutations in the proteasome and in SBMA flies that have impaired UPS function. (a) GMR-GAL4; UAS-DTS7 flies develop a rough eye phenotype when reared at 28°C. (b) In GMR-GAL4; UAS-DTS7; UAS-dHDAC6^{KD} flies the rough eye phenotype is enhanced. (c) GMR-GAL4; UAS-AR52 flies develop a rough eye phenotype when reared on food containing DHT. (d) In GMR-GAL4; UAS-AR52; UAS-dHDAC6^{KD} flies the rough eye phenotype is enhanced. ~200 fly eyes of each genotype have been examined. Quantitative analyses of eye phenotypes are presented in Supplemental Figure A4.2.

Supplemental Figure A4.6

Reaper   Reaper; dHDAC6

a   b

Supplemental Figure A4.6. Ectopic expression of dHDAC6 does not suppress the phenotype associated with mis-expression of the positive cell death regulator *reaper*. (**a**) GMR-GAL4; UAS-reaper flies develop a rough eye phenotype. (**b**) In GMR-GAL4; UAS-reaper; UAS-dHDAC6 flies the rough eye phenotype is unchanged. ~200 fly eyes of each genotype have been examined. Quantitative analyses of eye phenotypes are presented in Supplemental Figure A4.2.

Supplemental Figure A4.7. A *Drosophila* model of SBMA.

Supplemental Figure A4.7. A *Drosophila* model of SBMA. Expression of human AR resulted in ligand-dependent, polyQ length-dependent degeneration. Flies not treated with DHT had normal eyes (**top row**). Flies reared on food containing DHT showed polyQ length-dependent degeneration (**bottom row**). Degeneration was most severe at the posterior eye margin. There was disorganization of the ommatidial array, fusion of ommatidia, and abnormal bristles. Longer repeat length caused a more severe degenerative phenotype that extended further anteriorly. Ligand-dependent, polyQ length-dependent degeneration recapitulates two key features of human SBMA. >1000 fly eyes of each genotype have been examined. Quantitative analyses of eye phenotypes are presented in Supplemental Figure A4.2.
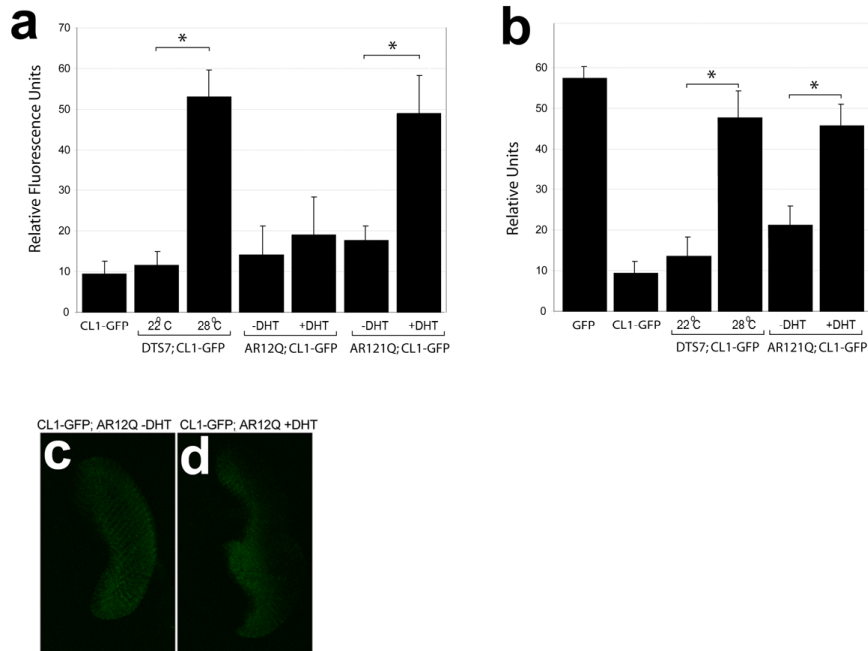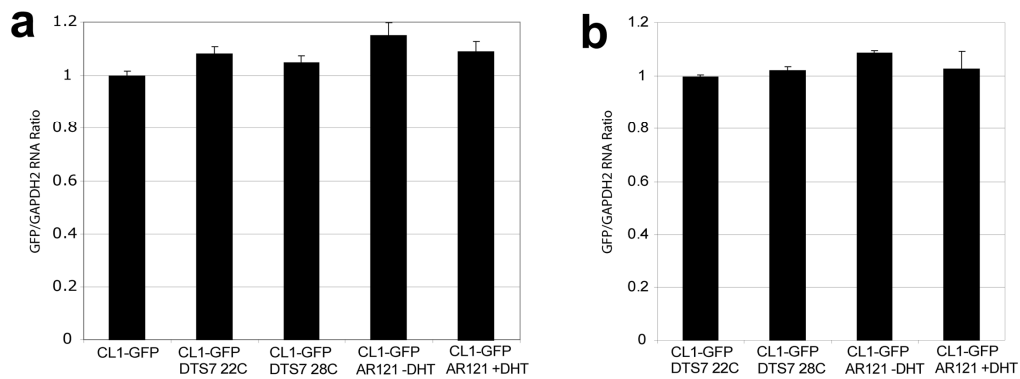
Supplemental Figure A4.8

Supplemental Figure A4.8. Monitoring UPS function in vivo. (**a**) Quantitation of fluorescent signal from 8-10 imaginal eye discs from each genotype and condition reveals significant UPS impairment in DTS7 flies reared at 28°C and in AR52 flies reared on DHT, but not in AR12 flies reared on DHT. (**b**) Quantitation of Western blots for GFP in adult flies expressing the indicated transgenes under the indicated conditions reveals significant UPS impairment in DTS7 flies reared at 28°C and in AR52 flies reared on DHT. Protein levels were normalized to actin. Comparisons were made using Student's t-test assuming equal variances. Data shows mean and standard deviation. *= p<0.01.(**c-d**) Detection of CL1-GFP reporter in imaginal eye discs from third instar larvae by confocal microscopy reveals no evidence of ligand-dependent UPS impairment in AR12 flies. (**c**)

GMR-GAL4; UAS-CL1-GFP; UAS-AR12Q (-DHT). (**d**) GMR-GAL4; UAS-CL1-GFP; UAS-AR12Q (+DHT).

Supplemental Figure A4.9

Supplemental Figure A4.9. Accumulation of CL1-GFP reporter protein with UPS impairment occurs without significant change in transcript levels as determined by real-time quantitative PCR. Total RNA was isolated from 5-10 flies and real time quantitative PCR was performed as described in Supplemental Methods. (**a**) RNA quantitation from larvae, corresponding to Figure A4.1 and Supplemental Figure A4.8a. (**b**) RNA quantitation from adult flies, corresponding to Supplemental Figure A4.8b. Data show mean GFP/GAPDH2 ratios and standard error.

Supplemental Figure A4.10
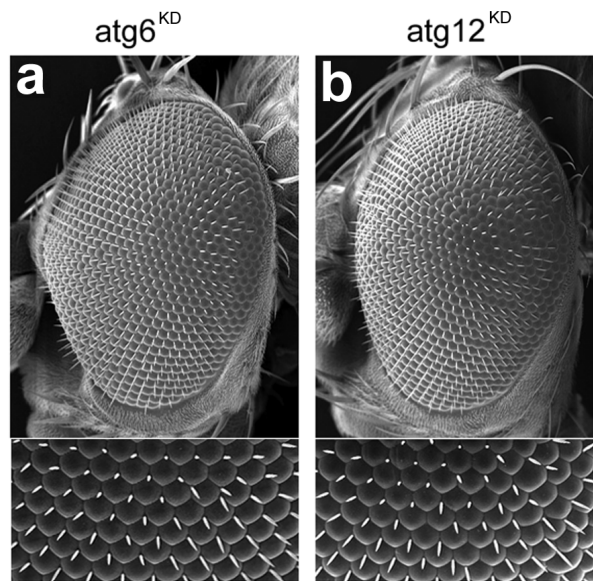
Supplemental Figure A4.10. Knockdown of atg6 and atg12 does not affect eye morphology. One-day-old (**a**) GMR-GAL4;UAS-atg6^{KD} and (**b**)GMR-GAL4;UAS-atg12^{KD} flies reared at 28°C were examined by SEM.

Supplemental Figure A4.11
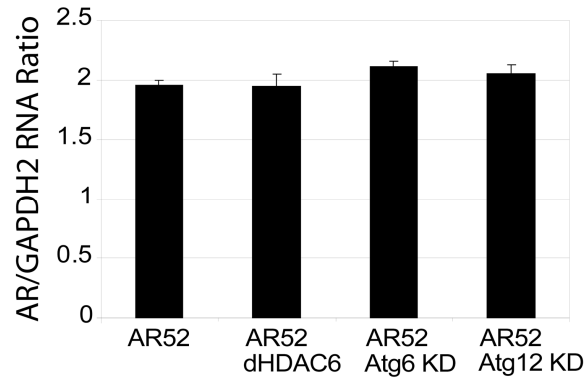
Supplemental Figure A4.11. Reduced levels of AR52 protein with ectopic expression of dHDAC6 occurs without significant change in AR transcript levels. This was determined by real-time quantitative PCR as described in Supplemental Methods. AR/GAPDH2 ratios and standard error for each condition are shown.

Supplemental Figure A4.12
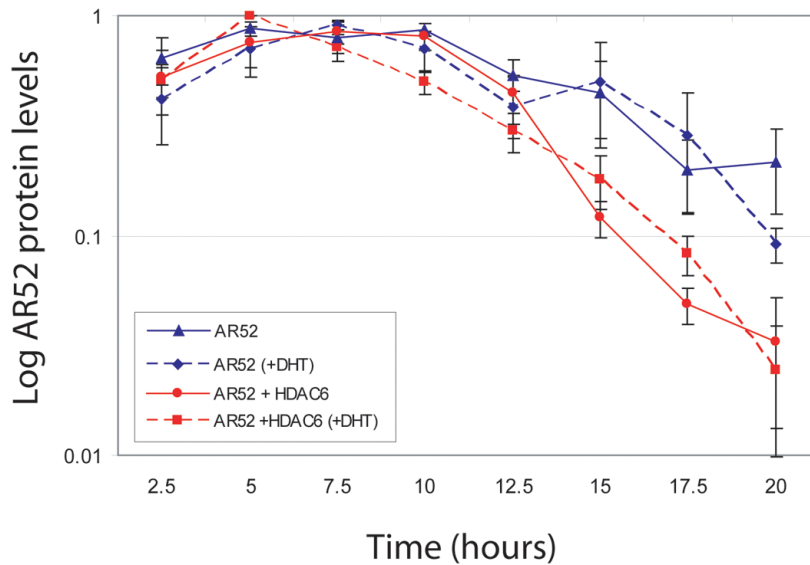
Supplemental Figure A4.12. HDAC6 accelerates the turnover of polyQ-expanded AR. A logarithmic plot of the AR52/actin ratio in 3-4 consecutive experiments showed accelerated turnover of AR52 with co-expression of dHDAC6. The experiment was performed with or without exposure to DHT, as indicated. Exposure to DHT did not significantly influence the rate of AR52 turnover. This data was used to determine the line of best fit by regression analysis ($y = Ae^{-Kx}$) as presented in Figure A4.3. The slope of the best fit line was used to estimate half-life with the equation $t_{1/2} = 0.693/K$. Half-life of AR52 *in vivo* was reduced approximately 2-fold in flies co-expressing dHDAC6 independent of exposure to DHT.

References

(1993) A novel gene containing a trinucleotide repeat that is expanded and unstable on Huntington's disease chromosomes. The Huntington's Disease Collaborative Research Group. Cell 72:971-983.

Abel A, Walcott J, Woods J, Duda J, Merry DE (2001) Expression of expanded repeat androgen receptor produces neurologic disease in transgenic mice. Hum Mol Genet 10:107-116.

Abeliovich H, Klionsky DJ (2001) Autophagy in yeast: mechanistic insights and physiological function. Microbiol Mol Biol Rev 65:463-479, table of contents.

Abida WM, Gu W (2008) p53-Dependent and p53-independent activation of autophagy by ARF. Cancer Res 68:352-357.

Adachi H, Waza M, Katsuno M, Tanaka F, Doyu M, Sobue G (2007) Pathogenesis and molecular targeted therapy of spinal and bulbar muscular atrophy. Neuropathol Appl Neurobiol 33:135-151.

Adachi H, Kume A, Li M, Nakagomi Y, Niwa H, Do J, Sang C, Kobayashi Y, Doyu M, Sobue G (2001) Transgenic mice with an expanded CAG repeat controlled by the human AR promoter show polyglutamine nuclear inclusions and neuronal dysfunction without neuronal cell death. Hum Mol Genet 10:1039-1048.

Adachi H, Katsuno M, Minamiyama M, Waza M, Sang C, Nakagomi Y, Kobayashi Y, Tanaka F, Doyu M, Inukai A, Yoshida M, Hashizume Y, Sobue G (2005) Widespread nuclear and cytoplasmic accumulation of mutant androgen receptor in SBMA patients. Brain 128:659-670.

Ahlberg J, Marzella L, Glaumann H (1982) Uptake and degradation of proteins by isolated rat liver lysosomes. Suggestion of a microautophagic pathway of proteolysis. Lab Invest 47:523-532.

Amaravadi RK, Yu D, Lum JJ, Bui T, Christophorou MA, Evan GI, Thomas-Tikhonenko A, Thompson CB (2007) Autophagy inhibition enhances therapy-induced apoptosis in a Myc-induced model of lymphoma. J Clin Invest 117:326-336.

Andrew DJ, Henderson KD, Seshaiah P (2000) Salivary gland development in Drosophila melanogaster. Mech Dev 92:5-17.

Anglade P, Vyas S, Javoy-Agid F, Herrero MT, Michel PP, Marquez J, Mouatt-Prigent A, Ruberg M, Hirsch EC, Agid Y (1997) Apoptosis and autophagy in nigral neurons of patients with Parkinson's disease. Histol Histopathol 12:25-31.

Arbizu T, Santamaria J, Gomez JM, Quilez A, Serra JP (1983) A family with adult spinal and bulbar muscular atrophy, X-linked inheritance and associated testicular failure. J Neurol Sci 59:371-382.

Arnason T, Ellison MJ (1994) Stress resistance in Saccharomyces cerevisiae is strongly correlated with assembly of a novel type of multiubiquitin chain. Mol Cell Biol 14:7876-7883.

Arrasate M, Mitra S, Schweitzer ES, Segal MR, Finkbeiner S (2004) Inclusion body formation reduces levels of mutant huntingtin and the risk of neuronal death. Nature 431:805-810.

Arstila AU, Trump BF (1968) Studies on cellular autophagocytosis. The formation of autophagic vacuoles in the liver after glucagon administration. Am J Pathol 53:687-733.

Baek SH, Ohgi KA, Nelson CA, Welsbie D, Chen C, Sawyers CL, Rose DW, Rosenfeld MG (2006) Ligand-specific allosteric regulation of coactivator functions of androgen receptor in prostate cancer cells. Proc Natl Acad Sci U S A 103:3100-3105.

Banno H, Katsuno M, Suzuki K, Takeuchi Y, Kawashima M, Suga N, Takamori M, Ito M, Nakamura T, Matsuo K, Yamada S, Oki Y, Adachi H, Minamiyama M, Waza M, Atsuta N, Watanabe H, Fujimoto Y, Nakashima T, Tanaka F, Doyu M, Sobue G (2009) Phase 2 trial of leuprorelin in patients with spinal and bulbar muscular atrophy. Ann Neurol 65:140-150.

Becher MW, Kotzuk JA, Sharp AH, Davies SW, Bates GP, Price DL, Ross CA (1998) Intranuclear neuronal inclusions in Huntington's disease and dentatorubral and pallidoluysian atrophy: correlation between the density of inclusions and IT15 CAG triplet repeat length. Neurobiol Dis 4:387-397.

Bence NF, Sampat RM, Kopito RR (2001) Impairment of the ubiquitin-proteasome system by protein aggregation. Science 292:1552-1555.

Benjamini Y, Hochberg Y (1995) Controlling the False Discovery Rate: a Practical and Powerful Approach to Multiple Testing. J R Statist Soc, B 57:289-300.

Bennett EJ, Bence NF, Jayakumar R, Kopito RR (2005) Global impairment of the ubiquitin-proteasome system by nuclear or cytoplasmic protein aggregates precedes inclusion body formation. Mol Cell 17:351-365.

Bennett MC, Bishop JF, Leng Y, Chock PB, Chase TN, Mouradian MM (1999) Degradation of alpha-synuclein by proteasome. J Biol Chem 274:33855-33858.

Berg TO, Fengsrud M, Stromhaug PE, Berg T, Seglen PO (1998) Isolation and characterization of rat liver amphisomes. Evidence for fusion of autophagosomes with both early and late endosomes. J Biol Chem 273:21883-21892.

Berger Z, Ravikumar B, Menzies FM, Oroz LG, Underwood BR, Pangalos MN, Schmitt I, Wullner U, Evert BO, O'Kane CJ, Rubinsztein DC (2006) Rapamycin alleviates toxicity of different aggregate-prone proteins. Hum Mol Genet 15:433-442.

Bhati M, Lee C, Nancarrow AL, Lee M, Craig VJ, Bach I, Guss JM, Mackay JP, Matthews JM (2008) Implementing the LIM code: the structural basis for cell type-specific assembly of LIM-homeodomain complexes. EMBO J 27:2018-2029.

Bichelmeier U, Schmidt T, Hubener J, Boy J, Ruttiger L, Habig K, Poths S, Bonin M, Knipper M, Schmidt WJ, Wilbertz J, Wolburg H, Laccone F, Riess O (2007) Nuclear localization of ataxin-3 is required for the manifestation of symptoms in SCA3: in vivo evidence. J Neurosci 27:7418-7428.

Bjorkoy G, Lamark T, Brech A, Outzen H, Perander M, Overvatn A, Stenmark H, Johansen T (2005) p62/SQSTM1 forms protein aggregates degraded by

autophagy and has a protective effect on huntingtin-induced cell death. J Cell Biol 171:603-614.

Bodner RA, Outeiro TF, Altmann S, Maxwell MM, Cho SH, Hyman BT, McLean PJ, Young AB, Housman DE, Kazantsev AG (2006) Pharmacological promotion of inclusion formation: a therapeutic approach for Huntington's and Parkinson's diseases. Proc Natl Acad Sci U S A 103:4246-4251.

Boutell JM, Thomas P, Neal JW, Weston VJ, Duce J, Harper PS, Jones AL (1999) Aberrant interactions of transcriptional repressor proteins with the Huntington's disease gene product, huntingtin. Hum Mol Genet 8:1647-1655.

Bowman AB, Yoo SY, Dantuma NP, Zoghbi HY (2005) Neuronal dysfunction in a polyglutamine disease model occurs in the absence of ubiquitin-proteasome system impairment and inversely correlates with the degree of nuclear inclusion formation. Hum Mol Genet 14:679-691.

Boyault C, Zhang Y, Fritah S, Caron C, Gilquin B, Kwon SH, Garrido C, Yao TP, Vourc'h C, Matthias P, Khochbin S (2007) HDAC6 controls major cell response pathways to cytotoxic accumulation of protein aggregates. Genes Dev 21:2172-2181.

Brand AH, Perrimon N (1993) Targeted gene expression as a means of altering cell fates and generating dominant phenotypes. Development 118:401-415.

Brooks BP, Paulson HL, Merry DE, Salazar-Grueso EF, Brinkmann AO, Wilson EM, Fischbeck KH (1997) Characterization of an expanded glutamine repeat androgen receptor in a neuronal cell culture system. Neurobiol Dis 3:313-323.

Bruggenwirth HT, Boehmer AL, Lobaccaro JM, Chiche L, Sultan C, Trapman J, Brinkmann AO (1998) Substitution of Ala564 in the first zinc cluster of the deoxyribonucleic acid (DNA)-binding domain of the androgen receptor by Asp, Asn, or Leu exerts differential effects on DNA binding. Endocrinology 139:103-110.

Brunet A, Bonni A, Zigmond MJ, Lin MZ, Juo P, Hu LS, Anderson MJ, Arden KC, Blenis J, Greenberg ME (1999) Akt promotes cell survival by phosphorylating and inhibiting a Forkhead transcription factor. Cell 96:857-868.

Callewaert L, Verrijdt G, Christiaens V, Haelens A, Claessens F (2003) Dual function of an amino-terminal amphipatic helix in androgen receptor-mediated transactivation through specific and nonspecific response elements. J Biol Chem 278:8212-8218.

Cao Y, Espinola JA, Fossale E, Massey AC, Cuervo AM, MacDonald ME, Cotman SL (2006) Autophagy is disrupted in a knock-in mouse model of juvenile neuronal ceroid lipofuscinosis. J Biol Chem 281:20483-20493.

Chan HY, Warrick JM, Andriola I, Merry D, Bonini NM (2002) Genetic modulation of polyglutamine toxicity by protein conjugation pathways in Drosophila. Hum Mol Genet 11:2895-2904.

Chang CY, McDonnell DP (2005) Androgen receptor-cofactor interactions as targets for new drug discovery. Trends Pharmacol Sci 26:225-228.

Chau V, Tobias JW, Bachmair A, Marriott D, Ecker DJ, Gonda DK, Varshavsky A (1989) A multiubiquitin chain is confined to specific lysine in a targeted short-lived protein. Science 243:1576-1583.

Chen HK, Fernandez-Funez P, Acevedo SF, Lam YC, Kaytor MD, Fernandez MH, Aitken A, Skoulakis EM, Orr HT, Botas J, Zoghbi HY (2003) Interaction of Akt-phosphorylated ataxin-1 with 14-3-3 mediates neurodegeneration in spinocerebellar ataxia type 1. Cell 113:457-468.

Chevalier-Larsen ES, O'Brien CJ, Wang H, Jenkins SC, Holder L, Lieberman AP, Merry DE (2004) Castration restores function and neurofilament alterations of aged symptomatic males in a transgenic mouse model of spinal and bulbar muscular atrophy. J Neurosci 24:4778-4786.

Ciechanover A (2005) Les Prix Nobel, The Nobel Prizes 2004. Stockholm: [Nobel Foundation].

Ciechanover A, Brundin P (2003) The ubiquitin proteasome system in neurodegenerative diseases: sometimes the chicken, sometimes the egg. Neuron 40:427-446.

Ciechanover A, Finley D, Varshavsky A (1984) Ubiquitin dependence of selective protein degradation demonstrated in the mammalian cell cycle mutant ts85. Cell 37:57-66.

Ciechanover A, Orian A, Schwartz AL (2000) Ubiquitin-mediated proteolysis: biological regulation via destruction. Bioessays 22:442-451.

Crighton D, Wilkinson S, O'Prey J, Syed N, Smith P, Harrison PR, Gasco M, Garrone O, Crook T, Ryan KM (2006) DRAM, a p53-induced modulator of autophagy, is critical for apoptosis. Cell 126:121-134.

Cuervo AM, Dice JF (1996) A receptor for the selective uptake and degradation of proteins by lysosomes. Science 273:501-503.

Cuervo AM, Palmer A, Rivett AJ, Knecht E (1995) Degradation of proteasomes by lysosomes in rat liver. Eur J Biochem 227:792-800.

Cuervo AM, Stefanis L, Fredenburg R, Lansbury PT, Sulzer D (2004) Impaired degradation of mutant alpha-synuclein by chaperone-mediated autophagy. Science 305:1292-1295.

Cummings CJ, Mancini MA, Antalffy B, DeFranco DB, Orr HT, Zoghbi HY (1998) Chaperone suppression of aggregation and altered subcellular proteasome localization imply protein misfolding in SCA1. Nat Genet 19:148-154.

Cummings CJ, Reinstein E, Sun Y, Antalffy B, Jiang Y, Ciechanover A, Orr HT, Beaudet AL, Zoghbi HY (1999) Mutation of the E6-AP ubiquitin ligase reduces nuclear inclusion frequency while accelerating polyglutamine-induced pathology in SCA1 mice. Neuron 24:879-892.

David G, Abbas N, Stevanin G, Durr A, Yvert G, Cancel G, Weber C, Imbert G, Saudou F, Antoniou E, Drabkin H, Gemmill R, Giunti P, Benomar A, Wood N, Ruberg M, Agid Y, Mandel JL, Brice A (1997) Cloning of the SCA7 gene reveals a highly unstable CAG repeat expansion. Nat Genet 17:65-70.

Davies JE, Sarkar S, Rubinsztein DC (2006) Trehalose reduces aggregate formation and delays pathology in a transgenic mouse model of oculopharyngeal muscular dystrophy. Hum Mol Genet 15:23-31.

Davies SW, Turmaine M, Cozens BA, DiFiglia M, Sharp AH, Ross CA, Scherzinger E, Wanker EE, Mangiarini L, Bates GP (1997) Formation of neuronal intranuclear inclusions underlies the neurological dysfunction in mice transgenic for the HD mutation. Cell 90:537-548.

236

Dice JF (1990) Peptide sequences that target cytosolic proteins for lysosomal proteolysis. Trends Biochem Sci 15:305-309.

Dice JF (2007) Chaperone-mediated autophagy. Autophagy 3:295-299.

DiFiglia M, Sapp E, Chase KO, Davies SW, Bates GP, Vonsattel JP, Aronin N (1997) Aggregation of huntingtin in neuronal intranuclear inclusions and dystrophic neurites in brain. Science 277:1990-1993.

Dubbink HJ, Hersmus R, Verma CS, van der Korput HA, Berrevoets CA, van Tol J, Ziel-van der Made AC, Brinkmann AO, Pike AC, Trapman J (2004) Distinct recognition modes of FXXLF and LXXLL motifs by the androgen receptor. Mol Endocrinol 18:2132-2150.

Elsasser S, Finley D (2005) Delivery of ubiquitinated substrates to protein-unfolding machines. Nat Cell Biol 7:742-749.

Emamian ES, Kaytor MD, Duvick LA, Zu T, Tousey SK, Zoghbi HY, Clark HB, Orr HT (2003) Serine 776 of ataxin-1 is critical for polyglutamine-induced disease in SCA1 transgenic mice. Neuron 38:375-387.

Estebanez-Perpina E, Arnold LA, Nguyen P, Rodrigues ED, Mar E, Bateman R, Pallai P, Shokat KM, Baxter JD, Guy RK, Webb P, Fletterick RJ (2007) A surface on the androgen receptor that allosterically regulates coactivator binding. Proc Natl Acad Sci U S A 104:16074-16079.

Evert BO, Schelhaas J, Fleischer H, de Vos RA, Brunt ER, Stenzel W, Klockgether T, Wullner U (2006) Neuronal intranuclear inclusions, dysregulation of cytokine expression and cell death in spinocerebellar ataxia type 3. Clin Neuropathol 25:272-281.

Fader CM, Sanchez D, Furlan M, Colombo MI (2008) Induction of autophagy promotes fusion of multivesicular bodies with autophagic vacuoles in k562 cells. Traffic 9:230-250.

Faus H, Haendler B (2008) Androgen receptor acetylation sites differentially regulate gene control. J Cell Biochem 104:511-524.

Feng Z, Zhang H, Levine AJ, Jin S (2005) The coordinate regulation of the p53 and mTOR pathways in cells. Proc Natl Acad Sci U S A 102:8204-8209.

Fernandez-Funez P, Nino-Rosales ML, de Gouyon B, She WC, Luchak JM, Martinez P, Turiegano E, Benito J, Capovilla M, Skinner PJ, McCall A, Canal I, Orr HT, Zoghbi HY, Botas J (2000) Identification of genes that modify ataxin-1-induced neurodegeneration. Nature 408:101-106.

Finley KD, Edeen PT, Cumming RC, Mardahl-Dumesnil MD, Taylor BJ, Rodriguez MH, Hwang CE, Benedetti M, McKeown M (2003) blue cheese mutations define a novel, conserved gene involved in progressive neural degeneration. J Neurosci 23:1254-1264.

Friedman MJ, Shah AG, Fang ZH, Ward EG, Warren ST, Li S, Li XJ (2007) Polyglutamine domain modulates the TBP-TFIIB interaction: implications for its normal function and neurodegeneration. Nat Neurosci 10:1519-1528.

Fu M, Wang C, Reutens AT, Wang J, Angeletti RH, Siconolfi-Baez L, Ogryzko V, Avantaggiati ML, Pestell RG (2000) p300 and p300/cAMP-response element-binding protein-associated factor acetylate the androgen receptor at sites governing hormone-dependent transactivation. J Biol Chem 275:20853-20860.

Fu M, Liu M, Sauve AA, Jiao X, Zhang X, Wu X, Powell MJ, Yang T, Gu W, Avantaggiati ML, Pattabiraman N, Pestell TG, Wang F, Quong AA, Wang C, Pestell RG (2006) Hormonal control of androgen receptor function through SIRT1. Mol Cell Biol 26:8122-8135.

Fu M, Rao M, Wang C, Sakamaki T, Wang J, Di Vizio D, Zhang X, Albanese C, Balk S, Chang C, Fan S, Rosen E, Palvimo JJ, Janne OA, Muratoglu S, Avantaggiati ML, Pestell RG (2003) Acetylation of androgen receptor enhances coactivator binding and promotes prostate cancer cell growth. Mol Cell Biol 23:8563-8575.

Fu YH, Pizzuti A, Fenwick RG, Jr., King J, Rajnarayan S, Dunne PW, Dubel J, Nasser GA, Ashizawa T, de Jong P, et al. (1992) An unstable triplet repeat in a gene related to myotonic muscular dystrophy. Science 255:1256-1258.

Fuertes G, Villarroya A, Knecht E (2003a) Role of proteasomes in the degradation of short-lived proteins in human fibroblasts under various growth conditions. Int J Biochem Cell Biol 35:651-664.

Fuertes G, Martin De Llano JJ, Villarroya A, Rivett AJ, Knecht E (2003b) Changes in the proteolytic activities of proteasomes and lysosomes in human fibroblasts produced by serum withdrawal, amino-acid deprivation and confluent conditions. Biochem J 375:75-86.

Galan JM, Haguenauer-Tsapis R (1997) Ubiquitin lys63 is involved in ubiquitination of a yeast plasma membrane protein. EMBO J 16:5847-5854.

Garcia-Mata R, Bebok Z, Sorscher EJ, Sztul ES (1999) Characterization and dynamics of aggresome formation by a cytosolic GFP-chimera. J Cell Biol 146:1239-1254.

Geetha T, Wooten MW (2002) Structure and functional properties of the ubiquitin binding protein p62. FEBS Lett 512:19-24.

Geng J, Klionsky DJ (2008) The Atg8 and Atg12 ubiquitin-like conjugation systems in macroautophagy. 'Protein modifications: beyond the usual suspects' review series. EMBO Rep 9:859-864.

Gidalevitz T, Ben-Zvi A, Ho KH, Brignull HR, Morimoto RI (2006) Progressive disruption of cellular protein folding in models of polyglutamine diseases. Science 311:1471-1474.

Graham RK, Deng Y, Slow EJ, Haigh B, Bissada N, Lu G, Pearson J, Shehadeh J, Bertram L, Murphy Z, Warby SC, Doty CN, Roy S, Wellington CL, Leavitt BR, Raymond LA, Nicholson DW, Hayden MR (2006) Cleavage at the caspase-6 site is required for neuronal dysfunction and degeneration due to mutant huntingtin. Cell 125:1179-1191.

Grozinger CM, Hassig CA, Schreiber SL (1999) Three proteins define a class of human histone deacetylases related to yeast Hda1p. Proc Natl Acad Sci U S A 96:4868-4873.

Gunawardena S, Goldstein LS (2005) Polyglutamine diseases and transport problems: deadly traffic jams on neuronal highways. Arch Neurol 62:46-51.

Gutierrez MG, Munafo DB, Beron W, Colombo MI (2004) Rab7 is required for the normal progression of the autophagic pathway in mammalian cells. J Cell Sci 117:2687-2697.

Haelens A, Tanner T, Denayer S, Callewaert L, Claessens F (2007) The hinge region regulates DNA binding, nuclear translocation, and transactivation of the androgen receptor. Cancer Res 67:4514-4523.

Hanada T, Noda NN, Satomi Y, Ichimura Y, Fujioka Y, Takao T, Inagaki F, Ohsumi Y (2007) The Atg12-Atg5 conjugate has a novel E3-like activity for protein lipidation in autophagy. J Biol Chem 282:37298-37302.

Hara T, Nakamura K, Matsui M, Yamamoto A, Nakahara Y, Suzuki-Migishima R, Yokoyama M, Mishima K, Saito I, Okano H, Mizushima N (2006) Suppression of basal autophagy in neural cells causes neurodegenerative disease in mice. Nature 441:885-889.

Harris TE, Lawrence JC, Jr. (2003) TOR signaling. Sci STKE 2003:re15.

He B, Bowen NT, Minges JT, Wilson EM (2001) Androgen-induced NH2- and COOH-terminal Interaction Inhibits p160 coactivator recruitment by activation function 2. J Biol Chem 276:42293-42301.

He B, Kemppainen JA, Voegel JJ, Gronemeyer H, Wilson EM (1999) Activation function 2 in the human androgen receptor ligand binding domain mediates interdomain communication with the NH(2)-terminal domain. J Biol Chem 274:37219-37225.

He B, Gampe RT, Jr., Kole AJ, Hnat AT, Stanley TB, An G, Stewart EL, Kalman RI, Minges JT, Wilson EM (2004) Structural basis for androgen receptor interdomain and coactivator interactions suggests a transition in nuclear receptor activation function dominance. Mol Cell 16:425-438.

Heinlein CA, Chang C (2002) Androgen receptor (AR) coregulators: an overview. Endocr Rev 23:175-200.

Helmlinger D, Hardy S, Abou-Sleymane G, Eberlin A, Bowman AB, Gansmuller A, Picaud S, Zoghbi HY, Trottier Y, Tora L, Devys D (2006) Glutamine-expanded ataxin-7 alters TFTC/STAGA recruitment and chromatin structure leading to photoreceptor dysfunction. PLoS Biol 4:e67.

Hicke L, Riezman H (1996) Ubiquitination of a yeast plasma membrane receptor signals its ligand-stimulated endocytosis. Cell 84:277-287.

Hild M, Beckmann B, Haas SA, Koch B, Solovyev V, Busold C, Fellenberg K, Boutros M, Vingron M, Sauer F, Hoheisel JD, Paro R (2003) An integrated gene annotation and transcriptional profiling approach towards the full gene content of the Drosophila genome. Genome Biol 5:R3.

Hockly E, Woodman B, Mahal A, Lewis CM, Bates G (2003) Standardization and statistical approaches to therapeutic trials in the R6/2 mouse. Brain Res Bull 61:469-479.

Hodgson JG, Agopyan N, Gutekunst CA, Leavitt BR, LePiane F, Singaraja R, Smith DJ, Bissada N, McCutcheon K, Nasir J, Jamot L, Li XJ, Stevens ME, Rosemond E, Roder JC, Phillips AG, Rubin EM, Hersch SM, Hayden MR (1999) A YAC mouse model for Huntington's disease with full-length mutant huntingtin, cytoplasmic toxicity, and selective striatal neurodegeneration. Neuron 23:181-192.

Holtz-Heppelmann CJ, Algeciras A, Badley AD, Paya CV (1998) Transcriptional regulation of the human FasL promoter-enhancer region. J Biol Chem 273:4416-4423.

Hsu CL, Chen YL, Yeh S, Ting HJ, Hu YC, Lin H, Wang X, Chang C (2003) The use of phage display technique for the isolation of androgen receptor interacting peptides with (F/W)XXL(F/W) and FXXLY new signature motifs. J Biol Chem 278:23691-23698.

Hughes T, Rusten TE (2007) Origin and evolution of self-consumption: autophagy. Adv Exp Med Biol 607:111-118.

Huynh DP, Figueroa K, Hoang N, Pulst SM (2000) Nuclear localization or inclusion body formation of ataxin-2 are not necessary for SCA2 pathogenesis in mouse or human. Nat Genet 26:44-50.

Ichimura Y, Kumanomidou T, Sou YS, Mizushima T, Ezaki J, Ueno T, Kominami E, Yamane T, Tanaka K, Komatsu M (2008) Structural basis for sorting mechanism of p62 in selective autophagy. J Biol Chem 283:22847-22857.

Ikeda H, Yamaguchi M, Sugai S, Aze Y, Narumiya S, Kakizuka A (1996) Expanded polyglutamine in the Machado-Joseph disease protein induces cell death in vitro and in vivo. Nat Genet 13:196-202.

Ishikawa K, Fujigasaki H, Saegusa H, Ohwada K, Fujita T, Iwamoto H, Komatsuzaki Y, Toru S, Toriyama H, Watanabe M, Ohkoshi N, Shoji S, Kanazawa I, Tanabe T, Mizusawa H (1999) Abundant expression and cytoplasmic aggregations of [alpha]1A voltage-dependent calcium channel protein associated with neurodegeneration in spinocerebellar ataxia type 6. Hum Mol Genet 8:1185-1193.

Iwata A, Riley BE, Johnston JA, Kopito RR (2005a) HDAC6 and microtubules are required for autophagic degradation of aggregated huntingtin. J Biol Chem 280:40282-40292.

Iwata A, Christianson JC, Bucci M, Ellerby LM, Nukina N, Forno LS, Kopito RR (2005b) Increased susceptibility of cytoplasmic over nuclear polyglutamine aggregates to autophagic degradation. Proc Natl Acad Sci U S A 102:13135-13140.

Jackson GR, Salecker I, Dong X, Yao X, Arnheim N, Faber PW, MacDonald ME, Zipursky SL (1998) Polyglutamine-expanded human huntingtin transgenes induce degeneration of Drosophila photoreceptor neurons. Neuron 21:633-642.

Jager S, Bucci C, Tanida I, Ueno T, Kominami E, Saftig P, Eskelinen EL (2004) Role for Rab7 in maturation of late autophagic vacuoles. J Cell Sci 117:4837-4848.

Johnston JA, Ward CL, Kopito RR (1998) Aggresomes: a cellular response to misfolded proteins. J Cell Biol 143:1883-1898.

Junn E, Lee SS, Suhr UT, Mouradian MM (2002) Parkin accumulation in aggresomes due to proteasome impairment. J Biol Chem 277:47870-47877.

Kaganovich D, Kopito R, Frydman J (2008) Misfolded proteins partition between two distinct quality control compartments. Nature 454:1088-1095.

Katsuno M, Adachi H, Doyu M, Minamiyama M, Sang C, Kobayashi Y, Inukai A, Sobue G (2003) Leuprorelin rescues polyglutamine-dependent phenotypes in a transgenic mouse model of spinal and bulbar muscular atrophy. Nat Med 9:768-773.

Katsuno M, Adachi H, Waza M, Banno H, Suzuki K, Tanaka F, Doyu M, Sobue G (2006) Pathogenesis, animal models and therapeutics in Spinal and bulbar muscular atrophy (SBMA). Exp Neurol.

Katsuno M, Adachi H, Kume A, Li M, Nakagomi Y, Niwa H, Sang C, Kobayashi Y, Doyu M, Sobue G (2002) Testosterone reduction prevents phenotypic expression in a transgenic mouse model of spinal and bulbar muscular atrophy. Neuron 35:843-854.

Kawaguchi Y, Kovacs JJ, McLaurin A, Vance JM, Ito A, Yao TP (2003) The deacetylase HDAC6 regulates aggresome formation and cell viability in response to misfolded protein stress. Cell 115:727-738.

Kawaguchi Y, Okamoto T, Taniwaki M, Aizawa M, Inoue M, Katayama S, Kawakami H, Nakamura S, Nishimura M, Akiguchi I, et al. (1994) CAG expansions in a novel gene for Machado-Joseph disease at chromosome 14q32.1. Nat Genet 8:221-228.

Kazemi-Esfarjani P, Benzer S (2000) Genetic suppression of polyglutamine toxicity in Drosophila. Science 287:1837-1840.

Kegel KB, Kim M, Sapp E, McIntyre C, Castano JG, Aronin N, DiFiglia M (2000) Huntingtin expression stimulates endosomal-lysosomal activity, endosome tubulation, and autophagy. J Neurosci 20:7268-7278.

Kennedy WR, Alter M, Sung JH (1968) Progressive proximal spinal and bulbar muscular atrophy of late onset. A sex-linked recessive trait. Neurology 18:671-680.

Kim I, Rodriguez-Enriquez S, Lemasters JJ (2007) Selective degradation of mitochondria by mitophagy. Arch Biochem Biophys 462:245-253.

Kim TW, Tanzi RE (1998) Neuronal intranuclear inclusions in polyglutamine diseases: nuclear weapons or nuclear fallout? Neuron 21:657-659.

Kimura S, Noda T, Yoshimori T (2007) Dissection of the autophagosome maturation process by a novel reporter protein, tandem fluorescent-tagged LC3. Autophagy 3:452-460.

Kimura S, Noda T, Yoshimori T (2008) Dynein-dependent Movement of Autophagosomes Mediates Efficient Encounters with Lysosomes. Cell Struct Funct 33:109-122.

King-Jones K, Thummel CS (2005) Nuclear receptors--a perspective from Drosophila. Nat Rev Genet 6:311-323.

Klement IA, Skinner PJ, Kaytor MD, Yi H, Hersch SM, Clark HB, Zoghbi HY, Orr HT (1998) Ataxin-1 nuclear localization and aggregation: role in polyglutamine-induced disease in SCA1 transgenic mice. Cell 95:41-53.

Klionsky DJ, Abeliovich H, Agostinis P, Agrawal DK, Aliev G, Askew DS, Baba M, Baehrecke EH, Bahr BA, Ballabio A, Bamber BA, Bassham DC, Bergamini E, Bi X, Biard-Piechaczyk M, Blum JS, Bredesen DE, Brodsky JL, Brumell JH, Brunk UT, Bursch W, Camougrand N, Cebollero E, Cecconi F, Chen Y, Chin LS, Choi A, Chu CT, Chung J, Clarke PG, Clark RS, Clarke SG, Clave C, Cleveland JL, Codogno P, Colombo MI, Coto-Montes A, Cregg JM, Cuervo AM, Debnath J, Demarchi F, Dennis PB, Dennis PA, Deretic V, Devenish RJ, Di Sano F, Dice JF, Difiglia M, Dinesh-Kumar S, Distelhorst CW, Djavaheri-Mergny M, Dorsey FC, Droge W, Dron M, Dunn WA, Jr., Duszenko M, Eissa NT, Elazar Z, Esclatine A,

Eskelinen EL, Fesus L, Finley KD, Fuentes JM, Fueyo J, Fujisaki K, Galliot B, Gao FB, Gewirtz DA, Gibson SB, Gohla A, Goldberg AL, Gonzalez R, Gonzalez-Estevez C, Gorski S, Gottlieb RA, Haussinger D, He YW, Heidenreich K, Hill JA, Hoyer-Hansen M, Hu X, Huang WP, Iwasaki A, Jaattela M, Jackson WT, Jiang X, Jin S, Johansen T, Jung JU, Kadowaki M, Kang C, Kelekar A, Kessel DH, Kiel JA, Kim HP, Kimchi A, Kinsella TJ, Kiselyov K, Kitamoto K, Knecht E, et al. (2008) Guidelines for the use and interpretation of assays for monitoring autophagy in higher eukaryotes. Autophagy 4:151-175.

Koide R, Ikeuchi T, Onodera O, Tanaka H, Igarashi S, Endo K, Takahashi H, Kondo R, Ishikawa A, Hayashi T, et al. (1994) Unstable expansion of CAG repeat in hereditary dentatorubral-pallidoluysian atrophy (DRPLA). Nat Genet 6:9-13.

Koike M, Nakanishi H, Saftig P, Ezaki J, Isahara K, Ohsawa Y, Schulz-Schaeffer W, Watanabe T, Waguri S, Kametaka S, Shibata M, Yamamoto K, Kominami E, Peters C, von Figura K, Uchiyama Y (2000) Cathepsin D deficiency induces lysosomal storage with ceroid lipofuscin in mouse CNS neurons. J Neurosci 20:6898-6906.

Kolling R, Hollenberg CP (1994) The ABC-transporter Ste6 accumulates in the plasma membrane in a ubiquitinated form in endocytosis mutants. EMBO J 13:3261-3271.

Komada M, Kitamura N (2005) The Hrs/STAM complex in the downregulation of receptor tyrosine kinases. J Biochem 137:1-8.

Komatsu M, Waguri S, Chiba T, Murata S, Iwata J, Tanida I, Ueno T, Koike M, Uchiyama Y, Kominami E, Tanaka K (2006) Loss of autophagy in the central nervous system causes neurodegeneration in mice. Nature 441:880-884.

Komatsu M, Waguri S, Koike M, Sou YS, Ueno T, Hara T, Mizushima N, Iwata J, Ezaki J, Murata S, Hamazaki J, Nishito Y, Iemura S, Natsume T, Yanagawa T, Uwayama J, Warabi E, Yoshida H, Ishii T, Kobayashi A, Yamamoto M, Yue Z, Uchiyama Y, Kominami E, Tanaka K (2007) Homeostatic levels of p62 control cytoplasmic inclusion body formation in autophagy-deficient mice. Cell 131:1149-1163.

Kopito RR (2003) The missing linker: an unexpected role for a histone deacetylase. Mol Cell 12:1349-1351.

Kovacs JJ, Murphy PJ, Gaillard S, Zhao X, Wu JT, Nicchitta CV, Yoshida M, Toft DO, Pratt WB, Yao TP (2005) HDAC6 regulates Hsp90 acetylation and chaperone-dependent activation of glucocorticoid receptor. Mol Cell 18:601-607.

Kundu M, Thompson CB (2008) Autophagy: basic principles and relevance to disease. Annu Rev Pathol 3:427-455.

Kuusisto E, Salminen A, Alafuzoff I (2001a) Ubiquitin-binding protein p62 is present in neuronal and glial inclusions in human tauopathies and synucleinopathies. Neuroreport 12:2085-2090.

Kuusisto E, Suuronen T, Salminen A (2001b) Ubiquitin-binding protein p62 expression is induced during apoptosis and proteasomal inhibition in neuronal cells. Biochem Biophys Res Commun 280:223-228.

Kuusisto E, Salminen A, Alafuzoff I (2002) Early accumulation of p62 in neurofibrillary tangles in Alzheimer's disease: possible role in tangle formation. Neuropathol Appl Neurobiol 28:228-237.

La Spada AR, Taylor JP (2003) Polyglutamines placed into context. Neuron 38:681-684.

La Spada AR, Taylor JP (2010) Repeat expansion disease: progress and puzzles in disease pathogenesis. Nat Rev Genet 11:247-258.

La Spada AR, Wilson EM, Lubahn DB, Harding AE, Fischbeck KH (1991) Androgen receptor gene mutations in X-linked spinal and bulbar muscular atrophy. Nature 352:77-79.

Laird FM, Farah MH, Ackerley S, Hoke A, Maragakis N, Rothstein JD, Griffin J, Price DL, Martin LJ, Wong PC (2008) Motor neuron disease occurring in a mutant dynactin mouse model is characterized by defects in vesicular trafficking. J Neurosci 28:1997-2005.

Lam YC, Bowman AB, Jafar-Nejad P, Lim J, Richman R, Fryer JD, Hyun ED, Duvick LA, Orr HT, Botas J, Zoghbi HY (2006) ATAXIN-1 interacts with the repressor Capicua in its native complex to cause SCA1 neuropathology. Cell 127:1335-1347.

Lee YS, Carthew RW (2003) Making a better RNAi vector for Drosophila: use of intron spacers. Methods 30:322-329.

Lenk SE, Dunn WA, Jr., Trausch JS, Ciechanover A, Schwartz AL (1992) Ubiquitin-activating enzyme, E1, is associated with maturation of autophagic vacuoles. J Cell Biol 118:301-308.

Levine B, Abrams J (2008) p53: The Janus of autophagy? Nat Cell Biol 10:637-639.

Li D (2006) Selective degradation of the IkappaB kinase (IKK) by autophagy. Cell Res 16:855-856.

Li M, Chevalier-Larsen ES, Merry DE, Diamond MI (2007) Soluble androgen receptor oligomers underlie pathology in a mouse model of spinobulbar muscular atrophy. J Biol Chem 282:3157-3164.

Li M, Miwa S, Kobayashi Y, Merry DE, Yamamoto M, Tanaka F, Doyu M, Hashizume Y, Fischbeck KH, Sobue G (1998) Nuclear inclusions of the androgen receptor protein in spinal and bulbar muscular atrophy. Ann Neurol 44:249-254.

Lieberman AP, Harmison G, Strand AD, Olson JM, Fischbeck KH (2002) Altered transcriptional regulation in cells expressing the expanded polyglutamine androgen receptor. Hum Mol Genet 11:1967-1976.

Lim J, Crespo-Barreto J, Jafar-Nejad P, Bowman AB, Richman R, Hill DE, Orr HT, Zoghbi HY (2008) Opposing effects of polyglutamine expansion on native protein complexes contribute to SCA1. Nature 452:713-718.

Lim KL, Chew KC, Tan JM, Wang C, Chung KK, Zhang Y, Tanaka Y, Smith W, Engelender S, Ross CA, Dawson VL, Dawson TM (2005) Parkin mediates nonclassical, proteasomal-independent ubiquitination of synphilin-1: implications for Lewy body formation. J Neurosci 25:2002-2009.

Lin X, Cummings CJ, Zoghbi HY (1999) Expanding our understanding of polyglutamine diseases through mouse models. Neuron 24:499-502.

Love KR, Catic A, Schlieker C, Ploegh HL (2007) Mechanisms, biology and inhibitors of deubiquitinating enzymes. Nat Chem Biol 3:697-705.

Maclean KH, Dorsey FC, Cleveland JL, Kastan MB (2008) Targeting lysosomal degradation induces p53-dependent cell death and prevents cancer in mouse models of lymphomagenesis. J Clin Invest 118:79-88.

Mahadevan M, Tsilfidis C, Sabourin L, Shutler G, Amemiya C, Jansen G, Neville C, Narang M, Barcelo J, O'Hoy K, et al. (1992) Myotonic dystrophy mutation: an unstable CTG repeat in the 3' untranslated region of the gene. Science 255:1253-1255.

Mahr A, Aberle H (2006) The expression pattern of the Drosophila vesicular glutamate transporter: a marker protein for motoneurons and glutamatergic centers in the brain. Gene Expr Patterns 6:299-309.

Mangiarini L, Sathasivam K, Seller M, Cozens B, Harper A, Hetherington C, Lawton M, Trottier Y, Lehrach H, Davies SW, Bates GP (1996) Exon 1 of the HD gene with an expanded CAG repeat is sufficient to cause a progressive neurological phenotype in transgenic mice. Cell 87:493-506.

Marsh JL, Walker H, Theisen H, Zhu YZ, Fielder T, Purcell J, Thompson LM (2000) Expanded polyglutamine peptides alone are intrinsically cytotoxic and cause neurodegeneration in Drosophila. Hum Mol Genet 9:13-25.

Martin DN, Baehrecke EH (2004) Caspases function in autophagic programmed cell death in Drosophila. Development 131:275-284.

Martin-Aparicio E, Yamamoto A, Hernandez F, Hen R, Avila J, Lucas JJ (2001) Proteasomal-dependent aggregate reversal and absence of cell death in a conditional mouse model of Huntington's disease. J Neurosci 21:8772-8781.

Massey AC, Kaushik S, Sovak G, Kiffin R, Cuervo AM (2006) Consequences of the selective blockage of chaperone-mediated autophagy. Proc Natl Acad Sci U S A 103:5805-5810.

Massey AC, Follenzi A, Kiffin R, Zhang C, Cuervo AM (2008) Early cellular changes after blockage of chaperone-mediated autophagy. Autophagy 4:442-456.

Matsumoto H, Sasaki Y (1989) Staurosporine, a protein kinase C inhibitor interferes with proliferation of arterial smooth muscle cells. Biochem Biophys Res Commun 158:105-109.

Mattson MP, Sherman M (2003) Perturbed signal transduction in neurodegenerative disorders involving aberrant protein aggregation. Neuromolecular Med 4:109-132.

McCampbell A, Taylor JP, Taye AA, Robitschek J, Li M, Walcott J, Merry D, Chai Y, Paulson H, Sobue G, Fischbeck KH (2000) CREB-binding protein sequestration by expanded polyglutamine. Hum Mol Genet 9:2197-2202.

McCray BA, Taylor JP (2008) The role of autophagy in age-related neurodegeneration. Neurosignals 16:75-84.

McGuire SE, Mao Z, Davis RL (2004) Spatiotemporal gene expression targeting with the TARGET and gene-switch systems in Drosophila. Sci STKE 2004:pl6.

McMahon SJ, Pray-Grant MG, Schieltz D, Yates JR, 3rd, Grant PA (2005) Polyglutamine-expanded spinocerebellar ataxia-7 protein disrupts normal SAGA and SLIK histone acetyltransferase activity. Proc Natl Acad Sci U S A 102:8478-8482.

Mizushima N (2005) The pleiotropic role of autophagy: from protein metabolism to bactericide. Cell Death Differ 12 Suppl 2:1535-1541.

Monks DA, Johansen JA, Mo K, Rao P, Eagleson B, Yu Z, Lieberman AP, Breedlove SM, Jordan CL (2007) Overexpression of wild-type androgen receptor in muscle recapitulates polyglutamine disease. Proc Natl Acad Sci U S A 104:18259-18264.

Montie HL, Cho MS, Holder L, Liu Y, Tsvetkov AS, Finkbeiner S, Merry DE (2009) Cytoplasmic retention of polyglutamine-expanded androgen receptor ameliorates disease via autophagy in a mouse model of spinal and bulbar muscular atrophy. Hum Mol Genet 18:1937-1950.

Morfini G, Pigino G, Szebenyi G, You Y, Pollema S, Brady ST (2006) JNK mediates pathogenic effects of polyglutamine-expanded androgen receptor on fast axonal transport. Nat Neurosci 9:907-916.

Moses K, Rubin GM (1991) Glass encodes a site-specific DNA-binding protein that is regulated in response to positional signals in the developing Drosophila eye. Genes Dev 5:583-593.

Moulder KL, Onodera O, Burke JR, Strittmatter WJ, Johnson EM, Jr. (1999) Generation of neuronal intranuclear inclusions by polyglutamine-GFP: analysis of inclusion clearance and toxicity as a function of polyglutamine length. J Neurosci 19:705-715.

Myllykangas L, Tyynela J, Page-McCaw A, Rubin GM, Haltia MJ, Feany MB (2005) Cathepsin D-deficient Drosophila recapitulate the key features of neuronal ceroid lipofuscinoses. Neurobiol Dis 19:194-199.

Nagafuchi S, Yanagisawa H, Sato K, Shirayama T, Ohsaki E, Bundo M, Takeda T, Tadokoro K, Kondo I, Murayama N, et al. (1994) Dentatorubral and pallidoluysian atrophy expansion of an unstable CAG trinucleotide on chromosome 12p. Nat Genet 6:14-18.

Nagaoka U, Kim K, Jana NR, Doi H, Maruyama M, Mitsui K, Oyama F, Nukina N (2004) Increased expression of p62 in expanded polyglutamine-expressing cells and its association with polyglutamine inclusions. J Neurochem 91:57-68.

Nakamura K, Jeong SY, Uchihara T, Anno M, Nagashima K, Nagashima T, Ikeda S, Tsuji S, Kanazawa I (2001) SCA17, a novel autosomal dominant cerebellar ataxia caused by an expanded polyglutamine in TATA-binding protein. Hum Mol Genet 10:1441-1448.

Narendra D, Tanaka A, Suen DF, Youle RJ (2008) Parkin is recruited selectively to impaired mitochondria and promotes their autophagy. J Cell Biol 183:795-803.

Neefjes J, Dantuma NP (2004) Fluorescent probes for proteolysis: tools for drug discovery. Nat Rev Drug Discov 3:58-69.

Nezis IP, Simonsen A, Sagona AP, Finley K, Gaumer S, Contamine D, Rusten TE, Stenmark H, Brech A (2008) Ref(2)P, the Drosophila melanogaster homologue of mammalian p62, is required for the formation of protein aggregates in adult brain. J Cell Biol 180:1065-1071.

Ning YP, Kanai K, Tomiyama H, Li Y, Funayama M, Yoshino H, Sato S, Asahina M, Kuwabara S, Takeda A, Hattori T, Mizuno Y, Hattori N (2008) PARK9-linked parkinsonism in eastern Asia: mutation detection in ATP13A2 and clinical phenotype. Neurology 70:1491-1493.

Nixon RA (2007) Autophagy, amyloidogenesis and Alzheimer disease. J Cell Sci 120:4081-4091.

Nixon RA, Yang DS, Lee JH (2008) Neurodegenerative lysosomal disorders: a continuum from development to late age. Autophagy 4:590-599.

Nixon RA, Wegiel J, Kumar A, Yu WH, Peterhoff C, Cataldo A, Cuervo AM (2005) Extensive involvement of autophagy in Alzheimer disease: an immuno-electron microscopy study. J Neuropathol Exp Neurol 64:113-122.

Nucifora FC, Jr., Ellerby LM, Wellington CL, Wood JD, Herring WJ, Sawa A, Hayden MR, Dawson VL, Dawson TM, Ross CA (2003) Nuclear localization of a non-caspase truncation product of atrophin-1, with an expanded polyglutamine repeat, increases cellular toxicity. J Biol Chem 278:13047-13055.

Nucifora FC, Jr., Sasaki M, Peters MF, Huang H, Cooper JK, Yamada M, Takahashi H, Tsuji S, Troncoso J, Dawson VL, Dawson TM, Ross CA (2001) Interference by huntingtin and atrophin-1 with cbp-mediated transcription leading to cellular toxicity. Science 291:2423-2428.

Ohtsu H, Xiao Z, Ishida J, Nagai M, Wang HK, Itokawa H, Su CY, Shih C, Chiang T, Chang E, Lee Y, Tsai MY, Chang C, Lee KH (2002) Antitumor agents. 217. Curcumin analogues as novel androgen receptor antagonists with potential as anti-prostate cancer agents. J Med Chem 45:5037-5042.

Olzmann JA, Chin LS (2008) Parkin-mediated K63-linked polyubiquitination: a signal for targeting misfolded proteins to the aggresome-autophagy pathway. Autophagy 4:85-87.

Olzmann JA, Li L, Chudaev MV, Chen J, Perez FA, Palmiter RD, Chin LS (2007) Parkin-mediated K63-linked polyubiquitination targets misfolded DJ-1 to aggresomes via binding to HDAC6. J Cell Biol 178:1025-1038.

Opal P, Zoghbi HY (2002) The role of chaperones in polyglutamine disease. Trends Mol Med 8:232-236.

Ordway JM, Tallaksen-Greene S, Gutekunst CA, Bernstein EM, Cearley JA, Wiener HW, Dure LSt, Lindsey R, Hersch SM, Jope RS, Albin RL, Detloff PJ (1997) Ectopically expressed CAG repeats cause intranuclear inclusions and a progressive late onset neurological phenotype in the mouse. Cell 91:753-763.

Orr HT (2001) Beyond the Qs in the polyglutamine diseases. Genes Dev 15:925-932.

Orr HT, Zoghbi HY (2007) Trinucleotide repeat disorders. Annu Rev Neurosci 30:575-621.

Orr HT, Chung MY, Banfi S, Kwiatkowski TJ, Jr., Servadio A, Beaudet AL, McCall AE, Duvick LA, Ranum LP, Zoghbi HY (1993) Expansion of an unstable trinucleotide CAG repeat in spinocerebellar ataxia type 1. Nat Genet 4:221-226.

Ortega Z, Diaz-Hernandez M, Maynard CJ, Hernandez F, Dantuma NP, Lucas JJ (2010) Acute polyglutamine expression in inducible mouse model unravels ubiquitin/proteasome system impairment and permanent recovery attributable to aggregate formation. J Neurosci 30:3675-3688.

Outeiro TF, Kontopoulos E, Altmann SM, Kufareva I, Strathearn KE, Amore AM, Volk CB, Maxwell MM, Rochet JC, McLean PJ, Young AB, Abagyan R, Feany MB, Hyman BT, Kazantsev AG (2007) Sirtuin 2 inhibitors rescue alpha-synuclein-mediated toxicity in models of Parkinson's disease. Science 317:516-519.

Palazzolo I, Burnett BG, Young JE, Brenne PL, La Spada AR, Fischbeck KH, Howell BW, Pennuto M (2007) Akt blocks ligand binding and protects against expanded polyglutamine androgen receptor toxicity. Hum Mol Genet 16:1593-1603.

Palazzolo I, Stack C, Kong L, Musaro A, Adachi H, Katsuno M, Sobue G, Taylor JP, Sumner CJ, Fischbeck KH, Pennuto M (2009) Overexpression of IGF-1 in muscle attenuates disease in a mouse model of spinal and bulbar muscular atrophy. Neuron 63:316-328.

Palhan VB, Chen S, Peng GH, Tjernberg A, Gamper AM, Fan Y, Chait BT, La Spada AR, Roeder RG (2005) Polyglutamine-expanded ataxin-7 inhibits STAGA histone acetyltransferase activity to produce retinal degeneration. Proc Natl Acad Sci U S A 102:8472-8477.

Pan T, Kondo S, Zhu W, Xie W, Jankovic J, Le W (2008) Neuroprotection of rapamycin in lactacystin-induced neurodegeneration via autophagy enhancement. Neurobiol Dis 32:16-25.

Pandey UB, Batlevi Y, Baehrecke EH, Taylor JP (2007a) HDAC6 at the intersection of autophagy, the ubiquitin-proteasome system and neurodegeneration. Autophagy 3:643-645.

Pandey UB, Nie Z, Batlevi Y, McCray BA, Ritson GP, Nedelsky NB, Schwartz SL, DiProspero NA, Knight MA, Schuldiner O, Padmanabhan R, Hild M, Berry DL, Garza D, Hubbert CC, Yao TP, Baehrecke EH, Taylor JP (2007b) HDAC6 rescues neurodegeneration and provides an essential link between autophagy and the UPS. Nature 447:859-863.

Pankiv S, Clausen TH, Lamark T, Brech A, Bruun JA, Outzen H, Overvatn A, Bjorkoy G, Johansen T (2007) p62/SQSTM1 binds directly to Atg8/LC3 to facilitate degradation of ubiquitinated protein aggregates by autophagy. J Biol Chem 282:24131-24145.

Paulson HL, Perez MK, Trottier Y, Trojanowski JQ, Subramony SH, Das SS, Vig P, Mandel JL, Fischbeck KH, Pittman RN (1997) Intranuclear inclusions of expanded polyglutamine protein in spinocerebellar ataxia type 3. Neuron 19:333-344.

Pennuto M, Fischbeck KH (2010) Therapeutic prospects for polyglutamine disease. In: Protein misfolding diseases: current and emerging principles (Dobson CM, Ramirez-Alvarado M, eds). Hoboken, NJ: John Wiley & Sons.

Perutz MF (1996) Glutamine repeats and inherited neurodegenerative diseases: molecular aspects. Curr Opin Struct Biol 6:848-858.

Perutz MF, Johnson T, Suzuki M, Finch JT (1994) Glutamine repeats as polar zippers: their possible role in inherited neurodegenerative diseases. Proc Natl Acad Sci U S A 91:5355-5358.

Peters MF, Nucifora FC, Jr., Kushi J, Seaman HC, Cooper JK, Herring WJ, Dawson VL, Dawson TM, Ross CA (1999) Nuclear targeting of mutant Huntingtin increases toxicity. Mol Cell Neurosci 14:121-128.

Pickart CM (2004) Back to the future with ubiquitin. Cell 116:181-190.

Pickford F, Masliah E, Britschgi M, Lucin K, Narasimhan R, Jaeger PA, Small S, Spencer B, Rockenstein E, Levine B, Wyss-Coray T (2008) The autophagy-

related protein beclin 1 shows reduced expression in early Alzheimer disease and regulates amyloid beta accumulation in mice. J Clin Invest 118:2190-2199.

Poletti A (2004) The polyglutamine tract of androgen receptor: from functions to dysfunctions in motor neurons. Front Neuroendocrinol 25:1-26.

Puls I, Oh SJ, Sumner CJ, Wallace KE, Floeter MK, Mann EA, Kennedy WR, Wendelschafer-Crabb G, Vortmeyer A, Powers R, Finnegan K, Holzbaur EL, Fischbeck KH, Ludlow CL (2005) Distal spinal and bulbar muscular atrophy caused by dynactin mutation. Ann Neurol 57:687-694.

Pulst SM, Nechiporuk A, Nechiporuk T, Gispert S, Chen XN, Lopes-Cendes I, Pearlman S, Starkman S, Orozco-Diaz G, Lunkes A, DeJong P, Rouleau GA, Auburger G, Korenberg JR, Figueroa C, Sahba S (1996) Moderate expansion of a normally biallelic trinucleotide repeat in spinocerebellar ataxia type 2. Nat Genet 14:269-276.

Quigley CA, Friedman KJ, Johnson A, Lafreniere RG, Silverman LM, Lubahn DB, Brown TR, Wilson EM, Willard HF, French FS (1992) Complete deletion of the androgen receptor gene: definition of the null phenotype of the androgen insensitivity syndrome and determination of carrier status. J Clin Endocrinol Metab 74:927-933.

Ramesh Babu J, Lamar Seibenhener M, Peng J, Strom AL, Kemppainen R, Cox N, Zhu H, Wooten MC, Diaz-Meco MT, Moscat J, Wooten MW (2008) Genetic inactivation of p62 leads to accumulation of hyperphosphorylated tau and neurodegeneration. J Neurochem 106:107-120.

Ravikumar B, Duden R, Rubinsztein DC (2002) Aggregate-prone proteins with polyglutamine and polyalanine expansions are degraded by autophagy. Hum Mol Genet 11:1107-1117.

Ravikumar B, Vacher C, Berger Z, Davies JE, Luo S, Oroz LG, Scaravilli F, Easton DF, Duden R, O'Kane CJ, Rubinsztein DC (2004) Inhibition of mTOR induces autophagy and reduces toxicity of polyglutamine expansions in fly and mouse models of Huntington disease. Nat Genet 36:585-595.

Reddy PH, Williams M, Charles V, Garrett L, Pike-Buchanan L, Whetsell WO, Jr., Miller G, Tagle DA (1998) Behavioural abnormalities and selective neuronal loss in HD transgenic mice expressing mutated full-length HD cDNA. Nat Genet 20:198-202.

Reggiori F, Klionsky DJ (2005) Autophagosomes: biogenesis from scratch? Curr Opin Cell Biol 17:415-422.

Rideout HJ, Lang-Rollin I, Stefanis L (2004) Involvement of macroautophagy in the dissolution of neuronal inclusions. Int J Biochem Cell Biol 36:2551-2562.

Riess O, Schols L, Bottger H, Nolte D, Vieira-Saecker AM, Schimming C, Kreuz F, Macek M, Jr., Krebsova A, Macek MS, Klockgether T, Zuhlke C, Laccone FA (1997) SCA6 is caused by moderate CAG expansion in the alpha1A-voltage-dependent calcium channel gene. Hum Mol Genet 6:1289-1293.

Riley BE, Orr HT (2006) Polyglutamine neurodegenerative diseases and regulation of transcription: assembling the puzzle. Genes Dev 20:2183-2192.

Ritson GP, Custer SK, Freibaum BD, Guinto JB, Geffel D, Moore J, Tang W, Winton MJ, Neumann M, Trojanowski JQ, Lee VM, Forman MS, Taylor JP (2010) TDP-

43 mediates degeneration in a novel Drosophila model of disease caused by mutations in VCP/p97. J Neurosci 30:7729-7739.

Ross CA (1997) Intranuclear neuronal inclusions: a common pathogenic mechanism for glutamine-repeat neurodegenerative diseases? Neuron 19:1147-1150.

Ross CA, Pickart CM (2004) The ubiquitin-proteasome pathway in Parkinson's disease and other neurodegenerative diseases. Trends Cell Biol 14:703-711.

Ross CA, Poirier MA (2004) Protein aggregation and neurodegenerative disease. Nat Med 10 Suppl:S10-17.

Rub U, de Vos RA, Brunt ER, Sebesteny T, Schols L, Auburger G, Bohl J, Ghebremedhin E, Gierga K, Seidel K, den Dunnen W, Heinsen H, Paulson H, Deller T (2006) Spinocerebellar ataxia type 3 (SCA3): thalamic neurodegeneration occurs independently from thalamic ataxin-3 immunopositive neuronal intranuclear inclusions. Brain Pathol 16:218-227.

Rubin GM, Spradling AC (1982) Genetic transformation of Drosophila with transposable element vectors. Science 218:348-353.

Rubinsztein DC (2006) The roles of intracellular protein-degradation pathways in neurodegeneration. Nature 443:780-786.

Sapp E, Schwarz C, Chase K, Bhide PG, Young AB, Penney J, Vonsattel JP, Aronin N, DiFiglia M (1997) Huntingtin localization in brains of normal and Huntington's disease patients. Ann Neurol 42:604-612.

Sarkar S, Ravikumar B, Floto RA, Rubinsztein DC (2008a) Rapamycin and mTOR-independent autophagy inducers ameliorate toxicity of polyglutamine-expanded huntingtin and related proteinopathies. Cell Death Differ.

Sarkar S, Davies JE, Huang Z, Tunnacliffe A, Rubinsztein DC (2007) Trehalose, a novel mTOR-independent autophagy enhancer, accelerates the clearance of mutant huntingtin and alpha-synuclein. J Biol Chem 282:5641-5652.

Sarkar S, Krishna G, Imarisio S, Saiki S, O'Kane CJ, Rubinsztein DC (2008b) A rational mechanism for combination treatment of Huntington's disease using lithium and rapamycin. Hum Mol Genet 17:170-178.

Saudou F, Finkbeiner S, Devys D, Greenberg ME (1998) Huntingtin acts in the nucleus to induce apoptosis but death does not correlate with the formation of intranuclear inclusions. Cell 95:55-66.

Schaffar G, Breuer P, Boteva R, Behrends C, Tzvetkov N, Strippel N, Sakahira H, Siegers K, Hayer-Hartl M, Hartl FU (2004) Cellular toxicity of polyglutamine expansion proteins: mechanism of transcription factor deactivation. Mol Cell 15:95-105.

Schapira M (2002) Pharmacogenomics opportunities in nuclear receptor targeted cancer therapy. Curr Cancer Drug Targets 2:243-256.

Schmidt BJ, Greenberg CR, Allingham-Hawkins DJ, Spriggs EL (2002) Expression of X-linked bulbospinal muscular atrophy (Kennedy disease) in two homozygous women. Neurology 59:770-772.

Schubert U, Anton LC, Gibbs J, Norbury CC, Yewdell JW, Bennink JR (2000) Rapid degradation of a large fraction of newly synthesized proteins by proteasomes. Nature 404:770-774.

Scott RC, Schuldiner O, Neufeld TP (2004) Role and regulation of starvation-induced autophagy in the Drosophila fat body. Dev Cell 7:167-178.

Seibenhener ML, Babu JR, Geetha T, Wong HC, Krishna NR, Wooten MW (2004) Sequestosome 1/p62 is a polyubiquitin chain binding protein involved in ubiquitin proteasome degradation. Mol Cell Biol 24:8055-8068.

Seo H, Sonntag KC, Kim W, Cattaneo E, Isacson O (2007) Proteasome activator enhances survival of huntington's disease neuronal model cells. PLoS ONE 2:e238.

Shacka JJ, Klocke BJ, Young C, Shibata M, Olney JW, Uchiyama Y, Saftig P, Roth KA (2007) Cathepsin D deficiency induces persistent neurodegeneration in the absence of Bax-dependent apoptosis. J Neurosci 27:2081-2090.

Shao J, Diamond MI (2007) Polyglutamine diseases: emerging concepts in pathogenesis and therapy. Hum Mol Genet 16 Spec No. 2:R115-123.

Sharp AH, Loev SJ, Schilling G, Li SH, Li XJ, Bao J, Wagster MV, Kotzuk JA, Steiner JP, Lo A, et al. (1995) Widespread expression of Huntington's disease gene (IT15) protein product. Neuron 14:1065-1074.

Sieradzan KA, Mann DM (2001) The selective vulnerability of nerve cells in Huntington's disease. Neuropathol Appl Neurobiol 27:1-21.

Sikorska B, Liberski PP, Giraud P, Kopp N, Brown P (2004) Autophagy is a part of ultrastructural synaptic pathology in Creutzfeldt-Jakob disease: a brain biopsy study. Int J Biochem Cell Biol 36:2563-2573.

Simonsen A, Birkeland HC, Gillooly DJ, Mizushima N, Kuma A, Yoshimori T, Slagsvold T, Brech A, Stenmark H (2004) Alfy, a novel FYVE-domain-containing protein associated with protein granules and autophagic membranes. J Cell Sci 117:4239-4251.

Skinner PJ, Koshy BT, Cummings CJ, Klement IA, Helin K, Servadio A, Zoghbi HY, Orr HT (1997) Ataxin-1 with an expanded glutamine tract alters nuclear matrix-associated structures. Nature 389:971-974.

Slow EJ, Graham RK, Osmand AP, Devon RS, Lu G, Deng Y, Pearson J, Vaid K, Bissada N, Wetzel R, Leavitt BR, Hayden MR (2005) Absence of behavioral abnormalities and neurodegeneration in vivo despite widespread neuronal huntingtin inclusions. Proc Natl Acad Sci U S A 102:11402-11407.

Smyth KA, Belote JM (1999) The dominant temperature-sensitive lethal DTS7 of Drosophila melanogaster encodes an altered 20S proteasome beta-type subunit. Genetics 151:211-220.

Sobue G, Hashizume Y, Mukai E, Hirayama M, Mitsuma T, Takahashi A (1989) X-linked recessive bulbospinal neuronopathy. A clinicopathological study. Brain 112 (Pt 1):209-232.

Sopher BL, Thomas PS, Jr., LaFevre-Bernt MA, Holm IE, Wilke SA, Ware CB, Jin LW, Libby RT, Ellerby LM, La Spada AR (2004) Androgen receptor YAC transgenic mice recapitulate SBMA motor neuronopathy and implicate VEGF164 in the motor neuron degeneration. Neuron 41:687-699.

Suzuki E, Zhao Y, Ito S, Sawatsubashi S, Murata T, Furutani T, Shirode Y, Yamagata K, Tanabe M, Kimura S, Ueda T, Fujiyama S, Lim J, Matsukawa H, Kouzmenko AP, Aigaki T, Tabata T, Takeyama K, Kato S (2009) Aberrant E2F activation by

polyglutamine expansion of androgen receptor in SBMA neurotoxicity. Proc Natl Acad Sci U S A 106:3818-3822.

Szebenyi G, Morfini GA, Babcock A, Gould M, Selkoe K, Stenoien DL, Young M, Faber PW, MacDonald ME, McPhaul MJ, Brady ST (2003) Neuropathogenic forms of huntingtin and androgen receptor inhibit fast axonal transport. Neuron 40:41-52.

Takeyama K, Ito S, Yamamoto A, Tanimoto H, Furutani T, Kanuka H, Miura M, Tabata T, Kato S (2002) Androgen-dependent neurodegeneration by polyglutamine-expanded human androgen receptor in Drosophila. Neuron 35:855-864.

Takeyama K, Ito S, Sawatsubashi S, Shirode Y, Yamamoto A, Suzuki E, Maki A, Yamagata K, Zhao Y, Kouzmenko A, Tabata T, Kato S (2004) A novel genetic system for analysis of co-activators for the N-terminal transactivation function domain of the human androgen receptor. Biosci Biotechnol Biochem 68:1209-1215.

Tamaoki T, Nomoto H, Takahashi I, Kato Y, Morimoto M, Tomita F (1986) Staurosporine, a potent inhibitor of phospholipid/Ca++dependent protein kinase. Biochem Biophys Res Commun 135:397-402.

Tan JM, Wong ES, Dawson VL, Dawson TM, Lim KL (2007) Lysine 63-linked polyubiquitin potentially partners with p62 to promote the clearance of protein inclusions by autophagy. Autophagy 4:251-253.

Tanaka M, Machida Y, Niu S, Ikeda T, Jana NR, Doi H, Kurosawa M, Nekooki M, Nukina N (2004) Trehalose alleviates polyglutamine-mediated pathology in a mouse model of Huntington disease. Nat Med 10:148-154.

Tasdemir E, Maiuri MC, Galluzzi L, Vitale I, Djavaheri-Mergny M, D'Amelio M, Criollo A, Morselli E, Zhu C, Harper F, Nannmark U, Samara C, Pinton P, Vicencio JM, Carnuccio R, Moll UM, Madeo F, Paterlini-Brechot P, Rizzuto R, Szabadkai G, Pierron G, Blomgren K, Tavernarakis N, Codogno P, Cecconi F, Kroemer G (2008) Regulation of autophagy by cytoplasmic p53. Nat Cell Biol 10:676-687.

Taylor J, Grote SK, Xia J, Vandelft M, Graczyk J, Ellerby LM, La Spada AR, Truant R (2006) Ataxin-7 can export from the nucleus via a conserved exportin-dependent signal. J Biol Chem 281:2730-2739.

Taylor JP, Hardy J, Fischbeck KH (2002) Toxic proteins in neurodegenerative disease. Science 296:1991-1995.

Taylor JP, Taye AA, Campbell C, Kazemi-Esfarjani P, Fischbeck KH, Min KT (2003a) Aberrant histone acetylation, altered transcription, and retinal degeneration in a Drosophila model of polyglutamine disease are rescued by CREB-binding protein. Genes Dev 17:1463-1468.

Taylor JP, Tanaka F, Robitschek J, Sandoval CM, Taye A, Markovic-Plese S, Fischbeck KH (2003b) Aggresomes protect cells by enhancing the degradation of toxic polyglutamine-containing protein. Hum Mol Genet 12:749-757.

Tearle RG, Belote JM, McKeown M, Baker BS, Howells AJ (1989) Cloning and characterization of the scarlet gene of Drosophila melanogaster. Genetics 122:595-606.

Terrell J, Shih S, Dunn R, Hicke L (1998) A function for monoubiquitination in the internalization of a G protein-coupled receptor. Mol Cell 1:193-202.

Thomas M, Dadgar N, Aphale A, Harrell JM, Kunkel R, Pratt WB, Lieberman AP (2004) Androgen receptor acetylation site mutations cause trafficking defects, misfolding, and aggregation similar to expanded glutamine tracts. J Biol Chem 279:8389-8395.

Thomas PS, Jr., Fraley GS, Damian V, Woodke LB, Zapata F, Sopher BL, Plymate SR, La Spada AR (2006) Loss of endogenous androgen receptor protein accelerates motor neuron degeneration and accentuates androgen insensitivity in a mouse model of X-linked spinal and bulbar muscular atrophy. Hum Mol Genet 15:2225-2238.

Trojanowski JQ, Lee VM (2000) "Fatal attractions" of proteins. A comprehensive hypothetical mechanism underlying Alzheimer's disease and other neurodegenerative disorders. Ann N Y Acad Sci 924:62-67.

Truant R, Atwal RS, Burtnik A (2007) Nucleocytoplasmic trafficking and transcription effects of huntingtin in Huntington's disease. Prog Neurobiol 83:211-227.

Truant R, Atwal RS, Desmond C, Munsie L, Tran T (2008) Huntington's disease: revisiting the aggregation hypothesis in polyglutamine neurodegenerative diseases. Febs J 275:4252-4262.

Tsuda H, Jafar-Nejad H, Patel AJ, Sun Y, Chen HK, Rose MF, Venken KJ, Botas J, Orr HT, Bellen HJ, Zoghbi HY (2005) The AXH domain of Ataxin-1 mediates neurodegeneration through its interaction with Gfi-1/Senseless proteins. Cell 122:633-644.

Vabulas RM, Hartl FU (2005) Protein synthesis upon acute nutrient restriction relies on proteasome function. Science 310:1960-1963.

van Royen ME, Cunha SM, Brink MC, Mattern KA, Nigg AL, Dubbink HJ, Verschure PJ, Trapman J, Houtsmuller AB (2007) Compartmentalization of androgen receptor protein-protein interactions in living cells. J Cell Biol 177:63-72.

Venkatraman P, Wetzel R, Tanaka M, Nukina N, Goldberg AL (2004) Eukaryotic proteasomes cannot digest polyglutamine sequences and release them during degradation of polyglutamine-containing proteins. Mol Cell 14:95-104.

Verhoeven K, De Jonghe P, Coen K, Verpoorten N, Auer-Grumbach M, Kwon JM, FitzPatrick D, Schmedding E, De Vriendt E, Jacobs A, Van Gerwen V, Wagner K, Hartung HP, Timmerman V (2003) Mutations in the small GTP-ase late endosomal protein RAB7 cause Charcot-Marie-Tooth type 2B neuropathy. Am J Hum Genet 72:722-727.

Verkerk AJ, Pieretti M, Sutcliffe JS, Fu YH, Kuhl DP, Pizzuti A, Reiner O, Richards S, Victoria MF, Zhang FP, et al. (1991) Identification of a gene (FMR-1) containing a CGG repeat coincident with a breakpoint cluster region exhibiting length variation in fragile X syndrome. Cell 65:905-914.

Vonsattel JP, Myers RH, Stevens TJ, Ferrante RJ, Bird ED, Richardson EP, Jr. (1985) Neuropathological classification of Huntington's disease. J Neuropathol Exp Neurol 44:559-577.

Wadman IA, Osada H, Grutz GG, Agulnick AD, Westphal H, Forster A, Rabbitts TH (1997) The LIM-only protein Lmo2 is a bridging molecule assembling an erythroid, DNA-binding complex which includes the TAL1, E47, GATA-1 and Ldb1/NLI proteins. EMBO J 16:3145-3157.

Waelter S, Boeddrich A, Lurz R, Scherzinger E, Lueder G, Lehrach H, Wanker EE (2001) Accumulation of mutant huntingtin fragments in aggresome-like inclusion bodies as a result of insufficient protein degradation. Mol Biol Cell 12:1393-1407.

Walcott JL, Merry DE (2002) Ligand promotes intranuclear inclusions in a novel cell model of spinal and bulbar muscular atrophy. J Biol Chem 277:50855-50859.

Walsh R, Storey E, Stefani D, Kelly L, Turnbull V (2005) The roles of proteolysis and nuclear localisation in the toxicity of the polyglutamine diseases. A review. Neurotox Res 7:43-57.

Warrick JM, Chan HY, Gray-Board GL, Chai Y, Paulson HL, Bonini NM (1999) Suppression of polyglutamine-mediated neurodegeneration in Drosophila by the molecular chaperone HSP70. Nat Genet 23:425-428.

Warrick JM, Paulson HL, Gray-Board GL, Bui QT, Fischbeck KH, Pittman RN, Bonini NM (1998) Expanded polyglutamine protein forms nuclear inclusions and causes neural degeneration in Drosophila. Cell 93:939-949.

Webb JL, Ravikumar B, Atkins J, Skepper JN, Rubinsztein DC (2003) Alpha-Synuclein is degraded by both autophagy and the proteasome. J Biol Chem 278:25009-25013.

Wei X, Henke VG, Strubing C, Brown EB, Clapham DE (2003) Real-time imaging of nuclear permeation by EGFP in single intact cells. Biophys J 84:1317-1327.

Wheatley DN, Inglis MS (1980) An intracellular perfusion system linking pools and protein synthesis. J Theor Biol 83:437-445.

Wigley WC, Fabunmi RP, Lee MG, Marino CR, Muallem S, DeMartino GN, Thomas PJ (1999) Dynamic association of proteasomal machinery with the centrosome. J Cell Biol 145:481-490.

Xie Z, Klionsky DJ (2007) Autophagosome formation: core machinery and adaptations. Nat Cell Biol 9:1102-1109.

Yamamoto A, Cremona ML, Rothman JE (2006) Autophagy-mediated clearance of huntingtin aggregates triggered by the insulin-signaling pathway. J Cell Biol 172:719-731.

Yang W, Dunlap JR, Andrews RB, Wetzel R (2002) Aggregated polyglutamine peptides delivered to nuclei are toxic to mammalian cells. Hum Mol Genet 11:2905-2917.

Yang Z, Chang YJ, Yu IC, Yeh S, Wu CC, Miyamoto H, Merry DE, Sobue G, Chen LM, Chang SS, Chang C (2007) ASC-J9 ameliorates spinal and bulbar muscular atrophy phenotype via degradation of androgen receptor. Nat Med 13:348-353.

Yeh E, Gustafson K, Boulianne GL (1995) Green fluorescent protein as a vital marker and reporter of gene expression in Drosophila. Proc Natl Acad Sci U S A 92\:7036-7040.

Yewdell JW (2005) Serendipity strikes twice: the discovery and rediscovery of defective ribosomal products (DRiPS). Cell Mol Biol (Noisy-le-grand) 51:635-641.

Yoshizawa T, Yoshida H, Shoji S (2001) Differential susceptibility of cultured cell lines to aggregate formation and cell death produced by the truncated Machado-Joseph disease gene product with an expanded polyglutamine stretch. Brain Res Bull 56:349-352.

Yu WH, Cuervo AM, Kumar A, Peterhoff CM, Schmidt SD, Lee JH, Mohan PS, Mercken M, Farmery MR, Tjernberg LO, Jiang Y, Duff K, Uchiyama Y, Naslund

J, Mathews PM, Cataldo AM, Nixon RA (2005) Macroautophagy--a novel Beta-amyloid peptide-generating pathway activated in Alzheimer's disease. J Cell Biol 171:87-98.

Yu Z, Dadgar N, Albertelli M, Gruis K, Jordan C, Robins DM, Lieberman AP (2006) Androgen-dependent pathology demonstrates myopathic contribution to the Kennedy disease phenotype in a mouse knock-in model. J Clin Invest 116:2663-2672.

Zatloukal K, Stumptner C, Fuchsbichler A, Heid H, Schnoelzer M, Kenner L, Kleinert R, Prinz M, Aguzzi A, Denk H (2002) p62 Is a common component of cytoplasmic inclusions in protein aggregation diseases. Am J Pathol 160:255-263.

Zeng X, Yan T, Schupp JE, Seo Y, Kinsella TJ (2007) DNA mismatch repair initiates 6-thioguanine--induced autophagy through p53 activation in human tumor cells. Clin Cancer Res 13:1315-1321.

Zhuchenko O, Bailey J, Bonnen P, Ashizawa T, Stockton DW, Amos C, Dobyns WB, Subramony SH, Zoghbi HY, Lee CC (1997) Autosomal dominant cerebellar ataxia (SCA6) associated with small polyglutamine expansions in the alpha 1A-voltage-dependent calcium channel. Nat Genet 15:62-69.

Zoghbi HY, Orr HT (2000) Glutamine repeats and neurodegeneration. Annu Rev Neurosci 23:217-247.

Zoghbi HY, Orr HT (2009) Pathogenic mechanisms of a polyglutamine-mediated neurodegenerative disease, spinocerebellar ataxia type 1. J Biol Chem 284:7425-7429.

Zuccato C, Ciammola A, Rigamonti D, Leavitt BR, Goffredo D, Conti L, MacDonald ME, Friedlander RM, Silani V, Hayden MR, Timmusk T, Sipione S, Cattaneo E (2001) Loss of huntingtin-mediated BDNF gene transcription in Huntington's disease. Science 293:493-498.